Inaugural dissertation

for

obtaining the doctoral degree

of the

Combined Faculty of Mathematics, Engineering and Natural Sciences

of the

Ruprecht - Karls - University

Heidelberg

Presented by

M.Med.Sc. Jia-Xiang See

born in: Johor, Malaysia

Oral examination: 18 July 2022

Immune-endothelial axis in liver homeostasis and inflammation

Referees:

Prof. Dr. Ana Martin-Villalba

Prof. Dr. Adelheid Cerwenka

Table of Contents

1 Zusammenfassung 1

2 Summary 3

3 Introduction 5

3.1 The immune system 5

3.1.1 Innate immunity 5

3.1.2 Adaptive immunity 7

3.2 Innate lymphocytes 8

3.2.1 Natural killer cells and innate lymphoid cells 8

3.2.2 Receptor activation 10

3.3 Adaptive lymphocytes 13

3.3.1 Naïve T cells 13

3.3.2 T helper cells and cytotoxic T cells 14

3.3.3 Memory T cells 16

3.3.4 Regulatory T cells 18

3.4 The vascular system 21

3.4.1 Endothelial cells 21

3.4.2 Role of endothelial cells in immune system 23

3.5 Liver 26

3.5.1 Liver architecture 26

3.5.2 NK cells and ILC1s 28

3.5.3 Liver sinusoidal endothelial cells (LSECs) 29

3.5.4 LSECs and immune cells 30

3.5.5 Liver diseases and murine models 31

3.6 Surface molecules studied on LSECs 34

3.6.1 Major histocompatibility class II (MHC II) 34

3.6.2 Herpes virus entry mediator (HVEM) 35

4 Aims of the study 39

5 Materials and Methods 41

5.1 Materials 41

5.1.1 Special laboratory equipment 41
5.1.2 Chemicals and biological reagents 41
5.1.3 Cell culture media and solutions 42
5.1.4 Cell culture products 43
5.1.5 Kits 44
5.1.6 Buffers and solutions 44
5.1.6 Primary anti-mouse antibodies for flow cytometry 46
5.1.7 Antibodies for functional assays 49
5.1.8 Isotype controls 49
5.1.9 Oligonucleotide primers 50
5.1.10 Mouse lines 50

5.2 Methods 52

5.2.1 Liver digestion for LSEC isolation 52
5.2.2 Lipopolysaccharide treatment 52
5.2.3 LSEC isolation and culture 52
5.2.4 Liver mononuclear cell (LMC) isolation for sorting and culture 53
5.2.5 LSECs and liver mononuclear cell isolation for immunophenotyping 53
5.2.6 Splenocyte isolation 54
5.2.7 Lung single cell suspension preparation 54
5.2.8 Cell number counting 54
5.2.9 LSEC and liver mononuclear cell (LMC) coculture 54
5.2.10 LSECs co-cultured with sorted NK cells and ILC1s 55
5.2.11 Co-culture with transwell inserts 55
5.2.12 LSEC sorting 56
5.2.13 RNA extraction 56
5.2.14 cDNA synthesis and real-time quantitative reverse transcription polymerase chain reaction (RT-PCR) 56
5.2.15 Gene expression analysis 57
5.2.16 Mouse genotyping 57
5.2.17 Flow cytometry staining and analysis 58
5.2.18 Flow cytometry analysis 58

6 Results 61

6.1 LSEC phenotypes 61

6.1.1 LSECs express surface molecules involved in immunology in steady-state 61

6.1.2 IFN-γ modulates HVEM, PD-L1 and MHC I expression on LSECs 63

6.2 MHC II on LSECs 64

6.2.1 MHC II expression on LSECs 64

6.2.2 MHC II defines a unique subset of LSECs 65

6.3 Regulation of MHC II expression on LSECs 67

6.3.1 The role of IFN-γ in regulating MHC II expression on LSECs 67

6.3.2 The role of IL-12 in regulating MHC II expression on LSECs 75

6.3.3 The role of microbiota in regulating MHC II expression on LSECs 77

6.3.4 The role of CIITA in regulating MHC II expression on LSECs 79

6.4 Functional roles of MHC II on LSECs 81

6.4.1 IFN-γ affects $CD4^+$ T cell phenotypes in the liver 81

6.5 Functional role of HVEM on LSECs 84

6.5.1 Phenotypes of LSEC-restricted Hvem knockout mice in steady-state 84

6.5.2 Phenotype of LSEC-restricted Hvem knockout mice in aging 87

6.5.3 Phenotypes of LSEC-restricted Hvem knockout mice in acute liver disease 91

6.6 Co-culture of LSECs with liver NK cells and ILC1s 94

6.6.1 LSECs regulate expression of surface receptors on NK cells and ILC1s 94

6.6.2 LSECs alter NK cell effector functions 96

6.6.3 NK cells co-cultured with LSECs reveal distinct transcriptomic profile 99

7 Discussion 101

7.1 MHC II on LSECs 101

7.1.1 MHC II in the context of liver zonation 101

7.1.2 $MHC\ II^{high}$ vs $MHC\ II^{low}$ LSECs 102

7.1.3 The role of IFN-γ in the liver and its redundant cellular sources 104

7.1.4 Other mechanisms for regulating MHC II expression in LSECs 104

7.1.5 Upstream inducers of IFN-γ in steady-state 106

7.1.6 Functional relevance of MHC II in livers 108

7.1.7 Summary I 109

7.2 HVEM on LSECs 111

7.2.1 Residual HVEM expression on LSECs of Hvem cKO mice 111

7.2.2 The role of HVEM in aging 112

7.2.3 The role of HVEM in liver disease 113

7.3 LSEC interaction with NK cells and ILC1s 117

7.3.1 Receptor and ligand interaction 117

7.3.2 Effector functions of NK cells and ILC1s 118

8 Conclusions 121

9 References 123

10 Abbreviations 145

11 Acknowledgements 151

1 Zusammenfassung

Die Leber ist ein zoniertes und stark vaskularisiertes Organ, das mit Immunzellen angereichert ist. Lebersinusoidale Endothelzellen (LSECs) bilden das Mikrogefäßsystem der Leber und sind die wichtigsten, nicht-parenchymalen Leberzellen. Sie bilden die Sinusoide, in denen sich Immunzellen aufhalten. In der Leber gibt es zwei große Untergruppen von angeborenen lymphoiden Zellen, zirkulierende Natürliche Killerzellen (NK) und gewebeständige angeborene lymphoide Zellen 1 (ILC1s). Da sich LSECs und ILCs in unmittelbarer Nähe zueinander befinden, könnten LSECs und NK-Zellen sowie ILC1s sich gegenseitig in der Homöostase und bei Erkrankungen der Leber regulieren.

Ich untersuchte den Crosstalk zwischen LSECs und Immunzellen in der Homöostase und bei Lebererkrankungen. Ich konnte einen neuen Mechanismus aufzeigen, bei dem LSECs als nicht-immune Zellen eine Brücke zwischen angeborener und adaptiver Immunität in der Leberhomöostase bilden. LSECs exprimierten unterschiedliche Mengen an Haupthistokompatibilitätskomplex II (MHC II) in einem zonierten Muster, hauptsächlich in midzonalen und perizentralen Acini. Die MHC-II-Expression auf LSECs war von *Interferon-gamma* (IFN-γ) abhängig, das von ILC1s, NK-Zellen und NKT-Zellen im Steady-State produziert wird. Die Verringerung der MHC-II-Expression auf LSECs korrelierte mit einer erhöhten Frequenz an naiven $CD4^+$ T-Zellen und einer Verringerung von $CD4^+$ T-Gedächtniszellen in der Leber. Daher reguliert IFN-γ, das von angeborenen Lymphozyten produziert wird, die Differenzierung von naiven zu Gedächtnis-T-Zellen, indem es die MHC-II-Expression auf LSECs in der Leber im Steady-State aufrechterhält.

Darüber hinaus induzierten LSECs nach der Ko-Kultur transkriptomische und phänotypische Veränderungen von NK-Zellen. Sie veranlassten die NK-Zellen dazu, bei Stimulation vermehrt IFN-γ zu produzieren. In einem durch Lipopolysaccharid (LPS) induzierten Mausmodell einer akuten Leberverletzung zeigten LSECs einen "aktivierten" Phänotypen durch Hochregulierung von Oberflächenproteinen, die an der Regulation von Immunfunktionen beteiligt sind, ähnlich den Phänotypen von LSECs, die durch IFN-γ stimuliert wurden. Darüber hinaus regulierten LSECs im LPS-Leberschadenmodell Adhäsionsmoleküle hoch, die für die Rekrutierung von NK-Zellen und Monozyten in die Leber während der Krankheit bedeutend sind. Schließlich führte die konditionale Deletion des Herpesvirus-Entry-Mediators (HVEM) in LSECs bei alten Mäusen zur Splenomegalie.

Zusammenfassend identifiziert meine Studie LSECs als Knotenpunkt, der angeborene und adaptive Immunantworten in der Homöostase, bei Entzündungen und während Krankheiten verbindet. Meine Studien beschreiben LSECs als einen unorthodoxen, nicht-immunen Akteur, der die Immunologie der Leber reguliert und bieten einen einzigartigen Einblick, wie die stromale Mikroumgebung die Funktionen der Immunzellen beeinflusst.

2 Summary

Liver is a zonated and highly vascularized organ, enriched with immune cells. Liver sinusoidal endothelial cells (LSECs) form the microvasculature in the liver, comprising the major non-parenchymal liver cells. They constitute the sinusoids where immune cells reside in. In the liver, there are two major subsets of innate lymphocytes, which are circulating natural killer (NK) cells and tissue-resident innate lymphoid cell 1 (ILC1s). As LSECs and innate lymphocytes are in close proximity, LSECs and NK cells, and ILC1s, might regulate each other functions in liver homeostasis and disease.

Here, I investigated LSEC-immune cell crosstalk in steady-state and liver disease. I illustrated a novel mechanism of LSECs to act as a non-immune cell bridging innate and adaptive immunity in liver homeostasis. LSECs expressed heterogeneous amounts of major histocompatibility II (MHC II) in a zonated manner, mainly in midzonal and pericentral acini. The MHC II expression on LSECs was dependent on interferon gamma (IFN-γ), produced by ILC1s, NK cells, and NKT cells in steady-state. The reduction of MHC II expression on LSECs correlated with an increased naïve $CD4^+$ T cell and a decreased memory $CD4^+$ T cell frequency in the liver. Hence, IFN-γ secreted by innate lymphocytes regulates naive to memory T cell differentiation, by maintaining MHC II expression on LSECs in the liver in steady-state.

In addition, LSECs induced transcriptomic and phenotypic changes of NK cells after co-culture. They also primed NK cells to produce a higher amount of IFN-γ upon stimulation. In a lipopolysaccharide (LPS)-induced acute liver injury model, LSECs displayed ‘activated’ phenotypes by upregulation of surface proteins involved in regulating immune functions, mimicking phenotypes of LSECs stimulated by IFN-γ. In addition, LSECs also upregulated adhesion molecules in the LPS liver injury model, important for NK cell and monocyte recruitment into the liver during the disease. Furthermore, in aged mice, conditional deletion of Herpesvirus Entry Mediator (HVEM) in LSECs led to splenomegaly.

In summary, my study highlights LSECs as the center mediating innate and adaptive immune responses in homeostasis, inflammation, and disease. I describe LSECs as an unorthodox non-immune player to regulate liver immunology, which provides a singular insight of how the stromal microenvironment shapes immune cell functions.

3 Introduction

3.1 The immune system

The immune system protects people from diseases. A functional and balanced immune system routinely performs several tasks: i. eliminate foreign harms such as bacteria, viruses and fungi, ii. eradicate self-derived threats such as cancer. An aberrant immune system, either too strong or too weak, causes diseases. A hyper-immune response can lead to destruction of own tissues, while a hypo-immune response causes inadequate clearance of pathogens. Thus, the purpose of studying immunology is to comprehend the immune system, so that we can fine-tune and harness its potential to treat various diseases. For instance, we have faced the greatest pandemic in 2020, namely COVID-19, since Spanish Flu that happened 100 years ago. Because of the accumulating knowledge in immunology, researchers were able to develop effective vaccines against COVID-19 in an unprecedented speed, which have largely restricted the transmission and mortality caused by the disease. An effective vaccine, and many other therapeutics, require optimal communication of two major aspects of the immune system: innate immunity and adaptive immunity.

3.1.1 Innate immunity

Innate immunity is the earliest form of immunity that is evolutionary conserved, and can be found in unicellular prokaryotes as well as in complex multicellular mammals like humans. One of the most well-known example of innate defense in prokaryotes is clustered regularly interspaced short palindromic repeats (CRISPR)-Cas9 system (Dimitriu, Szczelkun, & Westra, 2020). Cas9 protein in prokaryote uses CRISPR sequence derived from previous invading bacteriophage as a guide to recognize and cleave invaders (Mojica & Rodriguez-Valera, 2016). Jennifer Doudna and Emmanuelle Charpentier further developed this discovery into a genome editing tool that has revolutionized the genome editing field, culminating in their Nobel Prize award in Chemistry in 2020 (Jinek et al., 2012). Obviously, human innate immunity is far more advanced and complex than the archaic CRISPR-Cas9 system in prokaryotes.

In humans, there are three types of barriers acting as the first lines of defense, the mechanical, chemical, and microbiological barriers. Epithelial cells of skins and the inner body tracts have all these three barriers to protect against infection. Mechanical barrier includes tight junctions formed by epithelial cells. The chemical barrier includes stomach acid, tears, saliva, mucus, enzymes, and antibacterial peptides that can destroy invading pathogens, or prevent their survival and invasion. Microbiological barrier includes

commensal bacteria that reside on the epithelial surfaces, which compete with pathogenic microbes for nutrition and survival.

If a pathogen manages to penetrate through the first line of defense, innate immunity forms the second line of defense. Innate immune cells include natural killer (NK) cells, ILCs (innate lymphoid cells), monocytes, macrophages, dendritic cells, neutrophils, basophils, eosinophils, and mast cells. They are the early immune cells that encounter foreign invaders. One unique characteristic of innate immune cells is the ability to distinguish foreign cells from self through pattern recognition receptors (PRRs). These PRRs recognize pathogen-associated molecular patterns (PAMPs), which are only found on bacteria, viruses, and fungi. PRRs also recognize damage-associated molecular patterns (DAMPs), which are released after cell or tissue damage (Seong & Matzinger, 2004). There are various families of PRRs, and one important family is the Toll-like receptors (TLRs). Toll was initially discovered as an antifungal gene in Drosophila (Lemaitre, Nicolas, Michaut, Reichhart, & Hoffmann, 1996). There are 10 types of TLRs in humans and 12 types of TLRs in mice, expressed either on surface or intracellularly, which recognize different PAMPs of pathogens including lipopolysaccharide, nucleic acids, etc (Akira, Uematsu, & Takeuchi, 2006). Other families of PRRs include NOD-like receptors (NLRs), RIG-I-like receptors (RLRs), and C-type leptin receptors (CLRs), which play equally crucial role in recognizing PAMPs and DAMPs. After sensing PAMPs or DAMPs, innate immune cells are activated and initiate a cascade of signaling events leading to inflammatory responses. For example, TLRs signaling can lead to the activation of nuclear-factor-kappa B (NF-κβ), resulting in the release of inflammatory cytokines (Kawai & Akira, 2007). This further triggers activation of other immune cells in response to foreign pathogen.

Another part of the innate immunity is the complement system. It comprises a group of proteins produced by the liver, acting in a sequential manner to clear apoptotic cells or foreign invaders. There are three major pathways of complement activation: the classical, lectin, and alternative pathway. Homeostatic complement activation occurs at all time to remove apoptotic cells and survey foreign pathogens. In steady-state, complement pathways are only activated in a restricted manner to enhance phagocytosis and eliminate apoptotic cells without triggering host immune responses. However, when encountering foreign pathogens, the complement system can be activated in a way that leads to inflammation, phagocytosis and opsonization of the foreign pathogens (Merle, Church, Fremeaux-Bacchi, & Roumenina, 2015). Therefore, the complement system plays an indispensable role both in homeostasis and during inflammation.

Phagocytes are the crucial cells in innate immunity. Phagocytes comprise all cells that can ingest foreign substances or apoptotic cells, which include monocytes, macrophages, dendritic cells (DCs), neutrophils

and mast cells. They are either professional antigen presenting cells (APCs), like macrophages and DCs, or granulocytes as neutrophils and mast cells. Macrophages and dendritic cells are tissue-resident, while monocytes and neutrophils are patrolling and are recruited to the tissue during inflammation (Soehnlein & Lindbom, 2010). Phagocytes initiate phagocytosis once they have recognized ligands of foreign invaders. They start to engulf invaders through actin cytoskeleton remodeling and membrane extension. After that, phagosomes encapsulate foreign compounds, fusing with early endosomes and lysosome to become fully mature phagolysosome (Pauwels, Trost, Beyaert, & Hoffmann, 2017). Phagolysosomes, rich with hydrolytic enzymes and reactive oxygen species, kill the invaders in an acidic and highly hostile environment (Slauch, 2011). In addition, professional APCs, like macrophages and DCs, are able to cross-present antigens to adaptive T cells and activate them. APCs present peptide antigens in the context of major histocompatibility class (MHC) I or II molecules, as T cells are not able to recognize native antigens. Thus, phagocytes are also important in initiating adaptive immune responses after encountering foreign intruders.

3.1.2 Adaptive immunity

According to the current textbooks, adaptive immunity possesses several features that are not found in innate system: specificity and memory. There are two main types of cells involved in adaptive immunity, which are B cells and T cells. It has always been thought that the letter 'B' in B cells means bone marrow, as B cells develop in bone marrow. It is only partially true, as 'B' is derived bursa of Fabricus, which is the site of B cell development in birds. It was first described in 1956 that the chickens with bursa of Fabricus removed were not able to produce antibodies (Glick, Chang, & Jaap, 1956). Jacques Miller further described two major subsets of adaptive lymphocytes in mammals: T cells that develop in the thymus, and B cells which can produce antibodies develop fully in the bone marrow (Miller, 1999).

Memory is another hallmark of adaptive immunity. Once activated, a subpopulation of activated T cells and B cells will become antigen-specific memory T and B cells. These memory cells provide lifelong immunity against the antigen which they have encountered before. Memory cells can be both circulating and tissue-resident, enabling them to respond to antigens in an immediate manner (Palm & Henry, 2019; Sathaliyawala et al., 2013). Memory T cells proliferate and differentiate into effector memory T cells, while memory B cells differentiate into plasma cells that can produce abundant amount of antibodies, triggering secondary immune response. Because of immune memory, humans are protected against secondary reinfection of the same pathogen, such as viruses causing chicken pox and measles. Immunological memory is the foundation of vaccination, which educate T and B cells to form memory against pathogens causing diseases by injecting modified microorganism, viruses, RNAs, or proteins.

Naïve B cells are activated in secondary lymphoid organs, such as lymph nodes and spleen. They can be activated in a T cell-dependent or T-cell independent manner. Once activated, naïve B cells can differentiate into plasma cells that can produce one of the five main classes of antibodies, which are immunoglobulin (Ig) A, IgD, IgE, IgG, and IgM. The three most abundant classes in humans are IgG (75-80%), IgA (10-15%), and IgM (5-10%). IgA is produced abundantly in mucosal tissues in response to microbes or pollen. IgM is produced by short-lived plasmablasts/plasma cells after naïve B cell activation, often used as an indication of initial exposure to antigen (Sathe & Cusick, 2021). IgG and IgA are produced at a later stage after mature B cells undergo immunoglobulin class switching, if they receive additional receptor and cytokine signals from follicular B helper T cells in germinal centers(Cerutti, 2008; Nurieva & Chung, 2010; Stavnezer & Schrader, 2014). IgG and IgA are the most common form of antibody, and play crucial roles against viruses, bacteria, and fungi infections.

3.2 Innate lymphocytes

3.2.1 Natural killer cells and innate lymphoid cells

Innate lymphocytes include five major cell population: NK cells, ILC1s, ILC2s, ILC3s, and lymphoid-tissue inducer (LTi) cells. Developmentally, NK cells, ILCs (ILC1s, ILC2s, ILC3s), and LTis cells have distinct progenitors (Fig. 1.1). NK cells are derived from the NK progenitor (NKP), ILCs are from the ILC progenitor (ILCP), and LTi cells are from the LTi progenitor (LTiP). Thus, NK cells, ILCs, and LTi cells are different cell populations according to the lineage definition.

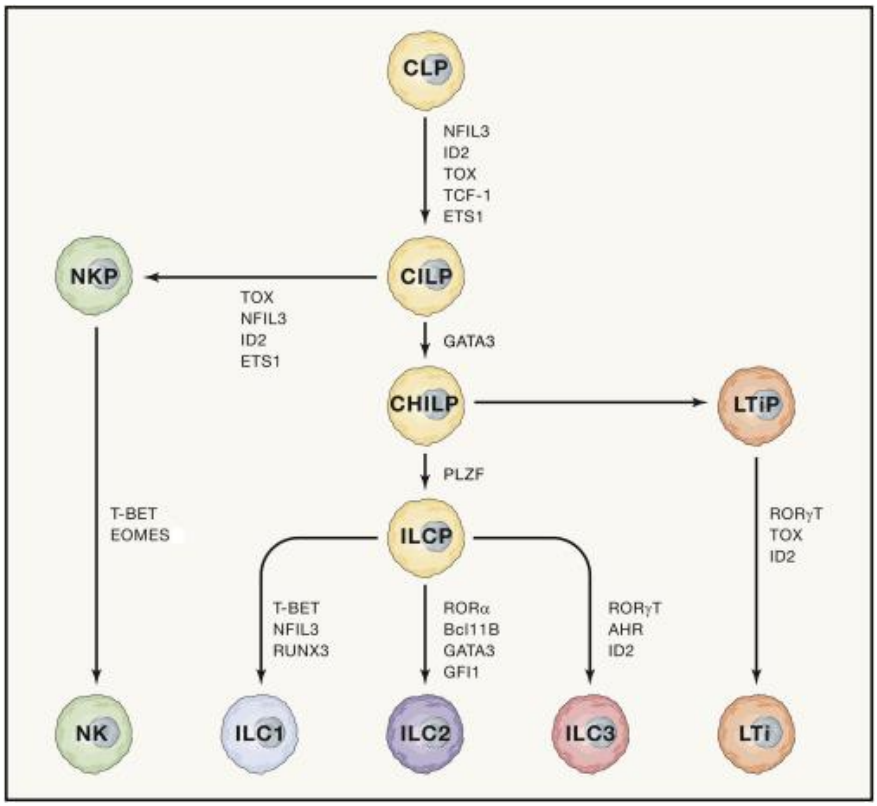

Figure 1.1 - Development lineages of NK cells, ILC1s, ILC2s, ILC3s and LTis. Names on the arrow show transcription factors expressed during the development. CLP - common lymphoid progenitor, CILP -common ILC progenitor, CHILP - common helper-like ILC progenitor, NKP - NK progenitor, LTiP - LTi progenitor. Image adapted from (Vivier et al., 2018).

NK cells are circulating, while ILC1s, ILC2s, ILC3s, and LTi cells are tissue-resident. NK cells are cytotoxic cells that kill pathogen-infected cells or transformed cells like tumor cells through granzyme and perforin. Besides, NK cells can produce an abundant amount of IFN-γ upon activation. NK cells can recognize and eliminate infected cells or transformed cells that downregulate MHC I, a concept known as the 'missing-self recognition' (Karre, Ljunggren, Piontek, & Kiessling, 1986; Ljunggren & Karre, 1990). All nucleated cells express high levels of MHC I in steady-state, and MHC I engages Ly49 receptors to inhibit NK cell activity in mouse (Karlhofer, Ribaudo, & Yokoyama, 1992), or Killer Ig-Like Receptors (KIRs) in human (Pende et al., 2019). When aberrant cells downregulate or lose MHC I, NK cells recognize them as 'foreign', unleashing their cytotoxic potential to eliminate the harmful cells (Karre et al., 1986). Thus, NK cells distinguish healthy cells from unhealthy cells through MHC I expression.

Despite having different progenitors, ILC1s resemble NK cells in their ability to produce high levels of IFN-γ upon stimulation with IL-12 and IL-18 (Ebbo, Crinier, Vely, & Vivier, 2017). However, ILC1s were also

reported to produce more granulocyte-macrophage colony-stimulating factor (GM-CSF) than NK cells. ILC1s are not thought to be 'cytotoxic', in the sense that they do not kill target cells via granzyme and perforin. However, ILC1s can also exert other modes of cytotoxicity through death receptor. The identification of bona-fide NK cells and ILC1s is difficult, as they express many similar surface proteins. In mouse, NK cells and ILC1s both express NK1.1 and NKp46. NK cells can be identified using Eomes, the transcription factor. However, it has been reported that Eomes can be downregulated on NK cells in the tumor microenvironment, and these NK cells acquired an ILC1-like phenotype (Y. Gao et al., 2017). Furthermore, as activated NK cells can start to express markers that are usually only expressed by ILC1s in steady-state, this makes it difficult to distinguish NK cells and ILC1s in diseases.

ILC2s produce type 2 cytokines, including IL-4, IL-5, and IL-13, upon stimulation with IL-25, IL-33 or thymic stromal lymphopoeitin (TSLP)(Vivier et al., 2018). They express GATA3 transcription factor, which is required for their development. In addition, they also can be identified via surface proteins including ST2 (IL-33R), KLRG1, CD25 and CRTH2.

Although derived from a different progenitor, ILC3s and LTi cells produce type 3 cytokines including IL-17 and IL-22, upon stimulation with IL-23 and IL-1β (Ebbo et al., 2017). Both express the RORγt transcription factor, which is indispensable for their development. In mouse, ILC3s can be separated into two subsets based on natural cytotoxicity receptor (NCR) expression: NKp46 -expressing ILC3s are called NCR^+ ILC3s, while the other subset is called NCR^- ILC3s. LTi cells do not express NCRs, but express c-Kit and CCR6. As both NCR^- ILC3s and LTi cells do not express NCR, identification between these two cell subsets remains challenging.

3.2.2 Receptor activation

NK cells express many activating and inhibitory receptors, which dictate the overall NK cell functions. If activating receptors receive more signals than inhibitory receptors, this would lead to NK activation, and vice versa. Moreover, ILC1s express activating and inhibitory receptors with NK cells. Here, I would mainly focus on four activating receptors/ligands: DNAM-1, TRAIL (ligand), NKG2D, and NKp46 (Table 1).

DNAX Accessory Molecule-1 (DNAM-1/CD226) was first described as an adhesion molecule, which played a crucial role in cytotoxicity and cytokine production of NK cells (Chan et al., 2010; Shibuya et al., 1996). The two identified ligands of DNAM-1 are CD155 (Poliovirus receptor, PVR) and CD112 (Nectin-2), which were frequently observed in various solid and lymphoid tumors (de Andrade, Smyth, & Martinet,

2014; Pende et al., 2005). It was reported that DNAM-1^+ NK cells produced higher amount of IFN-γ and exhibit more cytotoxicity against liver metastases than DNAM-1^- NK cells (Martinet et al., 2015). Accordingly, DNAM-1-deficient mice had increased tumor growth in a NK cell-sensitive tumor model, showing the importance of DNAM-1 on NK cell in eliminating tumor cells (Iguchi-Manaka et al., 2008). Interestingly, ILC1s express a higher amount of DNAM-1 in steady-state compared to NK cells, suggesting a potential function of DNAM-1 on ILC1s cells (Nabekura, Riggan, Hildreth, O'Sullivan, & Shibuya, 2020; Romero-Suarez et al., 2019). In liver disease, DNAM-1 on ILC1s was involved in IFN-γ production, which protected the mice from carbon tetrachloride (CCl_4)-induced acute liver injury. Thus, DNAM-1 apparently plays a similar role in both NK cells and ILC1s, as DNAM-1 activation leads to IFN-γ production. Nevertheless, whether DNAM-1engagement on ILC1s can lead to cytotoxicity against tumors, as observed in NK cells, would require more investigation.

Tumor necrosis factor-related apoptosis-inducing ligand (TRAIL), triggers programmed cell death, or apoptosis. TRAIL recognizes two receptors, TRAIL receptor 1/death receptor 1(TRAILR1/DR1) and TRAIL receptor 2/death receptor 2 (TRAILR2/DR2)(Schneider et al., 1997). Cancer cells are shown to express both TRAIL-R1 and TRAIL-R2. However, the mutation of TRAIL-R1 and TRAIL-R2 can lead to less apoptosis in tumor cells, associated with frequent metastasis (Shin et al., 2001). A subset of liver NK cells was shown to express TRAIL in steady-state, and these TRAIL-expressing NK cells can limit liver cancer metastases(Takeda et al., 2005; Takeda et al., 2001)}(Smyth et al., 2001). However, these studies were conducted before the discovery of ILC1s. It has now been discovered that liver ILC1s expressed TRAIL in steady-state, rather than NK cells (Robinette et al., 2015; Zhou et al., 2019). Therefore, more studies are warranted to pinpoint the role of TRAIL on NK cells versus ILC1s. In human NK cells, TRAIL was shown to play an important role in killing tumor cells (Zamai et al., 1998). Interestingly, NK cells were shown to first use Granzyme B (GzmB) to eliminate tumor cells, and switched to TRAIL as the main mechanism to perform sequential killing, indicating that NK cells exert distinct cytotoxicity modes in a temporal fashion (Prager et al., 2019).

NKG2D is a C-type lectin-like receptor first discovered in human NK cells in a library screen (Raulet, 2003). In mouse, NKG2D recognizes several ligands: Rae1, H60 and Mult1. In humans, NKG2D binds to MHC I Chain-related molecules A and B (MICA & MICB) and UL16 binding proteins (Dhar & Wu, 2018). Healthy cells usually do not express NKG2D ligands in homeostasis, and they only upregulate the ligand expression during disease. Nevertheless, it was reported that blood endothelial cells (ECs) and lymphatic ECs in lymph nodes expressed Rae-1 and desensitized NK cell activity in steady-state (Thompson et al., 2017). In disease, murine tumor models have shown the essential role of NKG2D on NK cells in restricting tumor growth

(Cerwenka, Baron, & Lanier, 2001; Diefenbach, Jensen, Jamieson, & Raulet, 2001). Although tumor cells can express NKG2D ligands, they frequently shed them to evade immune responses (Dhar & Wu, 2018). Elevated amounts of circulating soluble NKG2D ligands have been correlated with poor prognosis in various tumor malignancies (Lee, Lee, Kim, & Heo, 2004). Furthermore, a high plasma TGF-β concentration correlated with a decreased surface NKG2D expression on NK cells in cancer patients The authors showed that incubation with plasma samples from the cancer patients downregulated NKG2D on NK cells in a TGF-β-dependent manner, resulting in impaired cytotoxicity. These studies have demonstrated the importance of NKG2D on NK cells in cancers. While ILC1s also express NKG2D, its role remains unclear (Daussy et al., 2014; Klose et al., 2014).

NKp46, or NCR1, was first discovered as an activating receptor that was expressed by NK cells (Sivori et al., 1997). With the identification of the ILC family, it is now known that ILC1s and a subset of mouse ILC3s also express NKp46 (Vivier et al., 2018). Thus far, NKp46 has been demonstrated to bind different ligands of foreign pathogens, including influenza hemagglutinins, vimentin of *M. tuberculosis*, bacterial ligands, parasitic ligands and fungal ligands (Barrow, Martin, & Colonna, 2019). Some unknown ligands of NKp46 on tumor cells, which triggered NK cell cytotoxicity were also described (Glasner et al., 2012). A few years ago, complement factor P was discovered as a soluble ligand of NKp46 (Narni-Mancinelli et al., 2017). However, whether NKp46 has any membrane bound ligand still remains unclear. NKp46 is an essential activating receptor, as cross-linking NKp46 on NK cells *in vitro* triggered both IFN-γ production and cytotoxic functions. Indeed, NKp46 was required for preventing tumor growth and metastases, as revealed using NKp46-deficient mice (Glasner et al., 2012; Halfteck et al., 2009). Moreover, NKp46 was also crucial for fighting against various bacteria and viral infections (Barrow et al., 2019; Mandelboim et al., 2001). NKp46 was not involved in the IL-22 production of NCR^+ ILC3s during *Citrobacter rodentium* infection (Satoh-Takayama et al., 2009).

Table 1. Activating receptors and ligands expressed on NK cells and ILC1s

Receptors	**Ligands in mouse**	**Ligands in human**
DNAM-1 / CD226	CD155 (PVR), CD112 (Nectin-2)	CD155 (PVR), CD112 (Nectin-2)
TRAILR1 & TRAILR2	TRAIL	TRAIL
NKG2D	Rae1, H60, MULT1	MICA, MICB, ULBP1-6
NKp46	Various bacterial, viral, fungal ligands, Complement P, unknown tumor ligands	

3.3 Adaptive lymphocytes

3.3.1 Naïve T cells

Naïve T cells are T cells that has never encountered antigens. They develop in the thymus from T cell precursors, also known as thymocytes. The naïve T cell development is crucial, as inappropriate T cell development will result in autoimmune diseases. Therefore, the differentiation process from thymocytes to mature naïve T cells is strictly regulated.

In general, there are three stages for the development of mature naïve T cells. The first stage is double negative (DN) stage. It is called as DN stage as thymocytes (T cell precursors) do not express CD4 and CD8. The DN stage occurs in the thymic cortex. During this stage, RAG recombinase catalyzes V(D)J recombination forming a functional αβ T cell receptor (TCR) (Gellert, 2002). Thymocytes that do not form functional TCRs are eliminated by apoptosis. This process is known as the beta-selection checkpoint (Carpenter & Bosselut, 2010).

After the DN stage, thymocytes that express T cell receptors enter the positive selection stage. At this stage, thymocytes upregulate both CD4 and CD8, which are called double positive (DP) T cells. Cortical thymic epithelial cells (cTECs) serve as the APCs that present peptides in the form of MHC I and MHC II to DP T cells. DP T cells engage either MHC I with CD8, or MHC II with CD4, becoming single positive (SP) $CD4^+$ or $CD8^+$ T cells. DP T cells that cannot bind to MHC I or MHC II undergo apoptosis. This process is called positive selection because only T cells that can bind to MHC I or MHC II will be selected for further development (Germain, 2002).

Subsequently, the selected T cells enter the thymic medulla to finish their development. This stage is known as the negative selection stage. Medullary thymic epithelial cells (mTECs) serve as the APCs that present self-antigens from all parts of the body in the context of MHC I or MHC II. $CD4^+$ and $CD8^+$ T cells that bind strongly to the presented self-antigens are recognized as 'autoreactive T cells', and undergo apoptosis (Takaba & Takayanagi, 2017). This prevents self-reactive T cells from entering periphery, which will cause autoimmunity. Thus, non-self-reactive naïve $CD4^+$ or $CD8^+$ T cells are selected, and exit thymus as mature naïve $CD4^+$ or $CD8^+$ T cells. Naïve T cells express CD62L, which directs them to secondary lymphoid organs (SLOs), such as lymph nodes and spleens, where they can be activated by mature professional APCs during pathogen infections (Kumar, Connors, & Farber, 2018; Weinreich & Hogquist, 2008).

3.3.2 T helper cells and cytotoxic T cells

T cells can be subdivided into two major subsets: $CD4^+$ T cells and $CD8^+$ T cells. The activation of naïve $CD4^+$ and $CD8^+$ T cells requires three stimuli: TCR, CD28, and cytokines (Curtsinger & Mescher, 2010; Mondino, Khoruts, & Jenkins, 1996). $CD4^+$ and $CD8^+$ T cells bind to MHC II and MHC I, respectively. CD28 is an activating receptor binding to CD80 (B7-1) and CD86 (B7-2), which are the co-stimulatory molecules expressed by professional APCs. When receiving TCR (signal 1) and CD28 activation (signal 2), naïve $CD4^+$ and $CD8^+$ T cells can proliferate and secrete IL-2 for autocrine usage and survival. At this stage, $CD4^+$ and $CD8^+$ T cells also require inflammatory cytokines (signal 3) to differentiate into functional effector T cells. $CD4^+$ T cell require cytokines depending on polarizing conditions, while $CD8^+$ T cells required IL-12 with Type I (IFN α/β) or Type II IFN (IFN γ) for the differentiation (Curtsinger & Mescher, 2010; Curtsinger et al., 1999; Haring, Badovinac, & Harty, 2006). The activation process of naïve T cells usually takes place in SLOs, such as lymph nodes and spleen. Immature dendritic cells in the local tissues take up antigens, then migrate to SLOs, and complete their maturation. Mature dendritic cells present antigen to $CD4^+$ and $CD8^+$ in the context of MHC, priming them to become effector T cells (Alvarez, Vollmann, & von Andrian, 2008). Once activated, effector $CD4^+$ and $CD8^+$ T cells downregulate CD62L, which allows them to exit to SLO and migrate to peripheral tissues to exert their effector functions (Masopust & Schenkel, 2013).

Activated and differentiated $CD4^+$ T cells are known as T helper (T_h) cells, as they 'help' the functions of other immune cells by producing cytokines after differentiation. There are three main outcomes for $CD4^+$ T helper cells after activation: Th1, Th2, and Th17. The cells were named based on the cytokines that they produced after activation and polarization. For instance, Th1 cells produce type 1 cytokines, such as IFN-γ upon polarization with IL-12, and express the Tbet transcription factor. Th1 immunity is important for eliminating intracellular bacteria and viruses. Th2 cells secrete type 2 cytokines, like IL-4, IL-5, and IL-13, upon polarization with IL-4, and they express GATA3 transcription factor. Th2 cytokines are crucial for allergic responses and fighting helminth infections. Th17 cells produce type 3 cytokines, including IL-17 and IL-22 upon polarization with TGF-β and IL-6, and express the RORγt transcription factor. Th17 immunity is involved in combating fungi and extracellular bacteria infection, as well as in autoimmunity (Fig. 1.2). Depending on the tissue microenvironment, different Th cells are enriched in distinct organ in steady-state. For example, Th2 cells are enriched in lungs and skin, while Th17 cells are found in gut (Huang, Wang, & Chi, 2012). Functionally, Th1, Th2 and Th17 cells are the adaptive counterpart of ILC1s, ILC2s, and ILC3s, as they produce similar cytokines and express the same sets of transcription factors.

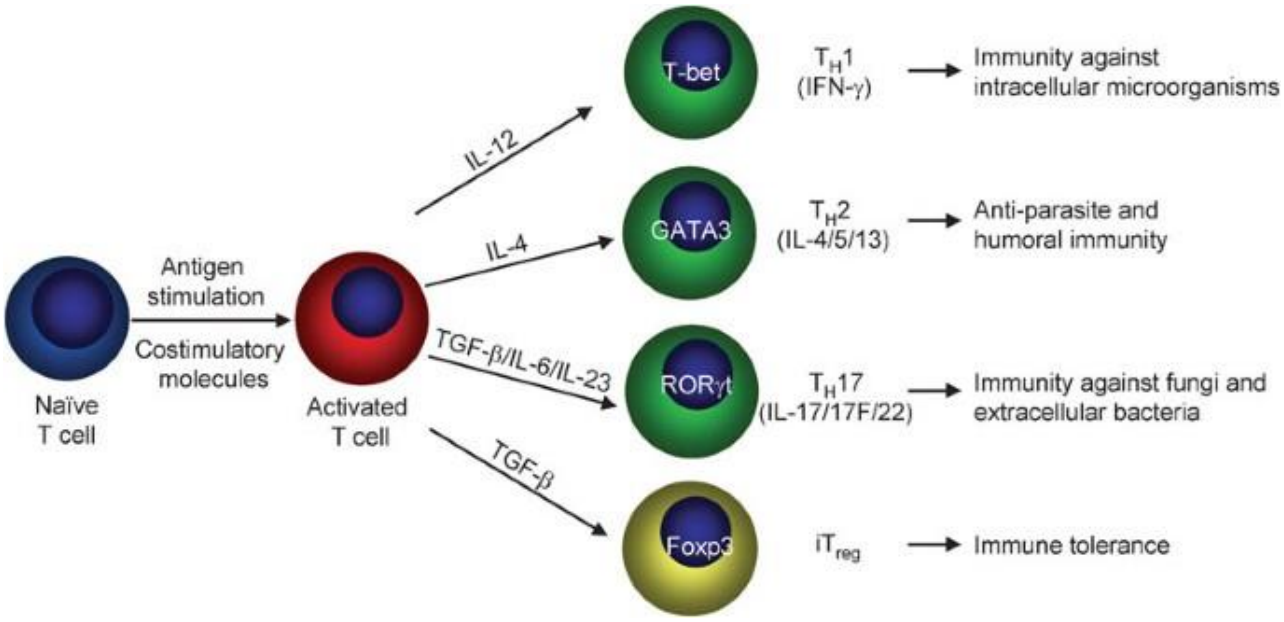

Figure 1.2 - Naïve $CD4^+$ T cell differentiation in depicted polarizing conditions and their functional roles. Th - helper T, iTreg - induced regulatory T cells. Figure adapted from (Huang et al., 2012).

Activated and differentiated $CD8^+$ T cells are known as cytotoxic T cells, as they perform cytotoxic functions against infected cells or cancer cells. $CD8^+$ T cells recognize antigens in the context of MHC I, which is expressed by all nucleated cells. Once $CD8^+$ T cells are activated in SLOs, they move to peripheral tissues to exert their functions. These effector $CD8^+$ T cells identify foreign antigens presented by infected cells, eliminating them with perforin and granzyme (Martinez-Lostao, Anel, & Pardo, 2015). Moreover, effector $CD8^+$ T cells also produce high amounts of IFN-γ and TNF-α that assist in their effector functions (Seder & Ahmed, 2003). They express Eomes and Tbet transcription factors (Pearce et al., 2003). Functionally, $CD8^+$ cytotoxic T cells are the adaptive counterpart of NK cells, as both of them produce similar cytokines and express similar transcription factors.

Taken together, $CD4^+$ and $CD8^+$ T cells mirror NK cells and ILC1s in various aspects, forming the adaptive arm of the innate lymphocytes (Fig. 1.3).

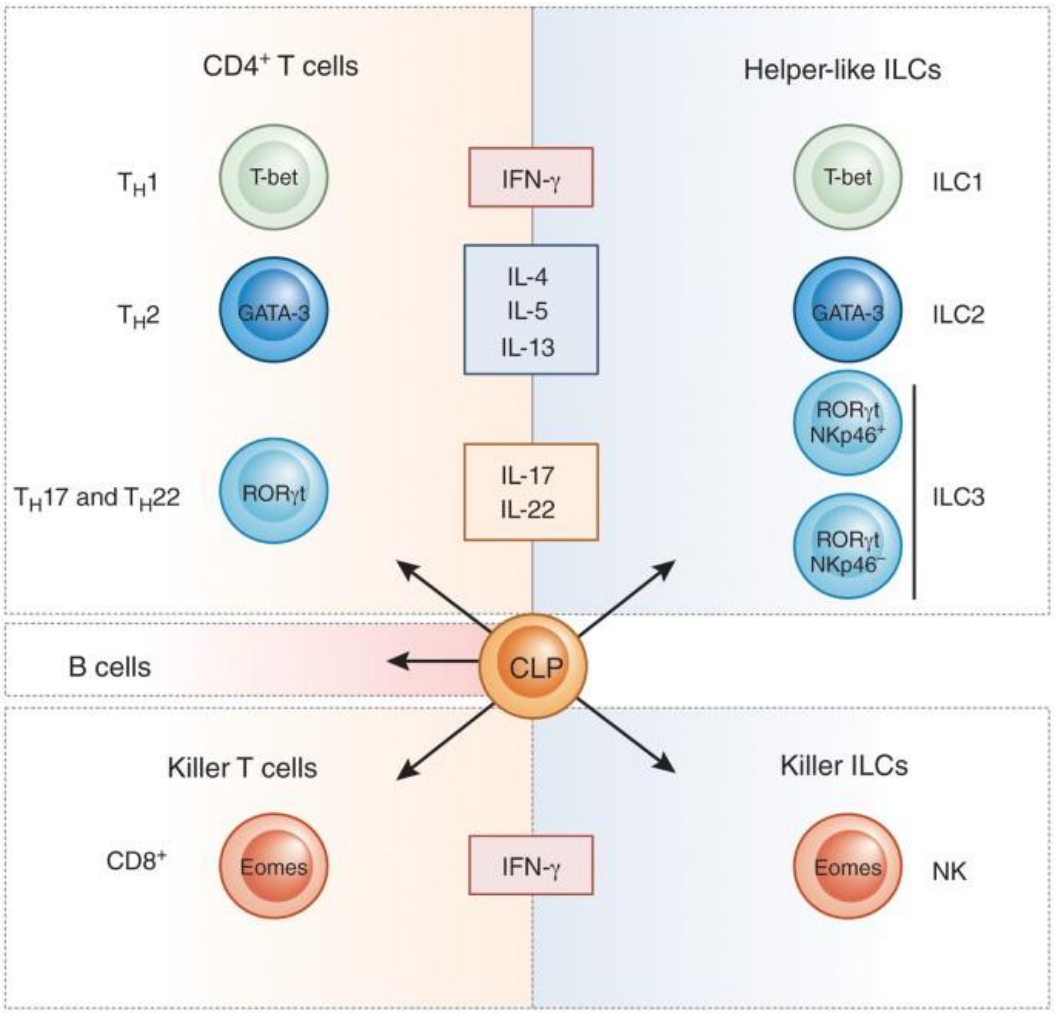

Figure 1.3 - NK cells and ILCs constitute the innate counterpart of effector $CD4^+$ and $CD8^+$ T cells. Transcription factor expressed are shown inside the circle (T-bet, GATA-3, RORγt and Eomes), and cytokine produced are shown inside the square (IFN-γ, IL-4, -5, -13, -17 and -22). CLP - common lymphoid progenitor. Image adapted from (Eberl, Di Santo, & Vivier, 2015).

3.3.3 Memory T cells

Memory T cells are antigen-specific T cells which can persist for years. Their differentiation is still controversial, with two models being proposed (Henning, Roychoudhuri, & Restifo, 2018). Circular model suggests that naïve T cells first differentiate into effector T cells (Fig. 1.4). After the infection is gone, most effector T cells die and some will become memory T cells. The memory T cells can differentiate into effector T cells again when they encounter the same antigen, and this cycle continues again. On the other hand, linear model suggests that depending on the strength and extent of antigen stimulation, naïve T cells differentiate into either effector T cells or memory T cells. During the differentiation process, naïve T cells

that repeatedly encounter strong antigen signal will differentiate into terminal effector stage, while those who receive weak antigen signal will stop at the intermediary memory stage. Therefore, in the beginning of the infection, there is always a large pool of effector T cells due to strong antigen stimulation. Once the infection subsides, those effector T cells die, leaving a small pool of memory T cells, which do not receive enough stimuli to fully differentiate into effector T cells (Henning et al., 2018).

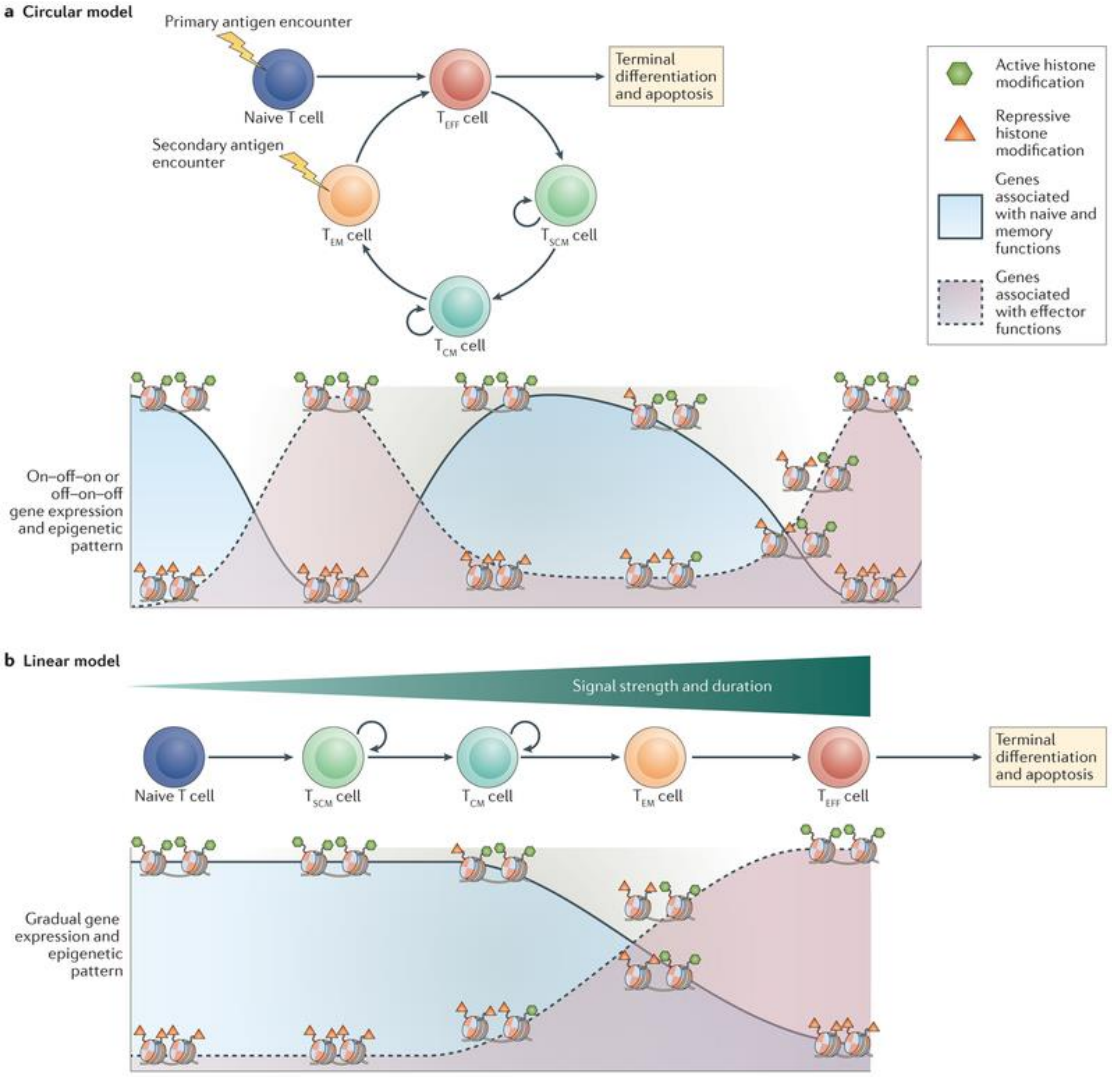

Fig. 1.4 - Two models of memory T cell differentiation: the circular model (a) and the linear model (b). T_{EFF} - effector T cell, T_{SCM} - stem cell memory T cell, T_{CM} - central memory T cell. Image adapted from (Henning et al., 2018).

Regardless of the model for the differentiation, memory T cells can react to pathogenic insult in an immediate manner. There seems to be controversy whether reactivation of memory T cells require priming by professional APCs (Berard & Tough, 2002; Zammit, Cauley, Pham, & Lefrancois, 2005). It was recently reported that circulating memory T cells required licensing from professional APCs, while tissue-resident

memory T cells can be reactivated by non-professional APCs (Low et al., 2020). Therefore, it would be crucial to distinguish between circulating and tissue-resident memory T cells due to their different requirements for reactivation.

There are two major subsets of circulating memory T cells, which are central memory T cells (T_{CM}) and effector memory T cells (T_{EM}) (Sallusto, Lenig, Forster, Lipp, & Lanzavecchia, 1999). T_{CM} can be distinguished from T_{EM} by the expression of CD62L and CCR7, which are two homing markers to SLOs. Thus, T_{CM} are enriched in SLOs, while T_{EM} are found in peripheral tissues (Sallusto, Geginat, & Lanzavecchia, 2004). Wherry et al. demonstrated that T_{EM} was an intermediate cell type that can subsequently differentiate into T_{CM} after infection subsided (Wherry et al., 2003). Thus, T_{CM} were considered the 'real' memory T cells, as they could self-renew and persist in homeostasis, and grant better protection with higher proliferative capacity upon secondary infection (Wherry et al., 2003). It was proposed that T_{EM} are first activated and confront foreign pathogens in the tissues, while T_{CM} are activated later in SLOs and act as the source to replenish T_{EM} in the tissues (Roberts, Ely, & Woodland, 2005; Sallusto et al., 2004). Therefore, T_{EM} and T_{CM} synergistically work together against re-exposure to same foreign invaders.

3.3.4 Regulatory T cells

Regulatory T cells (Treg) suppress activated T cell functions and play a crucial role in immune tolerance, autoimmune diseases and cancer. Treg can either develop in the thymus or can be induced in the peripheral organs. Treg which develop in the thymus are called thymic Treg or natural Treg (nTreg), while those that develop in the peripheral organs are named induced Treg (iTreg). Treg are $CD4^+$ T cells that express CD25 in steady-state. Sakaguchi et al first discovered that adoptive transfer of $CD4^+CD25^+$ T cells prevented autoimmune diseases in athymic nude mice, suggesting an immunosuppressive function of this population (Sakaguchi, Sakaguchi, Asano, Itoh, & Toda, 1995). Later, the transcription factor FoxP3 was identified to be expressed only by $CD4^+CD25^+$ T cells. FoxP3-deficient mice died within 4 weeks after birth due to defective Treg development, which resulted in lymphoproliferative autoimmune diseases (Fontenot, Gavin, & Rudensky, 2017). While Foxp3 is now often used as the transcription factor to identify Treg, iTreg in periphery also include type 1 regulatory cells (Tr1) and T helper 3 cells (Th3 cells), which do not express FoxP3, but still exert immunosuppressive functions (Fig 1.5) (Curotto de Lafaille & Lafaille, 2009). Hence, the identification of Treg based on FoxP3 alone might be insufficient. Several markers were identified to distinguish nTreg from iTreg. For instance, Neuropilin1 and Helios were demonstrated to be expressed by nTreg, but not iTreg (Weiss et al., 2012; Yadav et al., 2012).

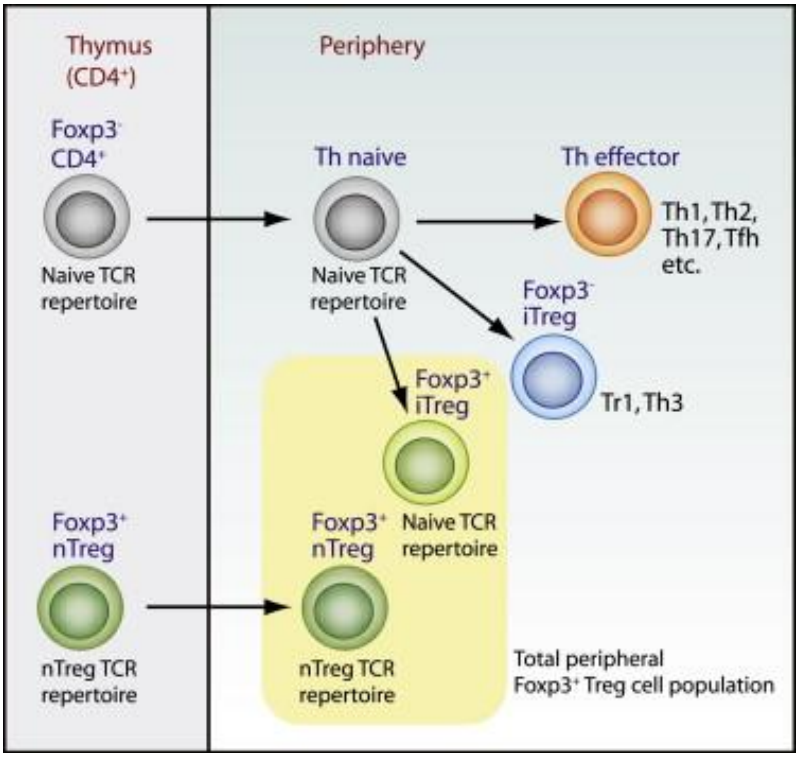

Fig 1.5 - Thymic-derived natural Treg (nTreg) and peripheral-induced Treg (iTreg) and their developmental sites. TCR - T cell receptor, Th - helper T, Tr1 - type 1 regulatory cells, Th3 - T helper 3 cells. Image adapted from (Curotto de Lafaille & Lafaille, 2009).

Treg achieve their immunoregulatory functions through various mechanisms. Treg can produce IL-10, TGF-β, and IL-35, which are immunosuppressive cytokines that can dampen effector functions of other immune cells(Sakaguchi, Wing, Onishi, Prieto-Martin, & Yamaguchi, 2009). They also express CD39 and CD73, which are involved in the hydrolysis of extracellular ATP/ADP to AMP and adenosine. Treg were demonstrated to utilize these ectoenyzmes to generate adenosine, which is known to be immunosuppressive (Deaglio et al., 2007). Other than soluble factors, Treg can also inhibit immune cell functions through their surface molecules. One of the important surface molecules is cytotoxic T-lymphocyte-associated protein 4 (CTLA-4), which is a co-inbibitory molecule that binds CD80 and CD86 on professional APCs. Treg constitutively express CTLA-4, allowing them to compete with naïve T cells for CD80/CD86 engagement, which eventually restricts naïve T cell activation (Schmidt, Oberle, & Krammer, 2012). Moreover, CTLA-4-expressing cells were shown to capture CD80/CD86 from APCs, a process known as trans-endocytosis or trogocytosis (Qureshi et al., 2011). Furthermore, it was also reported that CTLA-4 can exist as the soluble form resulting from alternative splicing, which could also bind CD80/86 (Ueda et al., 2003). Therefore, through various modes, Treg can limit the accessibility of CD80/86 on APCs to naïve T cells for their

optimal activation. Apart from acting through professional APCs, Treg can also limit the activation of naive T cells by sequestering IL-2 and calcium level (Fig. 1.6) (Schmidt et al., 2012).

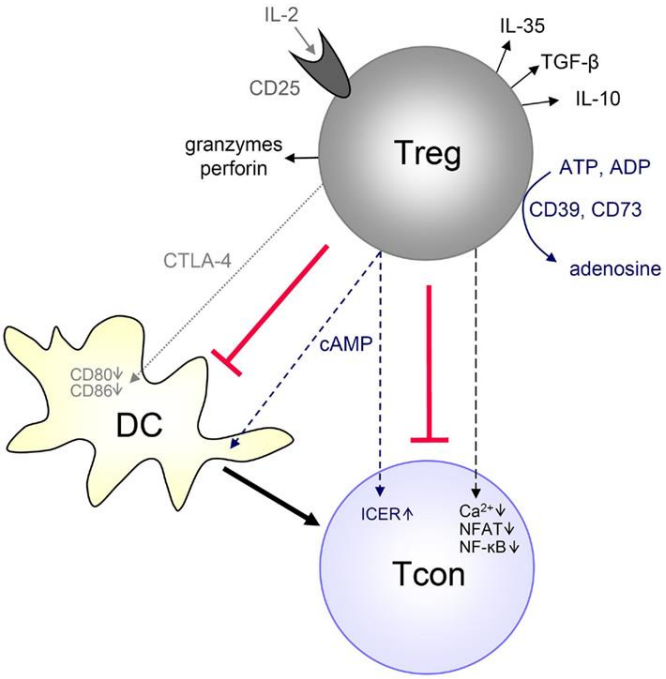

Fig. 1.6 - Different mechanisms of Treg in exerting immunosuppressive functions. Treg - regulatory T cells, DC - dendritic cells, Tcon - conventional T cells. Image adapted from (Schmidt et al., 2012).

3.4 The vascular system

3.4.1 Endothelial cells

Endothelial cells form the inner layer of blood and lymphatic vessels, which connect the whole body. They generate intricate blood and lymphatic vessels throughout the whole body during embroyonic development, a process known as angiogenesis. Endothelial cells play irreplaceable role in transporting gases, nutrients, blood, lymph, and waste. There are five major types of blood vessels: arteries, arteriole, capillaries, venules, and veins (Fig. 1.7). Perhaps the most important function of endothelial cells is to deliver oxygen to the whole body, which is required for every cell for its respiration and metabolic functions. In this aspect, arteries carry oxygenated blood from the heart, and branch into arterioles in the tissues, which further extend into a wide capillary network. Capillaries are the smallest blood vessels in the tissues, thus facilitating exchanges of substances between endothelial cells and tissues. Capillaries merge into venules, transporting deoxygenated blood containing waste. Venules integrate into veins, which transport deoxygenated blood back to heart. Gas, nutrient, and waste in blood diffuse to the interstitial fluid, which surrounds the cells in the tissues. Interstitial fluids form at the arterial end of capillaries, as the higher pressure in arteries drives the fluid out of permeable capillaries into tissues. Most of the interstitial fluid flows back into the blood at the venous end of the capillaries due to the lower pressure of veins. However, the remaining interstitial fluid is recycled as lymph by lymphatic capillaries and vessels back to the lymph nodes, and subclavian veins, where the lymph and blood mix again (Potente & Makinen, 2017).

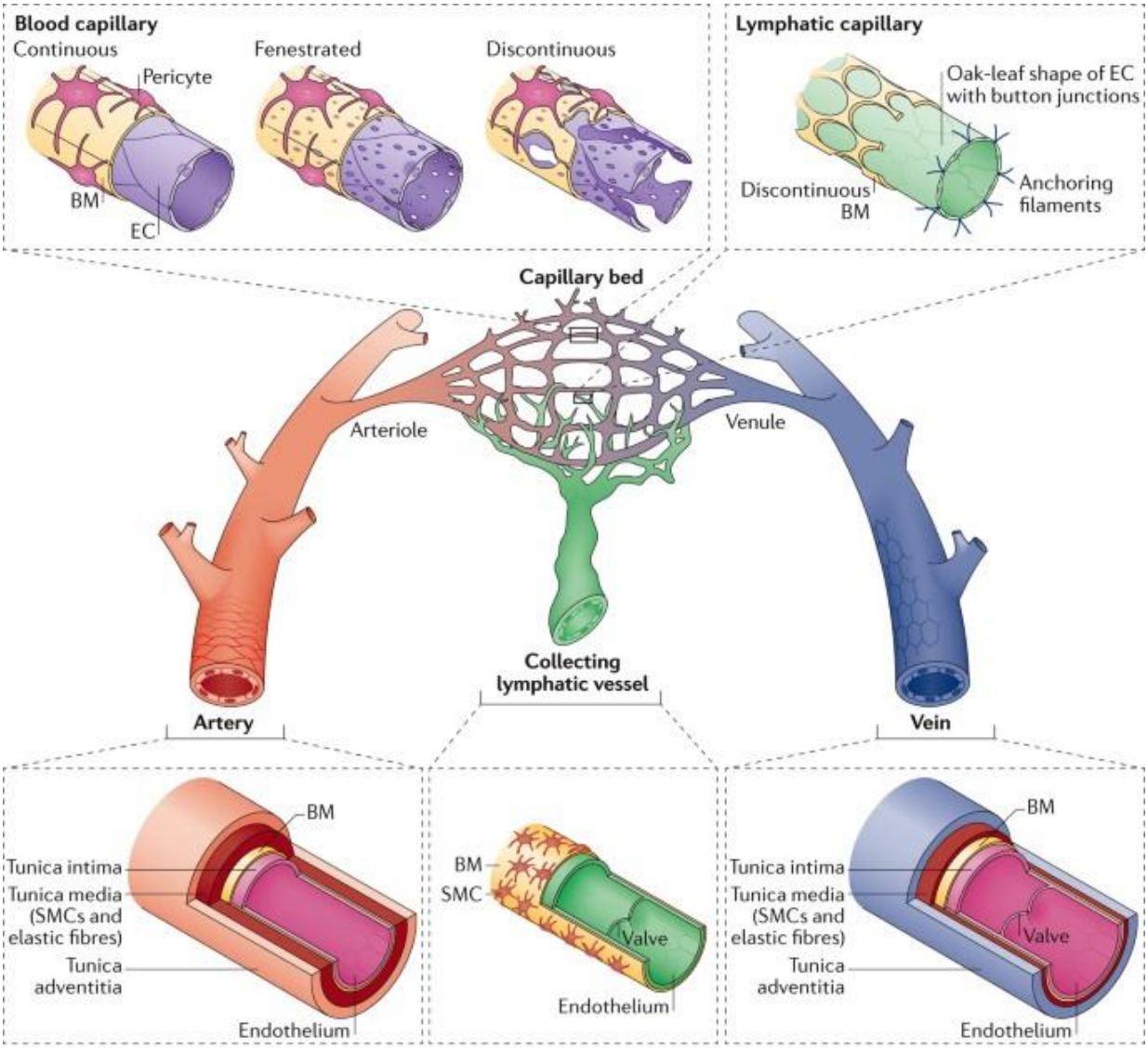

Figure 1.7 - Different types and sizes of blood vessels formed by endothelial cells: artery, arteriole, capillary, venule, and vein. There are three main types of blood capillaries: continuous, fenestrated, and discontinuous. Capillaries are the smallest blood vessels, connecting arteriole and venule. Artery and vein are the largest blood vessels, transporting blood from and to heart, respectively. Lymphatic capillary contains button-like junction and transports lymph across the body. BM - basement membrane, SMCs - smooth muscle cells, EC - endothelial cells. In red - oxygenated blood, in blue - deoxygenated blood. In green - lymph. Image adapted from (Potente & Makinen, 2017).

Endothelial cells can form the three main structures in capillaries: continuous, fenestrated, and sinusoidal. Continuous capillaries are formed if endothelial cells form tight junctions with each other without gaps in between cells. They are found in lung, skin, and heart. Fenestrated capillaries are similar to continuous capillaries, but endothelial cells possess small holes that allows small molecules to diffuse out directly. However, there is a network of diaphragm fibrils radiating out from the center of fenestrae, which largely

limits diffusion of large molecules (Bearer, Orci, & Sors, 1985; Stan, 2007). Fenestrated capillaries are found in intestine and kidneys. Sinusoidal capillaries are formed when endothelial cells do not connect via tight junction with each other, forming discontinuous structure. At the same time, they are fenestrated, and do not have diaphragm and organized basement membrane. This unique structure allows the diffusion of molecules directly through the fenestrae, which could facilitate material exchange. Sinusoidal capillaries are only found in liver, bone marrow, and spleen (Cleaver & Melton, 2003).

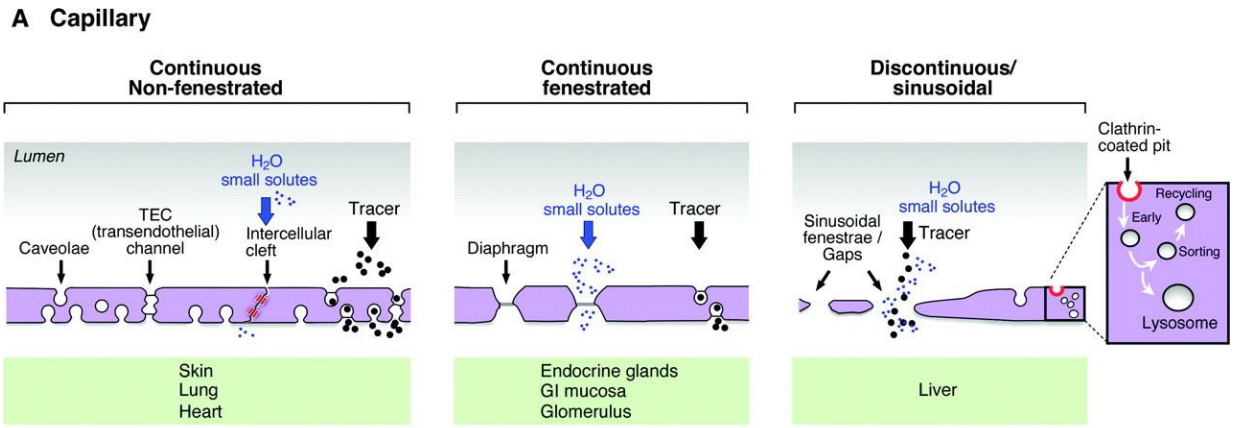

Figure 1.8 - Three types of capillaries formed by endothelial cells (ECs). ECs in continuous and non-fenestrated capillary form tight junction. ECs in fenestrated capillary contain fenestrate or small holes that allow the diffusion of small solutes. ECs in discontinuous or sinusoidal capillaries do not have diaphgram and complete basement membrane, allowing diffusion of small solutes directly to the local tissue. Image adapted from (Aird, 2007).

3.4.2 Role of endothelial cells in immune system

Endothelial cells function as an important mediator in immunology, as blood contains circulating leukocytes, including lymphocytes, neutrophils, and monocytes. Endothelial cells also play an active role in recruiting immune cells during tissue inflammation or injury. The process of endothelial cells recruiting leukocytes and transporting them across the blood vessels into local tissue is known as leucocyte transendothelial migration, which has been very extensively studied. The five main steps are capturing, rolling, arresting, crawling, and extravasating (Fig. 1.9). During tissue inflammation or injury, endothelial cells are activated by local inflammatory cytokines. This results in the upregulation of adhesion surface molecules, including P-selectin, E-selectin, intracellular adhesion molecule 1 and 2 (ICAM-1 and ICAM-2), and vascular cell adhesion protein (VCAM-1)(Schnoor, Alcaide, Voisin, & van Buul, 2015). The selectin family captures fast-flowing leukocytes in the bloodstream, slowing their speed, and allowing them to stay temporarily on the surface of endothelial cells, a process known as ‘rolling’. Leukocytes now are slowed down, and can further interact with ICAM-1, ICAM-2 and VCAM-1 upregulated by endothelial cells during tissue

inflammation and injury (Ley, Laudanna, Cybulsky, & Nourshargh, 2007). Concurrently, chemokines secreted by endothelial cells and other cells in the inflamed tissues also activate the leukocytes, leading to the 'arrest' of leukocytes on endothelial cells (Shamri et al., 2005). Now leukocytes adhered can 'crawl' to find a suitable endothelial junction to 'extravasate'. Leukocytes extravasate by squeezing themselves in a flat and elongated shape across endothelial layer, a process known as transendothelial migration or diapedesis. This can happen either in a paracellular or transcellular fashion. After that, leukocytes can further cross through the basement membrane and extracellular matrix in order to reach the local tissue to perform their functions (Vestweber, 2015).

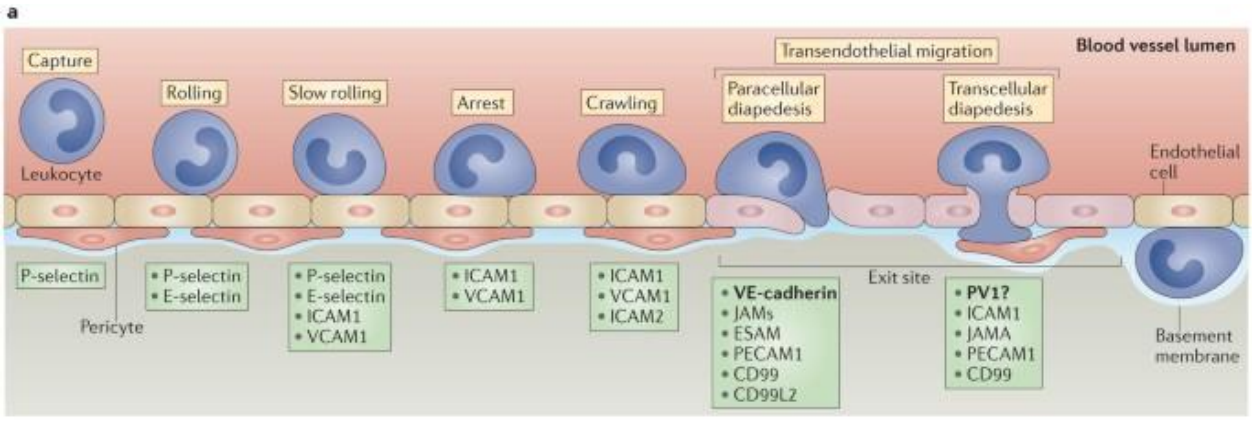

Figure 1.9 - Sequential events of leukocyte recruitment by endothelial cells during tissue inflammation. Five stages are involved: capture, rolling, arrest, crawling, and transendothelial migration. Selectins, ICAM, and VCAM, upregulated by ECs during inflammation, are crucial for the capture, rolling, arrest, and crawling of leukocytes. After crawling, leukocytes find suitable endothelial junction to extravasate, either in a paracellular or transcellular manner. Image adapted from (Vestweber, 2015).

Apart from recruiting lymphocytes during inflammation and injury, endothelial cells have been reported to function as innate immune cells. Endothelial cells have been reported to express various TLRs, which are the sensors of PAMPs and DAMPs (Shao et al., 2020). Therefore, just like other innate immune cells, endothelial cells can be the first responder upon pathogenic insult or during disease, particularly in case of bloodborne pathogens or cancer metastases. Once activated through TLRs, ECs produce chemokines and cytokines, such as IL-1, IL-8 and monocyte-chemotatic protein-1 (MCP-1), which assist in recruiting more immune cells to the site of injury (Danese, Dejana, & Fiocchi, 2007). Furthermore, endothelial cells have been reported to express MHC II, which is usually expressed only by professional APCs (Abrahimi et al., 2016; Muczynski, Ekle, Coder, & Anderson, 2003; Rose, Coles, Griffin, Pomerance, & Yacoub, 1986). The functional role of MHC II on endothelial cells remains obscure, but one study showed that MHC II on endothelial cells was involved in graft-versus-host disease (Abrahimi et al., 2016). Interestingly, blood and lymphatic endothelial cells in lymph nodes can acquire MHC II from DCs in steady-state, a process known

as trogocytosis. MHC II on these lymph node stromal cells was shown to induce $CD4^+$ T cell deletion, pointing a possible tolerogenic role of MHC II on endothelial cells (Dubrot et al., 2014). In addition to MHC II, endothelial cells have been demonstrated to express many immune co-stimulatory molecules, including CD80, CD86, 4-1BB ligand (4-1BBL), inducible co-stimulator ligand (ICOSL), and OX40 ligand (OX40L), which are involved in T cell activation (Mai, Virtue, Shen, Wang, & Yang, 2013).

3.5 Liver

3.5.1 Liver architecture

Liver is the metabolic hub of the body. Hepatocytes are the parenchymal cells in the liver, and constitute around 80% of the liver volume and 70% of all cells (B. Gao, Jeong, & Tian, 2008). Around 70%-80% of the blood in the liver comes from the portal vein, which drains the blood from gastrointestinal tracts (Carneiro et al., 2019). Blood flows from the portal vein and hepatic artery through sinusoids, constructed by liver sinusoidal endothelial cells (LSECs), to hepatic central vein. LSECs are the most abundant non-parenchymal cells in the liver that constitute around 50% of non-parenchymal cells (Racanelli & Rehermann, 2006). Apart from LSECs, immune cells also form the major part of non-parenchymal cells. Tissue-resident immune cells, such as Kupffer cells and ILC1s, reside in the sinusoids, thus having close interactions with LSECs (Ducimetiere et al., 2021; Wilkinson, Qurashi, & Shetty, 2020). Other non-parenchymal cells include hepatic stellate cells, biliary cells, tissue resident T cells and circulating immune cells.

Liver consists of hexagonal lobules, with each vertex of the hexagon occupied by a portal triad, and the middle of the hexagon occupied by a hepatic central vein. This typical liver architecture is known as the 'classical' model (Fig. 1.10 a). A portal triad consists of a portal vein, hepatic artery, and bile duct. Apart from the 'classical' model, the 'acinus' model has also been proposed and widely used due to its functional relevance. The 'acinus' model proposed existence of different zones from portal triad to central vein. Zone 1 is the periportal area, closest to the portal triad; zone 2 is the midzone; and zone 3 is the pericentral area (Fig. 1.10 b). Therefore, a liver acinus is the smallest functional unit in the liver.

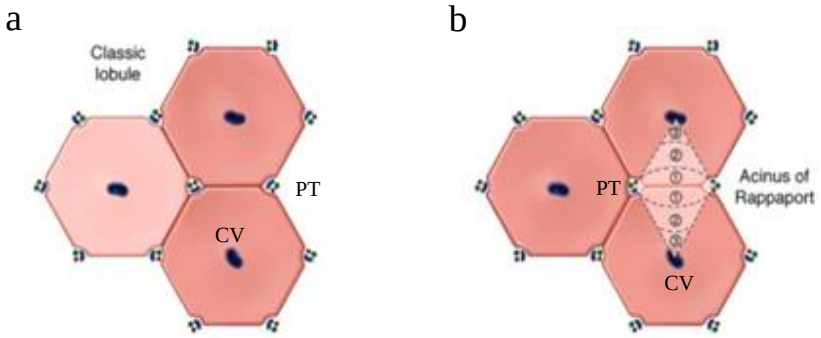

Figure 1.10 - Two models to illustrate liver architecture. a. The 'classical' model proposes the liver consists of a portal triad (PT) in each vertex of a hexagonal lobule, with the central vein (CV) in the middle. b. The 'acinus' model postulates the liver contains three zones. Zone 1 is the periportal area, Zone 2 is the midzone, and Zone 3 is the pericentral area. A liver acinus is the smallest functional unit of the liver. Image adapted from (C. Lau et al., 2021).

The ‘acinus’ model has been frequently applied because the liver is a zonated organ. Hepatocytes in periportal, midzonal, and pericentral regions perform distinct metabolic tasks due to the gradient of the oxygen concentration. The oxygen concentration is the highest near the portal vein, and gradually decreases to the lowest near the central vein (Fig. 1.11). Hepatocytes in the periportal region are involved in biochemical processes that require oxygen, such as β-oxidation and gluconeogenesis. On the other hand, hepatocytes in the pericentral region perform metabolic procedures including lipogenesis, ketogenesis, triglyceride synthesis, and glycolysis, which do not require so much oxygen. In addition, pericentral hepatocytes are enriched with Wnt target transcripts, which are indispensable for the development of liver zonation (Birchmeier, 2016). Due to metabolic zonation, hepatocytes from different regions have unique characteristics and can be identified with different markers. For instance, pericentral hepatocytes proximal to central vein express glutamine synthetase, while periportal hepatocytes express E-cadherin (Braeuning et al., 2006; Gebhardt, Baldysiak-Figiel, Krugel, Ueberham, & Gaunitz, 2007). Based on these unique markers expressed by hepatocytes in a spatial manner, liver biologists have been able to investigate and study the zonation pattern and its functional relevance in the liver.

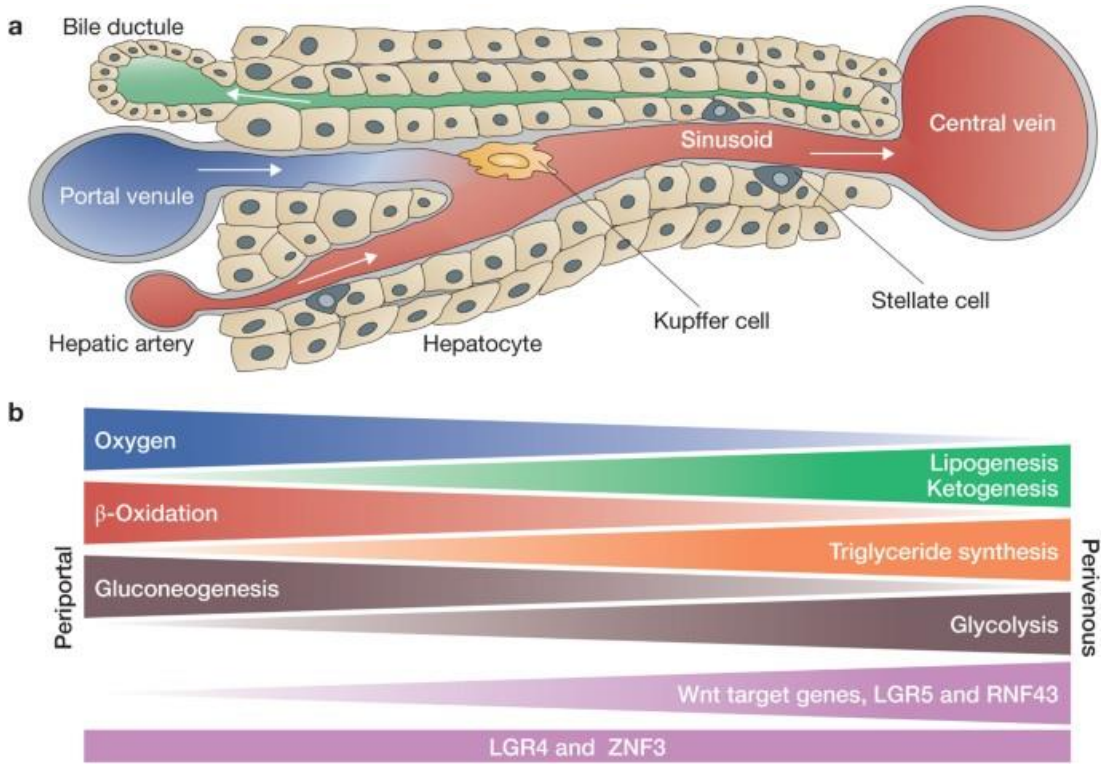

Figure 1.11 - Liver is a zonated organ. Metabolic functions and gene expressions are exerted in a spatial manner. Periportal and pericentral hepatocytes perform different metabolic tasks due to distinct oxygen concentration. Image adapted from (Birchmeier, 2016).

3.5.2 NK cells and ILC1s

In the mouse liver, there are two major subsets of innate lymphocytes: circulating NK cells and tissue-resident ILC1s. NK cells and ILC1s are enriched in the mouse liver compared to other organs, constituting around 5-10% of the total liver lymphocytes (Robinette et al., 2015; Tian, Chen, & Gao, 2013). Liver ILC1s reside in the sinusoids of the liver. In steady-state, liver ILC1s, but not NK cells, express CD49a (Peng et al., 2013). Other surface molecules were further identified to be exclusively expressed by liver ILC1s in steady-state, including CD200R, TRAIL, CXCR6 and PD-L1 (Daussy et al., 2014; Nabekura et al., 2020; Sojka et al., 2014; Zhou et al., 2019). Developmentally, liver ILC1s were distinct from NK cells, as ILC1s did not require Nfil3 nor Eomes, but required Tbet for the development (Seillet et al., 2014; Sojka et al., 2014). IFN-γ was recently revealed to be important for ILC1 development without affecting NK cells (Bai et al., 2021). Interestingly, livers from newborn mice were enriched with ILC1s, suggesting that ILC1s might play a crucial role in the liver development, and NK cells were only recruited postnatally (Daussy et al., 2014; Gordon et al., 2012). While both NK cells and ILC1s produced IFN-γ upon phorbol myristate acetate (PMA)/ionomycin stimulation, ILC1s in addition produced a higher amount of TNF-α and GM-CSF (Sojka et al., 2014).

The discovery that liver ILC1s expressed TRAIL in steady-state provided a new interpretation of papers that had been published before. For instance, a subset of liver NK cells was shown to express TRAIL and these TRAIL$^+$ NK cells limit liver metastases (Smyth et al., 2001; Takeda et al., 2005; Takeda et al., 2001). Moreover, activated liver TRAIL$^+$ NK cells were shown to kill syngeneic hepatocytes in vitro in a TRAIL-dependent manner (Ochi et al., 2004). The previously described TRAIL$^+$ NK cells most likely were ILC1s, and they were cytotoxic by utilizing TRAIL receptor. Interestingly, liver IL7Rα$^+$ ILC1s were found to be the precursors of more cytotoxic IL7Rα$^-$ ILC1s in steady-state (Friedrich et al., 2021). Apart from cytotoxicity, ILC1s were shown to have memory and mediate hapten-induced contact hypersensitivity (Peng et al., 2013). IL7Rα$^+$ ILC1s were recruited into lymph nodes and gained memory features after hapten sensitization. These memory IL7Rα$^+$ ILC1s resided in the liver and moved to skin-draining lymph nodes to mediate inflammation upon rechallenge (X. Wang et al., 2018).

NK cells play an essential role in the liver diseases due to their anti-fibrotic functions, achieved by killing activated hepatic stellate cells in a TRAIL-, FasL-, and NKG2D-dependent manner (Glassner et al., 2012; Melhem et al., 2006; Radaeva et al., 2006). NK cells were also demonstrated to cause liver injury due to their pro-inflammatory effector functions in several fulminant viral hepatitis murine models(B. Gao, Radaeva, & Park, 2009; Peng, Wisse, & Tian, 2016). Since the discovery of ILC1s, the relative contribution

of NK cells and ILC1s in liver metastases has become unclear. A recent paper discovered that both NK cells and ILC1s were crucial in controlling liver metastases. ILC1s mainly restricted metastases seeding, while NK cells limited both seeding and growth of metastases (Ducimetiere et al., 2021). Accordingly, another paper showed that NK cells sustained tumor dormancy through IFN-γ in the liver. However, activated stellate cells could lead to NK cell quiescence, resulting in tumor outgrowth and hepatic metastases (A. L. Correia et al., 2021). Therefore, both ILC1s and NK cells perform pivotal functions in various liver diseases.

3.5.3 Liver sinusoidal endothelial cells (LSECs)

LSECs constitute the microvasculature in sinusoids connecting hepatic portal vein and central vein. They are discontinuous, and do not have a diaphragm and basement membrane. They also possess fenestrae organized in sieve plates, allowing diffusion of small molecules directly to hepatocytes, which facilitates liver metabolism (Szafranska, Kruse, Holte, McCourt, & Zapotoczny, 2021). Like other blood endothelial cells, they express CD31 and CD146. LSECs have a high endocytosis rate. It was shown that each LSEC can clear up to 540 particles per hour (Mates et al., 2017). The high endocytosis function is facilitated by high expression of scavenging receptors, such as Stabilin1 (Stab1) and Stabilin2 (Stab2). Interestingly, a study showed that Stab1/Stab2 double knockout (DKO) mice developed glomerular fibrosis and died earlier compared to Stab1 KO and Stab2 KO (Schledzewski et al., 2011). Therefore, both Stab1 and Stab2 on LSECs might have redundant roles in removing harmful circulating factor in the blood to prevent diseases in distal organs. These data suggest that LSECs are crucial in maintaining homeostasis in the whole body.

Apart from their homeostatic role, LSECs are also indispensable for the liver development. In this aspect, GATA4 in LSECs was the key for proper liver development during embryonic stage. Conditional GATA4 deletion in LSECs resulted in a change from discontinuous to continuous ECs. The continuous capillaries led to liver hypoplasia and impaired hematopoietic stem cell recruitment, causing anemia and embryonic lethality (Geraud et al., 2017). The change from discontinuous to continuous ECs, named ‘capillarization’, has frequently been associated with aging and liver diseases. During this process, LSECs start to lose fenestrae, form basement membrane due to collagen deposition, and become capillarized (Szafranska et al., 2021). Not only during embryonic development, LSECs also play a role in neonatal liver. Hepatocyte zonation is a distinctive hallmark of the liver, and zonation starts around day 5 to 7 days post-natally. Interestingly, hepatocyte zonation was independent of microbiota, suggesting a possible internal cues in initiating zonation post-partum (Gola et al., 2021). Conditional deletion of Wnt cargo receptor Evi in LSECs led to aberrant hepatocyte zonation, demonstrating a vital function of LSEC-derived Wnt in liver zonation (Leibing et al., 2018; R. Ma, Martinez-Ramirez, Borders, Gao, & Sosa-Pineda, 2020). It has recently become

clear that LSECs also can have zonation pattern (Halpern et al., 2018; Inverso et al., 2021). Furthermore, LSECs also contribute to liver diseases. For instance, overexpression of Notch in LSECs led to reduced liver metastases due to a lower ICAM-1 expression, despite causing an aberration in zonated proteins expressed by LSECs (Wohlfeil et al., 2019). Taken together, LSECs have versatile functions during embryonic development, post-partum, homeostasis, and disease.

3.5.4 LSECs and immune cells

The role of LSECs in the immunology has been investigated, particularly their interaction with T cells. LSECs express several surface molecules related to immune responses, including TLRs, MHC I, MHC II, PD-L1 as well as CD80 and CD86 (Knolle et al., 1998; Limmer et al., 2000; Schurich et al., 2010; J. Wu et al., 2010). Similar to dendritic cells, LSECs can cross-present antigens in the format of MHC I to $CD8^+$ T cells in a (transporter associated with antigen processing) TAP-dependent manner (Limmer et al., 2000). Unlike dendritic cells, LSECs was thought to induce $CD8^+$ T cell tolerance rather than activation (Diehl et al., 2008; Schurich et al., 2010). The tolerance was regulated by PD-L1 on LSECs, and exogenous IL-2 could overwrite the tolerance induction. In addition, LSECs could activate naïve $CD8^+$ T cells in the presence of high antigen concentration, in a CD80/CD86-independent manner (Schurich et al., 2010). These results show that the strength of activation and inhibition signal provided by LSECs could determine the fate of naïve $CD8^+$ T cells. Nevertheless, it was shown that LSEC-primed tolerant $CD8^+$ T cells can be reactivated when encountering mature dendritic cells, thus showing a memory response. LSEC-primed $CD8^+$ memory T cells were similar to central memory T cells, but were generated under non-inflammatory condition. LSEC-primed T cells might be important to prevent immune escape of pathogens, as antigen presentation by immature DCs leads to T cell deletion under non-inflammatory condition (Bottcher et al., 2013). Interestingly, LSECs induce rapid and transient Grazyme B expression in naïve $CD8^+$ T cells during priming, and this requires trans-IL-6 signaling (Bottcher et al., 2014). All these data indicate that LSECs can function as non-professional APCs to activate $CD8^+$ T cells, in a mechanism distinct from dendritic cells. While LSECs can cross-present antigens and activate $CD8^+$ T cells, activated $CD8^+$ T cells were also shown to kill LSECs using perforin in an acute viral fulminant hepatitis model. This led to the destruction of blood vessels and hepatocyte death, and eventually liver failure (Welz et al., 2018).

On the other hand, the interaction between LSECs and $CD4^+$ T cells is less studied. In an early study, it was shown that LSECs were inefficient in generating Th1 cells, as they did not secrete IL-12 (Knolle et al., 1999). At least *in vitro*, LSECs could inhibit Th1 and Th17 cytokine production by activated T cells through PD-1 and IL-10 (Carambia et al., 2013). Moreover, LSECs was more efficient in generating $FoxP3^+$ Treg

in a TGF-β-dependent manner, compared to liver dendritic cells and Kupffer cells (Carambia et al., 2014). Another study showed that LSECs could only induce FoxP3$^-$ Treg (Kruse et al., 2009). The discrepancy between these studies could be due to the type of peptides used in respective experiments. LSECs could also be the therapeutic target for generating Treg, as one study showed that selective delivery of autoantigenic peptides to LSECs via nanoparticles could induce Treg (Carambia et al., 2015; Luth et al., 2008). This prevented experimental autoimmune encephalomyelitis disease. Beside CD4$^+$ and CD8$^+$ T cells, LSECs can also interact with NKT cells. It was reported that LSECs recruited and retained CXCR6$^+$ NKT cells through the ligand CXCL16. CXCR6-deficient mice had defects in retaining CXCR6$^+$ NKT cells in the liver, resulting in either a decreased T cell autoimmune hepatitis or more liver cancer metastases (Geissmann et al., 2005; C. Ma et al., 2018).

3.5.5 Liver diseases and murine models

Murine models have been used to study acute and chronic liver diseases. There are several models that have been well-established for acute or chronic liver diseases. Lipopolysaccharide (LPS) has been used to induce systemic endotoxin shock or septic shock. Rodents injected with LPS were shown to have an increased alanine aminotransferase (ALT) level, a clinical marker to determine liver damage (Ajuwon, Oguntibeju, & Marnewick, 2014; Jiang et al., 2018). Livers receive about 70%-80% of blood from the portal vein, which collects blood enriched with bacterial antigen from the intestines. Thus, livers are constantly exposed to LPS and act as the final refuge to remove LPS before transporting the blood to the rest of the body. It was shown that liver cleared most of the LPS after injection. The degree of liver failure often correlated with endotoxemia in patients with liver diseases (Su, 2002). In the LPS-mediated acute liver injury model, Kupffer cells recognized LPS through its TLR4 receptor, thus producing pro-inflammatory cytokines, such as TNF and IL-1 (Su, 2002). Apart from Kupffer cells, NK cells were also involved in LPS-mediated acute liver injury through the production of IFN-γ (Emoto et al., 2002). It was reported that NK cells played a detrimental role in mediating LPS-induced disease, as NK cell depletion prevented mice to succumb to endotoxic shock (Chan et al., 2014; Heremans, Dillen, van Damme, & Billiau, 1994). CD96, an inhibitory receptor on NK cells, was particularly crucial for limiting the liver damage caused by NK cells (Chan et al., 2014). In addition to LPS, the co-injection of D-Galactosamine (D-Gal) has also been frequently used as a liver injury model. However, LPS/D-gal mimicked fulminant hepatitis failure instead of septic shock, and this model induced a higher level of serum ALT, compared to LPS alone (Mignon et al., 1999; Nakama et al., 2001). Similar to the LPS model, NK cells also played an adverse role in LPS/D-gal model, as depletion prevented lethality (Vinay et al., 2004). However, the role of LSECs in this model remains unclear. Taken

together, these data suggested that NK cells exacerbated acute liver inflammation, leading to liver injury and eventually mortality.

ConcanavalinA (ConA) model has also been frequently used as an acute liver injury model. ConA is a mitogen that can activate T cells, independent of the antigen recognition. Thus, ConA model mimics autoimmune hepatitis disease. ConA model was shown to induce serum ALT in only 8 hours, manifesting a severe liver injury in a short period (Tiegs, Hentschel, & Wendel, 1992a). This model is T-cell dependent, as T cell-deficient mice did not develop liver damage after ConA-induced liver injury. It was shown that $CD4^+$ helper T cells were the subset mediating the liver damage (Tiegs, Hentschel, & Wendel, 1992b). Further investigation suggested that NKT cells were another key player in mediating ConA-inducted autoimmune hepatitis, demonstrating an adverse role of NKT cells in this disease (Geissmann et al., 2005; Kaneko et al., 2000). On the other hand, NK cell depletion did not ameliorate any ConA-induced liver damage, revealing a dispensable role of NK cells in this model (Toyabe et al., 1997). Interestingly, a sublethal dose of ConA injection led to liver T cell tolerance, mediated by Treg, Kupffer cells, and IL-10, revealing a unique liver microenvironment in generating tolerant T cells (Erhardt, Biburger, Papadopoulos, & Tiegs, 2007). Therefore, ConA could be a suitable model to study physiological role of $CD4^+$ T cells and NKT cells in acute liver diseases. The role of LSECs in the ConA model has rarely been investigated.

Another common liver damage model is the use of carbon tetrachloride (CCl_4), which causes chemical-induced liver damage. As CCl_4 is a toxic chemical that can directly cause hepatocyte cell death without the requirement of any specific receptor. It can be used as an acute liver injury inducer by either a single injection, or chronic liver fibrosis inducer by repeated injection (Weber, Boll, & Stampfl, 2003). There were contradicting results regarding the role of T cells in the CCl_4 model. Mice deficient in NKT cells showed elevated ALT activity in the serum and increased fibrosis in the early stage, indicating a protective role of NKT cells (Park et al., 2009). However, Rag1-deficient mice, which do not have T cells, did not show any change in serum ALT activity after CCl_4 injection (Nabekura et al., 2020). These two pieces of data suggest that different subsets of T cells might play different roles and regulate each other functions. Apart from T cells, ILC1s were shown to be activated through DNAM-1 in the CCl_4 acute liver injury model, and they promoted the survival of hepatocytes by secreting IFN-γ. NK cell depletion did not affect serum ALT level, revealing a limited role of NK cells in this model (Nabekura et al., 2020). Thus, tissue-resident ILC1s can act as the sentinel during acute liver damage. This model is suitable to investigate the function of ILC1s in conditional NK cell and ILC1s gene knockout murine models. LSECs were shown to lose fenestrate in chronic CCl_4 liver damage model, which precedes hepatic stellate cell activation (Lafoz, Ruart, Anton,

Oncins, & Hernandez-Gea, 2020). They also started to develop basement membrane, a process known as capillarization. The precise functional role of LSECs in the CCl_4 model has seldom been examined.

There are additional models, which have been well established for various liver diseases. These include acetaminophen (APAP)-induced acute liver injury, high fat diet, viral hepatitis models, diethyl nitrosamine (DEN)-induced hepatocarcinoma, liver metastasis models and others (Asgharpour et al., 2016; Y. Liu et al., 2013; C. Ma et al., 2018; Newsome, Plevris, Nelson, & Hayes, 2000; Welz et al., 2018). Depending on the research question and the etiology similarity to the human disease, different models should be considered to examine the role of various immune cells in liver diseases.

3.6 Surface molecules studied on LSECs

3.6.1 Major histocompatibility class II (MHC II)

MHC II is required for optimal T cell development and response, as it presents antigens to $CD4^+$ helper T cells. APCs actively uptake peptides from the extracellular environment, process them, and present them in the context of MHC II to $CD4^+$ helper T cells. They utilize different modes to facilitate antigen uptake, including micropinocytosis, receptor-mediated endocytosis, phagocytosis, autophagy, and endosomal and lysosomal protein proteolysis. These antigens, despite different uptaking routes, end up in endosomal/lysosomal antigen-processing compartments (also named as multivesicular bodies), a low pH and high proteolytic environment, where most antigen processing and loading take place. In these multivesicular bodies, antigens are processed and loaded to nascent MHC II, and antigen-loaded MHC II complexes traffic to the plasma membrane. However, these antigen-loaded MHC II complexes do not just stay on the plasma membrane in a static fashion. They are often internalized again, with some heading to lysosomes for subsequent degradation, and many enter early endosomes and recycle back to plasma membrane again (Roche & Furuta, 2015).

MHC II plays an indispensable role in the $CD4^+$ T cell development. During thymopoiesis, cortical and medullary thymic epithelial cells present self-antigens in the context of MHC II, directly participating in the positive and negative selection of $CD4^+$ T cells (Germain, 2002; Klein, Kyewski, Allen, & Hogquist, 2014). The regulation of MHC II has also been extensively studied. MHC II expression requires the master transcriptional co-gractivator, CIITA. CIITA-deficient mice were revealed to display aberrant expression of MHC II in the thymus, resulting in few $CD4^+$ T cells in the periphery (Chang, Guerder, Hong, van Ewijk, & Flavell, 1996). There are four promoters at the CIITA transcription site: pI, pII, pIII, and pIV. Both humans and mice share the conserved pI, pIII, and pIV promoters of CIITA gene, while humans also have an additional pII promoter (LeibundGut-Landmann et al., 2004). Different promoters are preferentially used by different cells for CIITA gene transcription. Myeloid cells mainly use pI promoter, while B cells mostly utilize pIII promoter, to drive constitutively CIITA expression in steady-state. More importantly, some non-professional APCs can express MHC II when stimulated with IFN-γ, as IFN-γ activates pIV promoter of CIITA (Muhlethaler-Mottet, Otten, Steimle, & Mach, 1997; Steimle, Siegrist, Mottet, Lisowska-Grospierre, & Mach, 1994). Interestingly, cTECs strictly depend on pIV, while mTEC depends on pIII and pIV of CIITA for MHC II expression (Irla et al., 2008), indicating that non-professional APCs can express CIITA in an IFN-γ-dependent manner. However, the usage of pII promoter in human is still unknown.

The functional role of MHC II on distinct cells are becoming clearer in the recent years due to the possibility to generate conditional deletion of MHC II gene using different murine models. It was shown that MHC II on lymph node stromal cells was crucial for maintaining peripheral T cell tolerance (Dubrot et al., 2018; Dubrot et al., 2014). MHC II on B cells also activated $CD4^+$ T cells in a murine lupus model, triggering a more severe lupus disease (Giles, Kashgarian, Koni, & Shlomchik, 2015). Interestingly, MHC II on alveolar cells in lungs had limited antigen presentation capability, having a moderate role in ameliorating viral diseases (Toulmin et al., 2021). In gut, MHC II on DCs was vital to prime and activate $CD4^+$ T cells, which prevented intestinal microbiota-mediated inflammation in steady-state (Loschko et al., 2016). Moreover, MHC II on intestinal epithelial cells was crucial for intraepithelial T cell development and played a role in aggravating graft-versus-host disease (Moon et al., 2021). In humans, different expression of MHC II alleles were shown to be involved in autoimmune diseases, including Celiac disease, type I diabetes, and multiple sclerosis (Rock, Reits, & Neefjes, 2016). Together, these data suggest the functional significance of MHC II on different cells in various diseases.

3.6.2 Herpes virus entry mediator (HVEM)

Herpes virus entry mediator (HVEM), as its name implies, was first discovered as the receptor for the entry of herpes simplex virus into the cells (Montgomery, Warner, Lum, & Spear, 1996). Since then, much research has been done to investigate its functional role in immunology. HVEM (encoded by the gene, *Tnfrsf14*) is widely expressed on both hematopoietic and non-hematopoietic cells. HVEM belongs to the tumor necrosis factor (TNF) superfamily. The cytoplasmic region of HVEM signals through TRAF and leads to NF-κB activation (Marsters et al., 1997). Apart from being the receptor that delivers intrinsic signal, HVEM can also act as a ligand, which modulates immune cell functions. It is known that HVEM can bind LIGHT, lymphotoxin α (Mauri et al., 1998), B and T lymphocyte attenuator (BTLA)(Sedy et al., 2005), and CD160 (Cai et al., 2008) (Fig. 1.12) through its cysteine rich domain (CRD). CRD1 of HVEM binds to either BTLA or CD160, with a higher affinity towards BLTA, without affecting LIGHT engagement (Cai & Freeman, 2009; W. Liu et al., 2019). Binding of LIGHT led to inflammatory responses (Granger & Ware, 2001), while binding of CD160 and BTLA on T cells inhibited T cell functions (Cai et al., 2008; Watanabe et al., 2003b))(Sedy et al., 2005) (Fig. 1.12). However, CD160 on activated NK cells, liver ILC1s and intraepithelial ILC1s contributed to IFN-γ production (Di Censo et al., 2021; Fuchs et al., 2013; T. C. Tu et al., 2015). Whether the engagement of HVEM with CD160 on NK cells and ILC1s leads to IFN-γ production remains to be investigated.

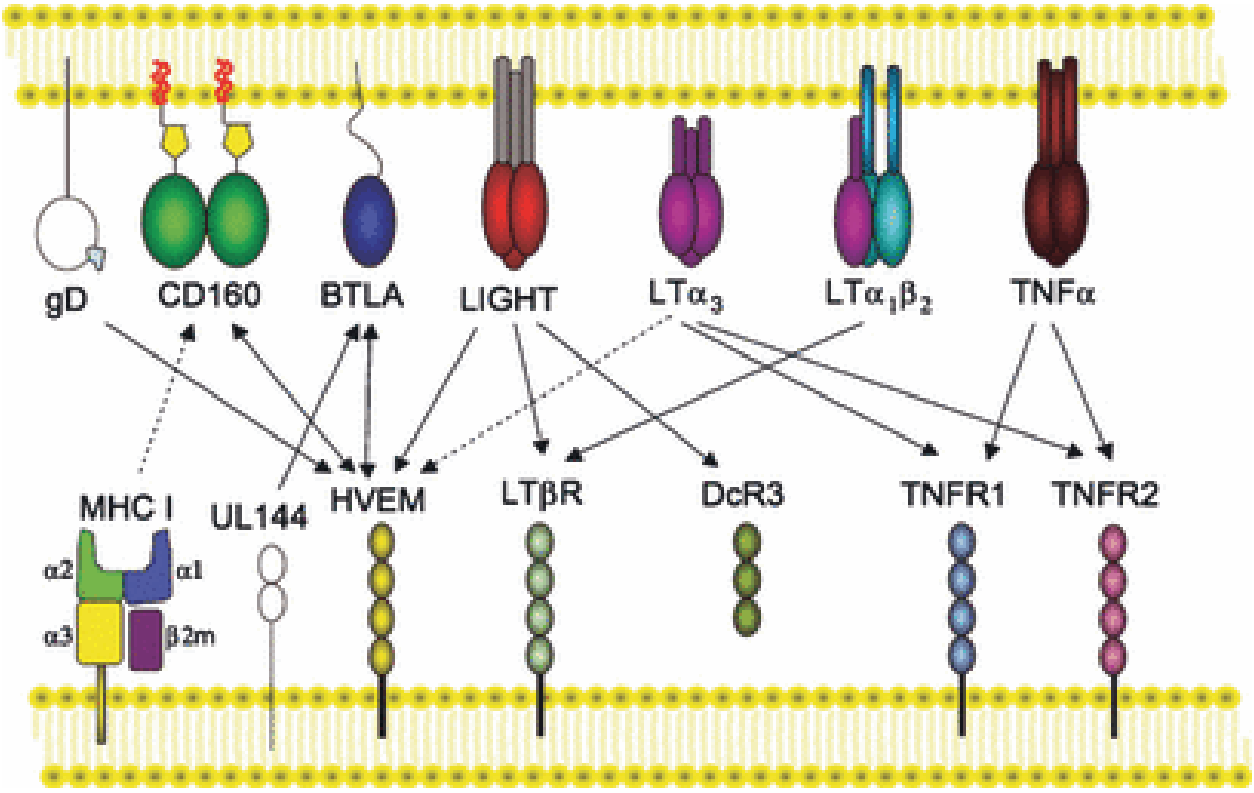

Figure 1.12 - HVEM can bind herpesvirus glycoprotein D (gD), CD160, BLTA, LIGHT, and LTα. Dotted arrow indicated weak binding affinity. Image adapted from (Cai & Freeman, 2009).

As HVEM is expressed by many cells and can act as both receptor and ligand, multiple roles have been described for HVEM, depending on the cell-type and the disease context. Adoptive transfer of HVEM-deficient T cells led to a reduction in colitis pathogenesis in the murine model (Steinberg et al., 2008). Another study also confirmed that adoptive transfer of HVEM-deficient T cells led to reduced weight loss and histopathology in the dextram sulfate sodium-induced and T-cell-induced colitis model (Schaer et al., 2011). Naive T cells express HVEM that acts as a costimulatory molecule (Cheung et al., 2009; Kwon et al., 1997). Nevertheless, HVEM-deficient T cells were shown to be more activated both *in vitro* and *in vivo* after stimulation with ConA, causing higher mortality in mice (Y. Wang et al., 2005). As T cells express HVEM, CD160, and BTLA, it is likely that depending on the stimulation and the disease context, the balance of HVEM, CD160, and BTLA-induced functions would dictate the overall activation of T cells. In addition, it was demonstrated that HVEM could stimulate NK cell activation to eliminate tumors (Fan et al., 2006). HVEM on ILC3s also contributed to IFN-γ production against intestinal bacteria infection (Seo et al., 2018). Furthermore, B cells, monocytes, and DCs all express HVEM and can be activated upon its engagement (Murphy, Nelson, & Sedy, 2006).

Apart from immune cells, HVEM on non-hematopoietic cells can also play a diverse role. It was shown that HVEM on radioresistant cells played an anti-inflammatory role in a colitis murine model, by binding to BTLA, which inhibited T cell functions (Steinberg et al., 2008). Moreover, HVEM on intestinal epithelial cells was vital for host immunity against mucosal pathogens by receiving activating signal from CD160 expressed by intraepithelial lymphocytes (Shui et al., 2012).

4 Aims of the study

The liver is a highly vascularized organ that performs various metabolic tasks. LSECs form the microvasculature networks connecting the hepatic portal vein, hepatic artery, and hepatic vein. Tissue-resident immune cells, like ILC1s and Kupffer cells, are enriched in the liver, and they reside in sinusoids formed by LSECs. The close proximity between LSECs and immune cells suggests their interaction and co-regulation. LSECs are crucial for a proper liver development, and their structural and functional abnormalities lead to liver diseases. On the other hand, NK cells and ILC1s play important role in liver homeostasis and diseases, such as restricting hepatic metastases. While NK cells and ILC1s are located in the niche formed by LSECs, the mechanism of the interaction between LSECs, and NK cells and ILC1s remains unexplored. Therefore, the understanding of the crosstalk between LSECs and innate lymphocytes will provide novel mechanisms of angio- and immuno-regulation in the liver during homeostasis and disease.

As NK cells and ILC1s are located in the sinusoids formed by LSECs, I proposed that interactions between these cells would be crucial for liver immune responses. The main objectives of the project are to investigate the crosstalk between LSECs with NK cells and ILC1s. In my project, I aim to dissect:

1. Functional relevance of LSECs NK/ILC1 crosstalk in liver immune homeostasis

2. Functional role of LSECs in regulating NK/ILC1 inflammatory responses

This research will help to understand how NK cell and ILC1 responses are shaped by their stromal microenvironment in the liver. In addition, it will provide a new perspective for the role of LSECs as the active participant in shaping liver immunity.

5 Materials and Methods

5.1 Materials

5.1.1 Special laboratory equipment

Product	Company
FACSAria Fusion cell sorter	BD Biosciences
Flow Cytometer, LSRfortessa	BD Biosciences
GentleMACS™ Octo Dissociator	Miltenyi
Plate reader Infinite 200 pro	Tecan
C1000 Touch™ Thermal Cycler	Bio-Rad
QuantStudio™ 5 Real-Time PCR System, 384-well	Applied Biosystems

5.1.2 Chemicals and biological reagents

Product	Company	Catalog no.
7-AAD	Biolegend	420404
Aqua zombie™	Biolegend	423102
Zombie UV™	Biolegend	423108
Cell Trace Violet™	Invitrogen	C34557
Dnase I	Sigma-Aldrich	DN25-1g
Ethanol		
Golgi Plug™	BD Bioscience	555029
Golgi Stop™	BD Bioscience	554724
Hyaluronidase type V	Sigma-Aldrich	H6254-1G
InVivoMab anti-mouse IFN-γ, Clone XMG1.2	Bio X cell	BE0055
Lipopolysaccharide E.coli O26:B6	Sigma-Alrich	L2654
Lympholyte-M™	Cedarlene	CL5035
Nuclease-Free Water (not DEPC treated)	Ambion	AM9937
Nycodenz	Axis-Shield	1002424

Percoll ®	Cytiva	17089101
Recombinant human IL-2	Hoffmann-La Roche	1104-0890
Recombinant mouse IFN-γ	Peprotech	315-05
Recombinant mouse IL-12	Peprotech	210-12
Recombinant mouse IL-18	MBL	B002-5
Recombinant murine IL-1b	Peprotech	211-11b
Recombinant murine IL-22	Peprotech	210-22
β-mercaptoethanol (50mM)	GIBCO-Invitrogen	31350010
Brilliant Stain Buffer	BD	566349
β-mercaptoethanol (99%)	VWR	97064-588
Sodium chloride	Sigma-Aldrich	31434-5KG

5.1.3 Cell culture media and solutions

Product	**Company**	**Catalog no.**
Cell Dissociation Solution Non-enzymatic (1x)	Sigma-Aldrich	C5914
Dimethylsulphoxide Hybri Max® (DMSO)	Sigma-Aldrich	D2650
Dulbecco's Modeified Eagle's Medium (DMEM), glucose, L-glutamine, sodium pyruvate, and sodium bicarbonate	Sigma-Aldrich	D6459
Dulbecco's phosphate buffered saline	Gibco	1490144
Fetal calf serum		
Gey's Balanced Salt Solution (GBSS)	Pancoll-biotech	P04-48500
Gibco™ RPMI 1640 Medium	Fisher Scientific	11530586
Gibco™ RPMI 1640 Medium, without Glucose	Fisher Scientific	11879020
Gibco™ RPMI-1640-Medium, without Glutamine	Fishers Scientific	11534446

L-Glutamine 200 mM (100x), 29.2 mg/mL	GIBCO-Invitrogen	25030
Non-essential amino acids (100x)	GIBCO-Invitrogen	11140035
Penicillin/Streptomycin-Solution 10000 U/mL penicillin, 10000 µg/mL streptomycin	GIBCO-Invitrogen	15140
Sodium pyruvate MEM 100mM	GIBCO-Invitrogen	11360088
Trypsin-EDTA (1x) HBSS w/o Ca2+/Mg2+ w/ EDTA	GIBCO-Invitrogen	25300
Detachin Cell Detachment Solution	Genlantis	T100106
β-mercaptoethanol 50mM	GIBCO-Invitrogen	31350010

5.1.4 Cell culture products

Product	**Company**	**Catalogue no.**
6.5 mm Transwell® with 0.4 µm Polyester (PET) Membrane Insert, Sterile	Corning	3470
CellAdhere™ Collagen I-Coated Plate, 96 well	Stem Cell Technologies	100-0366
Collagen I, Coated Plate, 24 well	Gibco	A1142802
Collagen I, Coated Plate, 96 well	Gibco	A1142803
GentleMACS™ C Tubes	Miltenyi	130-093-237
MACS LS columns	Miltenyi	130-042-401
RNase-free Microfuge Tubes (1.5 mL)	Thermofisher Ambion	AM12400
BD Falcon® 5mL round bottom tubes with 35µm nylon mesh strainer	Falcon	352235

5.1.5 Kits

Product	Company	Catalog no.
CD146 (LSEC) microbeads, mouse	Miltenyi	130-092-007
BD Cytofix/Cytoperm buffer™	BD	554714
eBioscience™ FoxP3 Transcription factor staining buffer set	eBioscience	00-5523-00
GeneChip™ Mouse Genome 430 2.0 Array	Affymetrix	900497
Liver Dissociation Kit, mouse	Miltenyi	130-105-807
MyTaq™ Extract-PCR Kit	Meridian Bioscience	BIO-21127
PowerUp™ SYBR™ Green Master Mix	Applied Biosystem	A25918
RNeasy Mini Kit (50 reactions)	Qiagen	74104
RNA Clean and Concentrator - 5	Zymo Research	R1013
TURBO DNA-free™ kit	Ambion	AM1907
ProtoScript® II First Strand cDNA Synthesis Kit	New England Biotechnology	E6560S

5.1.6 Buffers and solutions

Solution	Ingredients
FACS buffer	1x PBS 1% FCS 0.02% NaN_3 2 mM EDTA
Cell freezing medium	FCS 10% DMSO
MACS buffer	PBS 2% FCS 2 mM EDTA
ILCs sorting buffer	PBS 1% FCS 2mM EDTA
LSEC sorting buffer	GBSS 1% FCS 2mM EDTA
Primary cell culture media	RPMI 1640 with high glucose

	10% FCS 1% L-glutamine 1% Non-essential amino acid 1% Sodium Pyruvate 1% Penicillin/Streptomycin 0.1% β-mercaptoethanol (for cell culture)
LSEC media	DMEM with high glucose 10% FCS 1% L-glutamine 1% Non-essential amino acid 1% Sodium Pyruvate 1% Penicillin/Streptomycin 0.1% β-mercaptoethanol (for cell culture)
Complete DMEM	DMEM with high glucose 10% FCS 1% Penicillin/Streptomycin
Cell lysis buffer for RNA isolation	RLT buffer from Qiagen 1% β-mercaptoethanol (13.8M)
ACK lysis buffer	0.605g Tris base 4.01g Ammoniochloride Fill up to 500 mL with ddH_2O Adjust pH to 7.2
26% Nycodenz solution (freshly prepared)	10.4g of Nycodenz powder dissolved in GBSS Sterilized filter
1.5M Sodium Chloride (NaCl) Solution	87.66g of sodium chloride in 1 liter water
Isotonic Percoll solution (freshly prepared)	9 parts stock Percoll 1 part 1.5M NaCl solution
70% Percoll (freshly prepared)	7mL isotonic Percoll solution 3mL PBS
40% Percoll (freshly prepared)	4mL isotonic Percoll solution 6mL PBS
15% Percoll (freshly prepared)	1.5mL isotonic Percoll solution 8.5mL PBS

Liver and lung digestion media for gentleMACS dissociation	DMEM 1% L-glutamine

5.1.6 Primary anti-mouse antibodies for flow cytometry

Antigen	Fluorochrome	Clone	Company	Catalog no.
CD206	Alexa Fluor 647	C068C2	Biolegend	141708
CD31	Alexa Fluor 647	MEC13.3	Biolegend	102515
CD54/ICAM	Alexa Fluor 647	YN1/1.7.4	Biolegend	116114
cKit	Alexa Fluor 647	2B8	Biolegend	105818
CXCR6	Alexa Fluor 647	SA051D1	Biolegend	151115
FoxP3	Alexa Fluor 647	MF-14	Biolegend	126408
IA/IE	Alexa Fluor 647	M5/114.15.2	Biolegend	107618
IFN-γ	Alexa Fluor 647	XMG1.2	Biolegend	505814
CD106/VCAM	APC	429(MVCAM.A)	Biolegend	105712
CD25	APC	PC61	BD	553866
CD44	APC	IM7	eBioscience	17-0441-82
Eomes	APC	Dan-11mag	eBioscience	17-4875-82
GATA-3	APC	16E10A23	Biolegend	653809
HVEM	APC	C46	BD	564470
MULT-1	APC	237104	R&D	FAB2688A
NK1.1	APC	PK136	Biolegend	108710
NKG2D	APC	CX5	Biolegend	130212
NKp46	APC	29A1.4	Biolegend	137608
PD-1	APC	29F.1A12	Biolegend	135209
PVR / CD155	APC	TX56	Biolegend	131510
CD3	APC-Cy7	17A2	Biolegend	100222
CD19	APC-Cy7	6D5	Biolegend	115530
F4/80	APC-Cy7	BM8	Biolegend	123118
FcεRI	APC-Cy7	MAR-1	Biolegend	134325
Ly6G	APC-Cy7	1A8	Biolegend	127624
Siglec F	APC-Cy7	E50-2440	BD	565527
Ter119	APC-Cy7	Ter-119	Biolegend	116223
DNAM-1	APC-Cy7	10E5	Biolegend	128816

anti-human CD271	BUV395	C40-1457	BD	743362
CD3ε	BUV395	145-2C11	BD	563565
CD4	BUV563	GK1.5	BD	612923
CD45	BUV737	30-F11	BD	748371
CD45	BUV805	30-F11	BD	748370
TCRβ	BUV805	H57-597	BD	748405
CD31	BV421	390	Biolegend	102424
CTLA4	BV421	UC10-4B9	BD	106305
NKp46	BV421	29A1.4	Biolegend	137612
PD-L1	BV421	MIH5	BD	564716
TCRβ	BV421	H57-597	Biolegend	109230
CD3ε	BV510	145-2C11	Biolegend	100353
CD11b	BV650	M1/70	Biolegend	101259
CD62L	BV650	MEL-14	Biolegend	104453
NK1.1	BV650	PK136	Biolegend	108736
TCRγδ	BV711	GL3	BD	563994
CD103	BV785	2E7	Biolegend	121439
CD3ε	BV785	145-2C11	Biolegend	100355
CD45	BV785	30-F11	Biolegend	103149
LAG3	BV785	C9B7W	Biolegend	125219
Tbet	BV785	4B10	Biolegend	644835
TCRβ	BV785	H57-597	Biolegend	109249
Endomucin	eFluor660	eBioV.7C7	Invitrogen	50-5851-82
B220	FITC	RA3-6B2	Biolegend	103206
CD107a	FITC	1D4B	Biolegend	121606
CD200R	FITC	OX-2R	Biolegend	123910
CD206	FITC	C068C2	Biolegend	141704
CD86	FITC	GL-1	Biolegend	105006
CD8α	FITC	Ly-2	BD	553031
DNAM-1	FITC	10E5	Biolegend	128803
IFN-γ	FITC	XMG1.2	Biolegend	505806
Ly6C	FITC	RB6-8C5	BD Pharmingen	553126

Stabilin2	Alexa Fluor 488	34-2	MBL	D317-A48
Ly6G	Pacific Blue	1A8	Biolegend	127612
CD103	PE	M290	BD	557495
CD146	PE	ME-9F1	Biolegend	134704
CD200R	PE	OX-2R	Biolegend	123908
CD49a	PE	Hα31/8	BD	562115
CD62L	PE	MEL-14	Biolegend	104407
FoxP3	PE	FJK-16s	eBioscience	12-5773-82
H-2Db	PE	KH95	BD	553574
H-2Kb	PE	AF6-88.5	BD	561072
H60	PE	205326	R&D	FAB1155P
HVEM	PE	HMHV-1B18	Biolegend	136304
Ki-67	PE	SolA15	Invitrogen	12-5698-82
Lyve1	PE	FAB2125P	R & D	223322
Neuropilin1	PE	3E12	Biolegend	145204
NK1.1	PE	PK136	Biolegend	108708
PD-L1	PE	10F.9G2	Biolegend	124308
Rae-1	PE	186107	R&D	FAB17582P
TCRγ	PE	GL3	Biolegend	118108
TNFα	PE	MP6-XT22	Biolegend	506308
TRAIL	PE	N2B2	Biolegend	109305
Helios	PE/Dazzle 594	22F6	Biolegend	137232
NK1.1	PE/Dazzle 594	PK136	Biolegend	108748
F4/80	PE/Dazzle 594	BM8	Biolegend	123146
Gata3	PE-CF594	L50-823	BD	563510
CD11c	PE-Cy7	N418	Biolegend	117318
CD127	PE-Cy7	A7R34	Biolegend	135014
CD146	PE-Cy7	ME-9F1	Biolegend	134714
CD19	PE-Cy7	6D5	Biolegend	115520
CD69	PE-Cy7	H1.2F3	BD Pharmingen	552879
Eomes	PE-Cy7	Dan-11mag	eBioscience	25-4875-82
Neuropilin1	PE-Cy7	3E12	Biolegend	145211
NKp46	PE-Cy7	29A1.4	Biolegend	137618

TIGIT	PE-Cy7	1G9	Biolegend	142107
FoxP3	PE-eFluor 610	FJK-16s	eBiosciences	61-5773-80
CD11c	PerCP-Cy5.5	NF18	Biolegend	117327
CD31	PerCP-Cy5.5	390	Biolegend	102420
CD44	PerCP-Cy5.5	IM7	Biolegend	103031
CD49a	PerCP-Cy5.5	HA31/8	BD	564862
T-bet	PerCP-Cy5.5	4B10	Biolegend	644806

5.1.7 Antibodies for functional assays

Antibodies	Clone	Concentration	Company	Catalog no.
Ultra-LEAF Purified CD16/CD32	93	10μg/mL	Biolegend	101329
LEAF™ Purified anti-CD155	4.24.1	10μg/mL	Biolegend	132204
Purified Tag IgG2a, γ Isotype Ctrl Antibody	RTK2758	10μg/mL	Biolegend	400502

5.1.8 Isotype controls

Antibodies	Fluorochrome	Clone	Company	Catalog no.
Rat IgG2b	Alexa Fluor 647	RTK4530	Biolegend	400626
Rat IgG1	APC	RTK2071	Biolegend	400412
Rat IgG2a	APC	54447	R & D system	IC006A
Rat IgG2b	APC	RTK4530	Biolegend	400612
Rat IgG2b	APC/Fire	RTK4530	Biolegend	400670
Rat IgG2a	BV421	RTK2758	Biolegend	400549
Rat IgG1	FITC	RTK2071	Biolegend	400406
Rat IgG2a	FITC	RTK2758	Biolegend	400506
Rat IgG2b	FITC	RTK4530	Biolegend	400606
Arm Hamster	PE	A19-3	BD	553972
Mouse IgG2a	PE	MOPC-173	Biolegend	400212
Mouse IgG2b	PE	MPC-11	Biolegend	400312
Rat IgG2a	PE	RTK2758	Biolegend	400508
Rat IgG2b	PE	RTK4530	Biolegend	400608

5.1.9 Oligonucleotide primers

For PCR Genotyping

Gene/Protein	Forward sequence (5' → 3')	Reverse sequence (5' → 3')
HVEM	ACCAAATCAGACCTGGGAAG	TCCAGCTGTGTGATCTACCTC
PD-L1	AGAGGAGATACTCAGTGTTTGCC	TTCAAACTCAGCCAAGGACC
B2m	GGTTTCAGAATGCAAACTCTGG	CAACTTTCCAAACGTCACATCC
B2m	GCTACAGAAGGATCCTTTGGG	TACAAAGACAGCAAGCTCATCG

For qPCR

Gene/Protein	Forward sequence (5' → 3')	Reverse sequence ((5' → 3')
Ciita pI	CAGGGACCATGGAGACCATAGT	CAGGTAGCTGCCCTCTGGAG
Ciita pIII	GGTTCCTGGCCCTTCTGG	ATCCATGGTGGCACACAGACT
Ciita pIV	CAGCACTCAGAAGCACGGG	ATCCATGGTGGCACACAGACT
Tnfrsf14/HVEM	CCACTGTTCCACATGCTTGC	CCTGTTAGGCAGTCAGCACA
Actb/beta actin	CAGATGTGGATCAGCAAGCA	GGGTGTAAAACGCAGCTCAGTA
B2m/MHC I	TGCTATCCAGAAAACCCCTCA	GGCGGGTGGAACTGTGTTA

5.1.10 Mouse lines

Mouse line	Scientific name	Source
Rag2 knockout	B6.(MF;129)-Rag2tm1Fwa	Haus 111, UMM
Rag2 Ly5.1 knockout	B6.Rag2tm1Fwa Ptprca	Haus 111, UMM
Clec4g-cre	B57BL/6N-Tg(Clec4g-icre)1.1 Sgoe	Haus 111, UMM, by Prof. Philipp Reiners-Koch
C57BL/6n	C57BL/6NRj	Janvier Labs
C57BL/6j	C57BL/6JRj	The Jackson Laboratory
Ifng knockout	B6.129S7-Ifngtm1Ts/J	The Jackson Laboratory
Ifngr knockout	B6.129S7-Ifngr1tm1Agt/J	The Jackson Laboratory
Il12rb2 knockout	B6;129S1-Il12rb2tm1Jm/J	The Jackson Laboratory
Ciita knockout	B6.129S2-Ciitatm1Ccum/J	The Jackson Laboratory
$HVEM^{flox/flox}$	B6;SJL-Tnfrsf14tm1.1Kro/J	The Jackson Laboratory
Rag2γc double knockout	C57BL/6NTac.Cg-Rag2tm1Fwa Il2rgtm1Wjl	By Prof. Hans-Reimer Rodewald, DKFZ

Ifng-Il17a-Il-10 reporter	B6.129S4-Ifngtm3.1Lky/J B6.129S4-Il17atm1.1Lky/J B6(Cg)-Il10tm1.1Karp/J	By Prof. Thomas Korn, Charles River, Italy
Hobit knockout	Zfp683tm1a(KOMP)Wtsi	By Prof. Georg Gasteiger, Uni Würzburg
Tlr4 knockout	Tlr4tm Aki	DKFZ
Myd88 knockout	Myd88tm1 Aki	DKFZ
Germ-free C57BL/6		By Prof. Andreas Diefenbach, Charite, Berlin

All experiments were performed according to the local animal experimental ethics committee guidelines and permission.

5.2 Methods

5.2.1 Liver digestion for LSEC isolation

Mice were sacrificed in the carbon dioxide chamber and dissected. Livers were briefly perfused with PBS via portal vein or vena cava to remove red blood cells, dissected, and kept in PBS on ice. Gall bladders and connective tissues were removed and liver tissue was digested using Liver Dissociation Kit (Enzyme D, Enzyme R, and Enzyme A), gentleMACS C tubes, and gentle MACS Octo dissociator according to the manufacturer's protocol. After digestion, liver tissue suspension was centrifuged down briefly and filtered through 100μm strainer in a 50mL falcon tube. C tubes were washed with GBSS, and undigested small liver pieces on the strainers were homogenized manually. Each liver suspension was topped up with cold GBSS. Cells were centrifuged at 300g for 10 mins at 4ºC. Supernatant was removed and 4mL of ACK lysis buffer was added to remove red blood cells. After 4 minutes, GBSS was added, and the liver suspension was filtered through 70μm strainers, followed by wash and filtering through 40μm strainers. Liver cells were resuspended in 6mL of GBSS, and layered on 26% of Nycodenz in GBSS. The gradients were centrifuged at 1400g (acc:1, dec:1) for 18 mins at 4ºC. The interphase, represented the enriched non-parenchymal cells (NPCs), was collected and washed with GBSS. Cells were counted for downstream experiments.

5.2.2 Lipopolysaccharide treatment

12- to 16-week old male mice were injected with lipopolysaccharide (5mg/kg) via intraperitoneal route. After 20 hours, mice were sacrificed. Liver non-parenchymal cells were isolated as above.

5.2.3 LSEC isolation and culture

After cell counting, NPCs were resuspended in MACS buffer (10 million cells in 98uL of MACs buffer), and incubated with 10μg/mL of anti-mouse CD16/CD32 for 10 minutes at 4ºC. 2uL of anti-$CD146^+$ magnetic beads per 10 million cells was added and incubated for 15 minutes at 4ºC. Cells were washed with MACS buffer, centrifuged at 300g for 10 mins at 4ºC. 20 millions of cells were loaded into a LS column and purified with magnetic separation according to the manufacturer's instruction. The collected LSECs were washed and centrifuged. LSECs were resuspended in warm LSEC media, counted and seeded at 0.8-1 x 10^6 cells per well in a 24-well collagen I-coated plate, or 0.2 x 10^6 cells per well in a 96-well collagen I-coated plate to achieve 100% confluency. The optimized $CD146^+$ magnetic purification protocol routinely

gave >90% of pure LSECs after isolation. LSECs were washed carefully on the next day with warm PBS and unattached dead cells were removed. LSECs were stimulated with 100ng/mL of IFN-γ or left unstimulated after washing. After 20-24 hours, LSECs were detached using Detachin for immunophenotyping analysis. LSECs at this point usually yielded 99% purity.

5.2.4 Liver mononuclear cell (LMC) isolation for sorting and culture

Livers were briefly perfused via portal vein and harvested. Tissue was homogenized manually and digested with 10mL PBS containing 7-8mg of Hyaluronidase and 5-6mg of DNAse in a shaker water bath at 37ºC for 50 mins. Each liver tissue suspension was filtered through 100μm strainer and undigested tissue was homogenized manually through the cell strainer. Cells were washed with PBS, and centrifuged at 1500rpm for 10 mins at room temperature. They were filtered with 70μm strainers, washed, and centrifuged. Each liver cell suspension was resuspended in 6mL of PBS, and layered on 6mL of mouse lympholyte. The gradients were centrifuged at 1500g (acc:1, dec:1) for 25 mins at room temperature. The interphase, representing the enriched LMCs, was collected. The collected interphase was filtered with 40μm strainers, washed, and centrifuged. Cells were counted for downstream experiments.

5.2.5 LSECs and liver mononuclear cell isolation for immunophenotyping

Preparation of liver homogenate was performed as in 5.2.1. Depending on the experiment purpose, Enzyme R in the digestion step was excluded, as NK1.1 was sensitive to digestion. Cells were washed with PBS, and centrifuged at 1500rpm for 10 mins at room temperature. Isotonic Percoll was prepared by diluting 9 parts of stock Percoll and 1 part of 1.5M NaCl solution. 70% Percoll, 40% Percoll, 15% Percoll were prepared by diluting isotonic Percoll with PBS. 3mL of each Percoll concentration was layered carefully on top of each other, forming 15%-40%-70% gradient. After washing and filtering, each liver pellet was resuspended in 3mL of PBS, and layered on 15% of Percoll. Gradients were centrifuged at 1500g (acc:1, dec:1) for 25 minutes at room temperature. The interphase between 15% and PBS represented liver debris, between 15% and 40% represented enriched LSECs and Kupffer cells, between 40% and 70% represented enriched lymphocytes. LSECs/Kupffer cell interphase and lymphocyte interphase were collected independently and washed with PBS. Cells were counted and used for downstream experiments. This protocol allowed the separation of lymphocytes from abundant LSECs and cellular debris. It was only used when clean and enriched liver lymphocytes were required for accurate cell counting and immunophenotyping purposes.

5.2.6 Splenocyte isolation

Spleens were removed from mice and kept in PBS on ice. Spleens were placed in 40µm cell strainers and minced with the syringe plunger. Cells were centrifuged at 1500rpm for 10 mins at room temperature. Each spleen was treated with 3mL of ACK lysis buffer for 3 mins to remove erythrocytes, and filtered through 40 µm cell strainers. They were washed with PBS, centrifuged at 1500rpm for 10 mins at room temperature for two times, and counted for downstream experiments.

5.2.7 Lung single cell suspension preparation

Lungs were removed from mice and kept in PBS on ice. All connective tissue was removed carefully. Lungs were cut in small pieces and digested in digestion media with Enzyme A and Enzyme D using gentleMACS C tubes and gentle MACS Octo dissociator according to the manufacturer's protocol. After digestion, tissue suspension was filtered through 70µm strainer. Undigested tissue was homogenized manually through cell stainer. Cells were washed with PBS, and centrifuged at 1500rpm for 10 mins at 4ºC. Cells were treated with 4mL of ACK lysis buffer for 4 mins to remove erythrocytes, followed by two washing and filtration through 40µm strainers. Lung single cell suspension was counted and used for downstream experiments.

5.2.8 Cell number counting

10 µL of cell suspension was mixed with 10 µL of 0.05% Trypan blue solution (w/v) in a 1:1 ratio. Viable cells were counted using a Neubauer counting chamber (0.1mm depth). Number of viable cells are calculated as:

$$Total\ cell\ number\ per\ mL = \frac{cell\ count}{counted\ squares} \times dilution\ factor \times 10^4$$

5.2.9 LSEC and liver mononuclear cell (LMC) coculture

LMCs were isolated from livers of Rag2 knockout (KO) two days after seeding LSECs. LMCs were resuspended in a concentration of $1x10^6$ cells per mL in primary cell culture media (PCCM) with 1700U/mL of human IL-2. 1mL of LMCs were added to one well of LSECs in a 24-well plate. Plates were briefly centrifuged at 300rpm for 1 min to promote cell contact. LMCs were co-cultured with LSECs for 4 to 20 hours, and then harvested for immunophenotyping experiment.

5.2.10 LSECs co-cultured with sorted NK cells and ILC1s

LSECs were isolated from C57BL6/n mice and cultured. Liver mononuclear cells were isolated from C57BL6/n mice two days after seeding LSECs. They were counted and re-suspended in a concentration of $50x10^6$ per mL in ILC sorting buffer. The Fc receptors were blocked with 10μg/mL of anti-mouse CD16/CD32 for 10 minutes at 4ºC. Cells were stained with FITC-CD200R, PE-TRAIL, APC-Cy7-CD3, BV421-NKp46, BV650-NK1.1, and BV785-CD45 for 20 minutes 4ºC. After that, cells were washed with sorting buffer, centrifuged at 1500rpm for 10 mins at 4ºC. Cells were re-suspended in the sorting buffer and filtered through 5mL Falcon tubes with 35μm strainers. 7-AAD was added before sorting to distinguish live and dead cells. NK cells were sorted as $CD45^+CD3^-NK1.1^+NKp46^+CD200R^-TRAIL^-$, while ILC1s were sorted as $CD45^+CD3^-NK1.1^+NKp46^+CD200R^+TRAIL^+$ cells into PCCM media. Purity was determined after each sorting (>98%). Cells were centrifuged at 1500rpm for 10 mins at 4ºC and resuspended in warm PCCM with 300U/mL of human IL-2. 2-3 $x10^4$ cells in 200uL of PCCM were added into each well of LSECs cultured in 96-well-collagen-coated plate. Cells were briefly centrifuged at 300rpm to ensure NK cells and ILC1s were at the bottom to contact LSECs. After 14-16 hours of coculture, 40pg/mL of IL-12 and 800pg/mL of IL-18 was added. For intracellular IFN-γ detection, Golgi Plug was added after 1 hour of stimulation. After 5-6 hours, cells were harvested and downstream staining was performed.

For trascriptomic analysis, Golgi Plug was omitted after stimulation with IL-12 and IL-18. After 5-6 hours, NK cells were harvested, washed with PBS and centrifuged. Cells were resuspended in the sorting buffer and stained with APC-Cy7-CD3, BV421-NKp46, BV650-NK1.1, and BV785-CD45. 7AAD was added before sorting to distinguish live and dead cells. NK cells were sorted based on size as $CD45^+CD3^-NK1.1^+NKp46^+$ cells into PCCM. Sorted NK cells were then washed two times with PBS in 1.5mL microcentrifuge tubes at 5000rpm for 5 mins. Pellets were lysed for RNA extraction.

5.2.11 Co-culture with transwell inserts

Transwell inserts for 24-well plate were used according to the manufacturer's instruction. $1x10^6$ liver mononuclear cells (LMCs) were resuspended in 100μL of PCCM with 1700U/mL of IL-2, and loaded into the transwell insert that was placed in the well containing 600μL of the media. The experiment was performed for 4 hours to 20 hours. LMCs were harvested from the transwell insert to perform immunophenotyping.

Around 60,000 of sorted NK cells were resuspended in 100µL with PCCM in 300U/mL, and loaded into the transwell insert. After 14-16 hours, IL-12 and IL-18 master mix was added in a ratio of 1:6 into the transwell insert (1 part) and into the well (6 parts), respectively. After 1 hour, Golgi Plug was added. After 5-6 hours of stimulation, NK cells were harvested from the transwell to perform immunophenotyping.

5.2.12 LSEC sorting

Liver non-parenchymal cells (NPCs) were isolated, counted, and re-suspended in a concentration of $50x10^6$ per mL in the LSEC sorting buffer. The Fc receptors were blocked with 10µg/mL of anti-mouse CD16/CD32 for 10 minutes at 4ºC. NPCs were stained with FITC-Stabilin2, PE-Cy7-CD146, PE-TXR-F4/80, APC-IA/IE, APC-Cy7-Ly6G, BV421-CD31, BV650-CD11b, and BV785-CD45 for 20 minutes at 4ºC. After that, cells were washed with the sorting buffer, and centrifuged at 300g for 10 mins at 4ºC. NPCs were resuspended and filtered through 5mL Falcon tubes with 35µm strainers. 7AAD was added before sorting to distinguish live and dead cells. LSECs were defined as $CD45^{-/low}Stabilin2^{high}CD146^{high}CD31^{high}$. MHC II^{high} and MHC $II^{low/-}$ LSECs were sorted. Kupffer cells were sorted as $CD45^{high}Stabilin2^{low/-}Ly6G^{-}F4/80^{high}CD11b^{low}$. Immune cells other than Kupffer cells and LSECs were defined as $CD45^{high}$. Cells were sorted into LSEC media, and washed twice with PBS at 300g for 10 mins at 4ºC. Pellets were lysed for RNA extraction.

5.2.13 RNA extraction

RNA was isolated from pelleted cells using RNeasy® Mini Kit according to the manufacturer's instruction. Cells were lysed in RLT buffer with 1% β-mercaptoethanol, and vortexed for 2 mins. Lysates were stored at -80°C until isolation process. RNA were treated with TURBO DNA-free® Kit to eliminate genomic DNA contamination according to the manufacturer's protocol. For certain experiments, isolated RNA was concentrated with Zymo Research RNA Clean & Concentrator kit according to the manufacturer's procedure. RNA concentration was measured using TECAN instrument.

5.2.14 cDNA synthesis and real-time quantitative reverse transcription polymerase chain reaction (RT-PCR)

First strand cDNA was synthesized from 100 - 1000 ng of total RNA using ProtoScript® II First Strand cDNA Synthesis Kit using either Oligo d(T)23VN or random primer mix, depending on the target

transcripts. RT-PCR was performed in a QuantStudio™ 5 Real-Time 384-well PCR System, using PowerUp™ SYBR™ Green Master Mix. Primer efficiency was determined to be between 90% and 110% by obtaining standard curves of positive cDNA control with serial dilution. The program was run at 50ºC for 2 mins, 95ºC for 2 mins, 40 cycles of amplification at 95ºC for 1s and 60 ºC for 30 secs, and melt cult stage at 95ºC for 15s, 60ºC for 1 min, 95ºC for 15s. The gene expression was quantified using ΔΔCT (cycle threshold) method with using beta-actin (*Actb*) as the reference.

5.2.15 Gene expression analysis

Gene expression

Extracted RNA was processed by the bioinformatics core facility of Medical Faculty Mannheim. RNA was tested by capillary electrophoresis on an Agilent 2100 bioanalyzer (Agilent) and high-quality RNA samples were selected for experiment (RIN ≥ 7). Gene expression profiling was performed using Affymetrix GeneChip™ Mouse Gene 2.0 ST Arrays. Biotinylated antisense cDNA was then prepared according to the Affymetrix standard labelling protocol with the GeneChip® WT Plus Reagent Kit and the GeneChip® Hybridization, Wash and Stain Kit (both from Affymetrix, Santa Clara, USA). Afterwards, the hybridization was performed on a GeneChip Hybridization oven 640, then dyed in the GeneChip Fluidics Station 450 and thereafter scanned with a GeneChip Scanner 3000. All of the equipment used was from the Affymetrix-Company (Affymetrix, High Wycombe, UK).

Bioinformatics

A Custom CDF Version 21with ENTREZ based gene definitions was used to annotate the arrays (Dai et. al, 2005). The Raw fluorescence intensity values were normalized applying quantile normalization and RMA background correction. OneWay-ANOVA was performed to identify differential expressed genes using a commercial software package SAS JMP10 Genomics, version 6, from SAS (SAS Institute, Cary, NC, USA). A false positive rate of a=0.05 with FDR correction was taken as the level of significance.

5.2.16 Mouse genotyping

Mouse tails or ear punches were collected and lysed with MyTaq Extract-PCR Kit according to the manufacturer's protocol with slight modifications. PCR was performed with the optimized concentration of

primers, MyTaq HS Red Mix, and water, and run in Thermocylers with optimized conditions. PCR products were separated on 1.5-2% of Agarose Gel.

5.2.17 Flow cytometry staining and analysis

Surface staining

Cells were harvested from the culture or single cell suspensions from organs. $10^5 – 10^6$ cells were transferred into a 96 well round-bottom plate, centrifuged at 2100rpm for 4 mins at 4ºC. Each well was resuspended with 30uL of PBS containing 0.3uL of Aqua Zombie, and incubated for 15-20 mins at room temperature. 20uL of Fc block solution was added to each well and incubated for 15 mins at 4ºC. After that, 50mL of FACS buffer (or Brilliant Stain Buffer if both BV and BUV fluorochromes were used) containing a master mix of pre-titrated surface antibody was added to each well and incubated for 20 mins at 4ºC in the dark. Cells were then washed twice with FACS buffer. Depending on the purpose, if Aqua Zombie was not used for dead cell exclusion, 7AAD was added before acquisition.

Intracellular staining

After surface staining, cells were fixed with 200uL of Fixed/Perm concentrate, solution containing (3 parts) and diluent (1 part) (FoxP3 Transcription Factor Staining Buffer Set, ebioscience) at 4ºC for 35-60 minutes. Cells were then washed and incubated in 1 to 1 mixture of Perm buffer and Fc block solution for 15 mins. Next, master mix of pre-titrated intracellular antibodies diluted in Perm buffer was added and incubated for 20-30 mins at 4ºC in the dark. Cells were then washed twice with Perm buffer, and re-suspended in 200uL of FACS buffer before analysis.

5.2.18 Flow cytometry analysis

Samples were acquired with LSR Fortessa, or FACSAria fusion if BUV dyes were used. Data were analyzed with Flowjo™ v10.8. Gating strategy was as follow.

LSECs	$CD45^{-/low}Stabilin2^{high}CD146^{high}CD31^{high}$
LSECs after culture	$CD45^{-}CD146^{+}$
Kupffer cells	$CD45^{high}Stabilin2^{-/low}Ly6G^{-}F4/80^{high}CD11b^{low}$

Inflitrating monocytes	$CD45^{high}Stabilin2^{-/low}Ly6G^{-}CD11b^{high}F4/80^{low}$
Dendritic cells	$CD45^{high}Stabilin2^{-/low}Ly6G^{-}CD11c^{high}MHCII^{high}$
B cells /Plasmacytoid Dendritic cells	$CD45^{high}Stabilin2^{-/low}Ly6G^{-}CD3^{-}NK1.1^{-}B220^{high}$
Lung ECs	$CD45^{-}CD31^{high}$
ILC1s	$CD45^{high}Ly6G^{-}CD3\varepsilon^{-}NK1.1^{high}NKp46^{+}CD200R^{+}/CD49a^{+}/CXCR6^{+}/TRAIL^{+}$
NCR^{-} ILCs	$CD45^{high}Ly6G^{-}CD3\varepsilon^{-}NK1.1^{-}NKp46^{-}CD127^{+}$
NK cells	$CD45^{high}$ $CD3\varepsilon^{-}NK1.1^{+}NKp46^{+}Eomes^{+}$
NKT cells	$CD45^{high}Ly6G^{-}CD3\varepsilon^{+}TCR\beta^{int}NK1.1^{int}$
$CD4^{+}$ T cells	$CD45^{high}Ly6G^{-}CD3\varepsilon^{+}TCR\beta^{high}NK1.1^{-}CD4^{+}$
$CD8^{+}$ T cells	$CD45^{high}Ly6G^{-}CD3\varepsilon^{+}TCR\beta^{high}NK1.1^{-}CD8^{+}$
$CD4^{+}$ T_{EM}	$CD45^{high}Ly6G^{-}CD3\varepsilon^{+}TCR\beta^{high}NK1.1^{-}CD4^{+}CD44^{+}CD62L^{-}$
$CD4^{+}$ T_{N}	$CD45^{high}Ly6G^{-}CD3\varepsilon^{+}TCR\beta^{high}NK1.1^{-}CD4^{+}CD44^{-}CD62L^{+}$
$CD4^{+}$ Treg	$CD45^{high}Ly6G^{-}CD3\varepsilon^{+}TCR\beta^{high}NK1.1^{-}CD4^{+}FoxP3^{+}$
$CD8^{+}$ T_{EM}	$CD45^{high}Ly6G^{-}CD3\varepsilon^{+}TCR\beta^{high}NK1.1^{-}CD8^{+}CD44^{+}CD62L^{-}$
$CD8^{+}$ T_{N}	$CD45^{high}Ly6G^{-}CD3\varepsilon^{+}TCR\beta^{high}NK1.1^{-}CD8^{+}CD44^{-}CD62L^{+}$
γδ T cells	$CD45^{high}Ly6G^{-}CD3\varepsilon^{+}TCR\beta^{-}TCR\gamma^{+}$

5.2.19 Graphs and analysis

Graphs were generated using GraphPad PRISM version 7.04. Appropriate statistical analysis was computed using the statistical tests included in the PRISM. Data were considered significant if $*P < 0.05$, $**P < 0.01$, $***P < 0.001$.

6 Results

6.1 LSEC phenotypes

6.1.1 LSECs express surface molecules involved in immunology in steady-state

LSECs have been shown to modulate T cell functions by expressing various cell surface membrane proteins involved in immune responses (Wohlleber & Knolle, 2016). In addition, sinusoids are proposed to retain immune cells, and LSECs can interact closely with immune cells. Therefore, I first started by screening membrane proteins which were reported to modify NK cell, ILC1, and T cell functions. Gating strategy of LSECs was illustrated (Fig. 6.1 a). In steady-state, LSECs expressed many membrane proteins which are involved in immune responses, including MHC I, PD-L1, HVEM, and CD155 (Fig. 6.1 b). However, LSECs did not express RAE1, MULT1, and H60 in steady-state, which are the ligands of NKG2D (Fig. 6.1 c). The expression of receptors and ligands on different cells were listed in Table 6.1.

a

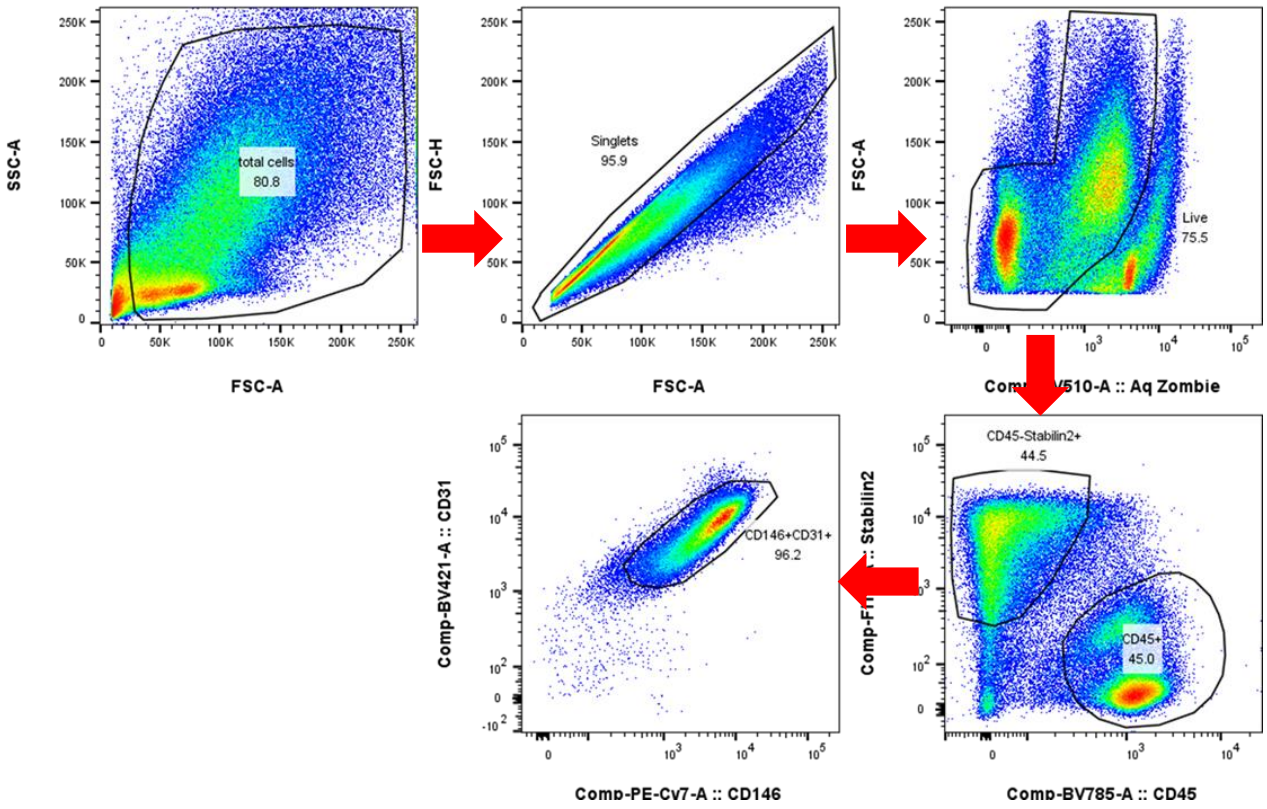

(Figure legend on the next page)

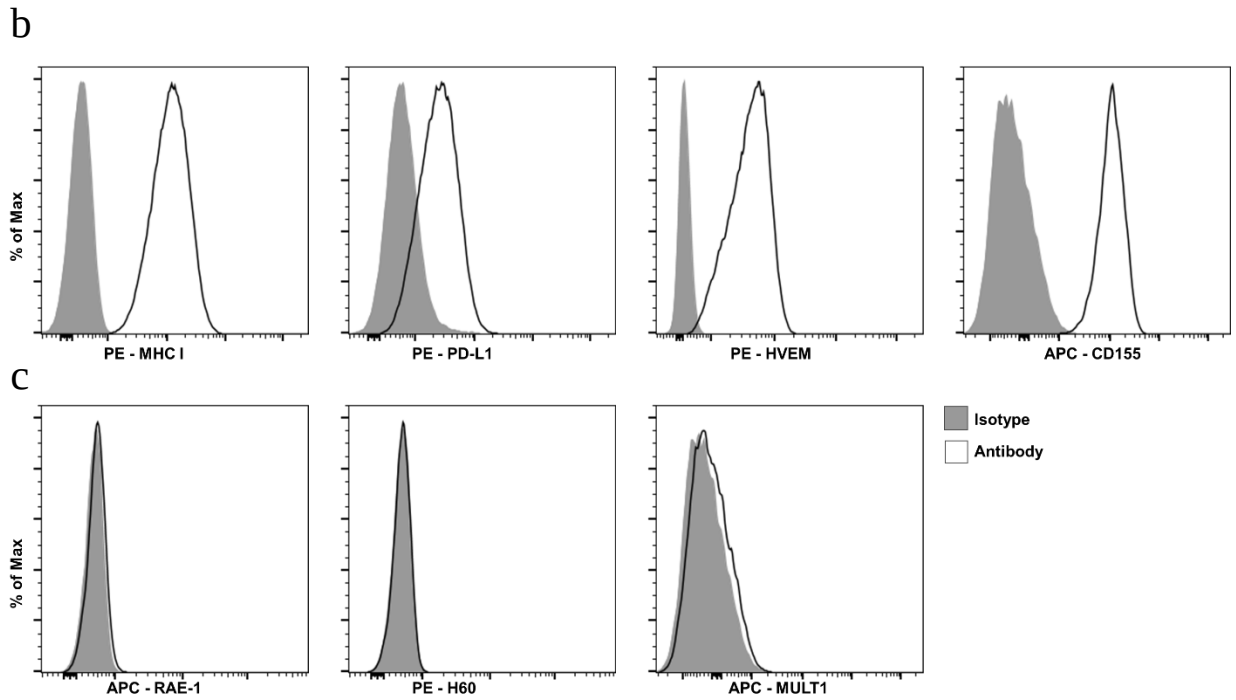

Fig. 6.1 - LSECs express surface molecules involved in immunology in steady-state. Liver non-parenchymal cells (NPCs) were isolated and analyzed with flow cytometry. **a**, Gating strategy used to define LSECs. LSECs were defined as $CD45^{-/low}Stabilin2^{high}CD146^{high}CD31^{high}$.**b**, Representative histograms of MHC I, PD-L1, HVEM, and CD155 expression on LSECs. **c**, Representative histograms of mouse NKG2D ligands: RAE,1 H60, and MULT1 expression on LSECs. Gray and white histograms depict isotype control staining and protein staining, respectively. Data shown are representative of at least two independent experiments.

Ligands on LSECs	Receptors	Cellular Distributions of Receptors
MHC I	Ly49	NK cells, ILC1s
PD-L1, can also function as a receptor	PD-1	Activated NK cells, ILC1s, T cells, myeloid cells
HVEM, can also function as a receptor	CD160, BTLA	NK cells, ILC1s, T cells
CD155, can also function as a receptor	DNAM-1, TIGIT	
RAE1	NKG2D	
MULT1		
H60		

Table 6.1. Membrane proteins screened on LSECs and their cognate ligands on immune cells.

6.1.2 IFN-γ modulates HVEM, PD-L1 and MHC I expression on LSECs

NK cells and ILC1s produce IFN-γ upon activation with cytokines or receptors. I hypothesized that NK cells and ILC1s could affect LSEC surface protein expression through the production of IFN-γ. Thus, I stimulated LSECs *in vitro* with IFN-γ. Indeed, LSECs upregulated MHC I, PD-L1, and HVEM protein expression after stimulation with IFN-γ, while CD155 expression remained unchanged (Fig. 6.2 a). LSECs also did not express RAE1, MULT1, and H60 expression after stimulation with IFN-γ (Fig. 6.2 b).

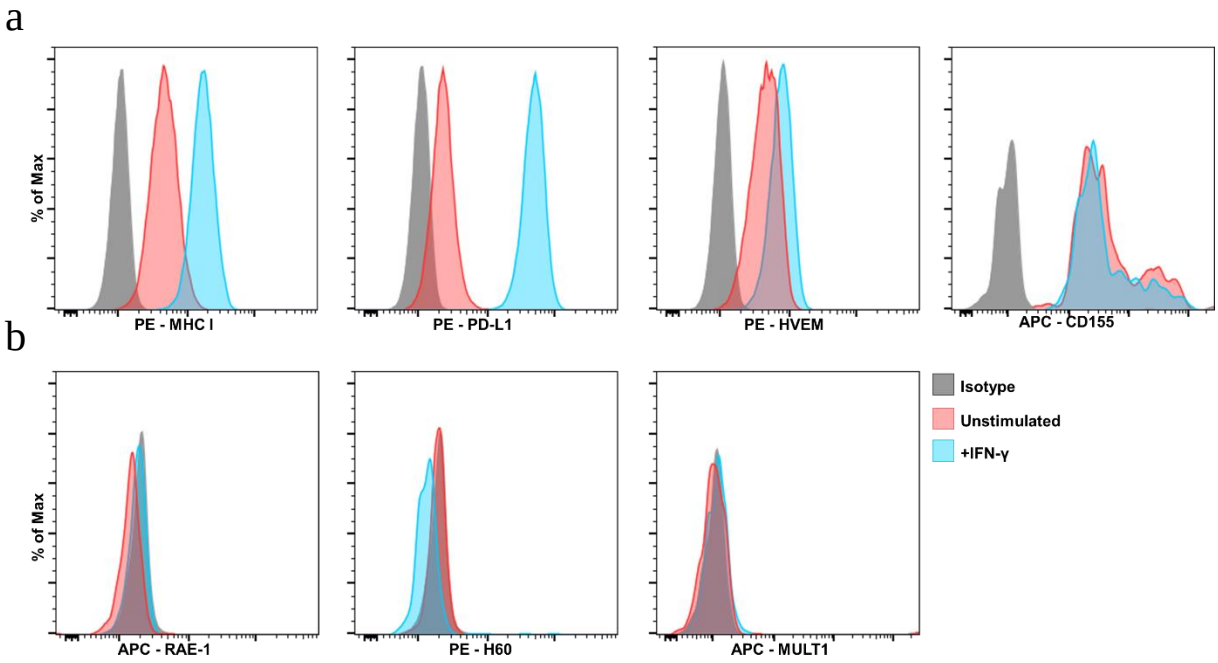

Fig. 6.2 - IFN-γ upregulates MHC I, PD-L1, and HVEM expression on LSECs. **a-b**, $CD146^{+}$ LSECs were magnetically purified and stimulated with IFN-γ for 24 hours. After stimulation, LSECs were detached, stained, and analyzed with flow cytometry. **a**, Representative histograms of MHC I, PD-L1, HVEM, and CD155 expression on LSECs. **b**, Representative histograms of RAE-1, H60, and MULT1 expression on LSECs. Data shown are representative of at least two independent experiments.

6.2 MHC II on LSECs

6.2.1 MHC II expression on LSECs

It was reported that LSECs constitutively express MHC II and regulate $CD4^+$ T cell polarization (Knolle & Wohlleber, 2016). Nevertheless, the expression pattern of MHC II on LSECs in different zones of the liver has not been investigated in detail. Hence, I analyzed MHC II expression on LSECs using flow cytometry. I observed that LSECs expressed heterogeneous and higher amounts of MHC II compared to venous ECs in the liver, but at a lower amount compared to Kupffer cells (KCs) (Fig. 6.3 a). Midzonal and pericentral LSECs were reported to express Lyve1 and Endomucin, respectively, using microscopy imaging (Leibing et al., 2018). Thus, I used these two markers to identify LSECs from periportal, midzonal, and pericentral acini (Fig. 6.3 b). I observed that the expression of $Lyve1^+$ midzonal marker correlated positively with MHC II expression on LSECs (Fig. 6.3 c). Accordingly, $Lyve1^+$ midzonal LSECs expressed the highest amount of MHC II, followed by $Endomucin^{high}$ pericentral LSECs and $Endomucin^{low}$ periportal LSECs (Fig. 6.3 c).

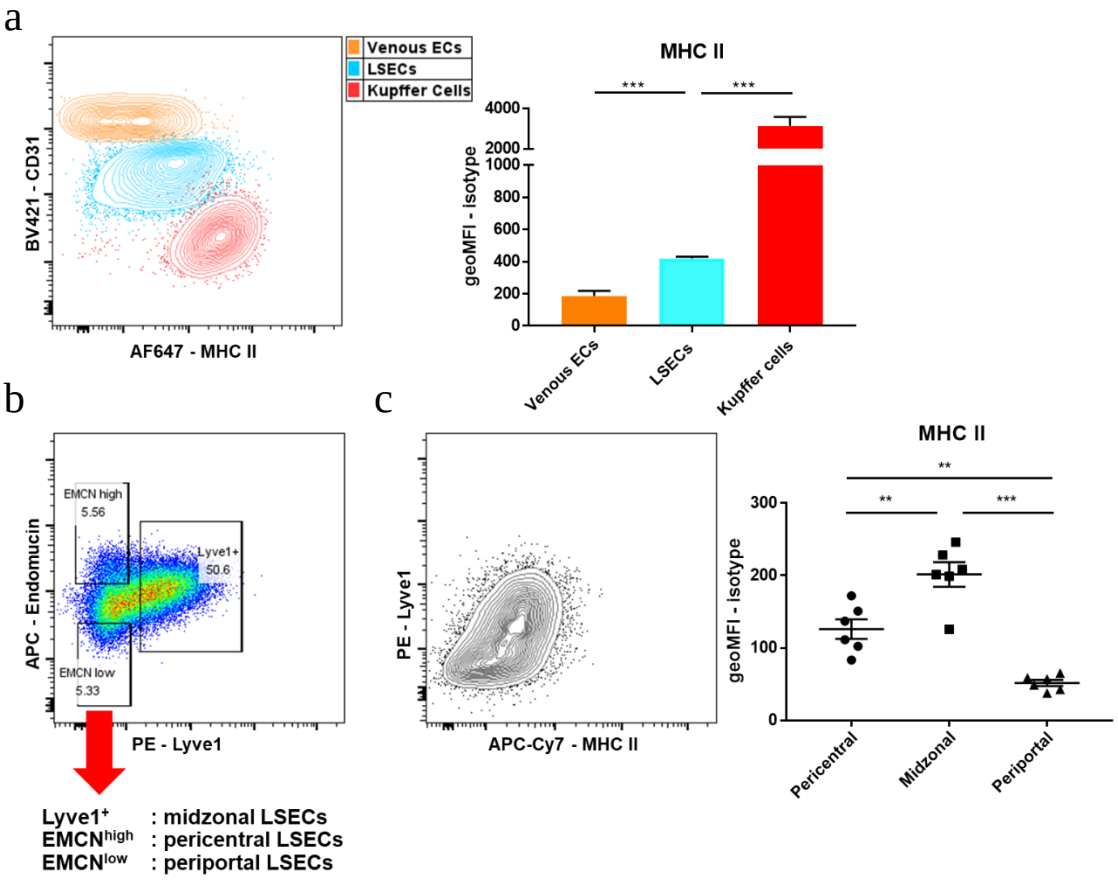

(Figure legend on the next page)

Fig. 6.3 - Midzonal LSECs express the highest amount of MHC II. **a-c**, Liver non-parenchymal cells (NPCs) were isolated and analyzed with flow cytometry for MHC II in steady-state. Venous ECs were defined as $CD45^{-/low}CD31^{bright}$, LSECs were defined as $CD45^{-/low}Stab2^{high}CD31^{high}CD146^{high}$, and Kupffer cells (KCs) were defined as $CD45^{high}Stabilin2^{-/low}Ly6G^{-}F4/80^{high}CD11b^{low}$. MHC II expression on venous EC, LSECs, and KCs was quantified by geometric Mean Fluorescence Intensity of the protein staining minus the respective isotype control staining (geoMFI-isotype). **a**, Representative contour plot of MHC II expression of venous ECs, LSECs, and KCs, and quantification (n = 3 per group). **b**, Gating strategy of LSECs from pericentral, midzonal, and periportal acini using Lyve1 and Endomucin. **c**, Co-staining of Lyve-1 and MHC II, and quantification of MHC II expression on pericentral, midzonal, and periportal LSECs (n = 5 per group). For all graphs, data are represented as mean ± SEM. Groups were analyzed by one-way ANOVA (**a, c**). $^{**}P < 0.01$, $^{***}P < 0.001$.

6.2.2 MHC II defines a unique subset of LSECs

Next, I sorted MHC II^{high} and MHC II^{low} LSECs with flow cytometer and performed transcriptomic analysis using microarray technology (Fig. 6.4 a). MHC II^{high} and MHC II^{low} LSECs had a distinct transcriptomic profile (Fig. 6.4 b). MHC II^{high} LSECs were enriched in MHC II-related transcripts (*H2-Eb1*, *H2-Aa*, *H2-Ab1*, *CD74*, *Ctss*), *Cxcl9* and *Cxcl10* (Fig. 6.4 c). As MHC II genes are involved in antigen-presentation (Roche & Furuta, 2015), and CXLC9 and CXLC10 are involved in chemotaxis (Metzemaekers, Vanheule, Janssens, Struyf, & Proost, 2018), MHC II^{high} LSECs appeared to show a more 'immune-like' phenotype. One of the midzonal marker, *Lyve1*, was also enriched in MHC II^{high} LSECs, confirming my previous data that $Lyve1^{+}$ midzonal LSECs expressed highest amounts of MHC II.

a

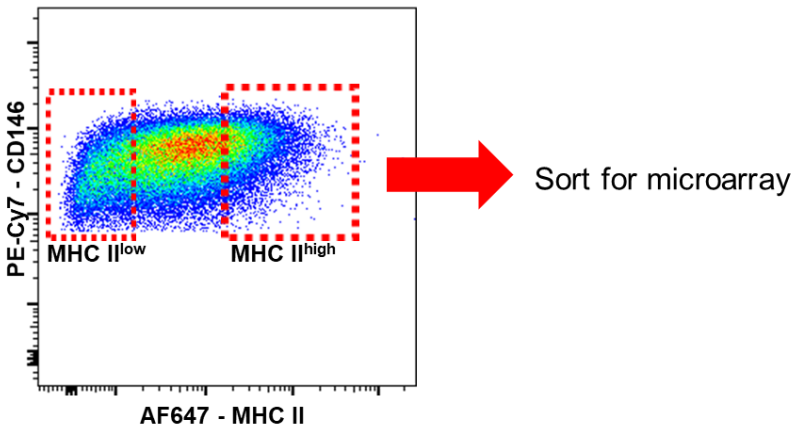

(Figure legend on the next page)

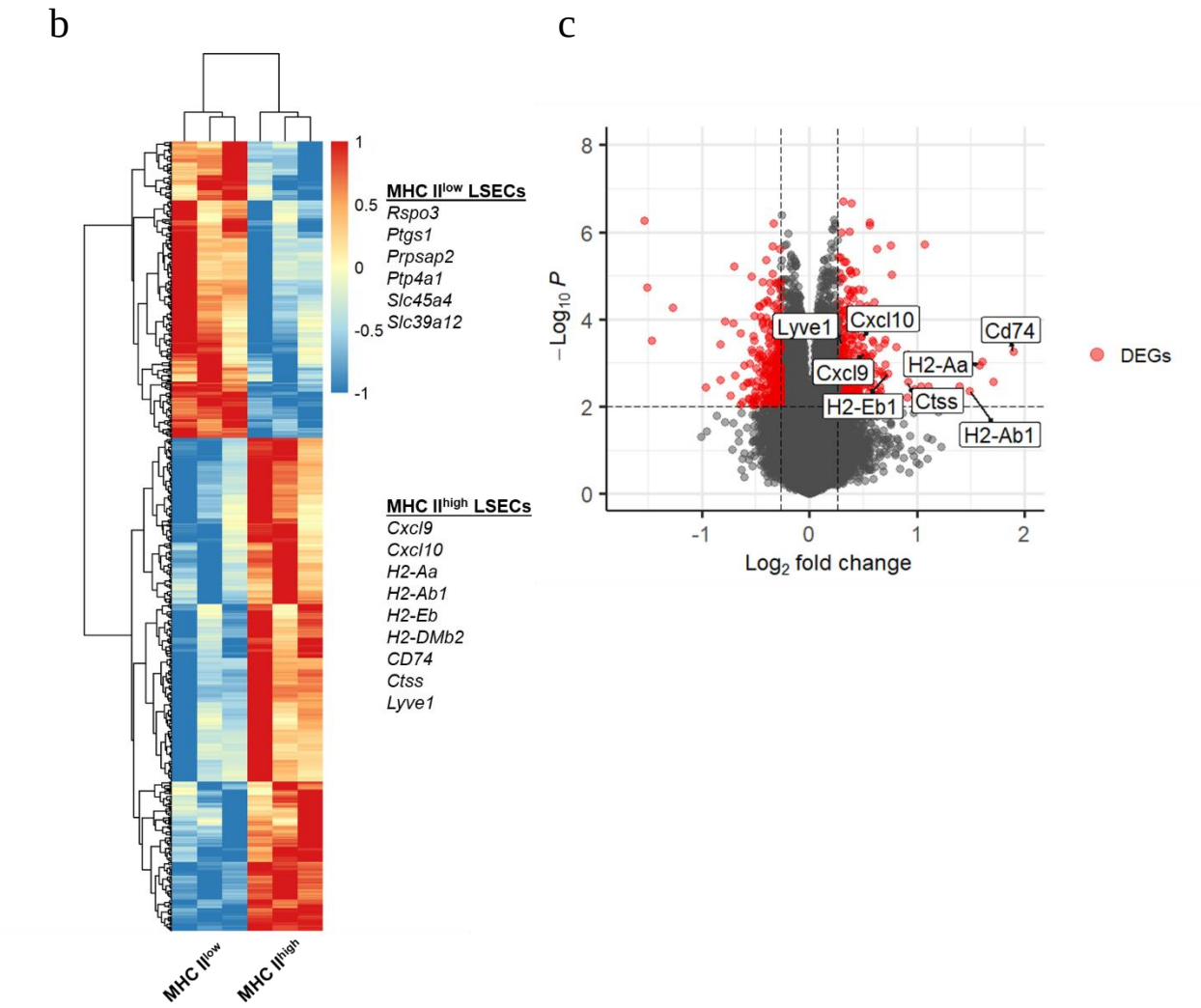

Fig. 6.4 - MHC II^{high} and MHC II^{low} LSECs are transcriptionally distinct. **a**, MHC II^{high} and MHC II^{low} LSECs were sorted with a flow cytometer for transcriptomic analysis with microarray technology. **b**, Heatmap of differentially regulated transcripts between MHC II^{high} and MHC II^{low} LSECs. Some enriched transcripts involved in immune responses, metabolic processes, and liver development with fold-change ≥ ±1.2 are listed. **c**, Volcano plots depicting *P*-value vs $\log_2$ fold change, and differentially regulated genes (DEGs) of MHC II^{high} LSECs vs MHC II^{low} LSECs.

6.3 Regulation of MHC II expression on LSECs

6.3.1 The role of IFN-γ in regulating MHC II expression on LSECs

I performed Ingenuity Pathway Analysis to predict the upstream regulators of DEGs in MHC II^{high} and MHC II^{low} LSECs (Fig. 6.5 a). IFN-γ was predicted to be one of the upstream regulators of DEGs in MHC II^{high} LSECs. IFN-γ is shown to regulate MHC II expression (Wosen, Mukhopadhyay, Macaubas, & Mellins, 2018). In order to investigate the role of IFN-γ in LSECs, I first neutralized IFN-γ *in vivo* for 28 days and examined MHC II expression on LSECs. While there was no change in the percentage of LSECs expressing MHC II, the mean fluorescence intensity (MFI) of MHC II was significantly reduced on LSECs in mice with neutralization of IFN-γ, compared to LSECs in control mice (Fig. 6.5 b-c). To further investigate the role of IFN-γ, I analyzed MHC II expression on LSECs in Ifnγ KO and Ifnγr KO mice. LSECs from Ifnγ KO and Ifnγr KO mice had a significant reduction of MHC II expression in both percentage and MFI (Fig. 6.5 d-e), compared to LSECs from WT mice. Different results between mice treated with anti-IFN-γ antibody and Ifnγ KO/Ifnγr KO mice suggest that IFN-γ could have a developmental role in the MHC II expression on LSECs.

a

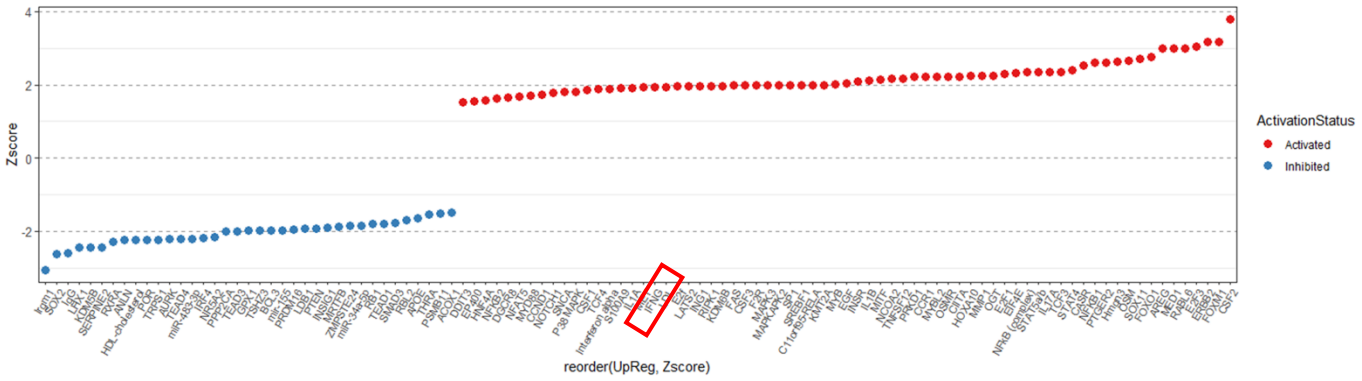

b

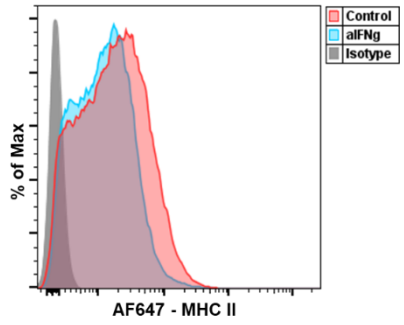

c

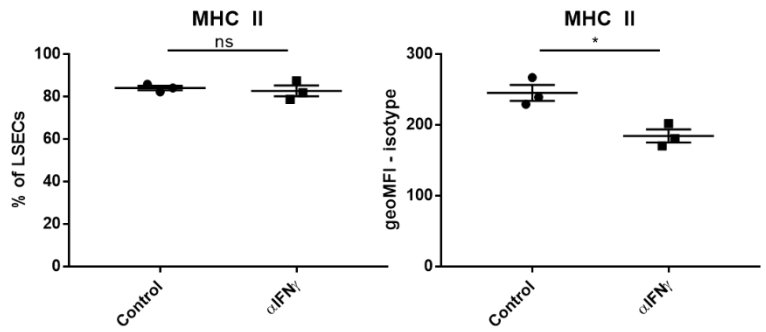

Figure legend on the next page)

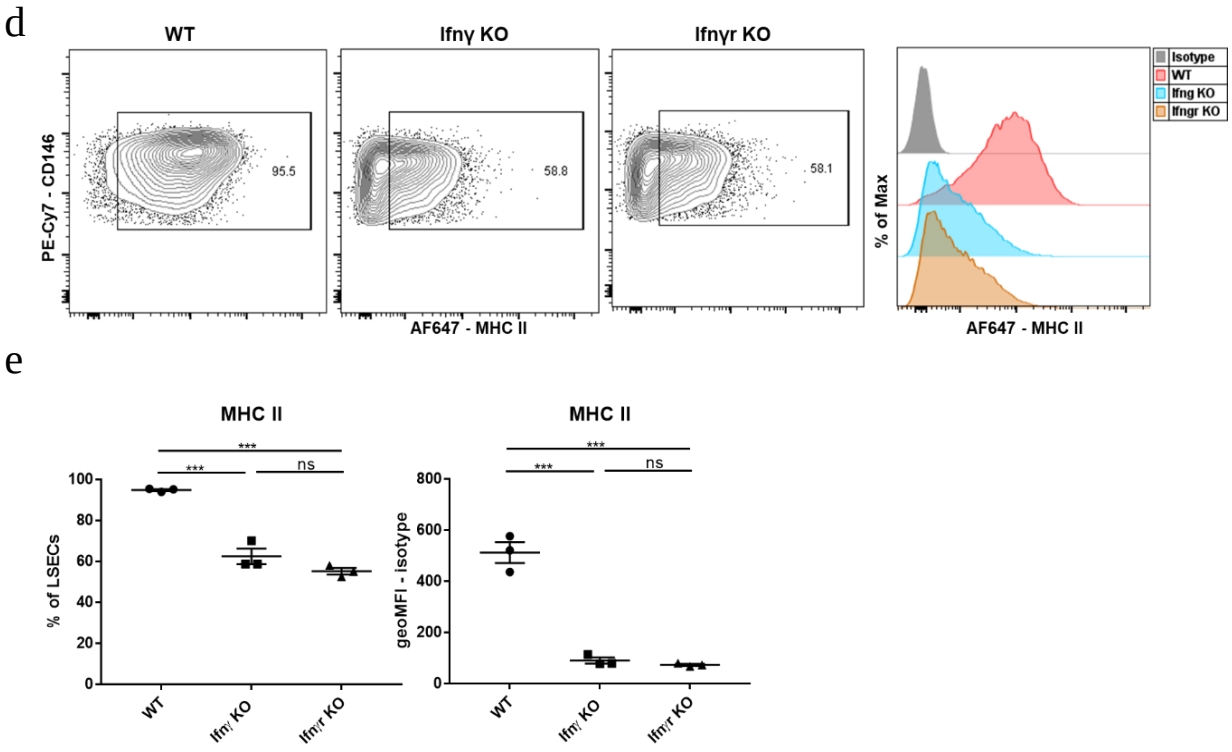

Fig. 6.5 - IFN-γ maintains MHC II expression on LSECs. **a**, Differentially expressed genes (DEGs) of MHC II^{high} and MHC II^{low} LSECs were subjected to Ingenuity Pathway Analysis to predict the upstream regulators. Highlighted in red shows IFN-γ to be the upstream regulator of DEGs in MHC II^{high} LSECs. **b-c**, Mice were treated with anti-IFN-γ antibody (200µg per mouse) or PBS, *i.p.* injection, for 28 days (Day-0, 2, 4, 7, 10, 14, 17, 21, 24 & 26). LSECs were analyzed with flow cytometry for MHC II expression. Representative contour plots and histograms of MHC II expression, and its quantification on LSECs (n = 3 per group). **d-e**, Liver NPCs were isolated from C57BL/6j (WT), Ifnγ KO, and Ifnγr KO mice and analyzed with flow cytometry for MHC II expression. Representative contour plots and histograms of MHC II expression, and its expression on LSECs (n = 3 per group). For all graphs, data are represented as mean ± SEM. Groups were analyzed by Student's t-test (**c**) and one-way ANOVA (**e**). *$P < 0.05$, ***$P < 0.001$, ns - not significant.

I also compared the effect of IFN-γ on MHC II expression between LSECs and liver professional APCs. Around 35% of LSECs from Ifnγ KO and Ifnγr KO mice did not express MHC II, compared to LSECs of WT mice (Fig. 6.5 e). In contrast, around 95% of liver KCs from Ifnγ KO and Ifnγr KO mice still expressed MHC II, compared to KCs of WT mice (Fig. 6.6 a-b). MHC II expression on liver dendritic cells and B cells was unaffected in Ifnγ KO and Ifnγr KO mice (Fig. 6.6 b). Furthermore, I also analyzed MHC II expression on lung ECs. All lung ECs from Ifnγ KO and Ifnγr KO mice still expressed MHC II, but at a lower amount compared to WT mice (Fig. 6.6 c-d). These data indicate that the absence of IFN-γ affected MHC II expression in LSECs the most, compared to other ECs and APCs.

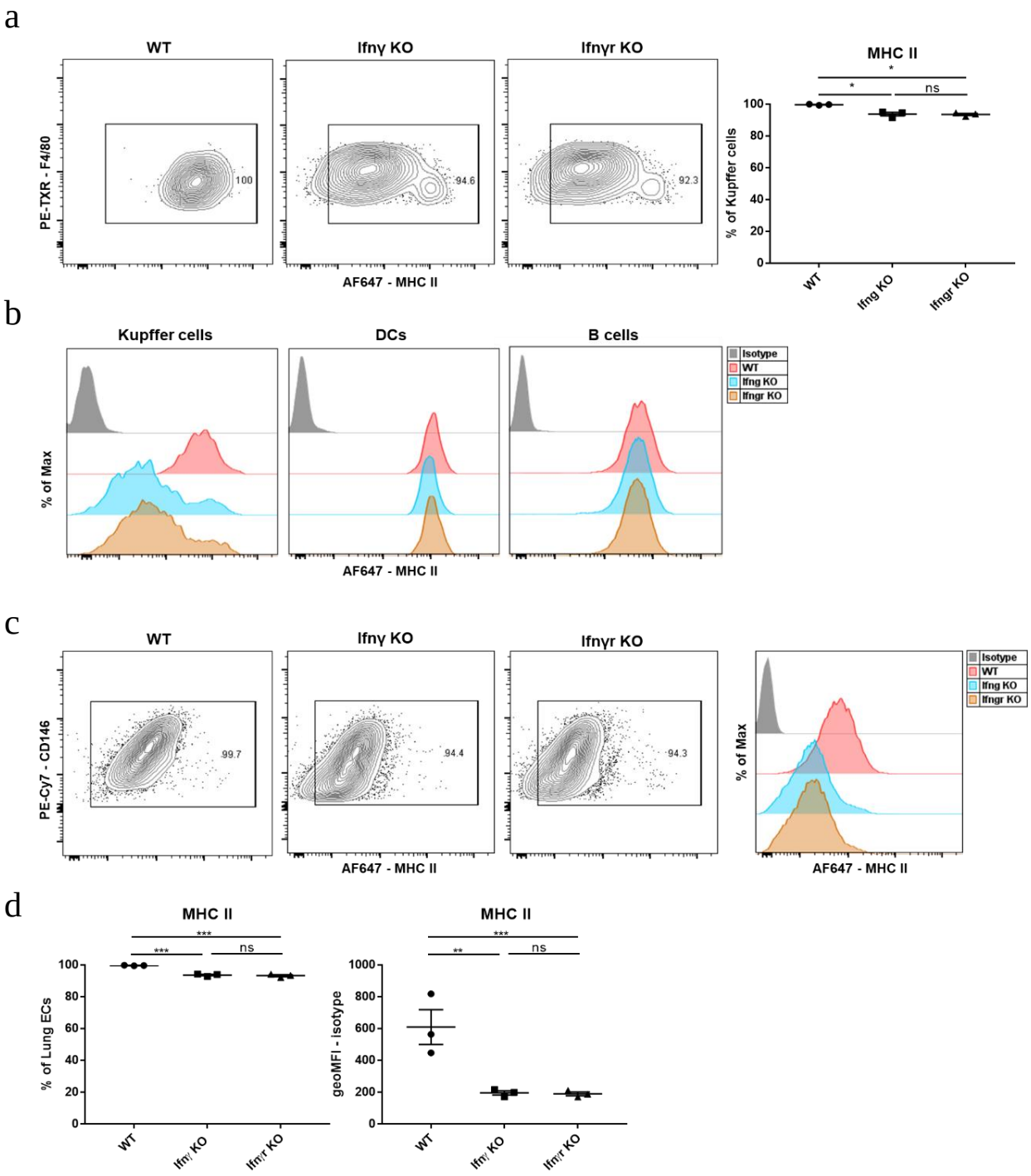

Fig. 6.6 - The absence of IFN-γ affects MHC II expression on Kupffer cells and lung ECs, but not B cells. Liver NPCs were analyzed with flow cytometry for MHC II expression. **a**, Representative contour plots of MHC II expression and its quantification on KCs (n = 3 mice per group). **b**, Representative histograms of MHC II expression on KCs, DCs and B cells (n = 3 mice per group). **c-d**, Representative contour plots and histograms of MHC II expression and its quantification on lung ECs (n = 3 per group). For all graphs, data are represented as mean ± SEM. Groups were analyzed by one-way ANOVA (**a**, **e**). $*P < 0.05$, $**P < 0.01$, $***P < 0.001$, ns - not significant.

Next, I purified and cultured LSECs to determine if IFN-γ affects MHC II expression. LSECs *in vitro* did not express MHC II after 2-day culture, and re-expressed MHC II after 24-hour of stimulation with IFN-γ (Fig. 6.7 a), further showing the crucial role of IFN-γ in maintaining MHC II expression. Besides, I also stimulated LSECs from Ifnγ KO and Ifnγr KO with IFN-γ to examine whether they can re-express MHC II *in vitro*. LSECs from Ifnγ KO could re-express MHC II, while LSECs from Ifnγr KO did not re-express MHC II after IFN-γ stimulation (Fig. 6.7 b). These data suggest that LSECs from Ifnγ KO were able to express MHC II when stimulated with IFN-γ, comparable to IFN-γ-stimulated LSECs from WT mice.

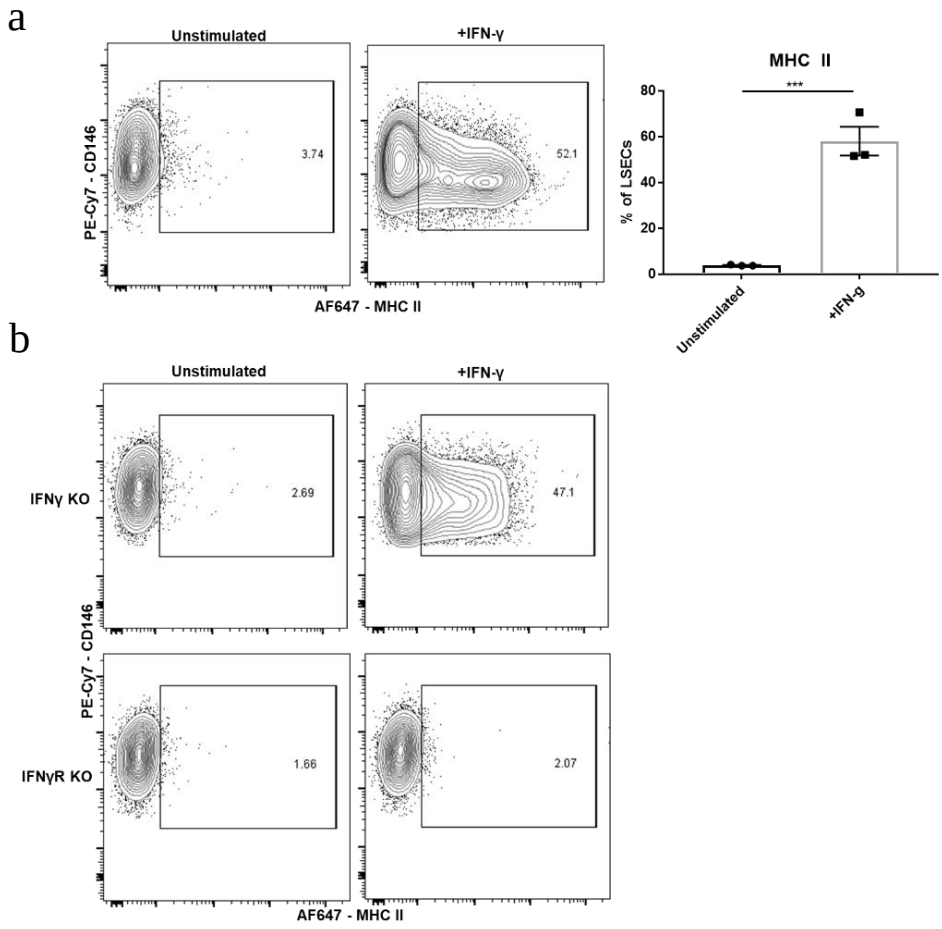

Fig. 6.7 - LSECs in the *in-vitro* culture re-express MHC II after stimulation with IFN-γ. LSECs were purified by magnetic separation using CD146 microbeads. On the next day, LSECs were either unstimulated or stimulated with 100ng/mL of IFN-γ for 24 hours. After stimulation, LSECs were harvested and analyzed with flow cytometry for MHC II expression. **a**, Representative contour plots of MHC II and its quantification on LSECs. Each dot represents one independent experiment. **b**, LSECs were purified from Ifnγ KO and Ifnγr KO mice, cultured, stimulated with IFN-γ, and analyzed with flow cytometry for MHC II expression. Data shown are representative of two independent experiments. For all graphs, data are represented as mean ± SEM. Groups were analyzed by Student t-test (**a**). ***$P < 0.001$, ns - not significant.

6.3.2 The source of IFN-γ in steady-state

As IFN-γ was important for the MHC II expression on LSECs, I sought to determine the cellular source of IFN-γ in the liver in steady state. To address this question, I used IFN-γ reporter mice, which contain an IRES-eYFP reporter cassette between the translational stop codon and 3'UTR/polyA tail of the *Ifng* gene (Sanmarco et al., 2021). I observed that around 30% of $Lin^{-}CD45^{+}$ immune cells produced IFN-γ in steady state (Fig. 6.8 a). Among the $Lin^{-}CD45^{+}$ population, NKT cells were the major IFN-γ producing cells, constituting around 50% of the population (Fig. 6.8 a-b). ILC1s were the second major IFN-γ producing source (~20%), followed by NK cells (~10%), and the rest were T cells. Qualitatively, ILC1s had the highest IFN-γ YFP expression, indicating that ILC1s produced the highest amount of IFN-γ in steady-state (Fig. 6.8 c-d), followed by NKT cells, NK cells, γδ T cells, $CD8^{+}$ T cells and $CD4^{+}$ T cells. Thus, NKT cells, ILC1s, NK cells appeared to be the major IFN-γ producers in the liver in the steady state.

a

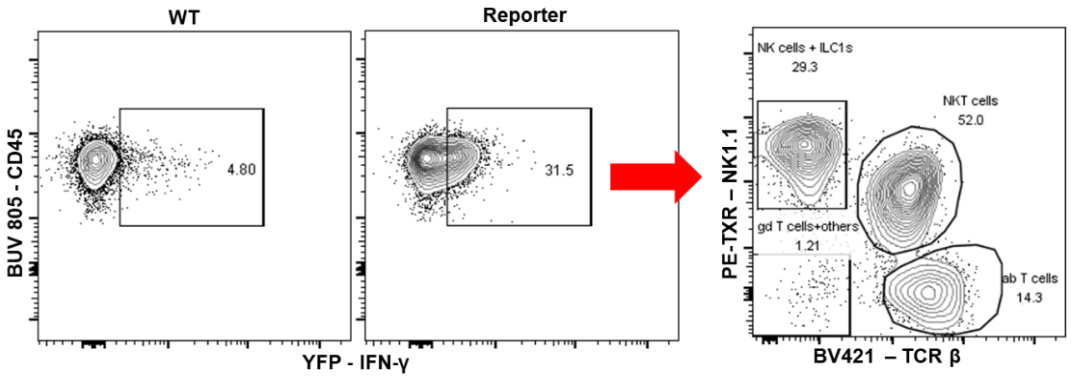

b

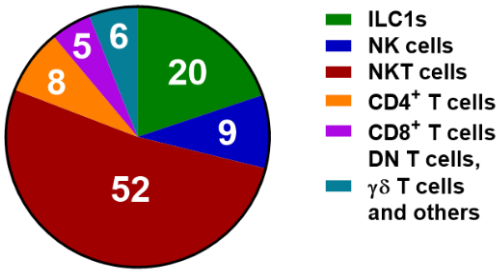

(Figure legend on the next page)

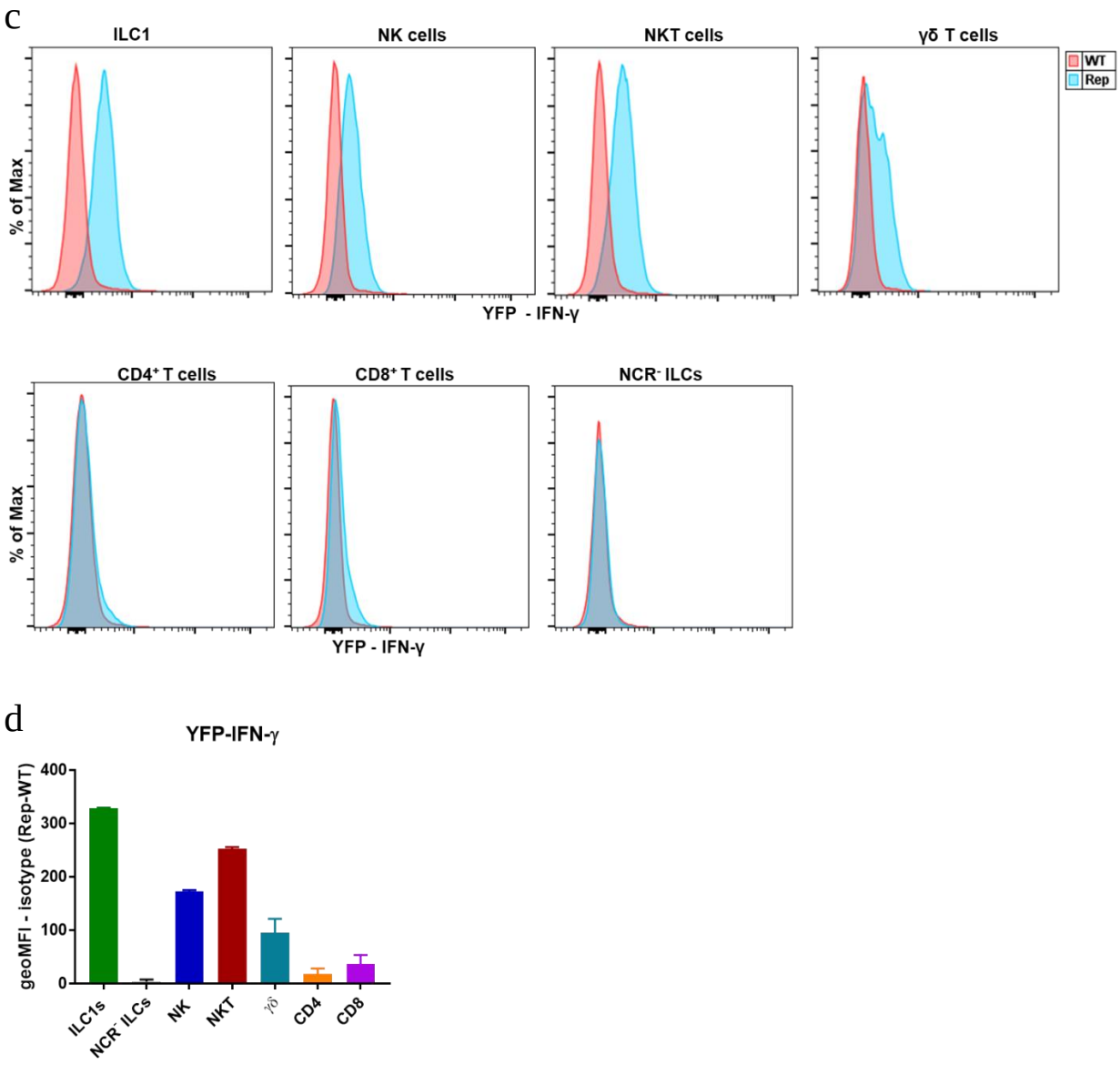

Fig. 6.8 - ILC1s, NK cells and NKT cells are the major cellular sources of IFN-γ in the liver in steady state. Liver mononuclear cells from *Ifng*-YFP reporter mice were isolated and analyzed with flow cytometry. **a**, Contour plots depicting YFP expression in the $Lin^{-}CD45^{+}$ immune cell population. WT mice were used as the control. YFP^{+} population was gated and separated into NK cells and ILC1s, NKT cells, and αβ T cells. **b**, Pie chart illustrating percentages of different cell populations in the gated $Lin^{-}CD45^{+}YFP^{+}$ immune cells. **c-d**, Different immune cell populations were gated and the YFP expression was analyzed. Representative histograms of YFP expression in each immune cell population using WT mice as the control, and quantification of the YFP expression. Data are representative of 2 individual mice (**a-b**).

As *Ifng*-YFP reporter mice showed that ILC1s, NK cells, and NKT cells were the major producers of IFN-γ in the steady-state in the liver, I used different KO models to dissect the contribution of each immune cell subset in producing IFN-γ. Hobit KO mice lack ILC1s (Mackay et al., 2016), thus I used Hobit KO mice as the ILC1-deficient model. Lacking ILC1s alone did not affect MHC II expression on LSECs (Fig. 6.9 a-b). Next, I used Rag2 KO, mice which are devoid of T and B cells, and Rag2γc double knockout (DKO), which are devoid of all lymphocytes. While LSECs from Rag2 KO mice did not show any changes in their MHC II expression, LSECs from Rag2γc DKO mice had a reduction in the percentage and MFI of MHC II expression, compared to LSECs from WT mice (Fig. 6.9 c-d). LSECs from Rag2γc DKO mice reproduced a similar phenotype as observed in Ifnγ KO and Ifnγr KO. This suggests that only the lack of all lymphocytes leads to significant reduction of MHC II expression on LSECs.

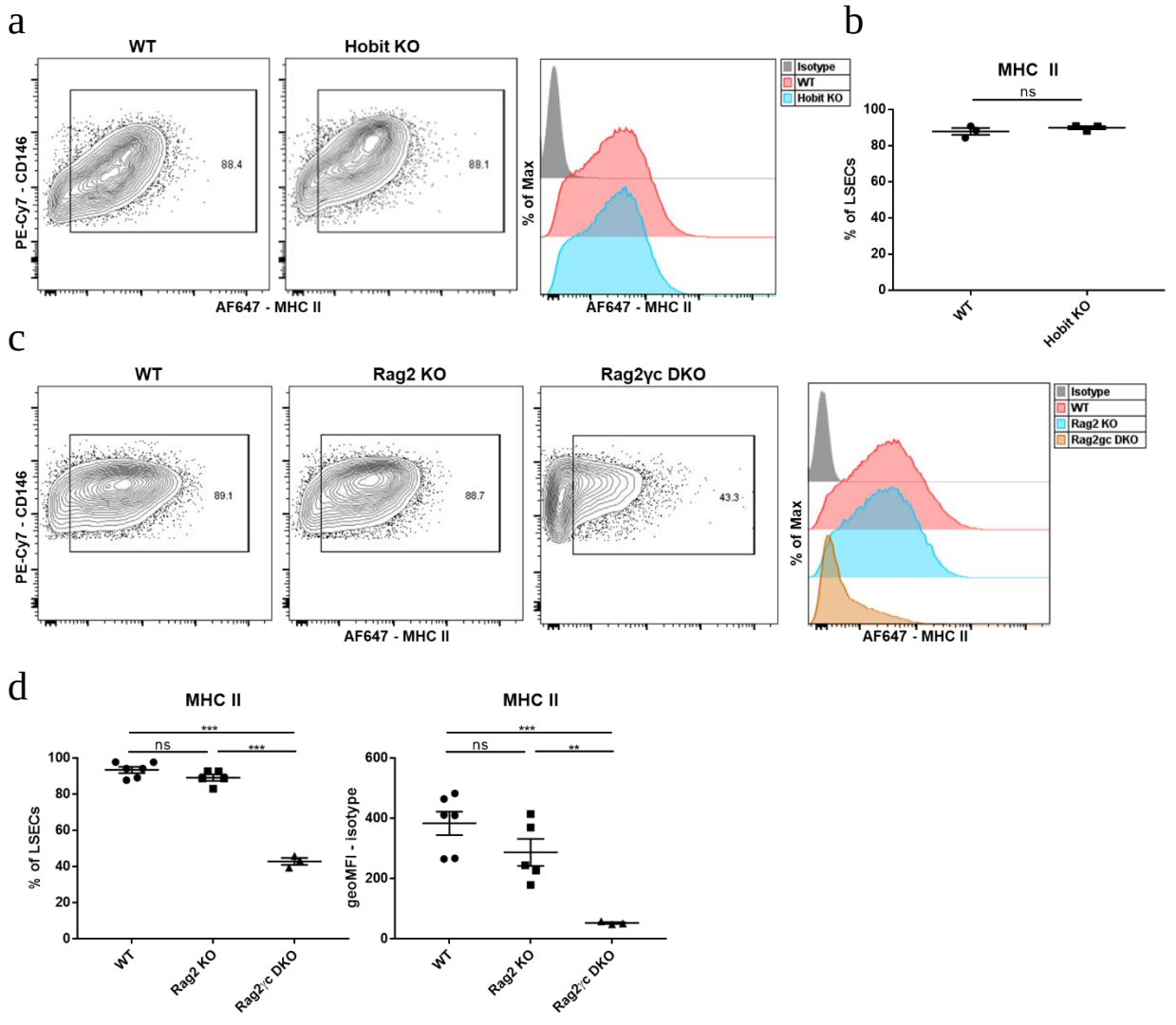

(Figure legend on the next page)

Fig. 6.9 - The absence of all lymphocytes leads to the reduction of MHC II expression on LSECs in steady-state. **a-b**, LSECs were isolated from WT and Hobit KO mice and analyzed with flow cytometry. Representative contour plots and histogram of MHC II expression, and its quantification on LSECs (n = 3 per group). **c-d**, LSECs were isolated from WT, Rag2 KO, and Rag2γc DKO mice and analyzed with flow cytometry for MHC II expression. Representative contour plots and histograms of MHC II expression, and quantification on LSECs (n = 3-5 per group). For all graphs, data are represented as mean ± SEM. Groups were analyzed by Student t-test (**b**) and one way ANOVA (**d**). $^{**}P < 0.01$, $^{***}P < 0.001$, ns - not significant.

I also compared the MHC II expression between LSECs and liver professional APCs in Rag2 KO and Rag2γc DKO mice. Around 45% of LSECs from Rag2γc DKO mice did not express MHC II, compared to LSECs from WT mice (Fig. 6.9 d). In contrast, around 95% of all liver KCs from Rag2γc DKO mice still expressed MHC II compared to KCs from Rag KO and WT mice (Fig. 6.10 a). KCs from Rag2γc DKO reproduced a similar phenotype as KCs in Ifnγ KO and Ifnγr KO mice. MHC II expression on liver DCs was unaffected in Rag2 KO and Rag2γc KO mice compared to DCs in control mice (Fig. 6.10 b).

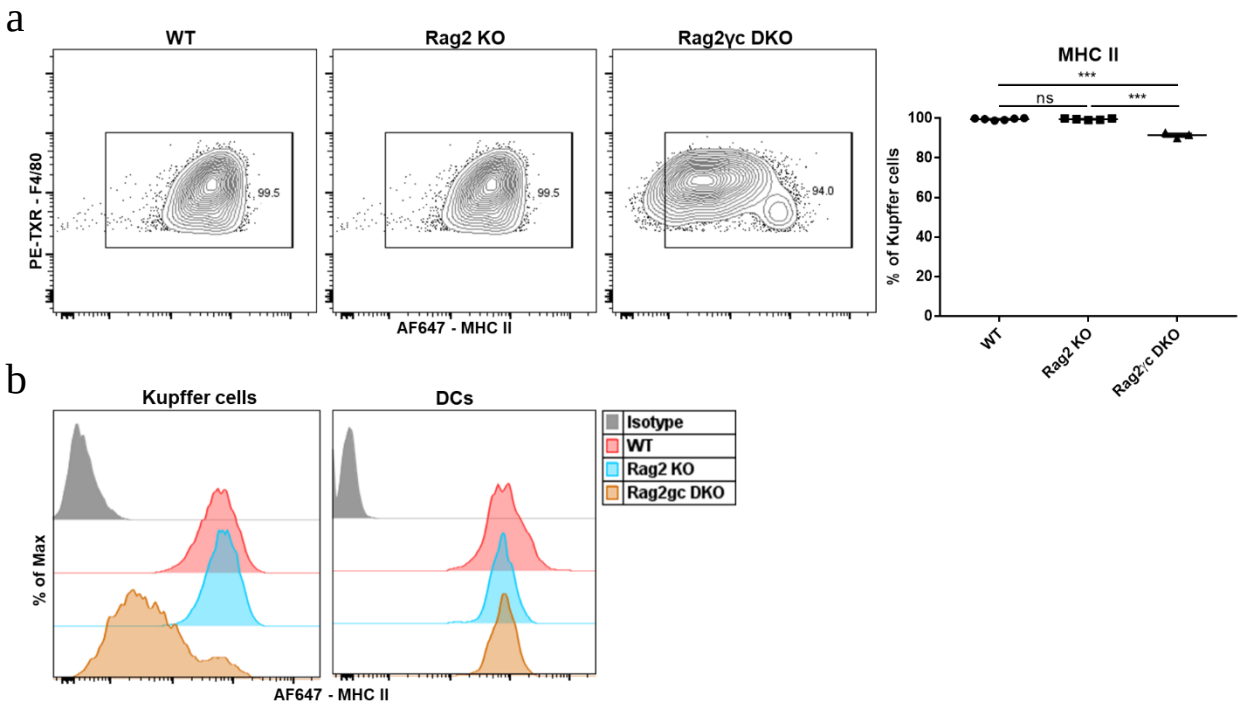

Fig. 6.10 - The absence of IFN-γ affects MHC II expression on Kupffer cells, but not dendritic cells. Liver NPCs were isolated from WT, Rag2 KO, and Rag2γc DKO mice and analyzed with flow cytometry for MHC II expression. **a,** Representative contour plots of MHC II expression and its quantification on KCs (n = 3-5 per group), mean ± SEM, one way ANOVA. **b**, Representative histograms of MHC II expression on KCs and DCs (n = 3-5 per group). $^{***}P < 0.001$

6.3.2 The role of IL-12 in regulating MHC II expression on LSECs

IL-12 is a Th1 cytokine that can stimulate immune cells to produce IFN-γ (Trinchieri, 2003). I hypothesized that IL-12 could be involved in the IFN-γ production by immune cells in the steady state. IL-12 binds to IL-12R, which consists of IL12Rβ1 and IL12Rβ2 subunits (Vignali & Kuchroo, 2012). To answer this question, I analyzed LSECs from Il12rb2 KO mice, which were reported to be deficient in IFN-γ production upon stimulation (C. Wu et al., 2000). LSECs from Il12rb2 KO mice had a significant reduction of the percentage of LSECs expressing MHC II, compared to LSECs from WT mice (Fig. 6.11 a-b). I also investigated if IL-12 could directly induce MHC II on LSECs. IL-12 was not able to upregulate MHC II directly on LSECs *in vitro* (6.11 c), suggesting that IL-12 maintains MHC II on LSECs through an indirect mechanism, most likely through inducing IFN-γ.

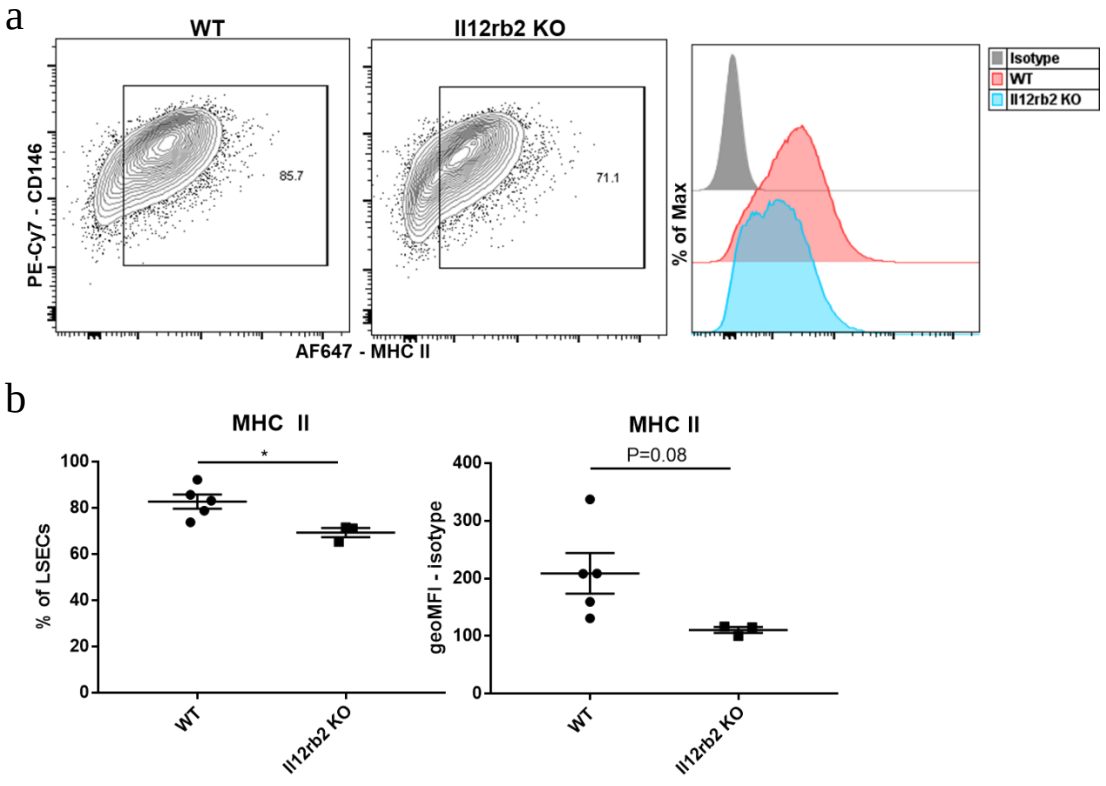

(Figure legend on the next page)

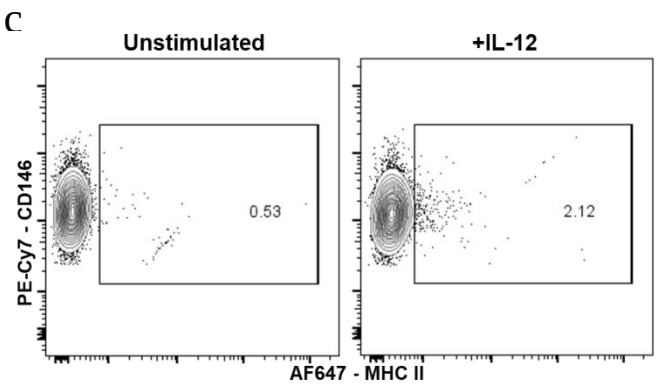

Fig. 6.11 - The absence of IL-12 alters MHC II expression on LSECs. **a-b**, LSECs were isolated from WT and Il12rb2 KO mice, and analyzed with flow cytometry for MHC II expression. Representative contour plots and histograms of MHC II expression on LSECs (n = 3-5 per group). **c**, LSECs were isolated from WT mice, cultured, and stimulated with IL-12 for 24-hour. After stimulation, LSECs were harvested and analyzed with flow cytometry for MHC II expression. Representative histogram of MHC II expression on unstimulated LSECs and LSECs stimulated with IL-12. Data are representative of 2 independent experiments (**c**). For all graphs, data are represented as mean ± SEM. Groups were analyzed by Student t-test (**b**). **P* < 0.05.

I also investigated MHC II expression on Kupffer cells from Il12rb2 KO mice. Around 15% of LSECs cells from Il12rb2 KO mice did not express MHC II, compared to LSECs from WT mice (Fig. 6.11). In contrast, KCs from Il12rb2 KO mice still expressed MHC II at a lower amount, compared to KCs from WT mice (Fig. 6.12 a). In addition, lung ECs from Il12rb2 KO mice expressed a lower amount of MHC II, compared to lung ECs from WT mice (Fig. 6.12 b-c).

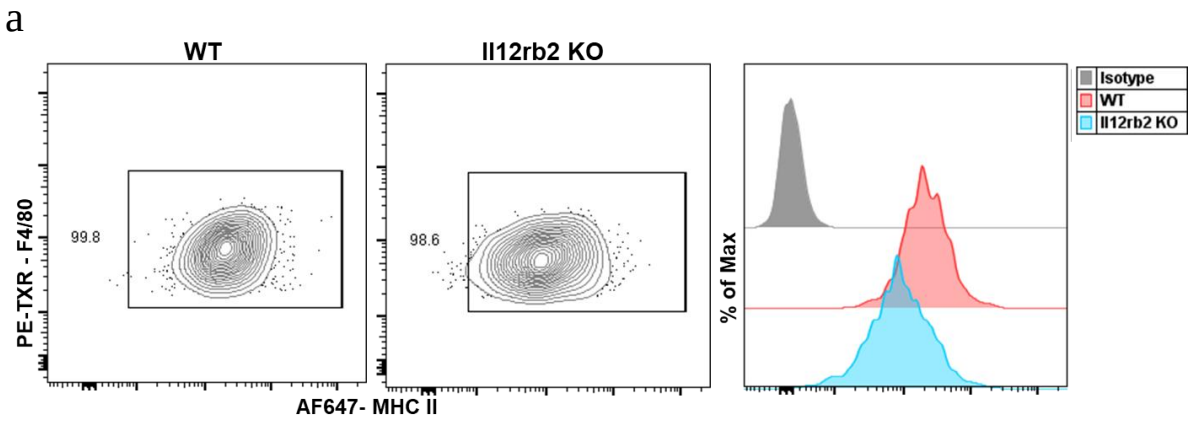

(Figure legend on the next page)

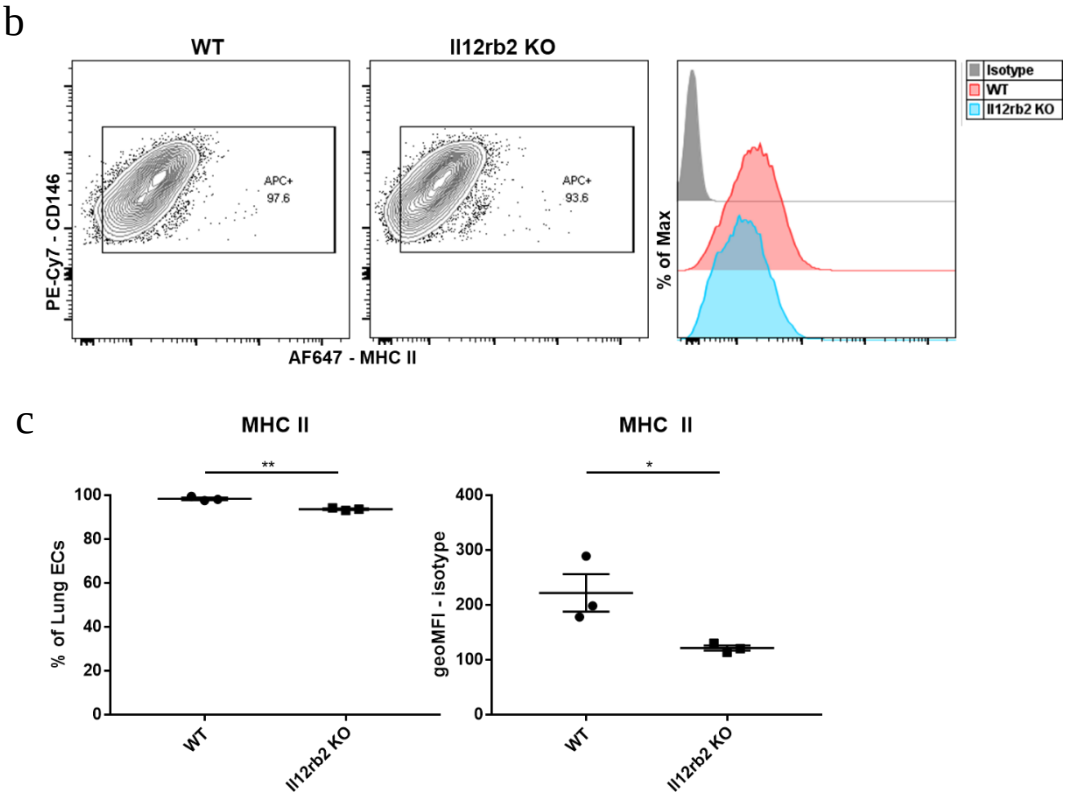

Fig. 6.12 - The absence of IL-12 affects MHC II expression on KCs and lung ECs. **a**, Liver NPCs were isolated from WT and Il12rb2 KO mice and analyzed with flow cytometry for MHC II expression. Representative contour plots and histograms of MHC II expression on KCs (n = 3 per group). **b-c**, Lung NPCs were isolated from WT and Il12rb2 KO mice and analyzed with flow cytometry for MHC II expression. Representative contour plots and histograms of MHC II expression on lung ECs and its quantification (n = 3 per group). For all graphs, data are represented as mean ± SEM. Groups were analyzed by Student t-test (**c**). $*P < 0.05$, $**P < 0.01$, $***P < 0.001$, ns - not significant.

6.3.3 The role of microbiota in regulating MHC II expression on LSECs

Microbiota was reported to be paramount for MHC II expression on intestinal epithelial cells, which are non-professional antigen-presenting cells (Koyama et al., 2019; Moon et al., 2021). I hypothesized that microbiota could be playing a role in stimulating IFN-γ production, as the liver is constantly being exposed to bacterial antigens coming from intestines through portal vein. For this reason, I examined MHC II on LSECs using various mouse models that were known to affect microbiota. Germ-free mice are housed in specialized mouse facility and do not have microbiota. Tlr4 KO mice do not have the receptor to respond to lipopolysaccharide, a bacterial antigen (Hoshino et al., 1999). Myd88 KO mice do not have the adaptor protein-MyD88, which mediates TLR signaling and downstream activation (Kawasaki & Kawai, 2014). Mice were treated with antibiotics containing a cocktail of ampicillin, neomycin, mereponem, and

ciprofloxacin in the drinking water (ABX) to eliminate microbiota. I did not observe any MHC II changes on LSECs in any of these models (Fig. 6.13 a-e). This indicates that MHC II expression in the liver was regulated in a microbiota-independent manner.

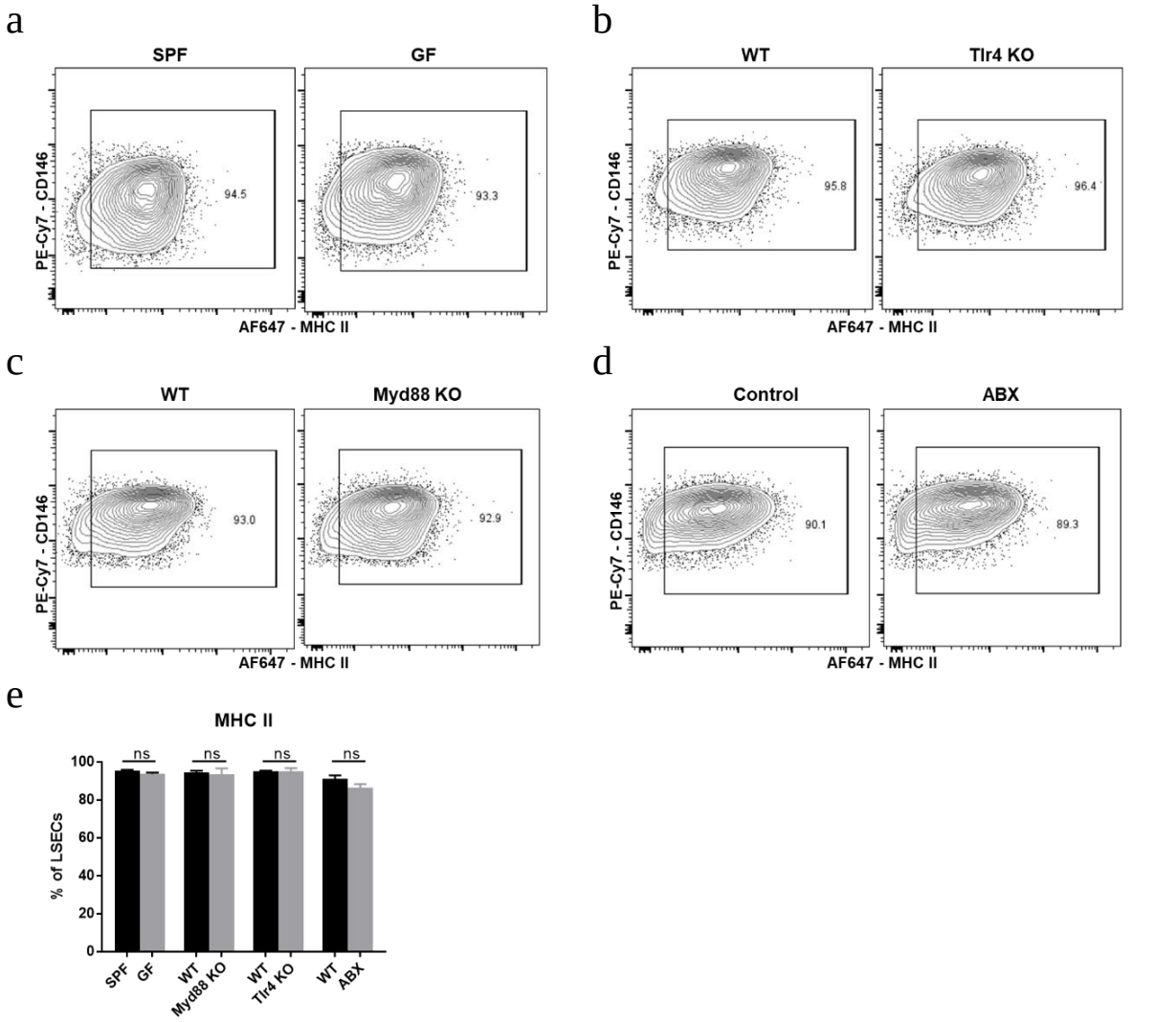

Fig. 6.13 - Microbiota does not regulate MHC II expression on LSECs. **a-d**, LSECs were isolated from specific-pathogen free (SPF) mice and germ-free (GF) mice, WT, Tlr4 KO, Myd88 KO, and ABX-treated mice. **a-d**, Representative contour plots of MHC II expression on LSECs from SPF and GF mice (**a**), from WT and Tlr4 KO mice (**b**), from WT and Myd88 KO mice (**c**), from control and ABX-treated mice (**d**). **e**, Quantification of MHC II expression on LSECs isolated in (**a-d**) (n = 3 per group). For all graphs, data represented as mean ± SEM. Groups were analyzed by Student t-test (**e**). ns - not significant.

6.3.4 The role of CIITA in regulating MHC II expression on LSECs

I also sought to determine the role of CIITA in regulating MHC II on LSECs, as CIITA is the master transcriptional co-activator of MHC II (Chang et al., 1996). CIITA was predicted to be the upstream regulator of DEGs in MHC II^{high} LSECs using Ingenuity Pathway Analysis. LSECs from Ciita KO mice were deficient in MHC II expression (Fig. 6.14 a-b). Moreover, Kupffer cells, B cells, and dendritic cells did not express MHC II in Ciita KO mice (Fig. 6.14 c-e). These results are in agreement with the previous studies showing that CIITA was the most essential player regulating MHC II expression (Chang et al., 1996). It was reported that IFN-γ drives MHC II expression mainly through the promoter IV (pIV) of CIITA (LeibundGut-Landmann et al., 2004). For this reason, I sorted LSECs and performed qRT-PCR to detect the promoter usage of *Ciita*. In general, LSECs expressed *Ciita* transcripts at a much lower level compared to Kupffer cells. I found that LSECs expressed pIII of *Ciita* the most, followed by pIV and pI in steady state (Fig. 6.14 f). However, LSECs *in vitro* stimulated with IFN-γ preferentially expressed pIV of *Ciita*. These data suggest LSECs can differentially utilize *Ciita* promoters depending on the context.

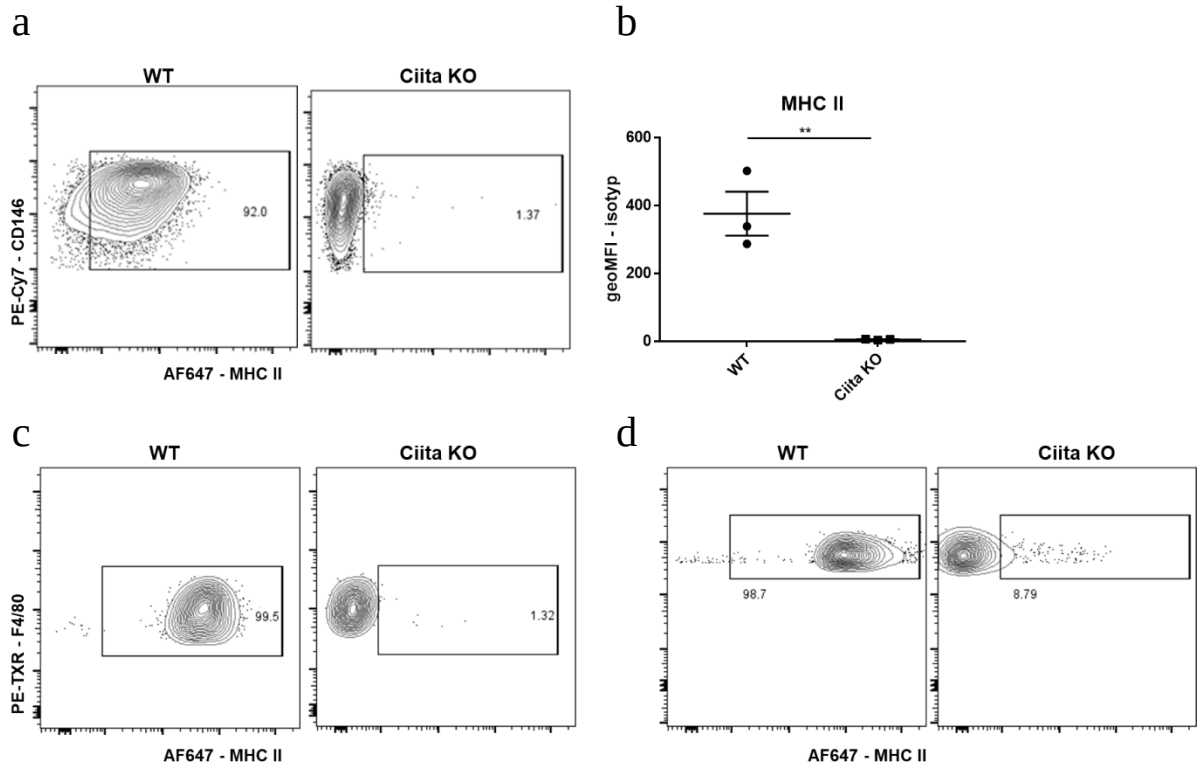

(Figure legend on the next page)

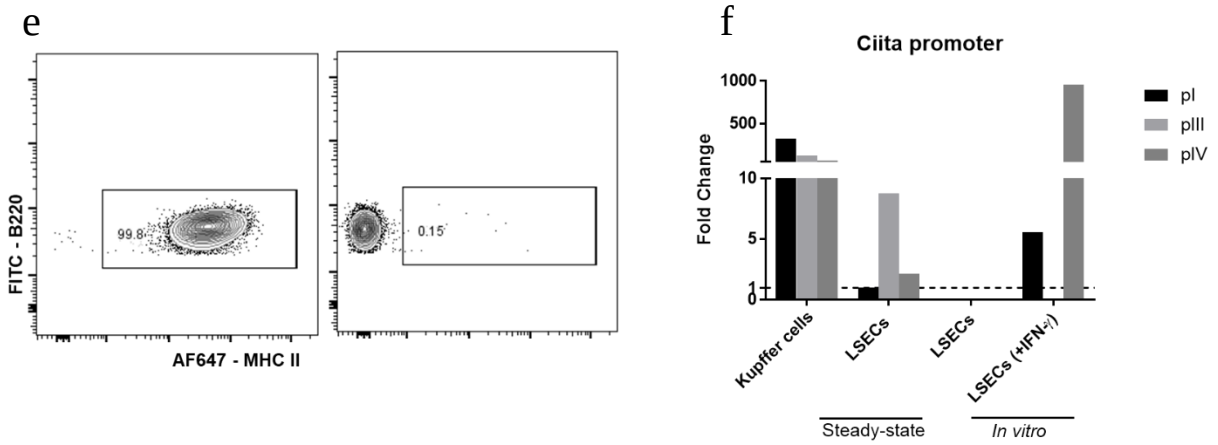

Fig 6.14 - CIITA is required for the MHC II expression on liver non-parenchymal cells. **a-d**, Liver NPCs were isolated from WT and Ciita KO mice, and analyzed with flow cytometry for MHC II expression. **a-b**, Representative contour plots of MHC II expression on LSECs and its quantification (n = 3 per group). **c**, Representative contour plots of MHC II expression on Kupffer cells (n = 3 per group). **d**, Representative contour plots of MHC II expression on DCs. **e**, Representative contour plot of MHC II expression on B cells (n = 3 per group). **f**, LSECs and Kupffer cells were sorted with flow cytometer. Cultured LSECs stimulated with IFN-γ for 24-hour were also harvested. cDNA was produced from the isolated RNA, and qRT-PCR was performed. Fold change of *Ciita* transcripts normalized to pIV *Ciita* transcripts of LSECs (dashed line) were computed using $2^{-\Delta\Delta Ct}$ method. Data shown are 1 experiment pooled from 8 mice (**f**). $^{**}P < 0.01$

6.4 Functional roles of MHC II on LSECs

6.4.1 IFN-γ affects CD4$^+$ T cell phenotypes in the liver

Ingenuity Pathway Analysis of the microarray data illustrated that MHC II^{high} LSECs were enriched in transcripts regulating immune cell responses, while MHC II^{low} LSECs were enriched in transcripts regulating liver development and metabolism (Fig. 6.15 a). MHC II on LSECs was shown to be involved in naïve CD4$^+$ T cell polarization and Treg induction *in vitro* (Knolle et al., 1999; Kruse et al., 2009). However, its *in vivo* role is still unclear. My results demonstrated that MHC II expression on LSECs was reduced in Ifnγ KO and Ifnγr KO, compared to LSECs in WT mice (Fig. 6.5 d-e). Thus, I hypothesized that the reduced MHC II expression on LSECs could affect liver T cell tolerance and differentiation in steady state. Therefore, I examined T cell phenotypes in Ifnγ KO and Ifnγr KO mice. I observed that among the CD4$^+$ T cell population, there was a higher frequency of CD62L$^+$CD44$^-$ naïve T cells (T_N) and a reduced frequency of CD44$^+$CD62L$^-$ effector memory T cells (T_{EM}) in Ifnγ KO and Ifnγr KO mice, compared to CD4$^+$ T cells in WT mice (Fig. 6.15 b-c). However, there was no change in T_N and T_{EM} among liver CD8$^+$ T cell population (Fig. 6.15 d). These data suggest a potential role of MHC II on LSECs in regulating peripheral naïve and memory CD4$^+$ T cell differentiation in the liver.

a

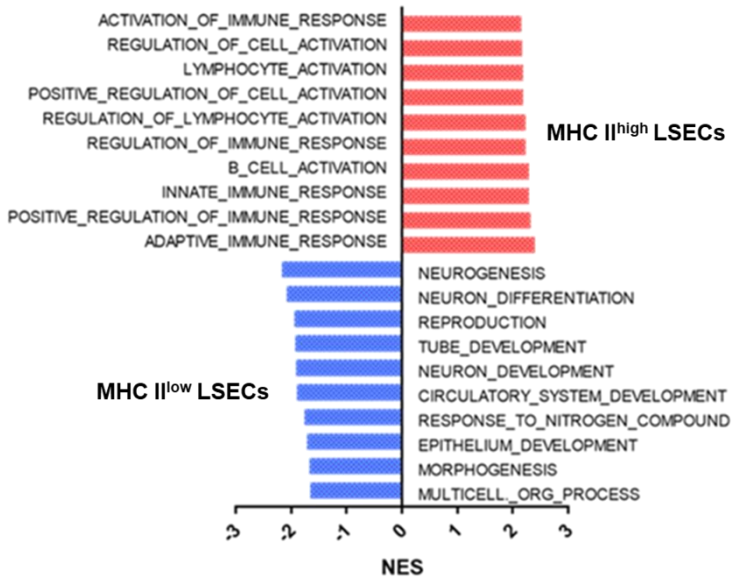

(Figure legend on the next page)

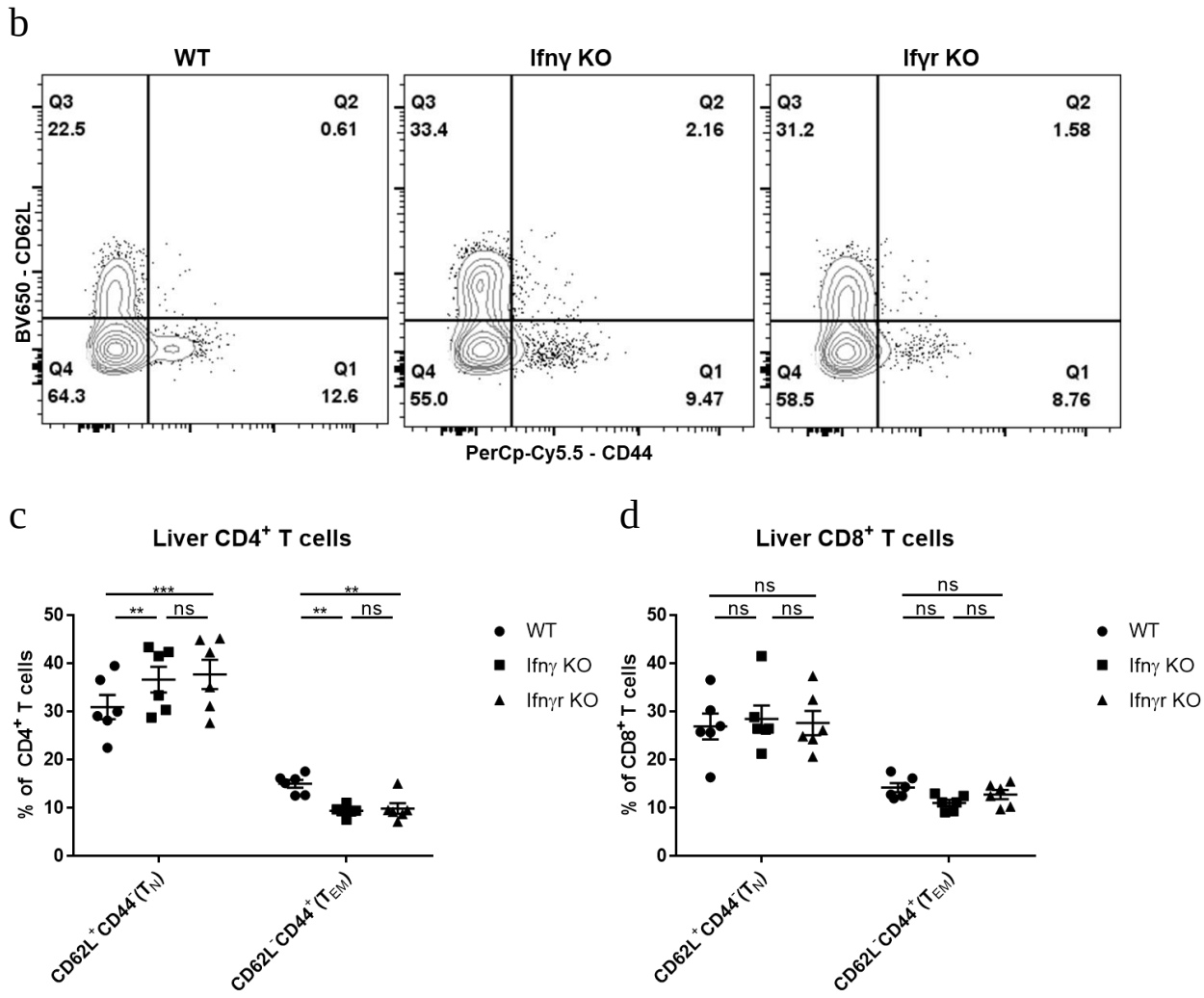

Fig. 6.15 - The reduction of MHC II expression on LSECs in Ifnγ KO and Ifnγr KO mice correlates with more naïve and less memory T cell frequencies. **a**, Ingenuity Pathway Analysis depicts pathways enriched in transcripts of MHC II^{high} and MHC II^{low} LSECs. NES - normalized enrichment score. **b-d**, Liver NPCs were isolated from WT, Ifnγ KO and Ifnγr KO mice, and analyzed with flow cytometry for T cell phenotypes. **b**, Representative contour plots of naive ($CD62L^+CD44^-$) and effector memory ($CD62L^-CD44^+$) T cells. **c**, Quantification of liver naïve (T_N) and effector memory (T_{EM}) percentages among $Lin^-CD45^+CD3^+TCR\beta^+CD4^+$ T cells (n = 6 per group). **d**, Quantification of liver naïve (T_N) and effector memory (T_{EM}) percentages among $Lin^-CD45^+CD3^+TCR\beta^+CD8^+$ T cells. Data are pooled from 2 independent experiments (**c-d**). For all graphs, data represented as mean ± SEM. Data were matched within each independent experiment, and two-way ANOVA is performed (**c-d**). $^{**}P < 0.01$, $^{***}P < 0.001$, ns, not significant.

I also investigated $CD4^+$ T cells in lungs and spleens to determine whether similar results as in livers would be observed. The changes in T_N and T_{EM} among $CD4^+$ T cells were not observed in lungs (Fig. 6.16 a). I also observed higher T_N and lower T_{EM} frequencies among $CD4^+$ T cells in Ifnγ KO mice in spleens, compared to WT and IFNγr KO mice (Fig. 6.16 b). The changes in T_N and T_{EM} in spleens of Ifnγ KO mice

need further investigation. I hypothesized that MHC II in the liver might be involved in generating regulatory T cells (Treg). However, I did not observe any change in the liver FoxP3$^+$ Treg population in Ifnγ KO and Ifnγr KO mice, compared to WT mice (Fig. 6.16 c).

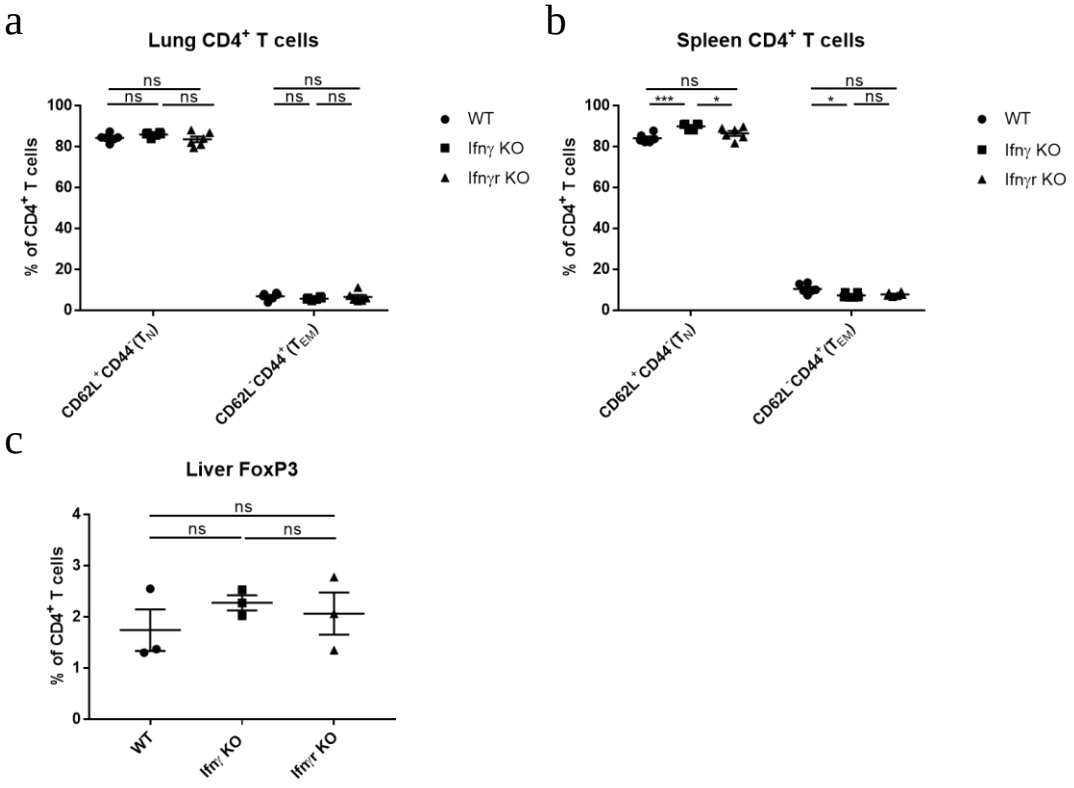

Fig. 6.16 - Naïve, memory, and regulatory T cells in lungs, livers, and spleens of WT, Ifnγ KO and Ifnγr KO mice. **a**, Lung NPCs were isolated and analyzed with flow cytometry. Quantification of lung naïve (T_N) and effector memory (T_{EM}) percentages among Lin$^-$CD45$^+$CD3$^+$TCRβ$^+$CD4$^+$ T cells (n = 6 per group). **b**, Splenocytes were isolated and analyzed with flow cytometry. Quantification of spleen naïve (T_N) and effector memory (T_{EM}) percentage among Lin$^-$CD45$^+$CD3$^+$TCRβ$^+$CD4$^+$ T cells (n = 6 per group). **c**, Liver NPCs were isolated and analyzed with flow cytometry for FoxP3$^+$ T cell percentage. Quantification of FoxP3$^+$ T cells among Lin$^-$CD45$^+$CD3$^+$TCRβ$^+$CD4$^+$ T cells (n = 3 per group). Data were pooled from 2 independent experiments (**a-b**). For all graphs, data represented as mean ± SEM. Data were matched within each independent experiment, and two-way ANOVA is performed (**a-b**). Groups were analyzed with one-way ANOVA (**c**). $*P < 0.05$, $**P < 0.01$, $***P < 0.001$, ns, not significant.

6.5 Functional role of HVEM on LSECs

My previous data showed that LSECs expressed HVEM in steady-state, and upregulated HVEM expression after stimulation with IFN-γ (Fig. 6.1-6.2) Mice expressing Cre-recombinase under the control of Clec4g promoter (Clec4g-cre) were shown to express Cre recombinase activity in LSECs and some ECs in the heart, but not in bone marrow, spleen, lung and kidney (Wohlfeil et al., 2019). Hvem$^{flox/flox}$ possess *loxP* sites flanking exons 3-6 of the *Tnfrsf14* (tumor necrosis factor receptor superfamily, member 14 (herpesvirus entry mediator)) gene (Seo et al., 2018). Therefore, I generated LSEC-restricted HVEM knockout mice by crossing Clec4g-cre with HVEM$^{flox/flox}$ mice, all in B6 mouse background. For convenience, I will refer Cre^{-} Hvem$^{flox/flox}$ mice as WT, Cre^{+} HVEM$^{flox/flox}$ as Hvem cKO hereafter.

6.5.1 Phenotypes of LSEC-restricted Hvem knockout mice in steady-state

Hvem cKO mice were born at the expected Mendelian ratio without any developmental abnormality. I first examined the efficacy of Clec4g-cre in driving Hvem knockout in LSECs. I observed residual surface HVEM expression on LSECs of Hvem cKO mice using flow cytometry, albeit the expression was significantly lower compared to LSECs of WT mice (Fig. 6.17 a-b). To confirm *Hvem* transcript was absent, I sorted LSECs, Kupffer cells, and other CD45^{+} immune cells with flow cytometer and performed RT-PCR. The gene expression result showed that *Hvem* transcript was not detected in LSECs of Hvem cKO mice, but it was not affected in Kupffer cells and other immune cells (Fig. 6.17 c). Furthermore, HVEM surface protein was not detected after 2-day of culture *in vitro*, and could not be upregulated after stimulation with IFN-γ (Fig. 6.17 d-e).

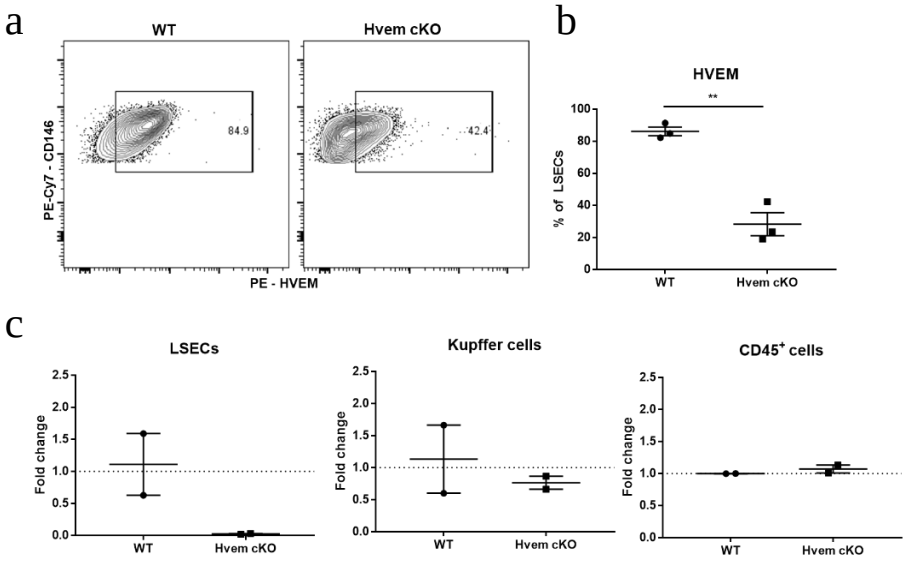

(Figure legend on the next page)

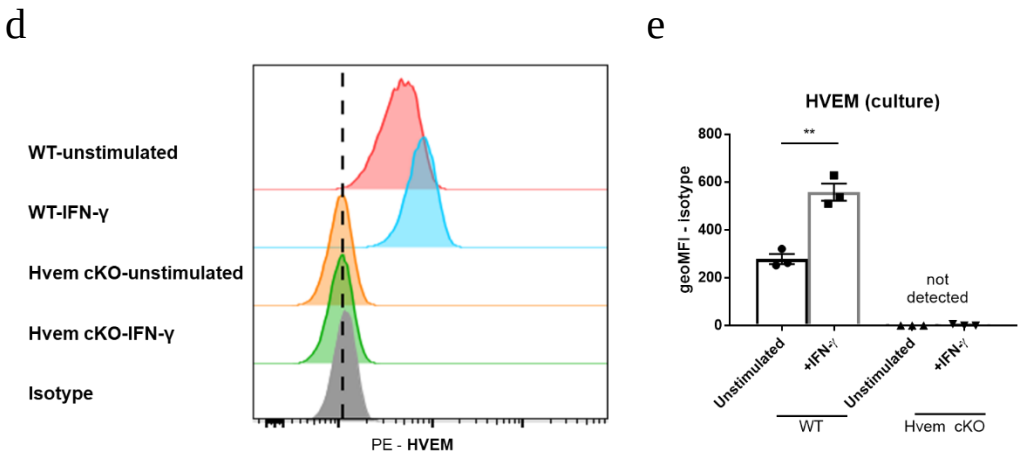

Fig. 6.17 - LSECs from Hvem cKO mice do not express *Hvem* transcript *ex vivo* and HVEM surface protein after culture. **a-b**, Liver NPCs were isolated and analyzed with flow cytometry. Representative contour plots of HVEM expression on LSECs and its quantification (n = 3 per group). **c**, Liver NPCs were isolated, and LSECs, Kupffer cells, or other $CD45^+$ cells were sorted with flow cytometer. cDNA was generated from the isolated RNA of these cells, and qRT-PCR was performed. Fold change of *Hvem* transcript of Hvem cKO normalized to WT was computed using $2^{-\Delta\Delta Ct}$ method (n = 2 per group). **d-e**, Liver NPCs were isolated, $CD146^+$ LSECs were purified and stimulated with IFN-γ for 24 hours. After stimulation, LSECs were harvested and analyzed with flow cytometry (n = 3 per group). For all graphs, data are represented as mean ± SEM. Groups were analyzed with one-way ANOVA (**c**). $^{**}P < 0.01$

Next, I analyzed blood sera of WT and Hvem cKO mice (2- to 4-month-old) to investigate whether the absence of HVEM on LSECs would lead to any liver damage or metabolic aberration in steady state. I measured Alanine Aminotransaminase (ALT) and Alkaline Phosphatase (ALP) activities in sera, which are used in clinical settings to determine liver damage. I also measured glucose, triglyceride, and cholesterol concentration in the sera as metabolic parameters. I did not observe any change in the parameters that I measured (Fig. 6.18 a-b). I also determined liver/body weight ratio, spleen weight, and total immune cell number per gram of liver, and I did not observe significant differences between WT and Hvem cKO (2 to 4 month old) (Fig. 6.18 c). These results suggest that HVEM on LSECs does not affect liver homeostasis and in adult mice (2- to 4-month old).

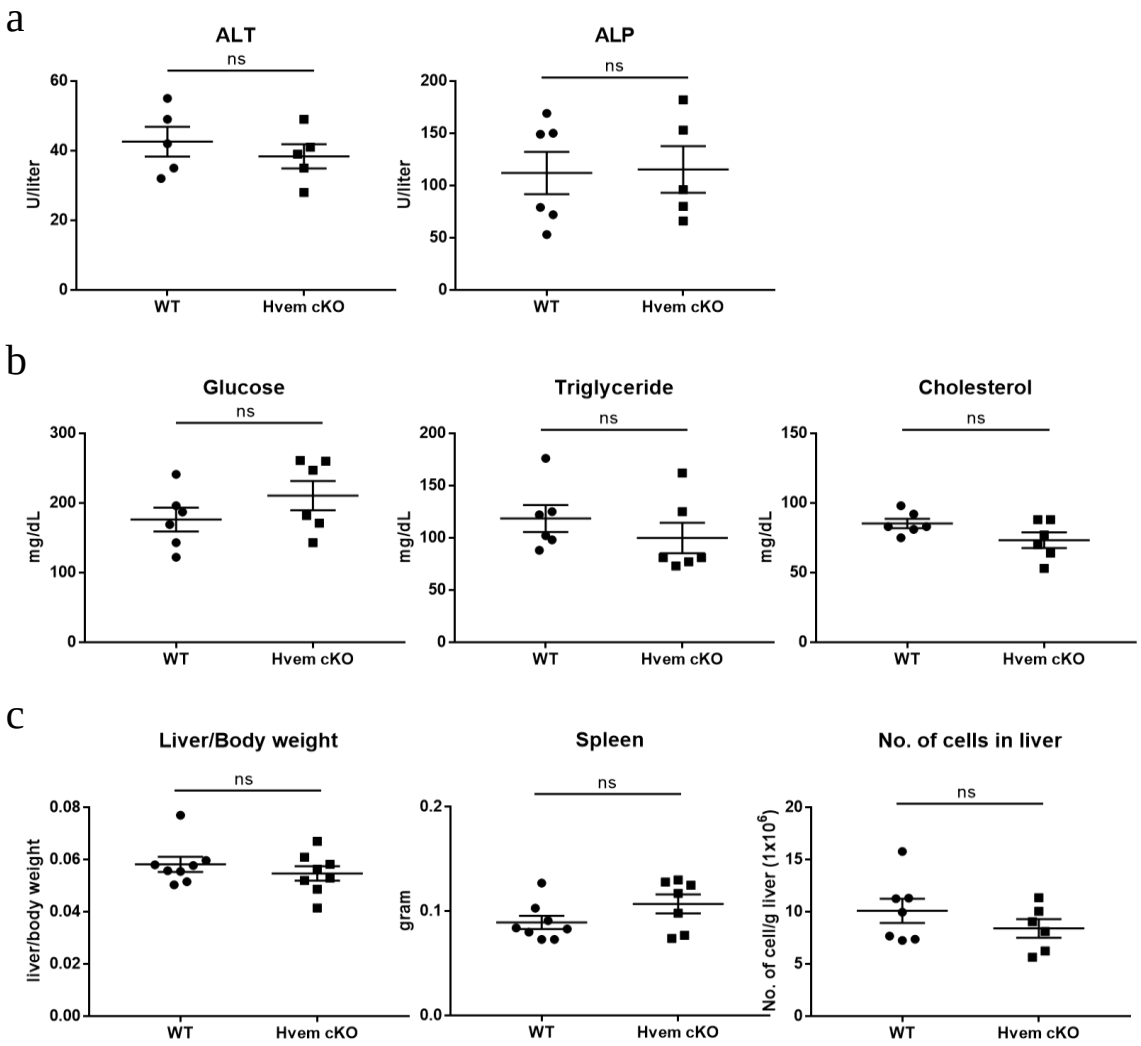

Fig. 6.18 - Hvem cKO mice do not show liver damage and systemic metabolic alterations in steady state. **a-b**, Blood were obtained from mice, and sera were collected from clotted blood after centrifugation. ALT and ALP activities (**a**), glucose, triglyceride, and cholesterol concentration (**b**) were measured. **c**, Liver, spleen, and body weight of mice were measured. Liver NPCs were isolated, and counted, and normalized to liver weight to obtain number of cells per liver. n $\geq$ 5 mouse per group (**a-c**). For all graphs, data are represented as mean ± SEM. Groups were analyzed with Student's t-test (**a-c**). ns - not significant.

Subsequently, I examined phenotype of LSECs in Hvem cKO mice. I did not observe any difference in the surface expression of endothelial cell markers including CD31, CD206, and VEGFR2 on LSECs between WT and Hvem cKO mice (Fig. 6.19 a). I also did not discover any difference in expressions of adhesion molecules including CD155, ICAM, and VCAM. (Fig. 6.19 b). In addition, I did not detect any difference in surface proteins including PD-L1, MHC I, and MHC II (Fig. 6.19 c).

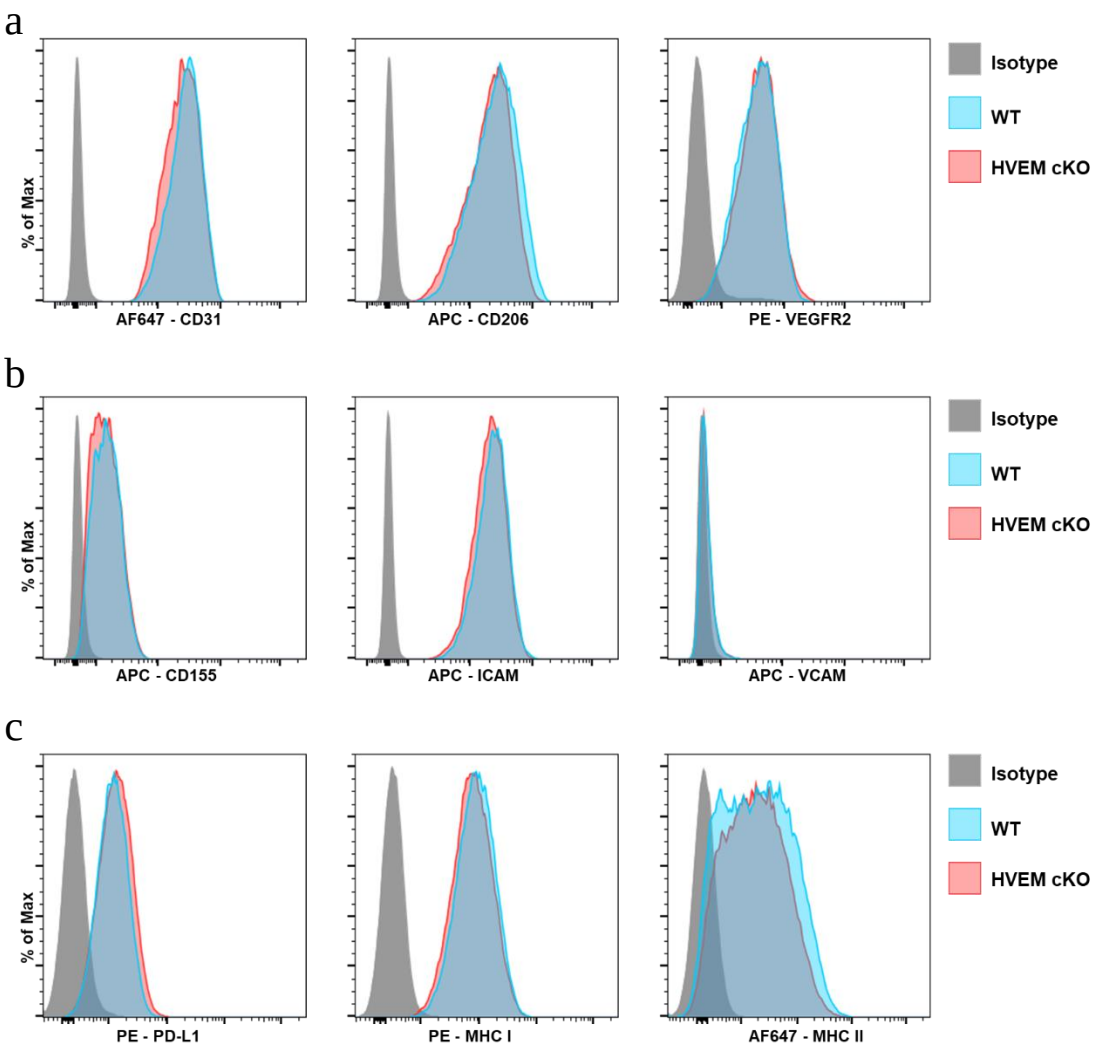

Fig. 6.19 - LSECs from Hvem cKO mice do not show phenotypic differences, compared LSECs of control mice. **a-c**, Liver NPCs were isolated and analyzed with flow cytometry. Representative histograms of CD31, CD206, VEGF2 (**a**), CD155, ICAM, VCAM (**b**), PD-L1, MHC I and MHC II (**c**) on LSECs. n = 3-5 mouse per group (**a-c**).

6.5.2 Phenotype of LSEC-restricted Hvem knockout mice in aging

Aging is a major risk factor for many vascular and inflammatory diseases (Franceschi et al., 2018). For this reason, I aged Hvem cKO mice to reach more than 1-year of age to determine whether this would result in any homeostatic alteration. I observed enlarged spleens, increased spleen weight, and increased number of immune cells in aged Hvem cKO mice, compared to the same parameters measured in WT mice (Fig. 6.20 a). However, I did not discover any changes in liver over body weight ratio (Fig. 6.20b). I also measured liver damage indicators, including ALT and ALP activities in serum, and there was no changes between

WT and Hvem cKO mice. In addition, I measured glucose, triglyceride, and cholesterol concetration in serum and did not observe any changes in these metabolic parameters (Fig. 6.20 b-c). The change in spleen size and cellularity in Hvem cKO mice suggests that HVEM could play a role in aged mice.

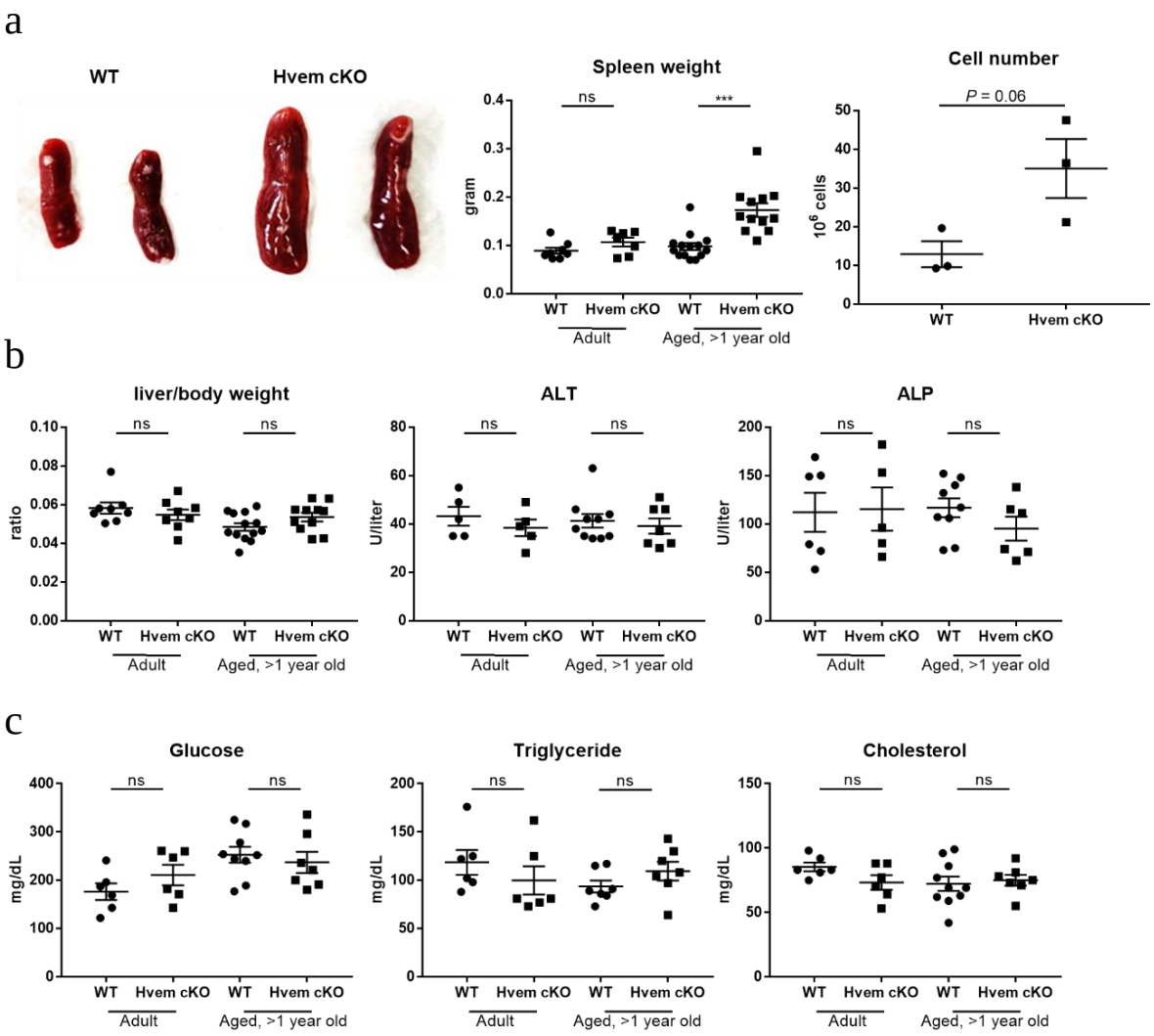

Fig. 6.20 - Spleens from aged Hvem cKO mice display splenomegaly. **a**, Gross image of spleens harvested from aged (>1 year old) WT and Hvem cKO mice. Spleens weight was measured. Splenocytes from aged mice were isolated and counted. **b-c**, Liver over body weight, ALT and ALP activities in serum (**b**), glucose, triglyceride, cholesterol concentration (**c**) in the sera of mice were quantified. Data were pooled from several independent experiments. Adult mice were 2 to 5 month-old, and aged mice were more than 1 year old (**a-c**). For all graphs, data are represented as mean ± SEM. Groups were analyzed with Student's t-test (**a-c**). ***$P < 0.001$, ns, not significant.

Next, I investigated the cellular composition of the enlarged spleens in aged (>1 year old) Hvem cKO mice. Flow cytometry identified several myeloid populations, including F4/80^{high}CD11b^{low} macrophages, Ly6C^{high}CD11b^{high} monocytes, Ly6C^{low}CD11b^{high}MHC II^{high} myeloid cells (myeloid I) and Ly6C^{low} CD11b^{high}MHC II^{high} myeloid cells (myeloid II) in aged WT and Hvem cKO mice (Fig. 6.21 a-c). These results showed that spleens in Hvem cKO mice had a tendency of reduced myeloid cell frequencies, compared to spleen in WT mice.

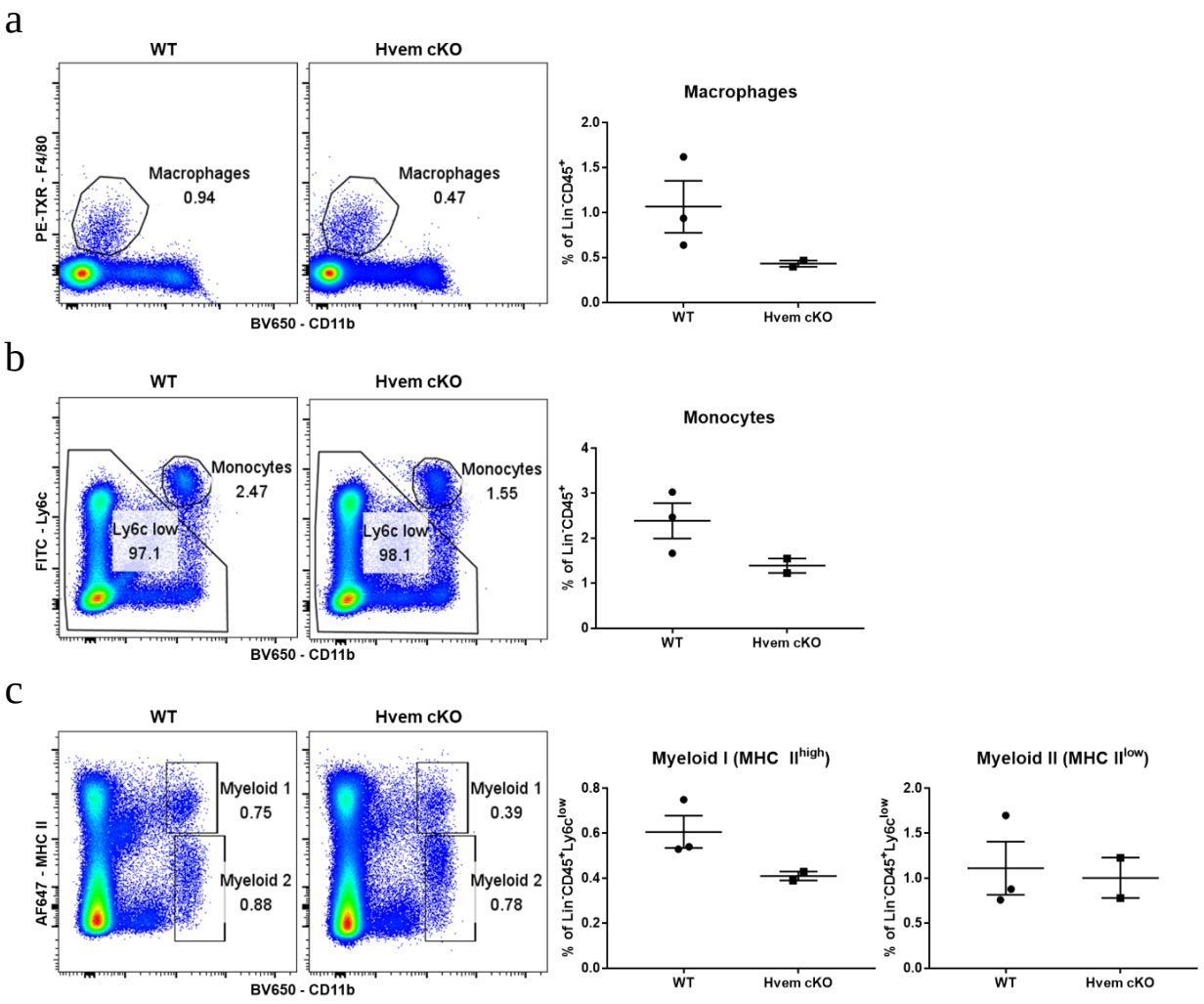

Fig. 6.21 - Myeloid composition in aged WT and Hvem cKO spleens. Spleens were harvested from aged (>1 year old) WT and Hvem cKO mice and analyzed with flow cytometry for myeloid cell composition. **a-c**, Representative plots of F4/80^{high}CD11b^{low} macrophages (**a**), Ly6c^{high}CD11b^{high} monocytes (**b**), and Ly6c^{low}CD11b^{high}MHC II^{high} myeloid cells (myeloid I) and Ly6c^{low}CD11b^{high}MHC II^{high} myeloid cells (myeloid II) (**c**) and their percentage quantification. n = 2-3 per group (**a-c**). For all graphs, data are represented as mean ± SEM.

I also determined the T cell composition in spleens of aged WT and Hvem cKO mice. Spleens in Hvem cKO mice had a trend of decreased $CD4^+$ T cells and increased $CD8^+$ T cell frequencies, compared to spleens in WT mice (Fig. 6.22a). Spleens in Hvem cKO mice also displayed a tendency of increased naïve T cell and decreased effector memory T cell frequencies, compared to spleens of WT mice (Fig. 6.22 b-c).

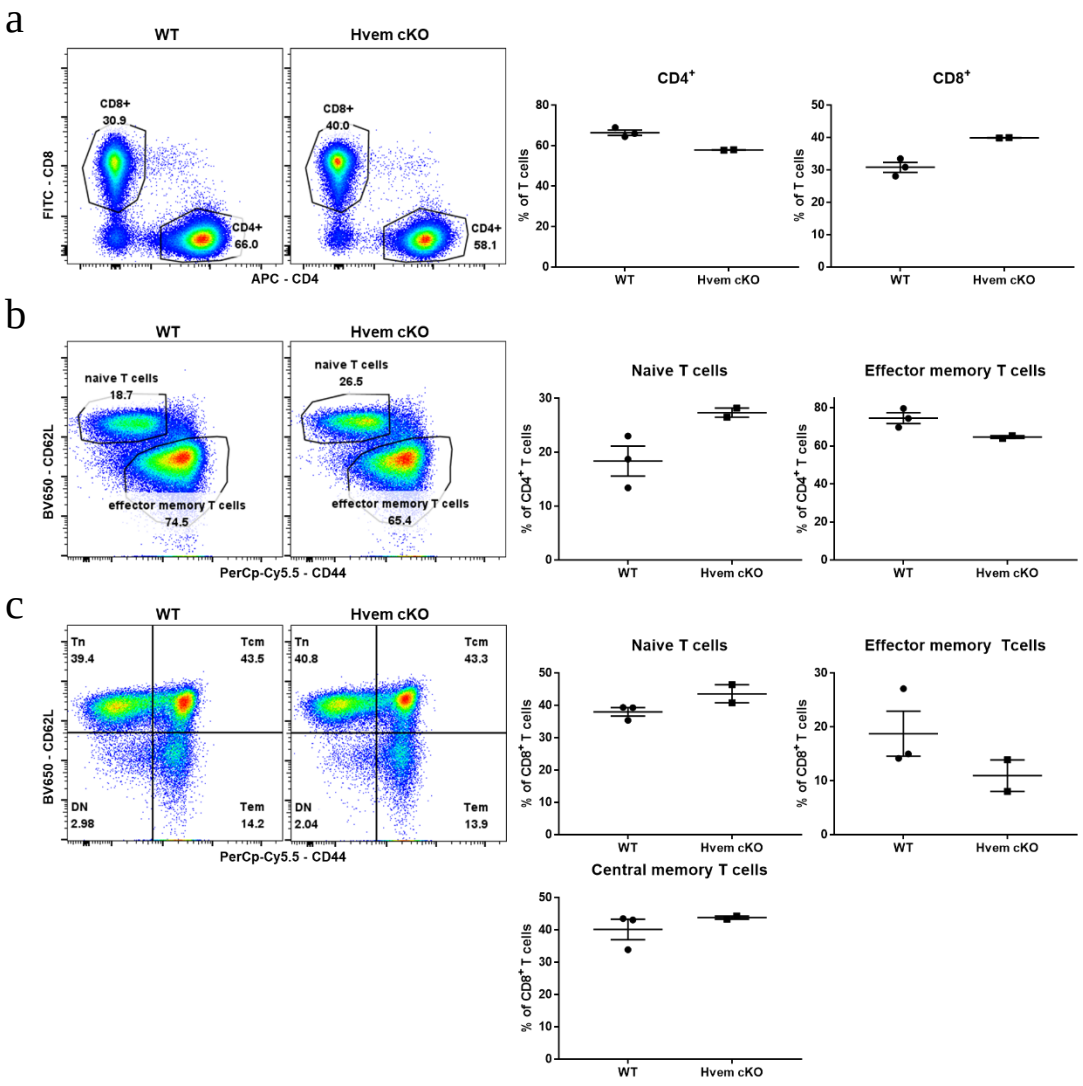

Fig. 6.22 - T cell composition in aged WT and Hvem cKO spleens. Spleens were harvested from aged (>1 year old) WT and Hvem cKO mice and analyzed with flow cytometry for T cell composition. **a**, Representative plots of $CD4^+$ and $CD8^+$ T cells and their quantification. **b**, Representative plots of naïve and effector memory T cells among $CD4^+$ T cell population and their quantification. **c**, Representative pseudocolor plots of naïve, central, and effector memory T cells among $CD8^+$ T cell population and their quantification. n = 2-3 per group (**a-c**). For all graphs, data represented as mean ± SEM. T_n- naïve T cells, T_{cm} - central memory T cell, T_{em} - effector memory T cells

6.5.3 Phenotypes of LSEC-restricted Hvem knockout mice in acute liver disease

Next, I determined the role of HVEM in a liver disease model. I injected adult (3 to 4-month old) male WT and Hvem cKO mice with 5mg/kg of lipopolysaccharide (LPS), *i.p.*, to induce endotoxicosis (Fig. 6.23 a). LPS injection led to a higher ALT activity in sera of mice, compared to PBS-treated mice (Fig. 6.23 b). I observed a decreased LSEC absolute cell number, but increased Kupffer cell, infiltrating monocyte and NK cell absolute cell numbers in livers after LPS injection (Fig. 6.23 c-d). There was a trend of decreased infiltrating monocyte absolute number in Hvem cKO livers of LPS-treated mice, compared to WT livers of LPS-treated mice. No changes were observed in liver ILC1 absolute cell number upon LPS injection (Fig 6.23 d). I did not detect any phenotypic difference between WT and Hvem cKO mice after LPS treatment.

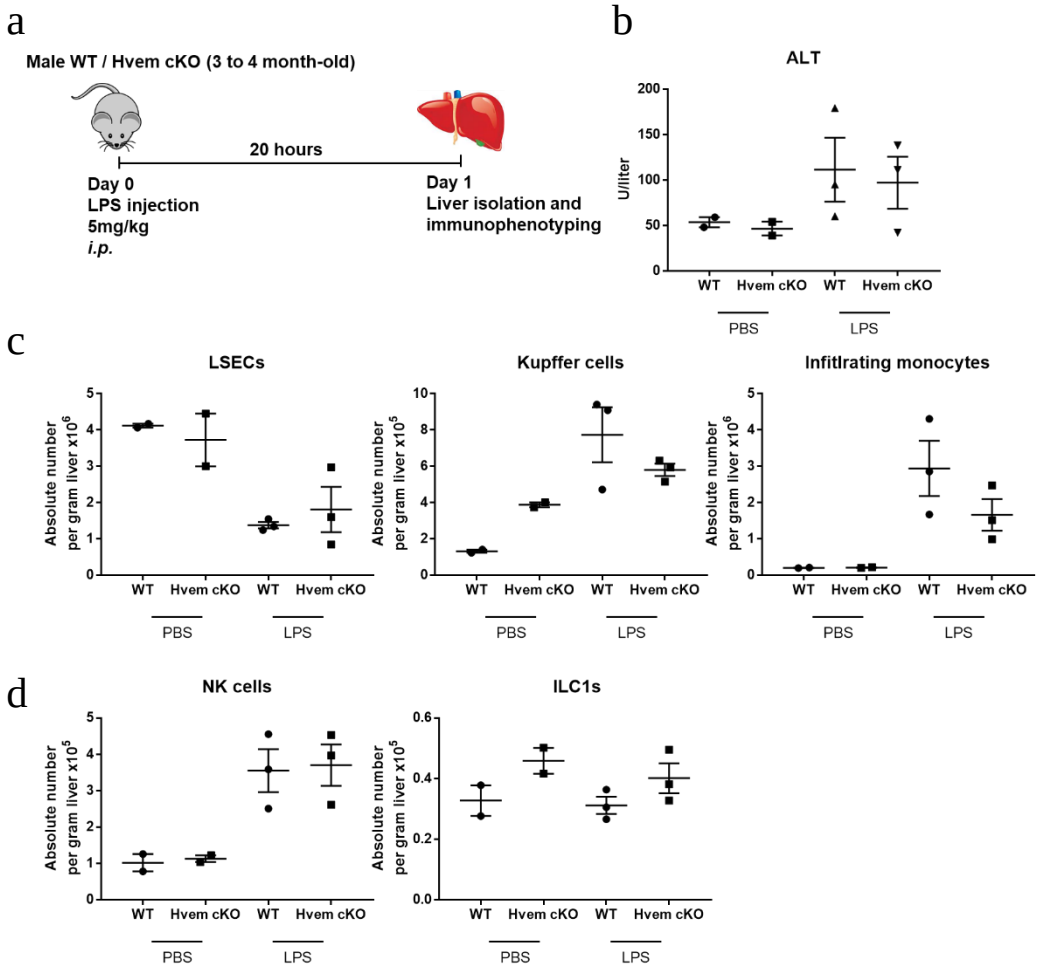

Fig. 6.23 - LPS treatment of WT and Hvem cKO mice results in increased absolute number of immune cells. **a**, Schematic diagram of the LPS treatment. **b**, Serum ALT activity was measured. **c-d**, Liver NPCs were isolated and analyzed with flow cytometry. **c-d**, Absolute number of LSECs, Kupffer cells, and infiltrating monocytes (**c**), NK cells and ILC1s (**d**) in livers. n = 2-3 per group (**a-d**). For all graphs, data are represented as mean ± SEM.

Furthermore, I analyzed phenotype of LSECs after LPS treatment. LPS injection consistently led to PD-L1, VCAM, and ICAM upregulation on LSECs in both WT and Hvem cKO mice (Fig. 6.24 a). I also constantly observed CD155, MHC I, and MHC II upregulation on LSECs upon LPS-treatment (Fig. 6.24 b). HVEM expression on LSECs remained unchanged after LPS injection (Fig. 6.24 c). I did not observe any phenotypic difference between LSECs in WT and Hvem cKO mice.

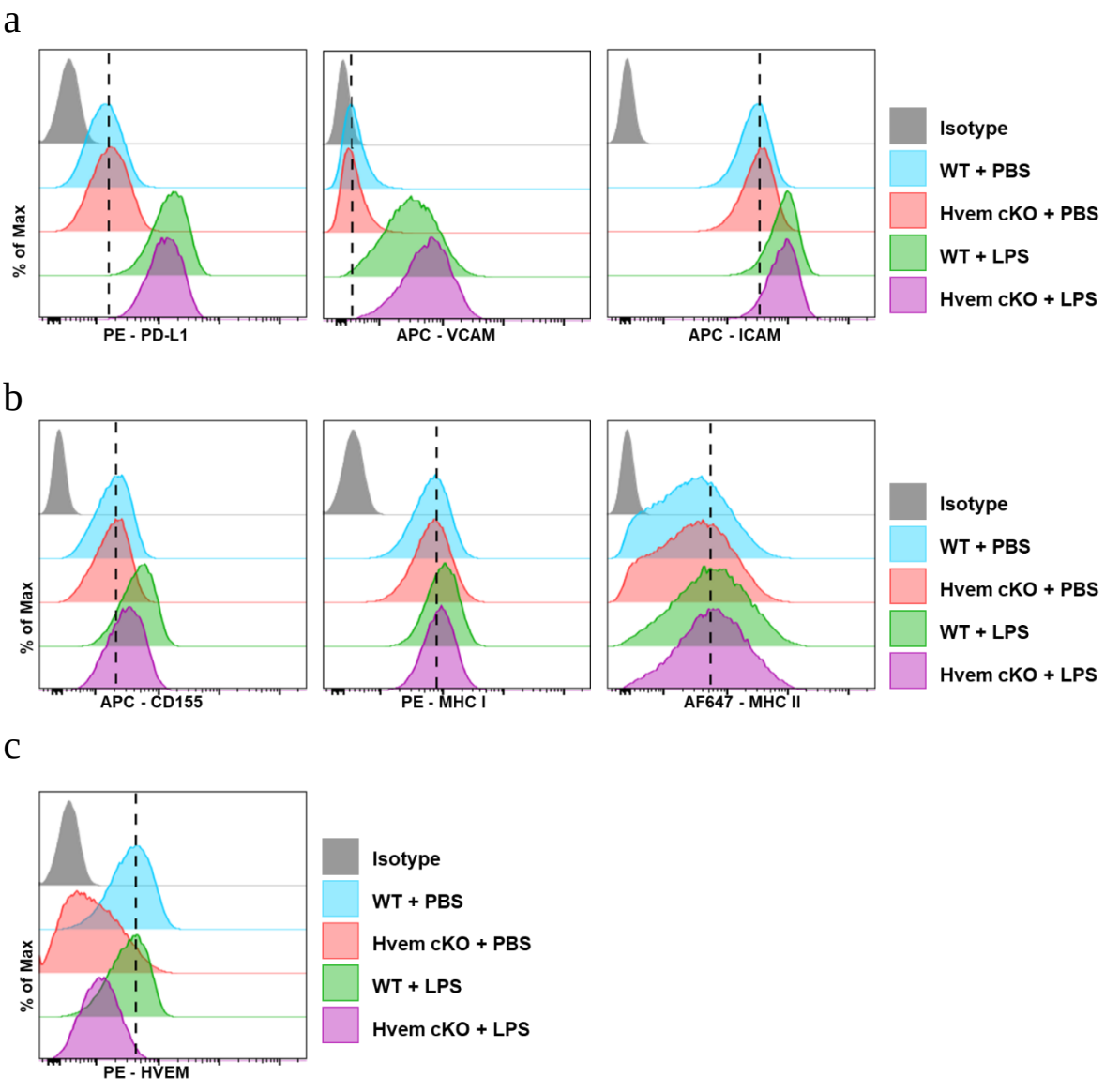

Fig. 6.24 - LPS injection induces phenotypic changes on LSECs. Liver NPCs were harvested from WT and Hvem cKO mice (3 to 4-old month) injected with PBS or LPS (5mg/kg) and analyzed with flow cytometry. **a-c**, Representative histograms of PD-L1, VCAM, ICAM (**a**), CD155, MHC I, MHC II (**b**) and HVEM (**c**) expression on LSECs. n = 2 to 3 per group (**a-c**).

I also investigated phenotype of liver NK cells and ILC1s in LPS-injected mice, as NK cells and ILC1s were shown to mediate LPS-induced septic shock (Chan et al., 2014; Emoto et al., 2002). CD25 and CD69 were reported to be the activation markers of NK cells and ILC1s (Borrego, Robertson, Ritz, Pena, & Solana, 1999; Nabekura et al., 2020). Liver NK cells consistently upregulated CD25 and CD69 expression after LPS injection (Fig. 6.25 a). Moreover, liver NK cells constantly expressed Eomes at a lower amount after LPS treatment (Fig. 6.25 a). ILC1s also consistently upregulated both CD69 and CD25 (Fig. 6.25 b), as well as PD-1 after LPS treatment, which was not observed on NK cells (Fig. 6.25 c). I did not observe phenotypic differences in liver NK cells and ILC1s between WT and Hvem cKO mice.

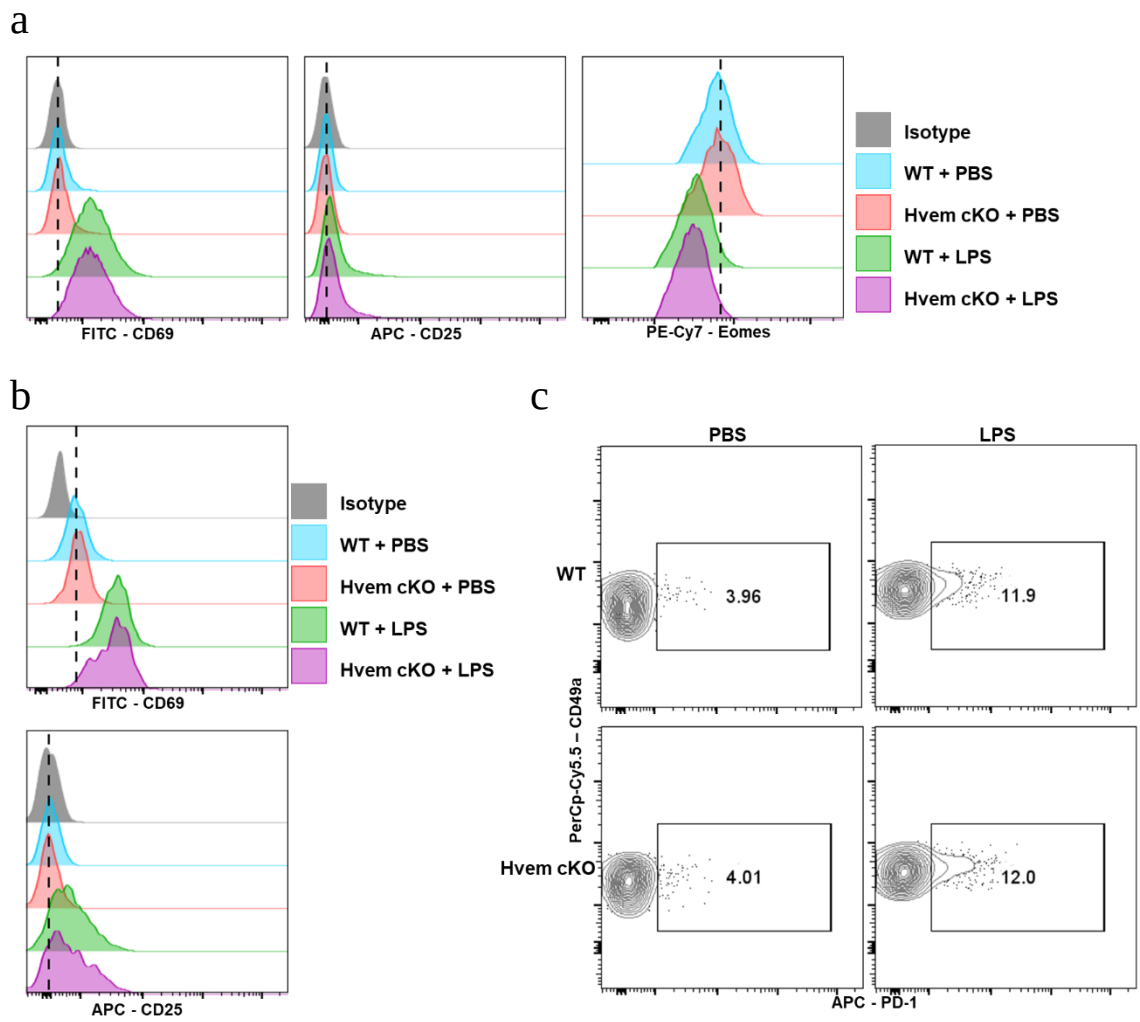

Fig. 6.25 - LPS treatment induces phenotypic changes on liver NK cells and ILC1s. Liver NPCs were harvested from WT and Hvem cKO mice (3 to 4-old month) injected with PBS or LPS (5mg/kg) and analyzed with flow cytometry. **a**, Representative histograms of CD69, CD25, and Eomes expression on NK cells. **b**, Representative histograms of CD69 and CD25 expression on ILC1s. **c**, Representative contour plots of PD-1 expression on ILC1s. n = 2 to 3 per group (**a-c**).

6.6 Co-culture of LSECs with liver NK cells and ILC1s

6.6.1 LSECs regulate expression of surface receptors on NK cells and ILC1s

To explore the interaction of LSECs with NK cells and ILC1s, I performed co-culture of LSECs and bulk liver mononuclear cells (LMCs) derived from Rag2 KO mice (deficient in T and B cells). Co-culture with LSECs led to DNAM-1 and NKG2D downregulation on liver NK cells and ILC1s (Fig. 6.26 a-b). In addition, co-culture with LSECs stimulated with IFN-γ triggered NKp46 downregulation on liver NK cells and ILC1s (Fig. 6.26 a-b).

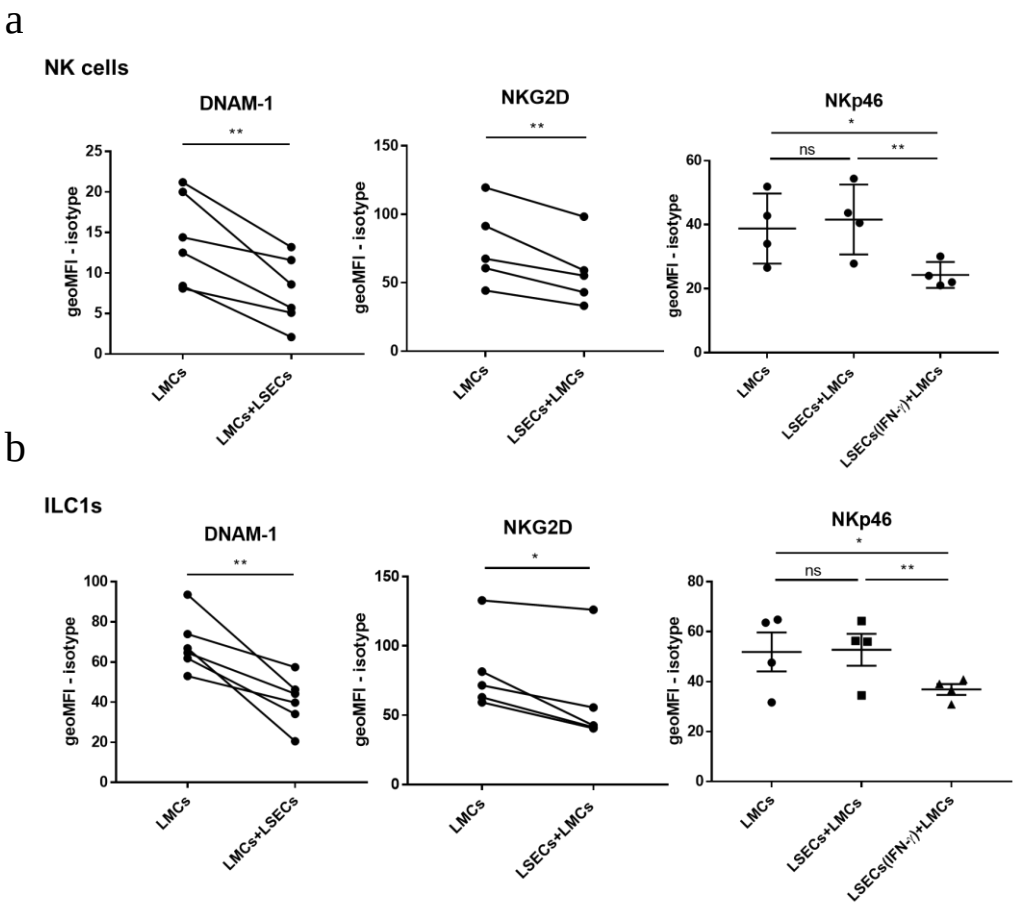

Fig. 6.26 - LSECs downregulate DNAM-1, NKG2D, and NKp46 on liver NK cells and ILC1s. Liver mononuclear cells (LMCs) from Rag2 KO mice were co-cultured with LSECs (unstimulated or stimulated with IFN-γ for 24 hours) for 4 to 18 hours, and harvested for flow cytometry analysis. **a**, Graphs depict DNAM-1, NKG2D, and NKp46 expression on $CD3^{-}NK1.1^{+}Eomes^{+}$ NK cells. **b**, Graphs depict DNAM-1, NKG2D, and NKp46 expression on $CD3^{-}NK1.1^{+}Eomes^{-}CD49a^{+}$ ILC1s. n = 4 to 6 independent experiments. Paired student t-test (DNAM-1 and NKG2D), one-way ANOVA (NKp46). $*P < 0.05$, $**P < 0.01$, ns-not significant. geoMFI - geometric mean fluorescence intensity

To investigate whether this downregulation required cell-to-cell contact, I performed co-culture experiment using a transwell insert. Co-culture with a transwell setup abrogated downregulation of DNAM-1, NKG2D, and NKp46 on NK cells and ILC1s, indicating that the downregulation was contact-dependent (Fig. 6.27 a-b). DNAM-1 is a ligand of CD155. Thus, I blocked CD155 with anti-CD155 antibody to examine if CD155-DNAM1 was engaged during co-culture, leading to DNAM-1 downregulation. Blocking CD155 abrogated DNAM-1 downregulation on NK cells/ILC1s (Fig. 6.28 a-b), showing that CD155-DNAM1 engagement led to DNAM-1 downregulation.

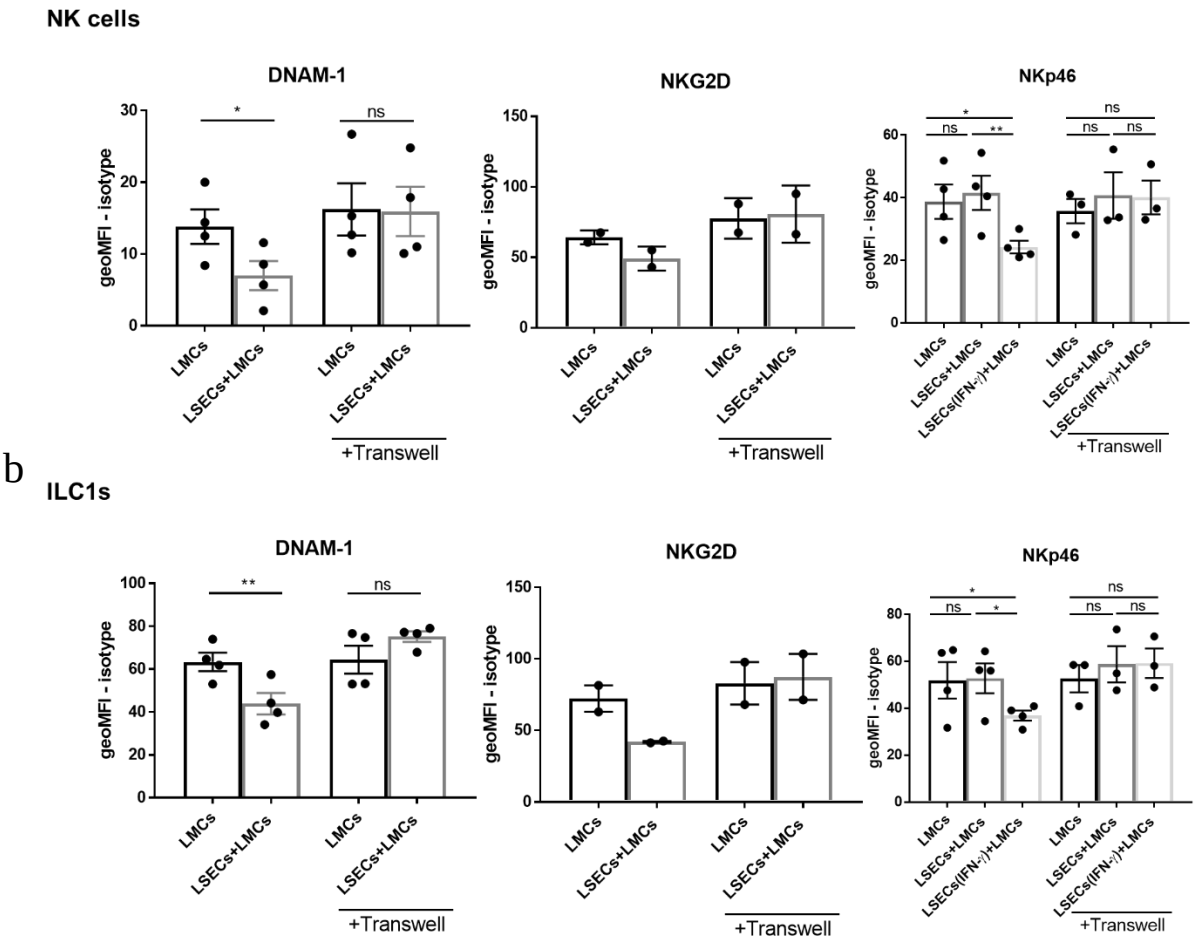

Fig. 6.27 - Cell-cell contact is required for downregulation of DNAM-1, NKG2D, and NKp46 expression on liver NK cells and ILC1s in co-culture with LSECs. Liver mononuclear cells (LMCs) from Rag2 KO mice were co-cultured with LSECs (unstimulated or stimulated with IFN-γ for 24 hours) for 4 to 20 hours, and were harvested for flow cytometry analysis. **a-b**, DNAM-1, NKG2D, and NKp46 expression on $CD3^{-}NK1.1^{+}Eomes^{+}$ NK cells (**a**) and $CD3^{-}NK1.1^{+}Eomes^{-}CD49a^{+}$ ILC1s (**b**). n = 2 to 4 independent experiments (**a-b**). For all graphs, data are represented as mean ± SEM. Paired t-test (**a-b**), one-way ANOVA (for NKp46). $*P < 0.05$, $**P < 0.01$, ns - not significant. geoMFI - geometric mean fluorescence intensity

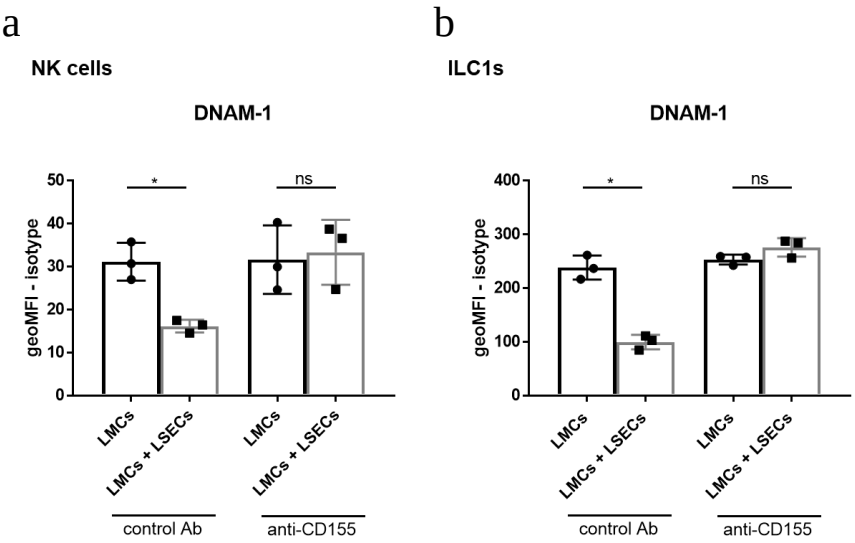

Fig. 6.28 - CD155 blockade prevents DNAM-1 downregulation on NK cells and ILC1s after co-cultured with LSECs. LMCs from Rag2 KO mice were co-cultured with LSECs for 4 - 18 hours with isotype control antibody or anti-CD155 antibody, and then harvested for flow cytometry analysis. **a-b**, DNAM-1 expression on $CD3^{-}NK1.1^{+}Eomes^{+}$ NK cells (**a**) and on $CD3^{-}NK1.1^{+}Eomes^{-}CD49a^{+}$ ILC1s (**b**). Each dot represents one independent experiment. For all graphs, data are represented as mean ± SEM. Paired t-test (**a-b**). *$P < 0.05$, ns - not significant.

6.6.2 LSECs alter NK cell effector functions

As I observed that LSECs regulate NK cell and ILC1 surface protein expression, I wanted to investigate if LSECs modulate NK cell and ILC1 effector functions. Hence, I determined IFN-γ production of NK cells and ILC1s after co-culture with LSECs. FACS-sorted NK cells and ILC1s were co-cultured with LSECs for 14-16 hours (Fig. 6.29 a). Afterwards, they were stimulated with IL-12 and IL-18 to induce IFN-γ production. NK cells produced a higher amount of IFN-γ after co-cultured with LSECs (Fig. 6.29 b). ILC1s produced a similar amount of IFN-γ after co-cultured with LSECs (Fig. 6.29 c).

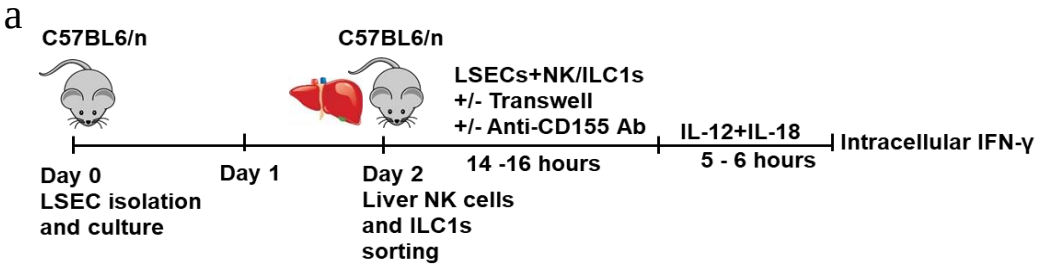

(Figure legend on the next page)

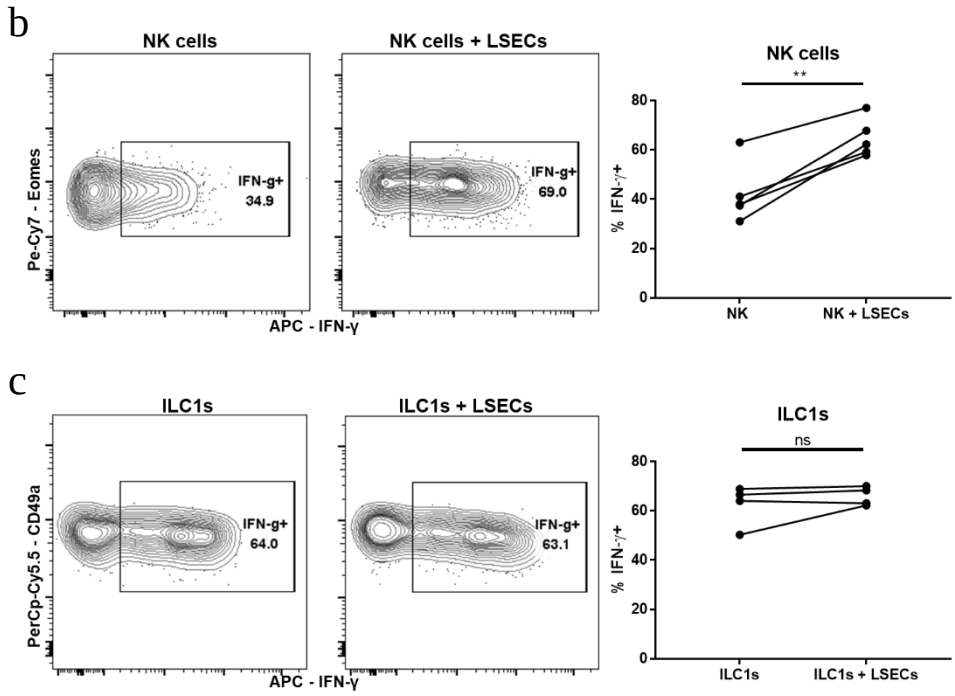

Fig. 6.29 - Co-culture of LSECs and liver NK cells leads to a higher IFNγ production in NK cells after stimulation with IL-12 and IL-18. **a**, Schematic illustration of the co-culture experiment. **b-c**, Sorted NK cells or ILC1s were co-cultured with LSECs for 14-16 hours, and stimulated with IL-12 and IL-18. Cells were harvested and intracellular staining was performed. **b-c**, Representative contour plots of intracellular IFN-γ staining of liver NK cells (**b**) and ILC1s (**c**) and its quantification. n = 4 independent experiments. For all graphs, data are represented as mean ± SEM. Paired t-test (**b-c**). $^{**}P < 0.01$, ns - not significant.

To determine whether the increase of IFN-γ production was contact-dependent, I performed co-culture experiment with transwell inserts. The increase in the IFN-γ production by NK cells after co-cultured with LSECs was abolished in a transwell insert (Fig. 6.30 a). This suggests that physical contact between LSECs and NK cells is required for the increase of IFN-γ amount upon stimulation with IL-12 and IL-18.

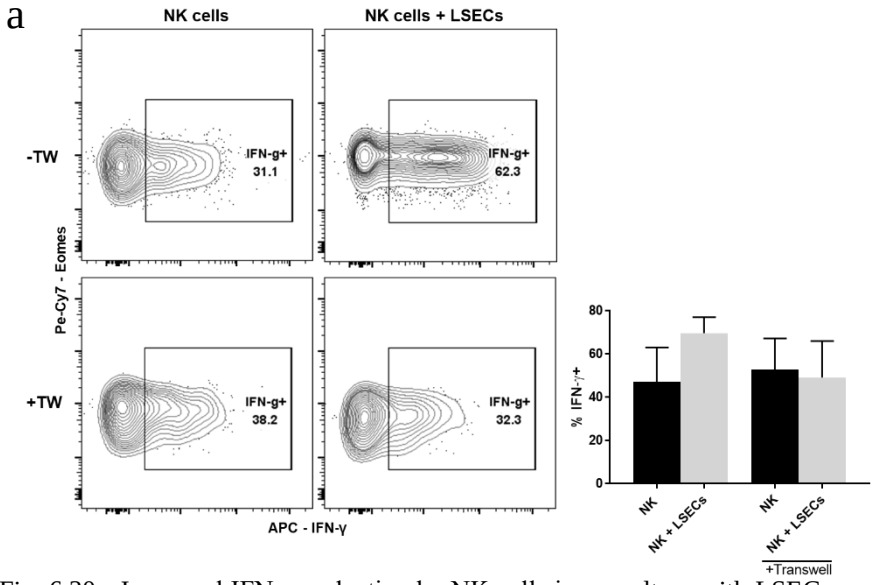

Fig. 6.30 - Increased IFNγ production by NK cells in co-culture with LSECs requires cell-cell interaction. **a**, Sorted NK cells or ILC1s were co-cultured with LSECs for 14-16 hours in the presence or absence of transwell (TW) inserts, and stimulated with IL-12 and IL-18. Cells were harvested and intracellular staining was performed. **a**, Representative contour plots of IFN-γ production by NK cells and quantification. n = 2 independent experiments. Graph is represented as mean ± SEM.

I previously showed that physical contact between LSECs and NK cells mediate receptor downregulation, and one of them was DNAM-1. My previous data showed that its cognate ligand, CD155, was expressed by LSECs in steady state. DNAM-1 was reported to be the activation receptor of NK cells, and was shown to regulate IFN-γ production(Martinet et al., 2015). I hypothesized that LSECs might regulate IFN-γ production by NK cells through CD155-DNAM-1 axis. Thus, I blocked CD155-DNAM-1 axis with anti-CD155 blocking antibody, and stimulated NK cells with IL-12 and IL-18. I did not observe any changes in IFN-γ production after CD155 blockade (Fig. 6.31 a), suggesting that CD155-DNAM-1 axis was not playing a role in the increased IFN-γ production upon stimulation with IL-12 and IL-18.

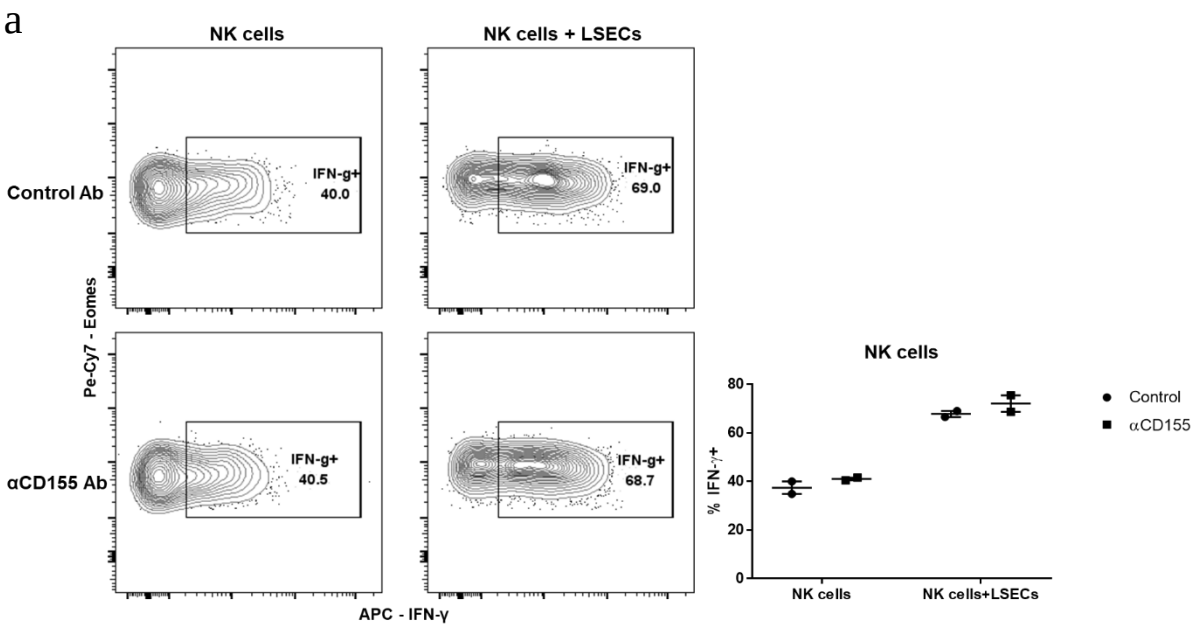

Fig. 6.31 - CD155-DNAM-1 axis does not regulate IFN-γ production of liver NK cells co-cultured with LSECs. **a**, Sorted liver NK cells or ILC1s were co-cultured with LSECs for 14-16 hours with control isotype antibody or anti-CD155 antibody, and stimulated with IL-12 and IL-18. Cells were harvested and intracellular staining was performed. **a**, Representative contour plots of IFN-γ production by NK cells and quantification. Data are representative of one experiment with two technical replicates, mean ± SEM is shown.

6.6.3 NK cells co-cultured with LSECs reveal distinct transcriptomic profile

I aimed to decipher the mechanisms of the increased IFN-γ production of NK cells after co-cultured with LSECs upon stimulation with IL-12 and IL-18. Thus, I sorted NK cells after co-culture with LSECs and used microarray technology to identify transcriptomic changes after interacting with LSECs. I included 4 conditions, NK cells, NK cells co-cultured with LSECs, NK cells stimulated with IL-12 and IL-18, and NK cells co-cultured with LSECs and stimulated with IL-12 and IL-18. I observed distinct transcriptomic profile among these 4 groups (Fig. 6.32 a). There were several upregulated and downregulated transcripts in NK cells after co-cultured with LSECs (Fig. 6.32 b - c). I validated some of the transcripts with flow cytometry. NK cells co-cultured with LSECs downregulated TRAIL, CD49a, and CD96, but upregulated CD62L (Fig 6.32 d). These data indicate that LSECs can affect NK cell functions, and the implications of the observed changes require further study.

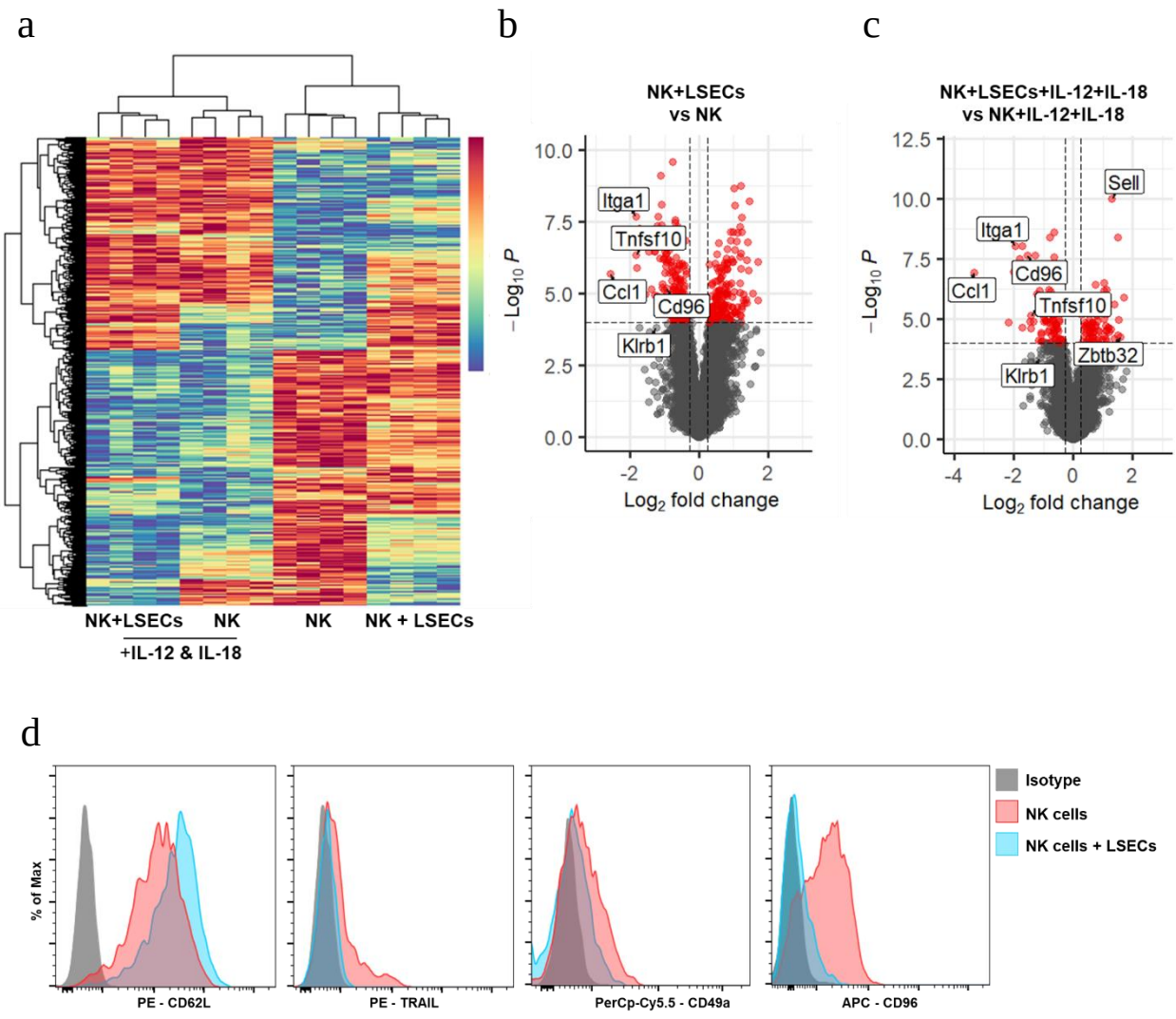

Fig. 6.32 - Liver NK cells co-cultured with LSECs reveal a distinct transcriptomic profile. **a-b**, Sorted NK cells were co-cultured with LSECs for 14-16 hours, stimulated with IL-12 and IL-18 for 5 to 6 hours, and re-sorted with flow cytometry to obtain highly purified NK cells. cDNA was synthesized from extracted RNA, and microarray experiment was conducted. **a**, Heatmap showing distinct transcriptomic profiles in 4 conditions: NK cells, NK cells+LSECs, NK cells+IL-12+IL-18, NK cells+LSECs+IL-12+IL-18. **b-c**, Volcano plots of NK cells+LSECs vs NK cells (**b**) and NK cells+LSECs+IL-12+IL-18 vs NK cells+IL-12+IL-18 (**c**), fold change > 1.2, $p < 0.0001$. **d**, Validation of the top changed transcripts with flow cytometry. After co-culture with LSECs, liver NK cells were harvested and analyzed with flow cytometry. Histograms depict the changes of CD62L, TRAIL, CD49a, and CD96 on NK cells after co-cultured with LSEC

7 Discussion

Despite forming microvessels and transporting nutrition and waste, LSECs are involved in immune responses. They are known to regulate T cell responses. For instance, LSECs can prime $CD8^+$ T cells and generate a unique liver primed memory $CD8^+$ T cells under non-inflammatory condition (Bottcher et al., 2013). This could be important in preventing immune escape, as priming by immature DCs leads to T cell deletion under non-inflammatory condition. Apart from that, LSECs can suppress $CD4^+$ T cell functions and induce T_{reg} *in vitro* (Carambia et al., 2013; Carambia et al., 2014). In agreement, Kruse et al. also showed that LSECs primed $CD4^+$ T cells *in vitro* to become T_{reg} (Kruse et al., 2009). While these T_{reg} did not express FoxP3, which is used to define T_{reg} cells, LSEC-primed T_{reg} suppressed liver inflammation in the murine autoimmune hepatitis model. The communication between LSECs and T cells is not only unidirectional, as $CD8^+$ T cells were shown to kill cross-presenting LSECs in a perforin-dependent manner in a fulminant viral hepatitis murine model (Welz et al., 2018). These studies together demonstrate that LSECs and T cells can regulate each other's functions during steady-state and disease.

NK cells and ILC1s have been defined as the innate counterparts of T cells. They are located in sinusoids, suggesting possible crosstalk between LSECs and NK cells, and ILC1s. However, the interactions between LSECs, NK cells and ILC1s remain unclear. Therefore, the aim of this study was to dissect the mechanisms of the LSEC-NK cell/ILC1 interaction.

7.1 MHC II on LSECs

MHC II is usually only expressed by professional APCs, such as DCs, macrophages, and B cells. Many papers also described MHC II expression on non-professional APCs, such as intestinal epithelial cells (IECs), LSECs, lymph node stromal cells, such as blood ECs and lymphatic ECs (Dubrot et al., 2014; Koyama et al., 2019; Lohse et al., 1996; Moon et al., 2021; Tuganbaev et al., 2020). Although the role of MHC II and its regulation was examined in IECs and lymph node stromal cells, its function and regulation in LSECs remain unclear.

7.1.1 **MHC II in the context of liver zonation**

It has been known the liver is a zonated organ, meaning that hepatocytes from different zones perform distinct metabolic tasks due to the gradient of oxygen level (Birchmeier, 2016). More recent studies revealed that LSECs mirror liver zonation pattern in both mouse and humans (Halpern et al., 2018; Strauss, Phillips,

Ruggiero, Bartlett, & Dunbar, 2017). In addition, 35 years ago Kupffer cells were reported to be mainly located in the periportal region , which was recently confirmed using more advanced imaging technology (Bouwens, Baekeland, De Zanger, & Wisse, 1986; Gola et al., 2021). Modelling showed that Kupffer cells located in the periportal region in livers were more efficient in preventing systemic bacterial spread (Gola et al., 2021). These studies indicate the importance of zonation for optimal liver metabolic and immune functions. Accordingly, my data demonstrated that LSECs expressed heterogenous amounts of MHC II on their cell surface in a zonated manner (Fig. 6.3). Lyve1^{+} midzonal LSECs expressed highest amounts of MHC II, followed by Emcn^{high} pericentral LSECs, and Emcn^{low} periportal LSECs. It is unclear why midzonal LSECs express the highest amount of MHC II, but it is expected to fulfill certain immune roles. Of note, there is a clear pattern of MHC II expression in different zones of acini. Dendritic cells (DCs) were reported to reside around portal triads (A. H. Lau & Thomson, 2003), while KCs were located in periportal region. DCs and KCs are professional APCs, so they express high amounts of MHC II. Therefore, I can appreciate a pattern from portal triad MHC II expressed by DCs, periportal MHCII expressed by KCs, and midzonal and pericentral MHC II expressed by LSECs (Fig. 7.1). Whether MHC II in different zones has distinct biological roles needs further investigations. Moreover, with advanced microscopy and imaging techniques, it will be possible to identify specialized niches of MHC II, containing immune cells like NK cells, ILC1s, and T cells.

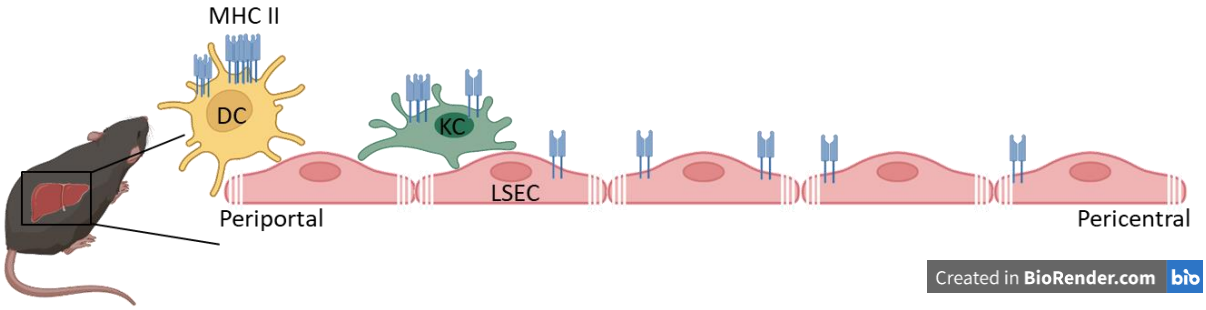

7.1 - Schematic illustration of MHC II expressed in a zonated manner by dendritic cells (DCs) near portal triad, Kupffer cells (KCs) in periportal region, and LSECs in midzonal and pericentral region of liver acinus.

7.1.2 MHC II^{high} vs MHC II^{low} LSECs

My results illustrated a distinct transcriptomic profile of MHC II^{high} compared to MHC II^{low} LSECs (Fig. 6.4). MHC II^{high} LSECs were enriched in MHC II-related transcripts, including *H2-Aa*, *H2-Ab*, *H2-Eb*, *Cd74*, and antigen degradation and presentation transcript-Cathepsin S (*Ctss*). This indicates that MHC II^{high} LSECs are equipped with the machinery required for antigen processing and presentation. Whether LSECs load antigenic peptides into the MHC II complex in a similar way as DCs and B cells, requires more investigation. Apart from that, MHC II^{high} LSECs also had higher amounts of chemokine transcripts,

including *Cxcl9* and *Cxcl10,* which encode the ligands of the CXCR3 receptor. *Cxcr3* transcript is expressed in a higher amount by liver ILC1s compared to NK cells a in single cell RNA (scRNA) sequencing database(Friedrich et al., 2021). Thus, I predict that these chemokines produced by MHC II^{high} LSECs could be important for the localization of ILCs in steady-state, and for recruiting NK cells during inflammation. Interestingly, *Cxcl9* and *Cxcl10* transcripts are mainly expressed by midzonal LSECs according to the single cell RMA expression of LSECs (Kalucka et al., 2020). In agreement, MHC II^{high} LSECs also expressed a higher amount of Lyve1 transcript, a midzonal LSEC marker, compared to MHC II^{low} LSECs. Ingenuity Pathway Analysis predicted that upstream regulators of MHC II^{high} LSEC transcript profile were involved in immune/regulation, further pinpointing their immune-like phenotypes (Fig. 6.5). The upstream regulators include CSF2 (GM-CSF), NFKB, STAT4, IL17A, STAT5a/b, CIITA, CCR1, TNFSF12, and IL1β, IFNγ, etc. It is known that ILC1s and ILC3s produce GM-CSF and IFN-γ, and ILC3s can also produce IL-17A upon activation with IL1β (Colonna, 2018). Thus, it might be postulated that MHC II^{high} LSECs are colocalized in immune niches abundant with these cytokines.

On the contrary, MHC II^{low} LSECs were enriched in transcripts involved in metabolism and development (Fig. 6.4). One of the most upregulated transcript in MHC II^{low}LSECs is *R-spondin3* (*Rspo3*). Rspo3 is the member of Wnt/β-catenin family, and angiocrine Wnt signaling was shown to be crucial for proper liver zonation and metabolic activities (Leibing et al., 2018). Rspo3 expression was reported to be restricted to central vein ECs, and Rspo3 KO mice exhibited embryonic lethality, showing an indispensable role in liver development (Rocha et al., 2015). Inducible Rspo3 deletion in adult mice also showed disrupted liver metabolic zonation, indicating its importance in liver metabolism. I postulate that my pericentral MHC II^{low} LSECs express low amount of Rspo3, thus participating in the liver development and metabolism. MHC II^{low} LSECs also express higher amount of *Jag1,* which is a Notch ligand. Jag1-Notch signaling is indispensable for blood vessel development (Akil et al., 2021), as both Jag1- and Notch-deficient mice had embryonic lethality (Conlon, Reaume, & Rossant, 1995; Xue et al., 1999). scRNA sequencing of LSECs showed that *Jag1* transcript is mainly expressed by periportal LSECs (Kalucka et al., 2020), suggesting that periportal LSECs might also participate in the liver development. MHC II^{low} LSECs were also enriched with transcripts enoding solute carrier families (*Slc39a12, Slc26a10, Slc45a4*) and *Ptgs1* involved in metabolic processes. In agreement, Ingenuity Pathway Analysis predicted MHC II^{low} LSECs to have upstream regulators involved in metabolic pathways, such as RXRα (Retinoic X receptor alpha), HDL Cholesterol and POR (Cytochrome P450 oxidoreductase) (Fig. 6.5) and organ development, such as SOX2, LHX1 (LIM hemeobox1), ANLN (Anilin actin binding protein). Therefore, my microarray data delineated that MHC II^{high} LSECs in the midzone were enriched in immune-related pathways, and MHC II^{low} LSECs in the periportal and pericentral zones were enriched in metabolic and developmental pathways.

7.1.3 The role of IFN-γ in the liver and its redundant cellular sources

IFN-γ was reported to regulate MHC II expression in non-professional APCs, such as epithelial cells and keratinocytes (Wosen et al., 2018). Here, I revealed that LSECs from Ifnγ KO and Ifnγr KO had a significant reduction in MHC II expression, suggesting a crucial role of IFN-γ in maintaining MHC II expression on LSECs (Fig 6.5). IFN-γ neutralization resulted in a significant reduction of fluorescence intensity of MHC II expression, while not affecting the percentage of LSECs expressing MHC II (Fig. 6.5). IFN-γ neutralization was not able to reduce MHC II expression on LSECs to the extent of the MHC II expression on LSECs in Ifmγ KO and Ifnγr KO mice. The data suggest that IFN-γ could be playing a developmental role, eg. modulating epigenetics of genes encoding MHC II proteins in LSECs. For instance, IFN-γ was shown to induce chromatin remodeling in macrophages, priming them to have a sustained IL-6 and TNF-γ production after TLR stimulation (Ivashkiv, 2018). In the context of my study, IFN-γ might remodel the chromatin landscape of genes required for MHC II expression in LSECs during early liver development, priming LSECs to be less dependent on IFN-γ for the MHC II expression in the later stage.

Tamoutounour et al. reported that keratinocytes expressed MHC II in Rag2 KO mice in a skin disease model, but did not express MHC II in Rag2γc DKO (Tamoutounour et al., 2019). Koyama et al. showed that intestinal epithelial cells (IECs) had a reduced MHC II expression in Rag2 KO mice, and did not express MHC II in Rag2γc DKO mice (Koyama et al., 2019). These studies suggest that NK cells, ILCs, and T cells can produce IFN-γ in steady-state and disease. Using *Ifng*-YFP reporter mice, I identified ILC1s, NK cells, and NKT cells as the predominant producers of IFN-γ in livers in steady-state, in terms of the number of cells that produce IFN-γ and their YFP-reporter expression (Fig. 6.8). Intriguingly, LSEC only had a significantly lower MHC II expression in Rag2γc DKO, but not in Rag2 KO (no T and B cells) and Hobit KO (no ILC1s), implying that only the lack of all subsets of IFN-γ-producing cells could result in the reduction of MHC II (Fig. 6.9). Therefore, these data suggest redundant IFN-γ cellular sources. Adoptive transfer of ILC1s, NK cells, and NKT cells into Rag2γc DKO will help us to confirm the capability of these immune subsets to restore MHC II expression on LSECs in steady-state.

7.1.4 Other mechanisms for regulating MHC II expression in LSECs

The identified key player which is indispensable for MHC II expression is Ciita, as Ciita KO mice did not express any MHC II on DCs, KCs, B cells, or LSECs (Fig. 6.14)(Chang et al., 1996). CIITA is the master co-transcriptional activator that assembles different proteins to initiate transcription of genes encoding MHC

II (Masternak et al., 2000). The *Ciita* gene has four promoters: pI used by dendritic cells and myeloid cells, pIII used by B cells, and pIV is used in various cells after stimulation with IFN-γ (Muhlethaler-Mottet et al., 1997). I predicted pIV to be utilized by LSECs in steady-state, as IFN-γ was required to maintain MHC II expression on LSECs. Unexpectedly, I observed that LSECs preferentially expressed pIII of *Ciita* in steady-state (Fig. 6.14). That could explain why IFN-γ neutralization in steady-state did not result in a similar MHC II reduction as observed in that of Ifnγ KO and Ifnγr KO (Fig. 6.5). In addition, deacetylase inhibitor trichostatin (TSA) was also reported to induce gene expression of different promoters of *Ciita* in a cell line-dependent manner (Chou, Khan, Magner, & Tomasi, 2005), showing a close connection between chromatin remodeling and CIITA expression. During early liver development, IFN-γ might modulate chromatin landscape of *Ciita* gene in a way that pIII is preferentially used in the later stage, resulting in less dependency on IFN-γ for MHC II expression in steady-state, as demonstrated by my IFN-γ neutralization experiment (Fig. 6.5).

Furthermore, several cytokines were reported to maintain or upregulate MHC II expression on different cells. GM-CSF was reported to upregulate MHC II expression on human monocytes and mouse DCs (Hamilton, 2019; Mausberg, Jander, & Reichmann, 2009). IL-22, which is secreted by ILC3s and Th17 cells, was the sole cytokine responsible for MHC II expression on keratinocytes during *S.epidermidis* infection (Tamoutounour et al., 2019). IL-18 was also reported to synergistically work with IFN-γ to induce a higher MHC II expression on human keratinocytes (Wittmann, Purwar, Hartmann, Gutzmer, & Werfel, 2005). In addition, IL-1β was described to upregulate MHC II on ILC3s (von Burg et al., 2014). Therefore, the residual expression of MHC II on LSECs in Ifnγ KO and Ifnγr KO mice, and after IFN-γ neutralization, could be explained by the presence of other cytokines which can maintain MHC II expression.

Another known biological process, apart from transcriptional regulation, allowing cells to express MHC II is trogocytosis. Trogocytosis is a process, through which one cell acquires membrane part of another cell in a contact-dependent manner (Nakayama, 2014). Hence, cells can start to express membrane proteins, whose genes are not transcriptionally active. For instance, lymph node stromal cells, T cells and NK cells were demonstrated to acquire MHC II from APCs, and the acquired MHC II was functionally competent (Dubrot et al., 2014; Nakayama et al., 2011; Tsang, Chai, & Lechler, 2003). Indeed, it was reported that LSECs were able to trogocytose MHC I from hepatic stellate cells (Scholzel et al., 2014). Moreover, LSECs could also acquire MHC II through exosomes. It was previously shown that MHC II-loaded exosomes from DCs were acquired by MHC II-deficient DCs, leading to $CD4^+$ T cell activation (Thery et al., 2002). It is not surprising that LSECs are taking up exosomes actively, given their high endocytic and scavenging capability. Thus, the residual MHC II level on LSECs in Ifnγ KO and Ifnγr KO mice could also be the consequence of either

trogocytosis or uptake of MHC II-containing exosomes. The ability of LSECs to uptake MHC II from other cells can be tested *in vitro* by co-culturing LSECs with MHC II-expressing cells, and determine whether LSECs will express MHC II after co-culture. Furthermore, conditional MHC II deletion in myeloid cells would allow us to determine if LSECs acquire MHC II from myeloid cells in steady-state. If LSECs acquire MHC II from myeloid cells, LSECs should express a lower amount of MHC II in steady-state in mice of conditional MHC II deletion in myeloid cells.

7.1.5 Upstream inducers of IFN-γ in steady-state

IL-12 is a Th1 cytokine that is known to induce lymphocytes to produce IFN-γ, and mice that lack IL-12 or IL-12R are defective in IFN-γ production and type I cytokine response (Magram et al., 1996; C. Wu, Ferrante, Gately, & Magram, 1997; C. Wu et al., 2000). I investigated if IL-12 was the upstream inducers of IFN-γ in livers in steady-state. Ingenuity Pathway Analysis depicted that STAT4 was the upstream regulator of MHC II^{high} LSEC phenotype. STAT4 acts downstream of IL-12R activation (Thierfelder et al., 1996), implying that MHC II^{high} LSECs might be residing in an IL-12-rich microenvironment. Hence, I examined MHC II expression on LSECs in Il12rb2 KO mice. LSECs in Il12rb2 KO mice showed a significant decrease in MHC II expression (Fig. 6.11), but not to the extent of the MHC II expression of LSECs in Ifnγ KO and Ifnγr KO mice (Fig. 6.5). This suggests that other signaling pathways could work together with IL-12 as the upstream of IFN-γ production. Alternatively, IL-12 might only contribute to the MHC II expression after postnatal liver development, as the pattern of MHC II reduction in Il12rb2 KO mice was comparable to IFN-γ neutralization (Fig. 6.11).

Microbiota can also play a role in inducing IFN-γ production in immune cells, as the liver is constantly exposed to bacterial antigens transported from intestines through the portal vein. The MHC II expression on intestinal epithelial cells (IECs) required presence of microbiota, as MHC II was absent on IECs from germ-free mice and Myd88-Trif double deficient mice (Koyama et al., 2019; Tuganbaev et al., 2020). I hypothesized that MHC II expression in LSECs might be regulated the same way as in IECs, since livers and guts are both part of the gastrointestinal tract system. To this end, I examined MHC II expression of LSECs in germ free mice, Myd88 KO mice, Tlr4 KO mice, and ABX-treated mice to investigate the role of microbiota. None of these models demonstrated a contribution of microbiota in MHC II regulation on LSECs (Fig 6.13), indicating a different mechanism of MHC II regulation compared to IECs. With no changes in the MHC II expression on LSECs in Myd88 KO mice, my data also ruled out the contribution of IL-18, which is a cytokine that stimulates lymphocytes to produce IFN-γ via the MyD88 signaling pathway (Adachi et al., 1998; Okamura et al., 1995).

Dendritic cells in gut were reported to secrete IL-12 in steady-state, independent of microbiota (Everts et al., 2016). DCs in lymph nodes also produce IL-12 in steady-state (Ashour et al., 2020). In agreement, a recent mouse liver scRNA sequencing data revealed that a subpopulation of DCs expresses the *Il12β* transcript in steady-state (Guilliams et al., 2022). My results indicate that IL-12 is produced independently of microbiota, but the source of IL-12 remains unclear. I hypothesize that the source could be liver dendritic cells. IL12p40-reporter mice are available and can be used to determine the source of IL-12 in the liver. Transgenic mice expressing the diphtheria toxin receptor under control of the *Cd11c* promoter can also be used to deplete DCs to determine whether this would result in a reduction of MHC II expression on LSECs. Hepatic DCs mainly reside around the portal triad of the liver. If DCs are the source of IL-12 in my experimental system, IL-12 might be released in the bloodstream towards the periportal region. It was reported that CXCR6-expressing cells (NKT cells and ILC1s) were located mostly in the periportal region (Gola et al., 2021). Therefore, lymphocytes in the periportal region might be activated by IL-12 to secrete IFN-γ, which will follow the direction of the bloodstream and move to the midzonal and pericentral acini. This would create an IFN-γ concentration gradient among different regions of the liver acini. This could explain why midzonal LSECs express the highest amount of MHC II, followed by pericentral LSECs, while periportal LSECs do not express MHC II.

IL-15 is a Th1 cytokine which can also stimulate production of IFN-γ(Carson et al., 1995). IL-15 is indispensable for lymphocyte development; thus, IL15 KO and IL15Rα KO mice lack NK cells, NKT cells, and ILC1s (Lodolce et al., 1998; Robinette et al., 2017). STAT5a/b acts downstream of IL-15R activation (Johnston et al., 1995). My Ingenuity Pathway Analysis predicted STAT5a/b to be an upstream regulator of the MHC II^{high} LSEC phenotype, implying that MHC II^{high} LSECs might be residing in an IL-15 abundant niche. Therefore, analyzing IL15 KO and IL15R KO mice could address whether the absence of IL-15 and IL-15R signaling would result in the reduction of MHC II expression on LSECs. In addition, IL-15 in mice can be neutralized to investigate the role of IL-15 without affecting immune cell development. The source of IL-15 in liver is less studied in steady-state, but it was reported that Kupffer cells and hepatocytes constitutively produce IL-15 (M. P. Correia et al., 2009; Golden-Mason et al., 2004). IL-15 is usually trans-presented to other cells through the IL-15Rα on the membrane of the IL-15-producing cells (Dubois, Mariner, Waldmann, & Tagaya, 2002). Thus, IL-15 and IL-15R gene and protein expression analysis could be done in different subsets of cells in livers to determine the predominant source of IL-15. Furthermore, it will be important to examine IL-15Rα on both liver parenchymal and non-parenchymal cells to determine whether these cells can trans-present IL-15. Conditional IL-15 KO on hepatocytes or myeloid cells would help to identify whether IL-15 produced by these cells is responsible for IFN-γ production in livers.

Another cytokine that signals upstream of STAT5a/b is IL-2 (Lin & Leonard, 2000). IL-2 and IL-15 share IL2Rβ and IL2Rγ. Therefore, IL-2 also plays an indispensable role in lymphocyte development. IL2 KO and IL2Rα (α chain only expressed by IL2R) KO mice show a severe T cell proliferation, autoimmune disease, and early mortality (Sadlack et al., 1994; Schultz et al., 1999; Willerford et al., 1995). The IL2Rγ KO (common γ chain shared by IL-2, -4, -7, -9, -15, -21) lacks all NK cells and ILCs (DiSanto, Muller, Guy-Grand, Fischer, & Rajewsky, 1995), and was further crossed to Rag2 KO mice to generate Rag2γc DKO that lacked all lymphocytes (Goldman et al., 1998). It was shown that IL-2 can stimulate NK cells and T cells to produce IFN-γ (Handa, Suzuki, Matsui, Shimizu, & Kumagai, 1983; Kasahara, Hooks, Dougherty, & Oppenheim, 1983). IL-2 neutralization could be performed to investigate if this will affect MHC II expression on LSECs in steady-state.

Beside cytokines, other factors might also be the upstream inducers of IFN-γ. For instance, Kupffer cells or LSECs might express ligands that can engage with activating receptors, like NK1.1 or NKp46, on NK cells, ILC1s, or NKT cells, which can activate tonic level of IFN-γ production in the liver microenvironment in steady-state. It was reported that NKG2D on NK cells was engaged by RAE-1 expressed by lymph node blood and lymphatic ECs in steady-state, leading to desensitization of NK effector functions (Thompson et al., 2017). Therefore, mouse models, which are deficient in Kupffer cells or myeloid cells, will be useful in the future to determine whether Kupffer cells or myeloid cells are the upstream inducers of IFN-γ production, and if LSECs from these models will induce a similar phenotypes as Ifnγ KO and Ifnγr KO mice. Kupffer cells and myeloid cells might modulate immune cells to produce IFN-γ through unknown receptor-ligand interactions or soluble factors, which requires further investigation.

7.1.6 Functional relevance of MHC II in livers

LSECs were reported to generate liver-primed memory $CD8^+$ T cells in non-inflammatory conditions, which were re-activated upon antigen re-challenge (Bottcher et al., 2013). In the absence of inflammation, priming by immature DCs results in T cell deletion or anergy. Thus, the ability LSECs to generate $CD8^+$ memory T cells under non-inflammatory conditions could enable effective immune responses against pathogens that inhibit DC maturation (Bottcher et al., 2013). My data demonstrate that the reduction of MHC II expression on LSECs coincided with an increased frequency of $CD62L^+CD44^-$ $CD4^+$ naïve T cells and a decreased frequency of $CD62^-CD44^+$ $CD4^+$ effector memory T cells in livers of Ifnγ KO and Ifmγr KO mice, compared to $CD4^+$ T cells of WT mice (Fig. 6.15). I did not observe alterations in liver $CD8^+$ T cell compartment, suggesting a specific $CD4^+$ T cell phenotype affected by the reduced MHC II expression. I also did not detect changes in lung $CD4^+$ T cells. I only detected an increase percentage of $CD62L^+CD44^-CD4^+$ naïve T

cells and a decrease percentage of $CD62^{-}CD44^{+}$ $CD4^{+}$ effector memory T cells in spleens of Ifnγ KO mice, but not Ifnγr KO mice, compared to that of WT mice, and this requires more exploration. However, the changes in the frequency of naïve and memory $CD4^{+}$ T cells in spleens were smaller compared to liver $CD4^{+}$ T cells in Ifnγ KO mice. These data suggest a liver-restricted role $CD4^{+}$ T cell phenotype. I was not able to conclusively demonstrate that the alteration in liver $CD4^{+}$ T cell phenotype was due to the reduction of MHC II expression on LSECs, as KCs also expressed lower amounts of MHC II in Ifnγ KO and Ifnγr KO mice, compared to KCs of WT mice. Nevertheless, the changes observed in liver $CD4^{+}$ T cells in Ifnγ KO and Ifnγr KO mice was most likely due to the reduction of MHC II expression on LSECs, as LSECs were the most affected population among all liver non-parenchymal cells. I hypothesize that MHC II expression on LSECs is crucial for liver $CD4^{+}$ T cell development and tolerance. LSECs might prime $CD4^{+}$ T cells in steady-state (non-inflammatory condition) to generate pool of memory T cells for future re-activation upon antigen re-encounter. Future studies should aim at generating conditional deletion of gene encoding MHC II in LSECs, and analyze T cell phenotypes in detail.

As LSECs are known to induce $CD4^{+}$ Treg cells (Carambia et al., 2014; Kruse et al., 2009), I also examined the Treg population in the liver in Ifnγ KO and Ifnγr KO mice. To identify the entire Treg population in livers by FoxP3 expression might be challenging, as LSEC-primed Treg *in vitro* did not express FoxP3, but they exhibited suppressive function in a hepatitis murine model (Kruse et al., 2009). I used FoxP3 expression as the marker for Treg identification (Fontenot et al., 2017), and I did not observe any difference in FoxP3 expression in the $CD4^{+}$ T cell population. It is unclear, whether all Treg in the liver express FoxP3, as some Treg populations can have suppressive functions without expressing FoxP3 (Curotto de Lafaille & Lafaille, 2009). Future studies should include more markers to identify different population.

7.1.7 Summary I

My data revealed that midzonal LSECs expressed the highest amounts of MHC II. MHC II^{high} and MHC II^{low} LSECs displayed distinct transcriptomic profiles, with MHC II^{high} LSECs being more ‘immune-like’. IFN-γ facilitated high levels of MHC II expression on the LSECs surface. The major cellular sources of IFN-γ in the liver were ILC1s, NK cells, and NKT cells. The lack of ILC1s or T cells did not affect MHC II expression on LSECs. Only the lack of all lymphocytes resulted in a reduced MHC II expression on LSECs, indicating redundant IFN-γ cellular sources. IL-12 was involved in the MHC II maintenance on LSECs, but it did not directly induce MHC II expression on LSECs *in vitro*. Hence, IL-12 might induce IFN-γ production of immune cells that is required for the MHC II maintenance on LSECs. I hypothesize that DCs are the source of IL-12 in steady-state. Microbiota was not involved in regulating MHC II

expression on LSECs. CIITA, the transcriptional co-activator of genes encoding MHC II, was indispensable for the MHC II expression on LSECs. The reduction of MHC II on LSECs correlated with an increased naïve $CD4^+$ T cell and a decreased memory $CD4^+$ T cell frequency in the liver. My findings discover the unconventional role of LSECs to act as a bridge between innate and adaptive immunity. The predicted model of LSEC and immune cell interactions based on my results is illustrated in Fig 7.2.

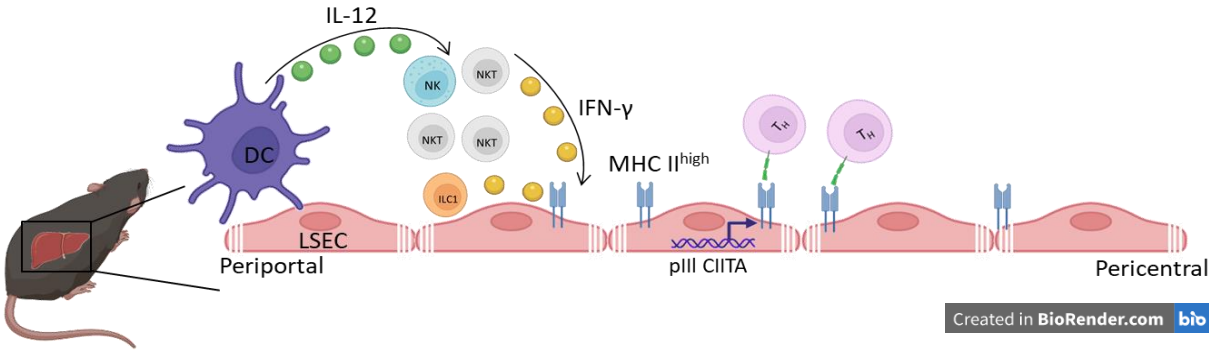

Fig- 7.2 - Schematic model of DCs - ILC1/NK/NKT - LSEC - $CD4^+$ T cell interaction.

7.2 HVEM on LSECs

7.2.1 Residual HVEM expression on LSECs of Hvem cKO mice

My data showed that HVEM was expressed by LSECs in steady-state (Fig. 6.1), and upregulated upon stimulation with IFN-γ (Fig. 6.2). Mice expressing cre recombinase under control Clec4g promoter (Clec4g-cre) to express Cre recombinase in LSECs and some ECs in the heart, but not in bone marrow, spleen, lung and kidney (Wohlfeil et al., 2019). Therefore, I generated conditional Hvem-deficient mice in LSECs by crossing Clec4g-cre mice with $Hvem^{flox/flox}$ mice to investigate its functional role. Peculiarly, LSECs still expressed residual HVEM protein in the Hvem cKO mice. Therefore, I sorted LSECs, KCs, and other myeloid cells to verify the HVEM gene expression (Fig. 6.17). RT-PCR results showed that *Hvem/Tnfrsf14* transcript was not detectable in Hvem cKO LSECs, confirming efficient *Hvem/Tnfrsf14* gene deletion. Furthermore, Hvem cKO LSECs lost all residual HVEM surface protein after *in vitro* culture and could not upregulate HVEM protein upon stimulation with IFN-γ. This indicates that *Hvem* transcript is absent in Hvem cKO LSECs and it is intriguing that HVEM protein is detectable. These data suggest that LSECs might take up HVEM protein from other cellular sources, either through direct interaction or exosomes, under homeostatic condition.

Trogocytosis is a mechanism through which LSECs can acquire membrane proteins from other cells (Joly & Hudrisier, 2003). It is a fast process, which happens within minutes after cell-cell direct contact. It is not surprising that LSECs trogocytose actively in steady-state, as they have high scavenging and endocytic capability (Mates et al., 2017). It was also reported that LSECs can acquire MHC I protein by trogocytosis from hepatic stellate cells (Scholzel et al., 2014). Thus, the residual HVEM protein expression on LSECs in Hvem cKO mice could be resulting from trogocytosis in homeostasis. Nonetheless, it has never been reported whether membrane expressing HVEM can be trogocytosed. To investigate whether LSECs can acquire HVEM by trogocytosis, Hvem cKO LSECs could be co-cultured with different liver parenchymal and non-parenchymal cells. If cKO LSECs start to express HVEM surface proteins after short time of culture, this would indicate trogocytosis. To investigate this *in vivo*, *Hvem/Tnfrsf14* gene will have to be conditionally deleted in different cells in the liver. If LSECs acquire HVEM from other cells in steady-state, I would expect a lower HVEM expression on LSECs in these conditional Hvem cKO murine models. Interestingly, my preliminary data depicted that LSECs expressed a lower amount of HVEM in Stabilin1 KO and Stabilin2 KO mice, compared to that of WT mice (data not shown). Stabilin1 and Stabilin2 are two vital scavenging receptors (Schledzewski et al., 2011), and the loss of these receptors could affect the ability of LSECs to trogocytose membrane from other cells. The trogocytosis capability of LSECs demands further

investigation, as it is posing big conceptual challenges to study the functional role of immune surface molecules on LSECs by generating LSEC-restricted conditional KO mouse models.

Another possible mechanism for Hvem cKO LSECs to express HVEM membrane protein is by uptaking extracellular vesicles including exosomes, microvesicles, or apoptotic bodies in steady-state (van Niel, D'Angelo, & Raposo, 2018). It is unclear whether HVEM can be packed on the membrane of extracellular vesicles. Several immune surface proteins like MHC I, MHC II, and PD-L1 can be expressed by exosomes, and have an impact on the host immune response (Chen et al., 2018; Zitvogel et al., 1998). Thus, it is likely that HVEM can also be expressed on vesicles, and these vesicles are taken up by LSECs in steady-state. In this way, Hvem cKO LSECs can express HVEM membrane protein derived from other cells. To address the cellular source of HVEM-containing vesicles might be difficult, as HVEM-containing vesicles can originate from any organ and can be circulating throughout the body. LSECs were reported to remove circulating factors through Stabilin-1 and Stabilin-2 receptor, and the loss of these scavenging receptors resulted in kidney glomerular fibrosis (Schledzewski et al., 2011). As my preliminary data showed that LSECs expressed a lower amount of HVEM in Stabilin1 KO and Stabilin2 KO mice, Stabilin1 and Stabilin2 might be involved in scavenging circulating vesicles in steady-state. Soluble HVEM-containing vesicles were also previously reported in human sera (Jung et al., 2003). Further investigation is required to study whether HVEM is expressed on vesicles and if LSECs can uptake extracellular vesicles in steady-state.

7.2.2 The role of HVEM in aging

To date, the role of HVEM in aging has not yet been reported. Clec4g-cre mice were revealed to express Cre recombinase in LSECs and some ECs in the heart, but not in spleens (Wohlfeil et al., 2019). Unexpectedly, aged Hvem cKO mice (>1year-old) displayed splenomegaly, but no changes of liver weight and liver/body weight ratio (Fig. 6.20). Metabolic parameters in the sera were unchanged. The enlarged spleens could be due to the loss of HVEM on LSECs, or the loss of HVEM on spleen endothelial cells. Spleen ECs are also sinusoidal ECs, possessing fenestrae and incomplete basement membrane (De Bruyn & Cho, 1974; Partanen et al., 2000). scRNA sequencing of spleen EC revealed that they expressed Clec4g (Kalucka et al., 2020). Recently, Clec4g was reported to also be expressed by a subset of Kupffer cells (Bleriot et al., 2021). Thus, I cannot rule out that certain subsets of myeloid cells in spleens might also express Clec4g, and the phenotype was due to the deletion of *Hvem/Tnfrsf14* gene in myeloid cells in addition to ECs. More detailed experiments are needed to confirm which cells in spleens and livers are affected by Clec4g-cre, in order to determine the mechanism underlying the phenotype in aged Hvem cKO mice.

Larger spleens in aged Hvem cKO mice could indicate infection or injury. However, aged Hvem cKO mice did not show signs of sickness. Aged Hvem cKO mice had an increased cell number in spleens, compare to spleens in WT mice (Fig. 6.20). Absence of increased massive myeloid infiltration suggested that these mice did not have on-going bacterial infection (Fig. 6.21). Histopathological examination did not reveal significant pathology in the spleens and other organs of Hvem WT and cKO mice (data not shown).

Naïve T cells express CD160, BTLA, and LIGHT molecules, which can bind to HVEM. CD160 and BTLA are inhibitory receptors, while LIGHT is an activating receptor on naïve T cells (Cai et al., 2008; Tamada et al., 2000; Watanabe et al., 2003a). It was reported that cysteine-rich domain 1 (CRD1) of HVEM binds to BTLA with a higher affinity than to CD160 (Liu et al., Structure, 2019). LIGHT does not compete with BTLA and CD160, as it binds to CRD2 and CRD3 of HVEM (Cai et al., 2008). Thus, HVEM can affect T cell activation and effector functions by engaging CD160, BTLA, and LIGHT on T cells. I analyzed $CD4^+$ and $CD8^+$ T cells in spleens, and the naïve T cell and memory T cell frequency among these populations. Despite some trends of alteration of T cell compartment, I was not able to draw conclusion due to the small sample size (Fig. 6.22). Further experiments are required to confirm the alteration in T cells. Future studies should aim at characterizing T cell phenotypes and functions in Hvem cKO mice using flow cytometry.

7.2.3 The role of HVEM in liver disease

HVEM was implicated in several diseases. It was first reported in a colitis model that HVEM expressed by radioresistant cells bound to BTLA and inhibited T cell functions, thus suppressing inflammation (Steinberg et al., 2008). A follow-up study implied that intrinsic HVEM-STAT3 signaling in intestinal epithelial cells provided defense against pathogenic bacteria by binding to CD160 on intraepithelial lymphocytes (Shui et al., 2012). The same research group also reported that HVEM on ILC3s was important for IFN-γ production and protection against intestinal bacterial infection by binding LIGHT (Seo et al., 2018). Thus, there are bi-directional signaling pathways resulting in cell activation or inhibition, when HVEM engages with CD160, BTLA, or LIGHT.

A few studies investigated the role of HVEM in liver diseases. HVEM on T cells was thought to be inhibitory, as T cells derived from global HVEM KO mice produced more cytokines upon activation both *in vitro* and *in vivo*. In a mouse model of T-cell mediated acute liver autoimmune hepatitis induced by injection of ConA, global HVEM KO mice showed increased inflammation, liver injury, and mortality, compared to WT mice (Y. Wang et al., 2005). It was also reported that blockade of LIGHT in the ConA model ameliorated liver injury in mice (An et al., 2006). In agreement, blockade of LIGHT protein prevented

ConA induced hepatitis in zebrafish, and HVEM was crucial for suppressing T cell functions by engaging BTLA (Shi et al., 2019). In general, HVEM played a consistent suppressive role in ConA-induced liver autoimmune hepatitis, but it is still unclear if the phenotype was due to T cells or other cell types which also express HVEM.

For this reason, I generated conditional Hvem cKO (Cleg4g-cre x $HVEM^{flox/flox}$) on LSECs to determine its functional role in liver diseases. I used LPS to induce systemic endotoxicosis and inflammation, as NK cells were reported to augment LPS-induced septic shock (Chan et al., 2014; Emoto et al., 2002; Heremans et al., 1994). Moreover, NK cells and NKT cells were shown to produce a high amount of IFN-γ in the LPS model (Varma, Lin, Toliver-Kinsky, & Sherwood, 2002). I observed that LPS injection caused major phenotypic changes on LSECs, as they upregulated PD-L1, ICAM, VCAM, CD155, MHC I, and MHC II expression (Fig. 6.24). I demonstrated that LSECs stimulated with IFN-γ *in vitro* upregulated PD-L1, MHC I, and MHC II expression (Fig. 6.2). Therefore, the upregulation of these molecules on LSECs in the LPS liver injury model might be due to IFN-γ secreted by NK cells, ILC1s, and NKT cells upon activation.

NK cells were reported to augment LPS-inducted liver injury (Chan et al., 2014; Emoto et al., 2002; Heremans et al., 1994). I detected a higher absolute number of NK cells in the liver after LPS injection (Fig. 6.23), which could indicate NK cell infiltration or *in situ* proliferation in the liver. The increased NK cells in the liver could lead to an enhanced acute liver inflammation and injury. CD69 and CD25 have been widely used in human and mouse T cells, and human NK cells, as activation markers (Borrego et al., 1999; Clausen et al., 2003). Accordingly, a recent study reported that liver ILC1s also upregulated CD69 and CD25 18 hours after CCl_4 injection, and the upregulation correlated with IFN-γ production (Nabekura et al., 2020). I observed that both liver NK cells and ILC1s upregulated CD69 and CD25 in the LPS liver injury model. Liver ILC1 upregulated CD69 and CD25 expression in both the LPS and CCl_4 model, suggesting a common mechanism upon activation. Furthermore, Nabekura et al. showed an increase in NK cell number, but no change in ILC1 cell number in the liver after CCl_4 injection. In agreement, I also observed an increase in NK cell number, but not ILC1 number in the liver after LPS injection (Fig. 6.23), possibly suggesting a common early response of NK cells and ILC1s in acute liver injury. The mechanism of NK cell infiltration or proliferation in the liver is still unclear. I hypothesize that LSECs might secrete chemokines or upregulate adhesion molecules during liver damage to recruit NK cells, which is one of the initial response of endothelial cells during inflammation (Vestweber, 2015).

PD-1 was described as an inhibitory receptor on T cells, and has become a promising target in immunotherapy to treat cancer (Sharpe & Pauken, 2018). PD-1 can be induced on NK mice in mice, but its

role on human NK cells remain controversial (Hsu et al., 2018; Judge et al., 2020; Quatrini et al., 2018). In addition, PD-1 is expressed by ILC progenitors, and can be upregulated on ILC2s during disease (Taylor et al., 2017; Yu et al., 2016). My results revealed that around 10% of liver ILC1s expressed PD-l after LPS injection (Fig. 6.25). Its role on ILCls remains unclear in my LPS model. Intriguingly, it was demonstrated that ILC1s expressed PD-L1, a ligand of PD-1, in steady-state (Zhou et al., 2019). Zhou et al. also showed that ILC1s upregulated PD-L1 in viral infection, that bound to PD-1 to suppress T cell functions (Zhou et al., 2019). The interaction between PD-1 and PD-L1 in cis on liver ILC1s remains to be investigated.

Monocytes were recruited into liver after CCl_4 and acetaminophen (APAP)-induced acute liver injury (Karlmark et al., 2009; Mossanen et al., 2016). I also detected an increased monocyte absolute number in LPS-treated mice in the liver. Hence, monocyte infiltration or proliferation might be a common mechanism during liver injury and inflammation. In APAP-induced acute liver injury, CCR2 KO mice that exhibited defective monocyte infiltration had a reduced Alanine Aminotransferease (ALT) activity, a liver damage marker (Mossanen et al., 2016). In CCl_4-induced liver injury, CCR2 KO mice did not have a lower ALT activity in sera, but they had a reduced hepatic fibrosis due to less hepatic stellate cell activation, compared to that of WT mice (Karlmark et al., 2009). It is still controversial whether depleting monocytes in the initial stage would prevent liver damage, and it could be dependent on the liver injury model (Brempelis & Crispe, 2016). My LPS liver injury model did not induce ALT activity as high as other reported liver injury models, such as CCl_4, ConA, or APAP (Mossanen et al., 2016; Nabekura et al., 2020; Tiegs et al., 1992a). Therefore, measuring ALT activity as the parameter in LPS liver injury model might not correlate with the severity of liver damage. Other indicators like serum TNF-α and IFN-γ could give better insights about the severity of liver damage in the LPS liver injury model. Alternatively, LPS and D-galactosamine co-injection was reported to induce high ALT activity in serum of mice, and this model mimics fulminant hepatitis, instead of septic shock (Mignon et al., 1999; Mohler et al., 1994). This might serve as a better model to use ALT activity to correlate with liver damage severity.

I first examined the LPS model, as NK cells were mediating LPS-induced endotoxemia (Chan et al., 2014; Emoto et al., 2002; Heremans et al., 1994). However, I did not observe any phenotypic changes on LSECs, NK cells, and ILC1s in all parameters that I measured between WT and Hvem cKO in adult mice (3-4 month old) 20 hours after LPS injection. Other parameters, such as serum TNF-α and IFN-γ, might help us to detect differences between WT and HVEM KO mice. Alternatively, LPS co-injected with D-galactosamine model can be used as another acute liver injury model. CD160, the ligand of HVEM, is expressed by ILC1s in steady-state (Di Censo et al., 2021). ILC1s were revealed to be protective in CCl_4-induced liver damage (Nabekura et al., 2020). Thus, the CCl_4 liver injury model will allow us to investigate the interaction of

HVEM on LSECs with CD160 on ILC1s. Global HVEM KO mice were shown to be more susceptible to ConA induced, T cell-mediated autoimmune hepatitis (Y. Wang et al., 2005). As T cells express CD160, BTLA, and LIGHT, it will also be interesting to use ConA-induced liver injury model to examine the role of HVEM on LSECs in modulating liver T cell functions.

7.3 LSEC interaction with NK cells and ILC1s

7.3.1 Receptor and ligand interaction

NK cells and ILC1s express activating and inhibiting receptors, and overall effector functions of NK cells and ILC1s are dictated by the signal strength received by the activating and inhibitory receptors (Long, Kim, Liu, Peterson, & Rajagopalan, 2013). In my study, I mainly focused on the receptors DNAM-1, NKG2D, and NKp46.

DNAM-1 was first described as an adhesion molecule, which played an important role in cytotoxicity and cytokine production of NK cells (Martinet et al., 2015; Shibuya et al., 1996). The two identified ligands of DNAM-1 are CD155 and CD112 (Pende et al., 2005). ILC1s were demonstrated to express higher amounts of DNAM-1 than NK cells (Romero-Suarez et al., 2019). DNAM-1 was also reported to be important for activating ILC1s to produce IFN-γ in a CCl_4 acute liver injury model, and this was crucial for preventing hepatocyte cell death (Nabekura et al., 2020). My data revealed that LSECs expressed CD155 in steady-state (Fig. 6.1), suggesting a possible close interaction between LSECs and tissue-resident ILC1s through the CD155-DNAM-1 axis. Upon co-culture with LSECs, NK cells and ILC1s downregulated DNAM-1 in a contact-dependent manner (Fig. 6.27). Blocking the CD155/DNAM-1 axis by adding anti-CD155 antibody in the co-culture abrogated DNAM-1 downregulation on NK cells and ILC1s. (Fig. 6.28), suggesting that the downregulation of DNAM-1 on NK cells and ILC1s was due to the direct engagement with CD155 on LSECs.

NKG2D was initially discovered in a screen for genes expressed by human NK cells (Raulet, 2003). In mouse, there are several identified ligands of NKG2D: Rae1, H60 and Mult1. In steady-state, blood ECs and lymphatic ECs in lymph nodes express RAE-1 human and NK cell desensitization(Thompson et al., 2017). However, my data revealed that LSECs neither express any of these NKG2D ligands in steady-state, nor were these NKG2D-ligands inducible by IFN-γ (Fig. 6.1 - 6.2). NK cells and ILC1s downregulated NKG2D in co-culture with LSECs in a contact-dependent manner (Fig. 6.27). This suggests that LSECs could express some unknown ligands in steady-state that can interact with NKG2D, causing NKG2D downregulation in co-culture. In addition, NK cells and ILC1s might be activated by LSECs during co-culture, and downregulate NKG2D as a result of activation.

NKp46 was first discovered as an activating receptor expressed by all NK cells (Sivori et al., 1997). To date, many ligands were reported to bind NKp46, including influenza hemagglutinins, vimentin of *M.*

tuberculosis, and various bacterial, parasitic, and fungal ligands (Barrow et al., 2019). Complement factor P was reported to be soluble ligand of NKp46 (Narni-Mancinelli et al., 2017). However, whether NKp46 has any natural membrane ligands still remains unclear. My results revealed that NK cells and ILC1s downregulated NKp46 in co-culture in a contact-dependent manner, only when LSECs were pre-stimulated with IFN-γ (Fig. 6.27). This could indicate that LSECs-stimulated with IFN-γ might express unknown ligands binding to NKp46, triggering its downregulation in the co-culture. More ligand screenings will reveal in the future to identify whether LSECs express unknown natural ligands of NKp46. Furthermore, NK cells and ILC1s might be activated by LSECs during co-culture, and they downregulate NKp46 as result of activation to possibly prevent overstimulation.

The downregulation of DNAM-1, NKG2D, and NKp46 in my co-culture system might have several implications. CD155 and RAE-1 were both reported to desensitize NK cell effector functions in the steady-state. CD155 KO mice challenged with tumors had a reduced tumor growth and a higher survival rate, as NK cells express a higher amount of DNAM-1 in CD155 KO mice (Li et al., 2018). Accordingly, RAE-1 KO mice injected with tumors had a decreased tumor growth and increased survival rate, as NK cells expressed a higher amount of NKG2D in RAE-1 KO mice (Thompson et al., 2017). My co-culture experiments suggest that LSECs might desensitize NK cells and ILC1s in steady-state by engaging DNAM-1, NKG2D, and NKp46. This could help to promote an immunotolerant microenvironment in the liver. Future experiments could aim at addressing the cytotoxicity of NK cells and ILC1s after co-cultured with LSECs against tumor cells, and examine the role of DNAM-1 and NKG2D on NK cells and ILC1against tumor cells after co-cultured with LSECs.

7.3.2 Effector functions of NK cells and ILC1s

Human Kupffer cells were reported to induce human NK cells to produce more IFN-γ after stimulation with IL-12 and IL-15 (Z. Tu et al., 2008). It is still unclear whether LSECs can modulate NK cell and ILC1 effector functions. I show that LSECs increased IFN-γ production of NK cells to IL-12 and IL-18 (Fig 6.29). This was specific for NK cells, as LSECs did not alter the IFN-γ production of ILC1s (Fig. 6.31). The increase of IFN-γ production of NK cells was contact-dependent. DNAM-1 was reported to be involved in the IFN-γ production of NK cells (Martinet et al., 2015), and I showed that the CD155 ligand was expressed by LSECs in steady-state (Fig. 6.1). Other stimuli such as NK1.1 and NKp46 receptor activation can be employed to determine differences between various kinds of stimuli in inducing IFN-γ of NK cells after co-cultured with LSECs.

I performed transcriptomic analysis of NK cells after co-cultured with LSECs to determine mechanisms mediating the increased IFN-γ production. Co-culture with LSECs induced significant transcriptomic changes in NK cells. Of note, several transcripts were enriched in NK cells after co-culture with LSECs, and I validated proteins encoded by these transcripts with flow cytometry. I observed that NK cells upregulated CD62L, while downregulated TRAIL, CD49a, and CD96, after co-cultured with LSECs (Fig. 6.32). CD49a and TRAIL were reported to be expressed by ILC1 (Peng et al., 2013; Sojka et al., 2014). I observed that NK cells cultured in the presence of IL-2 expressed TRAIL and CD49a (Fig. 6.32). Co-culture of NK cells with LSECs prevented the upregulation of TRAIL and CD49a expression on NK cells, retaining their homeostatic NK phenotype. The implications of changes in expressions of these molecules require further investigation. For instance, TRAIL is a ligand of a death receptor involved in NK cell cytotoxicity against tumors (Zamai et al., 1998). Hence, downregulation of TRAIL expression on NK cells by LSECs after co-culture might result in less NK cell cytotoxicity against cancer cells.

The precise mechanisms of how LSECs regulate NK cells and ILC1s distinctly, boosting only IFN-γ production of NK cells, remains to be investigated. It is possible that LSECs express some ligands that can only interact with NK cells, but not with ILC1s. As ILC1s are tissue-resident cells in sinusoids, they might have been transcriptionally wired by LSECs in steady-state. Thus, ILC1s co-cultured with LSECs did not have an increased IFN-γ production as observed in NK cells. I detected that NK cells co-cultured with LSECs produced comparable amounts of IFN-γ to ILC1s, upon stimulation with IL-12 and IL-18 (Fig. 6.29). This suggests that LSECs might prime circulating NK cells to be effective IFN-γ producers as ILC1s. Future experiments should aim at measuring other cytokines, such as TNF-α and GM-CSF, which were reported to be produced in higher amounts by ILC1s than NK cells (Sojka et al., 2014). I hypothesize that in acute liver disease models like LPS injection, LSECs are activated and release chemokines to recruit NK cells (Fig. 6.23). With IL-12 and IL-18 produced by Kupffer cells upon LPS stimulation (Seki et al., 2001; Varma et al., 2002), LSECs can boost NK cell function in a direct contact-dependent manner to produce higher amounts of IFN-γ. The schematic model of LSEC and NK cell interaction is illustrated in Fig. 7.3.

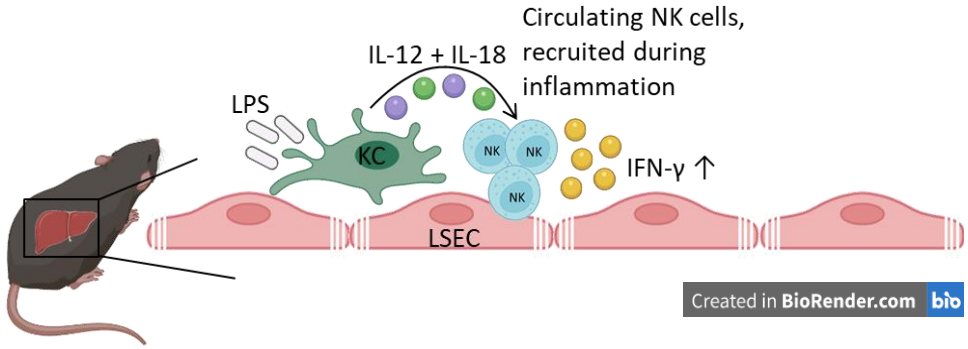

Fig. 7.3 - Schematic model of NK cell activation during LPS injection.

8 Conclusions

The crosstalk of NK cells and ILC1s with their stromal microenvironment is greatly underappreciated. Here, I attempted to understand interactions of NK cells and ILC1s with LSECs, as these cells are located in close proximity to each other.

I described a novel mechanism of LSECs to act as a non-immune cell bridging innate and adaptive immunity in liver homeostasis. I showed that LSECs expressed heterogeneous amounts of MHC II in a zonated manner, with Lyve1^{+} midzonal LSECs expressed the highest amount of MHC II. MHC II^{high} LSECs and MHC II^{low} LSECs had a distinct transcriptomic profile. IFN-γ, derived from ILC1s, NK cells, and NKT cells, was important to maintain MHC II expression on LSECs in steady-state. The absence of IL-12, an upstream inducer of IFN-γ in immune cells, affected MHC II expression on LSECs. The reduction of MHC II expression on LSECs correlated with an increased frequency of naïve CD4^{+} T cells and a decreased frequency of memory CD4^{+} T cells in the liver. Hence, innate lymphocyte-derived IFN-γ regulates naive to memory T cell differentiation, by maintaining MHC II expression on LSECs in the liver in steady-state.

LSECs induced transcriptomic and phenotypic changes of NK cells after co-culture. They also primed NK cells to produce a higher amount of IFN-γ upon cytokine stimulation. In a LPS-induced acute liver injury model, LSECs displayed 'activated' phenotypes by upregulation of surface proteins involved in regulating immune functions, mimicking phenotypes of LSECs stimulated by IFN-γ. In addition, LSECs also upregulated adhesion molecules in the LPS liver injury model, crucial for NK cell and monocyte recruitment into the liver during the disease. Using mice more than 1-year-old, I observed that conditional deletion of HVEM in LSECs led to splenomegaly. Thus, LSECs could modulate immune cell functions not only during liver disease but also during aging.

In conclusion, my study highlights LSECs as the center mediating innate and adaptive immune responses in homeostasis, inflammation, and disease. I describe LSECs as a novel non-immune player to regulate liver immunology, which provides a new insight of how stromal microenvironment shapes immune cell functions.

9 References

1. Abrahimi, P., Qin, L., Chang, W. G., Bothwell, A. L., Tellides, G., Saltzman, W. M., & Pober, J. S. (2016). Blocking MHC class II on human endothelium mitigates acute rejection. *JCI Insight, 1*(1). doi:10.1172/jci.insight.85293
2. Adachi, O., Kawai, T., Takeda, K., Matsumoto, M., Tsutsui, H., Sakagami, M., . . . Akira, S. (1998). Targeted disruption of the MyD88 gene results in loss of IL-1- and IL-18-mediated function. *Immunity, 9*(1), 143-150. doi:10.1016/s1074-7613(00)80596-8
3. Aird, W. C. (2007). Phenotypic heterogeneity of the endothelium: II. Representative vascular beds. *Circ Res, 100*(2), 174-190. doi:10.1161/01.RES.0000255690.03436.ae
4. Ajuwon, O. R., Oguntibeju, O. O., & Marnewick, J. L. (2014). Amelioration of lipopolysaccharide-induced liver injury by aqueous rooibos (Aspalathus linearis) extract via inhibition of pro-inflammatory cytokines and oxidative stress. *BMC Complement Altern Med, 14*, 392. doi:10.1186/1472-6882-14-392
5. Akil, A., Gutierrez-Garcia, A. K., Guenter, R., Rose, J. B., Beck, A. W., Chen, H., & Ren, B. (2021). Notch Signaling in Vascular Endothelial Cells, Angiogenesis, and Tumor Progression: An Update and Prospective. *Front Cell Dev Biol, 9*, 642352. doi:10.3389/fcell.2021.642352
6. Akira, S., Uematsu, S., & Takeuchi, O. (2006). Pathogen recognition and innate immunity. *Cell, 124*(4), 783-801. doi:10.1016/j.cell.2006.02.015
7. Alvarez, D., Vollmann, E. H., & von Andrian, U. H. (2008). Mechanisms and consequences of dendritic cell migration. *Immunity, 29*(3), 325-342. doi:10.1016/j.immuni.2008.08.006
8. An, M. M., Fan, K. X., Cao, Y. B., Shen, H., Zhang, J. D., Lu, L., . . . Jiang, Y. Y. (2006). Lymphtoxin beta receptor-Ig protects from T-cell-mediated liver injury in mice through blocking LIGHT/HVEM signaling. *Biol Pharm Bull, 29*(10), 2025-2030. doi:10.1248/bpb.29.2025
9. Asgharpour, A., Cazanave, S. C., Pacana, T., Seneshaw, M., Vincent, R., Banini, B. A., . . . Sanyal, A. J. (2016). A diet-induced animal model of non-alcoholic fatty liver disease and hepatocellular cancer. *J Hepatol, 65*(3), 579-588. doi:10.1016/j.jhep.2016.05.005
10. Ashour, D., Arampatzi, P., Pavlovic, V., Forstner, K. U., Kaisho, T., Beilhack, A., . . . Lutz, M. B. (2020). IL-12 from endogenous cDC1, and not vaccine DC, is required for Th1 induction. *JCI Insight, 5*(10). doi:ARTN e135143
11. 10.1172/jci.insight.135143
12. Bai, L., Vienne, M., Tang, L., Kerdiles, Y., Etiennot, M., Escaliere, B., . . . Tian, Z. (2021). Liver type 1 innate lymphoid cells develop locally via an interferon-gamma-dependent loop. *Science, 371*(6536). doi:10.1126/science.aba4177
13. Barrow, A. D., Martin, C. J., & Colonna, M. (2019). The Natural Cytotoxicity Receptors in Health and Disease. *Front Immunol, 10*, 909. doi:10.3389/fimmu.2019.00909
14. Bearer, E. L., Orci, L., & Sors, P. (1985). Endothelial Fenestral Diaphragms - a Quick-Freeze, Deep-Etch Study. *Journal of Cell Biology, 100*(2), 418-428. doi:DOI 10.1083/jcb.100.2.418
15. Berard, M., & Tough, D. F. (2002). Qualitative differences between naive and memory T cells. *Immunology, 106*(2), 127-138. doi:10.1046/j.1365-2567.2002.01447.x
16. Birchmeier, W. (2016). Orchestrating Wnt signalling for metabolic liver zonation. *Nat Cell Biol, 18*(5), 463-465. doi:10.1038/ncb3349

17. Bleriot, C., Barreby, E., Dunsmore, G., Ballaire, R., Chakarov, S., Ficht, X., . . . Ginhoux, F. (2021). A subset of Kupffer cells regulates metabolism through the expression of CD36. *Immunity, 54*(9), 2101-2116 e2106. doi:10.1016/j.immuni.2021.08.006
18. Borrego, F., Robertson, M. J., Ritz, J., Pena, J., & Solana, R. (1999). CD69 is a stimulatory receptor for natural killer cell and its cytotoxic effect is blocked by CD94 inhibitory receptor. *Immunology, 97*(1), 159-165. doi:10.1046/j.1365-2567.1999.00738.x
19. Bottcher, J. P., Schanz, O., Garbers, C., Zaremba, A., Hegenbarth, S., Kurts, C., . . . Knolle, P. A. (2014). IL-6 trans-signaling-dependent rapid development of cytotoxic CD8+ T cell function. *Cell Rep, 8*(5), 1318-1327. doi:10.1016/j.celrep.2014.07.008
20. Bottcher, J. P., Schanz, O., Wohlleber, D., Abdullah, Z., Debey-Pascher, S., Staratschek-Jox, A., . . . Knolle, P. A. (2013). Liver-primed memory T cells generated under noninflammatory conditions provide anti-infectious immunity. *Cell Rep, 3*(3), 779-795. doi:10.1016/j.celrep.2013.02.008
21. Bouwens, L., Baekeland, M., De Zanger, R., & Wisse, E. (1986). Quantitation, tissue distribution and proliferation kinetics of Kupffer cells in normal rat liver. *Hepatology, 6*(4), 718-722. doi:10.1002/hep.1840060430
22. Braeuning, A., Ittrich, C., Kohle, C., Hailfinger, S., Bonin, M., Buchmann, A., & Schwarz, M. (2006). Differential gene expression in periportal and perivenous mouse hepatocytes. *FEBS J, 273*(22), 5051-5061. doi:10.1111/j.1742-4658.2006.05503.x
23. Brempelis, K. J., & Crispe, I. N. (2016). Infiltrating monocytes in liver injury and repair. *Clin Transl Immunology, 5*(11), e113. doi:10.1038/cti.2016.62
24. Cai, G., Anumanthan, A., Brown, J. A., Greenfield, E. A., Zhu, B., & Freeman, G. J. (2008). CD160 inhibits activation of human CD4+ T cells through interaction with herpesvirus entry mediator. *Nat Immunol, 9*(2), 176-185. doi:10.1038/ni1554
25. Cai, G., & Freeman, G. J. (2009). The CD160, BTLA, LIGHT/HVEM pathway: a bidirectional switch regulating T-cell activation. *Immunol Rev, 229*(1), 244-258. doi:10.1111/j.1600-065X.2009.00783.x
26. Carambia, A., Frenzel, C., Bruns, O. T., Schwinge, D., Reimer, R., Hohenberg, H., . . . Herkel, J. (2013). Inhibition of inflammatory CD4 T cell activity by murine liver sinusoidal endothelial cells. *J Hepatol, 58*(1), 112-118. doi:10.1016/j.jhep.2012.09.008
27. Carambia, A., Freund, B., Schwinge, D., Bruns, O. T., Salmen, S. C., Ittrich, H., . . . Herkel, J. (2015). Nanoparticle-based autoantigen delivery to Treg-inducing liver sinusoidal endothelial cells enables control of autoimmunity in mice. *J Hepatol, 62*(6), 1349-1356. doi:10.1016/j.jhep.2015.01.006
28. Carambia, A., Freund, B., Schwinge, D., Heine, M., Laschtowitz, A., Huber, S., . . . Herkel, J. (2014). TGF-beta-dependent induction of CD4(+)CD25(+)Foxp3(+) Tregs by liver sinusoidal endothelial cells. *J Hepatol, 61*(3), 594-599. doi:10.1016/j.jhep.2014.04.027
29. Carneiro, C., Brito, J., Bilreiro, C., Barros, M., Bahia, C., Santiago, I., & Caseiro-Alves, F. (2019). All about portal vein: a pictorial display to anatomy, variants and physiopathology. *Insights into Imaging, 10*(1). doi:ARTN 38
30. 10.1186/s13244-019-0716-8
31. Carpenter, A. C., & Bosselut, R. (2010). Decision checkpoints in the thymus. *Nat Immunol, 11*(8), 666-673. doi:10.1038/ni.1887
32. Carson, W. E., Ross, M. E., Baiocchi, R. A., Marien, M. J., Boiani, N., Grabstein, K., & Caligiuri, M. A. (1995). Endogenous production of interleukin 15 by activated human monocytes is critical

for optimal production of interferon-gamma by natural killer cells in vitro. *J Clin Invest, 96*(6), 2578-2582. doi:10.1172/JCI118321

33. Cerutti, A. (2008). The regulation of IgA class switching. *Nat Rev Immunol, 8*(6), 421-434. doi:10.1038/nri2322
34. Cerwenka, A., Baron, J. L., & Lanier, L. L. (2001). Ectopic expression of retinoic acid early inducible-1 gene (RAE-1) permits natural killer cell-mediated rejection of a MHC class I-bearing tumor in vivo. *Proc Natl Acad Sci U S A, 98*(20), 11521-11526. doi:10.1073/pnas.201238598
35. Chan, C. J., Andrews, D. M., McLaughlin, N. M., Yagita, H., Gilfillan, S., Colonna, M., & Smyth, M. J. (2010). DNAM-1/CD155 interactions promote cytokine and NK cell-mediated suppression of poorly immunogenic melanoma metastases. *J Immunol, 184*(2), 902-911. doi:10.4049/jimmunol.0903225
36. Chan, C. J., Martinet, L., Gilfillan, S., Souza-Fonseca-Guimaraes, F., Chow, M. T., Town, L., . . . Smyth, M. J. (2014). The receptors CD96 and CD226 oppose each other in the regulation of natural killer cell functions. *Nat Immunol, 15*(5), 431-438. doi:10.1038/ni.2850
37. Chang, C. H., Guerder, S., Hong, S. C., van Ewijk, W., & Flavell, R. A. (1996). Mice lacking the MHC class II transactivator (CIITA) show tissue-specific impairment of MHC class II expression. *Immunity, 4*(2), 167-178. doi:10.1016/s1074-7613(00)80681-0
38. Chen, G., Huang, A. C., Zhang, W., Zhang, G., Wu, M., Xu, W., . . . Guo, W. (2018). Exosomal PD-L1 contributes to immunosuppression and is associated with anti-PD-1 response. *Nature, 560*(7718), 382-386. doi:10.1038/s41586-018-0392-8
39. Cheung, T. C., Steinberg, M. W., Oborne, L. M., Macauley, M. G., Fukuyama, S., Sanjo, H., . . . Ware, C. F. (2009). Unconventional ligand activation of herpesvirus entry mediator signals cell survival. *Proc Natl Acad Sci U S A, 106*(15), 6244-6249. doi:10.1073/pnas.0902115106
40. Chou, S. D., Khan, A. N., Magner, W. J., & Tomasi, T. B. (2005). Histone acetylation regulates the cell type specific CIITA promoters, MHC class II expression and antigen presentation in tumor cells. *Int Immunol, 17*(11), 1483-1494. doi:10.1093/intimm/dxh326
41. Clausen, J., Vergeiner, B., Enk, M., Petzer, A. L., Gastl, G., & Gunsilius, E. (2003). Functional significance of the activation-associated receptors CD25 and CD69 on human NK-cells and NK-like T-cells. *Immunobiology, 207*(2), 85-93. doi:10.1078/0171-2985-00219
42. Cleaver, O., & Melton, D. A. (2003). Endothelial signaling during development. *Nat Med, 9*(6), 661-668. doi:10.1038/nm0603-661
43. Colonna, M. (2018). Innate Lymphoid Cells: Diversity, Plasticity, and Unique Functions in Immunity. *Immunity, 48*(6), 1104-1117. doi:10.1016/j.immuni.2018.05.013
44. Conlon, R. A., Reaume, A. G., & Rossant, J. (1995). Notch1 Is Required for the Coordinate Segmentation of Somites. *Development, 121*(5), 1533-1545.
45. Correia, A. L., Guimaraes, J. C., Auf der Maur, P., De Silva, D., Trefny, M. P., Okamoto, R., . . . Bentires-Alj, M. (2021). Hepatic stellate cells suppress NK cell-sustained breast cancer dormancy. *Nature, 594*(7864), 566-571. doi:10.1038/s41586-021-03614-z
46. Correia, M. P., Cardoso, E. M., Pereira, C. F., Neves, R., Uhrberg, M., & Arosa, F. A. (2009). Hepatocytes and IL-15: a favorable microenvironment for T cell survival and CD8+ T cell differentiation. *J Immunol, 182*(10), 6149-6159. doi:10.4049/jimmunol.0802470
47. Curotto de Lafaille, M. A., & Lafaille, J. J. (2009). Natural and adaptive foxp3+ regulatory T cells: more of the same or a division of labor? *Immunity, 30*(5), 626-635. doi:10.1016/j.immuni.2009.05.002

48. Curtsinger, J. M., & Mescher, M. F. (2010). Inflammatory cytokines as a third signal for T cell activation. *Current Opinion in Immunology, 22*(3), 333-340. doi:10.1016/j.coi.2010.02.013
49. Curtsinger, J. M., Schmidt, C. S., Mondino, A., Lins, D. C., Kedl, R. M., Jenkins, M. K., & Mescher, M. F. (1999). Inflammatory cytokines provide a third signal for activation of naive CD4(+) and CD8(+) T cells. *Journal of Immunology, 162*(6), 3256-3262.
50. Danese, S., Dejana, E., & Fiocchi, C. (2007). Immune regulation by microvascular endothelial cells: directing innate and adaptive immunity, coagulation, and inflammation. *J Immunol, 178*(10), 6017-6022. doi:10.4049/jimmunol.178.10.6017
51. Daussy, C., Faure, F., Mayol, K., Viel, S., Gasteiger, G., Charrier, E., . . . Walzer, T. (2014). T-bet and Eomes instruct the development of two distinct natural killer cell lineages in the liver and in the bone marrow. *J Exp Med, 211*(3), 563-577. doi:10.1084/jem.20131560
52. de Andrade, L. F., Smyth, M. J., & Martinet, L. (2014). DNAM-1 control of natural killer cells functions through nectin and nectin-like proteins. *Immunol Cell Biol, 92*(3), 237-244. doi:10.1038/icb.2013.95
53. De Bruyn, P. P., & Cho, Y. (1974). Contractile structures in endothelial cells of splenic sinusoids. *J Ultrastruct Res, 49*(1), 24-33. doi:10.1016/s0022-5320(74)90075-6
54. Deaglio, S., Dwyer, K. M., Gao, W., Friedman, D., Usheva, A., Erat, A., . . . Robson, S. C. (2007). Adenosine generation catalyzed by CD39 and CD73 expressed on regulatory T cells mediates immune suppression. *J Exp Med, 204*(6), 1257-1265. doi:10.1084/jem.20062512
55. Dhar, P., & Wu, J. D. (2018). NKG2D and its ligands in cancer. *Curr Opin Immunol, 51*, 55-61. doi:10.1016/j.coi.2018.02.004
56. Di Censo, C., Marotel, M., Mattiola, I., Muller, L., Scarno, G., Pietropaolo, G., . . . Sciume, G. (2021). Granzyme A and CD160 expression delineates ILC1 with graded functions in the mouse liver. *Eur J Immunol*. doi:10.1002/eji.202149209
57. Diefenbach, A., Jensen, E. R., Jamieson, A. M., & Raulet, D. H. (2001). Rae1 and H60 ligands of the NKG2D receptor stimulate tumour immunity. *Nature, 413*(6852), 165-171. doi:10.1038/35093109
58. Diehl, L., Schurich, A., Grochtmann, R., Hegenbarth, S., Chen, L., & Knolle, P. A. (2008). Tolerogenic maturation of liver sinusoidal endothelial cells promotes B7-homolog 1-dependent CD8+ T cell tolerance. *Hepatology, 47*(1), 296-305. doi:10.1002/hep.21965
59. Dimitriu, T., Szczelkun, M. D., & Westra, E. R. (2020). Evolutionary Ecology and Interplay of Prokaryotic Innate and Adaptive Immune Systems. *Curr Biol, 30*(19), R1189-R1202. doi:10.1016/j.cub.2020.08.028
60. DiSanto, J. P., Muller, W., Guy-Grand, D., Fischer, A., & Rajewsky, K. (1995). Lymphoid development in mice with a targeted deletion of the interleukin 2 receptor gamma chain. *Proc Natl Acad Sci U S A, 92*(2), 377-381. doi:10.1073/pnas.92.2.377
61. Dubois, S., Mariner, J., Waldmann, T. A., & Tagaya, Y. (2002). IL-15Ralpha recycles and presents IL-15 In trans to neighboring cells. *Immunity, 17*(5), 537-547. doi:10.1016/s1074-7613(02)00429-6
62. Dubrot, J., Duraes, F. V., Harle, G., Schlaeppi, A., Brighouse, D., Madelon, N., . . . Hugues, S. (2018). Absence of MHC-II expression by lymph node stromal cells results in autoimmunity. *Life Science Alliance, 1*(6). doi:ARTN e201800164
63. 10.26508/lsa.201800164

64. Dubrot, J., Duraes, F. V., Potin, L., Capotosti, F., Brighouse, D., Suter, T., . . . Hugues, S. (2014). Lymph node stromal cells acquire peptide-MHCII complexes from dendritic cells and induce antigen-specific CD4(+) T cell tolerance. *J Exp Med, 211*(6), 1153-1166. doi:10.1084/jem.20132000
65. Ducimetiere, L., Lucchiari, G., Litscher, G., Nater, M., Heeb, L., Nunez, N. G., . . . Tugues, S. (2021). Conventional NK cells and tissue-resident ILC1s join forces to control liver metastasis. *Proc Natl Acad Sci U S A, 118*(27). doi:10.1073/pnas.2026271118
66. Ebbo, M., Crinier, A., Vely, F., & Vivier, E. (2017). Innate lymphoid cells: major players in inflammatory diseases. *Nat Rev Immunol, 17*(11), 665-678. doi:10.1038/nri.2017.86
67. Eberl, G., Di Santo, J. P., & Vivier, E. (2015). The brave new world of innate lymphoid cells. *Nat Immunol, 16*(1), 1-5. doi:10.1038/ni.3059
68. Emoto, M., Miyamoto, M., Yoshizawa, I., Emoto, Y., Schaible, U. E., Kita, E., & Kaufmann, S. H. (2002). Critical role of NK cells rather than V alpha 14(+)NKT cells in lipopolysaccharide-induced lethal shock in mice. *J Immunol, 169*(3), 1426-1432. doi:10.4049/jimmunol.169.3.1426
69. Erhardt, A., Biburger, M., Papadopoulos, T., & Tiegs, G. (2007). IL-10, regulatory T cells, and Kupffer cells mediate tolerance in concanavalin A-induced liver injury in mice. *Hepatology, 45*(2), 475-485. doi:10.1002/hep.21498
70. Everts, B., Tussiwand, R., Dreesen, L., Fairfax, K. C., Huang, S. C. C., Smith, A. M., . . . Pearce, E. J. (2016). Migratory CD103(+) dendritic cells suppress helminth-driven type 2 immunity through constitutive expression of IL-12. *Journal of Experimental Medicine, 213*(1), 35-51. doi:10.1084/jem.20150235
71. Fan, Z., Yu, P., Wang, Y., Wang, Y., Fu, M. L., Liu, W., . . . Fu, Y. X. (2006). NK-cell activation by LIGHT triggers tumor-specific CD8+ T-cell immunity to reject established tumors. *Blood, 107*(4), 1342-1351. doi:10.1182/blood-2005-08-3485
72. Fontenot, J. D., Gavin, M. A., & Rudensky, A. Y. (2017). Pillars Article: Foxp3 Programs the Development and Function of CD4+CD25+ Regulatory T Cells. Nat. Immunol. 2003. 4: 330-336. *J Immunol, 198*(3), 986-992.
73. Franceschi, C., Garagnani, P., Morsiani, C., Conte, M., Santoro, A., Grignolio, A., . . . Salvioli, S. (2018). The Continuum of Aging and Age-Related Diseases: Common Mechanisms but Different Rates. *Front Med (Lausanne), 5*, 61. doi:10.3389/fmed.2018.00061
74. Friedrich, C., Taggenbrock, R., Doucet-Ladeveze, R., Golda, G., Moenius, R., Arampatzi, P., . . . Gasteiger, G. (2021). Effector differentiation downstream of lineage commitment in ILC1s is driven by Hobit across tissues. *Nat Immunol, 22*(10), 1256-1267. doi:10.1038/s41590-021-01013-0
75. Fuchs, A., Vermi, W., Lee, J. S., Lonardi, S., Gilfillan, S., Newberry, R. D., . . . Colonna, M. (2013). Intraepithelial type 1 innate lymphoid cells are a unique subset of IL-12- and IL-15-responsive IFN-gamma-producing cells. *Immunity, 38*(4), 769-781. doi:10.1016/j.immuni.2013.02.010
76. Gao, B., Jeong, W. I., & Tian, Z. (2008). Liver: An organ with predominant innate immunity. *Hepatology, 47*(2), 729-736. doi:10.1002/hep.22034
77. Gao, B., Radaeva, S., & Park, O. (2009). Liver natural killer and natural killer T cells: immunobiology and emerging roles in liver diseases. *J Leukoc Biol, 86*(3), 513-528. doi:10.1189/JLB.0309135
78. Gao, Y., Souza-Fonseca-Guimaraes, F., Bald, T., Ng, S. S., Young, A., Ngiow, S. F., . . . Smyth, M. J. (2017). Tumor immunoevasion by the conversion of effector NK cells into type 1 innate lymphoid cells. *Nat Immunol, 18*(9), 1004-1015. doi:10.1038/ni.3800

79. Gebhardt, R., Baldysiak-Figiel, A., Krugel, V., Ueberham, E., & Gaunitz, F. (2007). Hepatocellular expression of glutamine synthetase: an indicator of morphogen actions as master regulators of zonation in adult liver. *Prog Histochem Cytochem, 41*(4), 201-266. doi:10.1016/j.proghi.2006.12.001
80. Geissmann, F., Cameron, T. O., Sidobre, S., Manlongat, N., Kronenberg, M., Briskin, M. J., . . . Littman, D. R. (2005). Intravascular immune surveillance by CXCR6+ NKT cells patrolling liver sinusoids. *PLoS Biol, 3*(4), e113. doi:10.1371/journal.pbio.0030113
81. Gellert, M. (2002). V(D)J recombination: RAG proteins, repair factors, and regulation. *Annu Rev Biochem, 71*, 101-132. doi:10.1146/annurev.biochem.71.090501.150203
82. Geraud, C., Koch, P. S., Zierow, J., Klapproth, K., Busch, K., Olsavszky, V., . . . Goerdt, S. (2017). GATA4-dependent organ-specific endothelial differentiation controls liver development and embryonic hematopoiesis. *J Clin Invest, 127*(3), 1099-1114. doi:10.1172/JCI90086
83. Germain, R. N. (2002). T-cell development and the CD4-CD8 lineage decision. *Nat Rev Immunol, 2*(5), 309-322. doi:10.1038/nri798
84. Giles, J. R., Kashgarian, M., Koni, P. A., & Shlomchik, M. J. (2015). B Cell-Specific MHC Class II Deletion Reveals Multiple Nonredundant Roles for B Cell Antigen Presentation in Murine Lupus. *J Immunol, 195*(6), 2571-2579. doi:10.4049/jimmunol.1500792
85. Glasner, A., Ghadially, H., Gur, C., Stanietsky, N., Tsukerman, P., Enk, J., & Mandelboim, O. (2012). Recognition and prevention of tumor metastasis by the NK receptor NKp46/NCR1. *J Immunol, 188*(6), 2509-2515. doi:10.4049/jimmunol.1102461
86. Glassner, A., Eisenhardt, M., Kramer, B., Korner, C., Coenen, M., Sauerbruch, T., . . . Nattermann, J. (2012). NK cells from HCV-infected patients effectively induce apoptosis of activated primary human hepatic stellate cells in a TRAIL-, FasL- and NKG2D-dependent manner. *Laboratory Investigation, 92*(7), 967-977. doi:10.1038/labinvest.2012.54
87. Glick, B., Chang, T. S., & Jaap, R. G. (1956). The Bursa of Fabricius and Antibody Production. *Poultry Science, 35*(1), 224-225. doi:DOI 10.3382/ps.0350224
88. Gola, A., Dorrington, M. G., Speranza, E., Sala, C., Shih, R. M., Radtke, A. J., . . . Germain, R. N. (2021). Commensal-driven immune zonation of the liver promotes host defence. *Nature, 589*(7840), 131-136. doi:10.1038/s41586-020-2977-2
89. Golden-Mason, L., Kelly, A. M., Doherty, D. G., Traynor, O., McEntee, G., Kelly, J., . . . O'Farrelly, C. (2004). Hepatic interleuklin 15 (IL-15) expression: implications for local NK/NKT cell homeostasis and development. *Clin Exp Immunol, 138*(1), 94-101. doi:10.1111/j.1365-2249.2004.02586.x
90. Goldman, J. P., Blundell, M. P., Lopes, L., Kinnon, C., Di Santo, J. P., & Thrasher, A. J. (1998). Enhanced human cell engraftment in mice deficient in RAG2 and the common cytokine receptor gamma chain. *Br J Haematol, 103*(2), 335-342. doi:10.1046/j.1365-2141.1998.00980.x
91. Gordon, S. M., Chaix, J., Rupp, L. J., Wu, J., Madera, S., Sun, J. C., . . . Reiner, S. L. (2012). The transcription factors T-bet and Eomes control key checkpoints of natural killer cell maturation. *Immunity, 36*(1), 55-67. doi:10.1016/j.immuni.2011.11.016
92. Granger, S. W., & Ware, C. F. (2001). Turning on LIGHT. *J Clin Invest, 108*(12), 1741-1742. doi:10.1172/JCI14651
93. Guilliams, M., Bonnardel, J., Haest, B., Vanderborght, B., Wagner, C., Remmerie, A., . . . Scott, C. L. (2022). Spatial proteogenomics reveals distinct and evolutionarily conserved hepatic macrophage niches. *Cell*. doi:10.1016/j.cell.2021.12.018

94. Halfteck, G. G., Elboim, M., Gur, C., Achdout, H., Ghadially, H., & Mandelboim, O. (2009). Enhanced in vivo growth of lymphoma tumors in the absence of the NK-activating receptor NKp46/NCR1. *J Immunol, 182*(4), 2221-2230. doi:10.4049/jimmunol.0801878
95. Halpern, K. B., Shenhav, R., Massalha, H., Toth, B., Egozi, A., Massasa, E. E., . . . Itzkovitz, S. (2018). Paired-cell sequencing enables spatial gene expression mapping of liver endothelial cells. *Nat Biotechnol, 36*(10), 962-970. doi:10.1038/nbt.4231
96. Hamilton, J. A. (2019). GM-CSF-Dependent Inflammatory Pathways. *Front Immunol, 10*, 2055. doi:10.3389/fimmu.2019.02055
97. Handa, K., Suzuki, R., Matsui, H., Shimizu, Y., & Kumagai, K. (1983). Natural killer (NK) cells as a responder to interleukin 2 (IL 2). II. IL 2-induced interferon gamma production. *J Immunol, 130*(2), 988-992.
98. Haring, J. S., Badovinac, V. P., & Harty, J. T. (2006). Inflaming the CD8+ T cell response. *Immunity, 25*(1), 19-29. doi:10.1016/j.immuni.2006.07.001
99. Henning, A. N., Roychoudhuri, R., & Restifo, N. P. (2018). Epigenetic control of CD8(+) T cell differentiation. *Nat Rev Immunol, 18*(5), 340-356. doi:10.1038/nri.2017.146
100. Heremans, H., Dillen, C., van Damme, J., & Billiau, A. (1994). Essential role for natural killer cells in the lethal lipopolysaccharide-induced Shwartzman-like reaction in mice. *Eur J Immunol, 24*(5), 1155-1160. doi:10.1002/eji.1830240522
101. Hoshino, K., Takeuchi, O., Kawai, T., Sanjo, H., Ogawa, T., Takeda, Y., . . . Akira, S. (1999). Cutting edge: Toll-like receptor 4 (TLR4)-deficient mice are hyporesponsive to lipopolysaccharide: evidence for TLR4 as the Lps gene product. *J Immunol, 162*(7), 3749-3752.
102. Hsu, J., Hodgins, J. J., Marathe, M., Nicolai, C. J., Bourgeois-Daigneault, M. C., Trevino, T. N., . . . Ardolino, M. (2018). Contribution of NK cells to immunotherapy mediated by PD-1/PD-L1 blockade. *J Clin Invest, 128*(10), 4654-4668. doi:10.1172/JCI99317
103. Huang, G., Wang, Y., & Chi, H. (2012). Regulation of TH17 cell differentiation by innate immune signals. *Cell Mol Immunol, 9*(4), 287-295. doi:10.1038/cmi.2012.10
104. Iguchi-Manaka, A., Kai, H., Yamashita, Y., Shibata, K., Tahara-Hanaoka, S., Honda, S., . . . Shibuya, A. (2008). Accelerated tumor growth in mice deficient in DNAM-1 receptor. *J Exp Med, 205*(13), 2959-2964. doi:10.1084/jem.20081611
105. Inverso, D., Shi, J., Lee, K. H., Jakab, M., Ben-Moshe, S., Kulkarni, S. R., . . . Augustin, H. G. (2021). A spatial vascular transcriptomic, proteomic, and phosphoproteomic atlas unveils an angiocrine Tie-Wnt signaling axis in the liver. *Dev Cell, 56*(11), 1677-1693 e1610. doi:10.1016/j.devcel.2021.05.001
106. Irla, M., Hugues, S., Gill, J., Nitta, T., Hikosaka, Y., Williams, I. R., . . . Reith, W. (2008). Autoantigen-specific interactions with CD4+ thymocytes control mature medullary thymic epithelial cell cellularity. *Immunity, 29*(3), 451-463. doi:10.1016/j.immuni.2008.08.007
107. Ivashkiv, L. B. (2018). IFN gamma: signalling, epigenetics and roles in immunity, metabolism, disease and cancer immunotherapy. *Nature Reviews Immunology, 18*(9), 545-558. doi:10.1038/s41577-018-0029-z
108. Jiang, Z., Meng, Y., Bo, L., Wang, C., Bian, J., & Deng, X. (2018). Sophocarpine Attenuates LPS-Induced Liver Injury and Improves Survival of Mice through Suppressing Oxidative Stress, Inflammation, and Apoptosis. *Mediators Inflamm, 2018*, 5871431. doi:10.1155/2018/5871431

109. Jinek, M., Chylinski, K., Fonfara, I., Hauer, M., Doudna, J. A., & Charpentier, E. (2012). A programmable dual-RNA-guided DNA endonuclease in adaptive bacterial immunity. *Science, 337*(6096), 816-821. doi:10.1126/science.1225829
110. Johnston, J. A., Bacon, C. M., Finbloom, D. S., Rees, R. C., Kaplan, D., Shibuya, K., . . . et al. (1995). Tyrosine phosphorylation and activation of STAT5, STAT3, and Janus kinases by interleukins 2 and 15. *Proc Natl Acad Sci U S A, 92*(19), 8705-8709. doi:10.1073/pnas.92.19.8705
111. Joly, E., & Hudrisier, D. (2003). What is trogocytosis and what is its purpose? *Nature Immunology, 4*(9), 815-815. doi:10.1038/ni0903-815
112. Judge, S. J., Dunai, C., Aguilar, E. G., Vick, S. C., Sturgill, I. R., Khuat, L. T., . . . Murphy, W. J. (2020). Minimal PD-1 expression in mouse and human NK cells under diverse conditions. *J Clin Invest, 130*(6), 3051-3068. doi:10.1172/JCI133353
113. Jung, H. W., La, S. J., Kim, J. Y., Heo, S. K., Kim, J. Y., Wang, S., . . . Kwon, B. S. (2003). High levels of soluble herpes virus entry mediator in sera of patients with allergic and autoimmune diseases. *Exp Mol Med, 35*(6), 501-508. doi:10.1038/emm.2003.65
114. Kalucka, J., de Rooij, L., Goveia, J., Rohlenova, K., Dumas, S. J., Meta, E., . . . Carmeliet, P. (2020). Single-Cell Transcriptome Atlas of Murine Endothelial Cells. *Cell, 180*(4), 764-779 e720. doi:10.1016/j.cell.2020.01.015
115. Kaneko, Y., Harada, M., Kawano, T., Yamashita, M., Shibata, Y., Gejyo, F., . . . Taniguchi, M. (2000). Augmentation of Valpha14 NKT cell-mediated cytotoxicity by interleukin 4 in an autocrine mechanism resulting in the development of concanavalin A-induced hepatitis. *J Exp Med, 191*(1), 105-114. doi:10.1084/jem.191.1.105
116. Karlhofer, F. M., Ribaudo, R. K., & Yokoyama, W. M. (1992). MHC class I alloantigen specificity of Ly-49+ IL-2-activated natural killer cells. *Nature, 358*(6381), 66-70. doi:10.1038/358066a0
117. Karlmark, K. R., Weiskirchen, R., Zimmermann, H. W., Gassler, N., Ginhoux, F., Weber, C., . . . Tacke, F. (2009). Hepatic recruitment of the inflammatory Gr1+ monocyte subset upon liver injury promotes hepatic fibrosis. *Hepatology, 50*(1), 261-274. doi:10.1002/hep.22950
118. Karre, K., Ljunggren, H. G., Piontek, G., & Kiessling, R. (1986). Selective Rejection of H-2-Deficient Lymphoma Variants Suggests Alternative Immune Defense Strategy. *Nature, 319*(6055), 675-678. doi:DOI 10.1038/319675a0
119. Kasahara, T., Hooks, J. J., Dougherty, S. F., & Oppenheim, J. J. (1983). Interleukin 2-mediated immune interferon (IFN-gamma) production by human T cells and T cell subsets. *J Immunol, 130*(4), 1784-1789.
120. Kawai, T., & Akira, S. (2007). Signaling to NF-kappaB by Toll-like receptors. *Trends Mol Med, 13*(11), 460-469. doi:10.1016/j.molmed.2007.09.002
121. Kawasaki, T., & Kawai, T. (2014). Toll-like receptor signaling pathways. *Front Immunol, 5*, 461. doi:10.3389/fimmu.2014.00461
122. Klein, L., Kyewski, B., Allen, P. M., & Hogquist, K. A. (2014). Positive and negative selection of the T cell repertoire: what thymocytes see (and don't see). *Nat Rev Immunol, 14*(6), 377-391. doi:10.1038/nri3667
123. Klose, C. S. N., Flach, M., Mohle, L., Rogell, L., Hoyler, T., Ebert, K., . . . Diefenbach, A. (2014). Differentiation of type 1 ILCs from a common progenitor to all helper-like innate lymphoid cell lineages. *Cell, 157*(2), 340-356. doi:10.1016/j.cell.2014.03.030
124. Knolle, P. A., Schmitt, E., Jin, S., Germann, T., Duchmann, R., Hegenbarth, S., . . . Lohse, A. W. (1999). Induction of cytokine production in naive CD4(+) T cells by antigen-presenting murine

liver sinusoidal endothelial cells but failure to induce differentiation toward Th1 cells. *Gastroenterology, 116*(6), 1428-1440. doi:10.1016/s0016-5085(99)70508-1

125. Knolle, P. A., Uhrig, A., Hegenbarth, S., Loser, E., Schmitt, E., Gerken, G., & Lohse, A. W. (1998). IL-10 down-regulates T cell activation by antigen-presenting liver sinusoidal endothelial cells through decreased antigen uptake via the mannose receptor and lowered surface expression of accessory molecules. *Clin Exp Immunol, 114*(3), 427-433. doi:10.1046/j.1365-2249.1998.00713.x
126. Knolle, P. A., & Wohlleber, D. (2016). Immunological functions of liver sinusoidal endothelial cells. *Cell Mol Immunol, 13*(3), 347-353. doi:10.1038/cmi.2016.5
127. Koyama, M., Mukhopadhyay, P., Schuster, I. S., Henden, A. S., Hulsdunker, J., Varelias, A., . . . Hill, G. R. (2019). MHC Class II Antigen Presentation by the Intestinal Epithelium Initiates Graft-versus-Host Disease and Is Influenced by the Microbiota. *Immunity, 51*(5), 885-898 e887. doi:10.1016/j.immuni.2019.08.011
128. Kruse, N., Neumann, K., Schrage, A., Derkow, K., Schott, E., Erben, U., . . . Klugewitz, K. (2009). Priming of CD4(+) T Cells by Liver Sinusoidal Endothelial Cells Induces CD25(low) Forkhead Box Protein 3(-) Regulatory T Cells Suppressing Autoimmune Hepatitis. *Hepatology, 50*(6), 1904-1913. doi:10.1002/hep.23191
129. Kumar, B. V., Connors, T. J., & Farber, D. L. (2018). Human T Cell Development, Localization, and Function throughout Life. *Immunity, 48*(2), 202-213. doi:10.1016/j.immuni.2018.01.007
130. Kwon, B. S., Tan, K. B., Ni, J., Oh, K. O., Lee, Z. H., Kim, K. K., . . . Young, P. R. (1997). A newly identified member of the tumor necrosis factor receptor superfamily with a wide tissue distribution and involvement in lymphocyte activation. *J Biol Chem, 272*(22), 14272-14276. doi:10.1074/jbc.272.22.14272
131. Lafoz, E., Ruart, M., Anton, A., Oncins, A., & Hernandez-Gea, V. (2020). The Endothelium as a Driver of Liver Fibrosis and Regeneration. *Cells, 9*(4). doi:ARTN 929

132. 10.3390/cells9040929
133. Lau, A. H., & Thomson, A. W. (2003). Dendritic cells and immune regulation in the liver. *Gut, 52*(2), 307-314. doi:10.1136/gut.52.2.307
134. Lau, C., Kalantari, B., Batts, K. P., Ferrell, L. D., Nyberg, S. L., Graham, R. P., & Moreira, R. K. (2021). The Voronoi theory of the normal liver lobular architecture and its applicability in hepatic zonation. *Sci Rep, 11*(1), 9343. doi:10.1038/s41598-021-88699-2
135. Laydon, D. J., Bangham, C. R., & Asquith, B. (2015). Estimating T-cell repertoire diversity: limitations of classical estimators and a new approach. *Philos Trans R Soc Lond B Biol Sci, 370*(1675). doi:10.1098/rstb.2014.0291
136. Lee, J. C., Lee, K. M., Kim, D. W., & Heo, D. S. (2004). Elevated TGF-beta1 secretion and down-modulation of NKG2D underlies impaired NK cytotoxicity in cancer patients. *J Immunol, 172*(12), 7335-7340. doi:10.4049/jimmunol.172.12.7335
137. Leibing, T., Geraud, C., Augustin, I., Boutros, M., Augustin, H. G., Okun, J. G., . . . Koch, P. S. (2018). Angiocrine Wnt signaling controls liver growth and metabolic maturation in mice. *Hepatology, 68*(2), 707-722. doi:10.1002/hep.29613
138. LeibundGut-Landmann, S., Waldburger, J. M., Krawczyk, M., Otten, L. A., Suter, T., Fontana, A., . . . Reith, W. (2004). Mini-review: Specificity and expression of CIITA, the master regulator of MHC class II genes. *Eur J Immunol, 34*(6), 1513-1525. doi:10.1002/eji.200424964

139. Lemaitre, B., Nicolas, E., Michaut, L., Reichhart, J. M., & Hoffmann, J. A. (1996). The dorsoventral regulatory gene cassette spatzle/Toll/cactus controls the potent antifungal response in Drosophila adults. *Cell, 86*(6), 973-983. doi:10.1016/s0092-8674(00)80172-5
140. Ley, K., Laudanna, C., Cybulsky, M. I., & Nourshargh, S. (2007). Getting to the site of inflammation: the leukocyte adhesion cascade updated. *Nat Rev Immunol, 7*(9), 678-689. doi:10.1038/nri2156
141. Li, X. Y., Das, I., Lepletier, A., Addala, V., Bald, T., Stannard, K., . . . Smyth, M. J. (2018). CD155 loss enhances tumor suppression via combined host and tumor-intrinsic mechanisms. *J Clin Invest, 128*(6), 2613-2625. doi:10.1172/JCI98769
142. Limmer, A., Ohl, J., Kurts, C., Ljunggren, H. G., Reiss, Y., Groettrup, M., . . . Knolle, P. A. (2000). Efficient presentation of exogenous antigen by liver endothelial cells to CD8+ T cells results in antigen-specific T-cell tolerance. *Nat Med, 6*(12), 1348-1354. doi:10.1038/82161
143. Lin, J. X., & Leonard, W. J. (2000). The role of Stat5a and Stat5b in signaling by IL-2 family cytokines. *Oncogene, 19*(21), 2566-2576. doi:10.1038/sj.onc.1203523
144. Liu, W., Garrett, S. C., Fedorov, E. V., Ramagopal, U. A., Garforth, S. J., Bonanno, J. B., & Almo, S. C. (2019). Structural Basis of CD160:HVEM Recognition. *Structure, 27*(8), 1286-1295 e1284. doi:10.1016/j.str.2019.05.010
145. Liu, Y., Meyer, C., Xu, C., Weng, H., Hellerbrand, C., ten Dijke, P., & Dooley, S. (2013). Animal models of chronic liver diseases. *Am J Physiol Gastrointest Liver Physiol, 304*(5), G449-468. doi:10.1152/ajpgi.00199.2012
146. Ljunggren, H. G., & Karre, K. (1990). In Search of the Missing Self - Mhc Molecules and Nk Cell Recognition. *Immunology Today, 11*(7), 237-244. doi:Doi 10.1016/0167-5699(90)90097-S
147. Lodolce, J. P., Boone, D. L., Chai, S., Swain, R. E., Dassopoulos, T., Trettin, S., & Ma, A. (1998). IL-15 receptor maintains lymphoid homeostasis by supporting lymphocyte homing and proliferation. *Immunity, 9*(5), 669-676. doi:10.1016/s1074-7613(00)80664-0
148. Lohse, A. W., Knolle, P. A., Bilo, K., Uhrig, A., Waldmann, C., Ibe, M., . . . Meyer Zum Buschenfelde, K. H. (1996). Antigen-presenting function and B7 expression of murine sinusoidal endothelial cells and Kupffer cells. *Gastroenterology, 110*(4), 1175-1181. doi:10.1053/gast.1996.v110.pm8613007
149. Long, E. O., Kim, H. S., Liu, D. F., Peterson, M. E., & Rajagopalan, S. (2013). Controlling Natural Killer Cell Responses: Integration of Signals for Activation and Inhibition. *Annual Review of Immunology, Vol 31, 31*, 227-258. doi:10.1146/annurev-immunol-020711-075005
150. Loschko, J., Schreiber, H. A., Rieke, G. J., Esterhazy, D., Meredith, M. M., Pedicord, V. A., . . . Nussenzweig, M. C. (2016). Absence of MHC class II on cDCs results in microbial-dependent intestinal inflammation. *J Exp Med, 213*(4), 517-534. doi:10.1084/jem.20160062
151. Low, J. S., Farsakoglu, Y., Amezcua Vesely, M. C., Sefik, E., Kelly, J. B., Harman, C. C. D., . . . Kaech, S. M. (2020). Tissue-resident memory T cell reactivation by diverse antigen-presenting cells imparts distinct functional responses. *J Exp Med, 217*(8). doi:10.1084/jem.20192291
152. Luth, S., Huber, S., Schramm, C., Buch, T., Zander, S., Stadelmann, C., . . . Lohse, A. W. (2008). Ectopic expression of neural autoantigen in mouse liver suppresses experimental autoimmune neuroinflammation by inducing antigen-specific Tregs. *J Clin Invest, 118*(10), 3403-3410. doi:10.1172/JCI32132

153. Ma, C., Han, M., Heinrich, B., Fu, Q., Zhang, Q., Sandhu, M., . . . Greten, T. F. (2018). Gut microbiome-mediated bile acid metabolism regulates liver cancer via NKT cells. *Science, 360*(6391). doi:10.1126/science.aan5931
154. Ma, R., Martinez-Ramirez, A. S., Borders, T. L., Gao, F., & Sosa-Pineda, B. (2020). Metabolic and non-metabolic liver zonation is established non-synchronously and requires sinusoidal Wnts. *Elife, 9*. doi:10.7554/eLife.46206
155. Mackay, L. K., Minnich, M., Kragten, N. A., Liao, Y., Nota, B., Seillet, C., . . . van Gisbergen, K. P. (2016). Hobit and Blimp1 instruct a universal transcriptional program of tissue residency in lymphocytes. *Science, 352*(6284), 459-463. doi:10.1126/science.aad2035
156. Magram, J., Connaughton, S. E., Warrier, R. R., Carvajal, D. M., Wu, C. Y., Ferrante, J., . . . Gately, M. K. (1996). IL-12-deficient mice are defective in IFN gamma production and type 1 cytokine responses. *Immunity, 4*(5), 471-481. doi:10.1016/s1074-7613(00)80413-6
157. Mai, J., Virtue, A., Shen, J., Wang, H., & Yang, X. F. (2013). An evolving new paradigm: endothelial cells--conditional innate immune cells. *J Hematol Oncol, 6*, 61. doi:10.1186/1756-8722-6-61
158. Mandelboim, O., Lieberman, N., Lev, M., Paul, L., Arnon, T. I., Bushkin, Y., . . . Porgador, A. (2001). Recognition of haemagglutinins on virus-infected cells by NKp46 activates lysis by human NK cells. *Nature, 409*(6823), 1055-1060. doi:10.1038/35059110
159. Marsters, S. A., Ayres, T. M., Skubatch, M., Gray, C. L., Rothe, M., & Ashkenazi, A. (1997). Herpesvirus entry mediator, a member of the tumor necrosis factor receptor (TNFR) family, interacts with members of the TNFR-associated factor family and activates the transcription factors NF-kappaB and AP-1. *J Biol Chem, 272*(22), 14029-14032. doi:10.1074/jbc.272.22.14029
160. Martinet, L., Ferrari De Andrade, L., Guillerey, C., Lee, J. S., Liu, J., Souza-Fonseca-Guimaraes, F., . . . Smyth, M. J. (2015). DNAM-1 expression marks an alternative program of NK cell maturation. *Cell Rep, 11*(1), 85-97. doi:10.1016/j.celrep.2015.03.006
161. Martinez-Lostao, L., Anel, A., & Pardo, J. (2015). How Do Cytotoxic Lymphocytes Kill Cancer Cells? *Clinical Cancer Research, 21*(22), 5047-5056. doi:10.1158/1078-0432.Ccr-15-0685
162. Masopust, D., & Schenkel, J. M. (2013). The integration of T cell migration, differentiation and function. *Nat Rev Immunol, 13*(5), 309-320. doi:10.1038/nri3442
163. Masternak, K., Muhlethaler-Mottet, A., Villard, J., Zufferey, M., Steimle, V., & Reith, W. (2000). CIITA is a transcriptional coactivator that is recruited to MHC class II promoters by multiple synergistic interactions with an enhanceosome complex. *Genes Dev, 14*(9), 1156-1166.
164. Mates, J. M., Yao, Z. L., Cheplowitz, A. M., Suer, O., Phillips, G. S., Kwiek, J. J., . . . Anderson, C. L. (2017). Mouse Liver Sinusoidal Endothelium Eliminates HIV-Like Particles from Blood at a Rate of 100 Million per Minute by a Second-Order Kinetic Process. *Frontiers in Immunology, 8*. doi:ARTN 35

165. 10.3389/fimmu.2017.00035
166. Mauri, D. N., Ebner, R., Montgomery, R. I., Kochel, K. D., Cheung, T. C., Yu, G. L., . . . Ware, C. F. (1998). LIGHT, a new member of the TNF superfamily, and lymphotoxin alpha are ligands for herpesvirus entry mediator. *Immunity, 8*(1), 21-30. doi:10.1016/s1074-7613(00)80455-0
167. Mausberg, A. K., Jander, S., & Reichmann, G. (2009). Intracerebral granulocyte-macrophage colony-stimulating factor induces functionally competent dendritic cells in the mouse brain. *Glia, 57*(12), 1341-1350. doi:10.1002/glia.20853

168. Melhem, A., Muhanna, N., Bishara, A., Alvarez, C. E., Ilan, Y., Bishara, T., . . . Safadi, R. (2006). Anti-fibrotic activity of NK cells in experimental liver injury through killing of activated HSC. *J Hepatol, 45*(1), 60-71. doi:10.1016/j.jhep.2005.12.025
169. Merle, N. S., Church, S. E., Fremeaux-Bacchi, V., & Roumenina, L. T. (2015). Complement System Part I - Molecular Mechanisms of Activation and Regulation. *Front Immunol, 6*, 262. doi:10.3389/fimmu.2015.00262
170. Metzemaekers, M., Vanheule, V., Janssens, R., Struyf, S., & Proost, P. (2018). Overview of the Mechanisms that May Contribute to the Non-Redundant Activities of Interferon-Inducible CXC Chemokine Receptor 3 Ligands. *Frontiers in Immunology, 8*. doi:ARTN 1970
171. 10.3389/fimmu.2017.01970
172. Mignon, A., Rouquet, N., Fabre, M., Martin, S., Pages, J. C., Dhainaut, J. F., . . . Joulin, V. (1999). LPS challenge in D-galactosamine-sensitized mice accounts for caspase-dependent fulminant hepatitis, not for septic shock. *Am J Respir Crit Care Med, 159*(4 Pt 1), 1308-1315. doi:10.1164/ajrccm.159.4.9712012
173. Miller, J. F. (1999). Discovering the origins of immunological competence. *Annu Rev Immunol, 17*, 1-17. doi:10.1146/annurev.immunol.17.1.1
174. Mohler, K. M., Sleath, P. R., Fitzner, J. N., Cerretti, D. P., Alderson, M., Kerwar, S. S., . . . et al. (1994). Protection against a lethal dose of endotoxin by an inhibitor of tumour necrosis factor processing. *Nature, 370*(6486), 218-220. doi:10.1038/370218a0
175. Mojica, F. J., & Rodriguez-Valera, F. (2016). The discovery of CRISPR in archaea and bacteria. *FEBS J, 283*(17), 3162-3169. doi:10.1111/febs.13766
176. Mondino, A., Khoruts, A., & Jenkins, M. K. (1996). The anatomy of T-cell activation and tolerance. *Proceedings of the National Academy of Sciences of the United States of America, 93*(6), 2245-2252. doi:DOI 10.1073/pnas.93.6.2245
177. Montgomery, R. I., Warner, M. S., Lum, B. J., & Spear, P. G. (1996). Herpes simplex virus-1 entry into cells mediated by a novel member of the TNF/NGF receptor family. *Cell, 87*(3), 427-436. doi:10.1016/s0092-8674(00)81363-x
178. Moon, S., Park, Y., Hyeon, S., Kim, Y. M., Kim, J. H., Kim, H., . . . Lee, S. W. (2021). Niche-specific MHC II and PD-L1 regulate CD4+CD8alphaalpha+ intraepithelial lymphocyte differentiation. *J Exp Med, 218*(4). doi:10.1084/jem.20201665
179. Mossanen, J. C., Krenkel, O., Ergen, C., Govaere, O., Liepelt, A., Puengel, T., . . . Tacke, F. (2016). Chemokine (C-C motif) receptor 2-positive monocytes aggravate the early phase of acetaminophen-induced acute liver injury. *Hepatology, 64*(5), 1667-1682. doi:10.1002/hep.28682
180. Muczynski, K. A., Ekle, D. M., Coder, D. M., & Anderson, S. K. (2003). Normal human kidney HLA-DR-expressing renal microvascular endothelial cells: characterization, isolation, and regulation of MHC class II expression. *J Am Soc Nephrol, 14*(5), 1336-1348. doi:10.1097/01.asn.0000061778.08085.9f
181. Muhlethaler-Mottet, A., Otten, L. A., Steimle, V., & Mach, B. (1997). Expression of MHC class II molecules in different cellular and functional compartments is controlled by differential usage of multiple promoters of the transactivator CIITA. *EMBO J, 16*(10), 2851-2860. doi:10.1093/emboj/16.10.2851
182. Murphy, K. M., Nelson, C. A., & Sedy, J. R. (2006). Balancing co-stimulation and inhibition with BTLA and HVEM. *Nat Rev Immunol, 6*(9), 671-681. doi:10.1038/nri1917

183. Nabekura, T., Riggan, L., Hildreth, A. D., O'Sullivan, T. E., & Shibuya, A. (2020). Type 1 Innate Lymphoid Cells Protect Mice from Acute Liver Injury via Interferon-gamma Secretion for Upregulating Bcl-xL Expression in Hepatocytes. *Immunity, 52*(1), 96-108 e109. doi:10.1016/j.immuni.2019.11.004
184. Nakama, T., Hirono, S., Moriuchi, A., Hasuike, S., Nagata, K., Hori, T., . . . Tsubouchi, H. (2001). Etoposide prevents apoptosis in mouse liver with D-galactosamine/lipopolysaccharide-induced fulminant hepatic failure resulting in reduction of lethality. *Hepatology, 33*(6), 1441-1450. doi:10.1053/jhep.2001.24561
185. Nakayama, M. (2014). Antigen Presentation by MHC-Dressed Cells. *Front Immunol, 5*, 672. doi:10.3389/fimmu.2014.00672
186. Nakayama, M., Takeda, K., Kawano, M., Takai, T., Ishii, N., & Ogasawara, K. (2011). Natural killer (NK)-dendritic cell interactions generate MHC class II-dressed NK cells that regulate CD4(+) T cells. *Proceedings of the National Academy of Sciences of the United States of America, 108*(45), 18360-18365. doi:10.1073/pnas.1110584108
187. Narni-Mancinelli, E., Gauthier, L., Baratin, M., Guia, S., Fenis, A., Deghmane, A. E., . . . Vivier, E. (2017). Complement factor P is a ligand for the natural killer cell-activating receptor NKp46. *Sci Immunol, 2*(10). doi:10.1126/sciimmunol.aam9628
188. Newsome, P. N., Plevris, J. N., Nelson, L. J., & Hayes, P. C. (2000). Animal models of fulminant hepatic failure: a critical evaluation. *Liver Transpl, 6*(1), 21-31. doi:10.1002/lt.500060110
189. Nurieva, R. I., & Chung, Y. (2010). Understanding the development and function of T follicular helper cells. *Cell Mol Immunol, 7*(3), 190-197. doi:10.1038/cmi.2010.24
190. Ochi, M., Ohdan, H., Mitsuta, H., Onoe, T., Tokita, D., Hara, H., . . . Asahara, T. (2004). Liver NK cells expressing TRAIL are toxic against self hepatocytes in mice. *Hepatology, 39*(5), 1321-1331. doi:10.1002/hep.20204
191. Okamura, H., Tsutsui, H., Komatsu, T., Yutsudo, M., Hakura, A., Tanimoto, T., . . . Kurimoto, M. (1995). Cloning of a New Cytokine That Induces Ifn-Gamma Production by T-Cells. *Nature, 378*(6552), 88-91. doi:DOI 10.1038/378088a0
192. Palm, A. E., & Henry, C. (2019). Remembrance of Things Past: Long-Term B Cell Memory After Infection and Vaccination. *Front Immunol, 10*, 1787. doi:10.3389/fimmu.2019.01787
193. Park, O., Jeong, W. I., Wang, L., Wang, H., Lian, Z. X., Gershwin, M. E., & Gao, B. (2009). Diverse roles of invariant natural killer T cells in liver injury and fibrosis induced by carbon tetrachloride. *Hepatology, 49*(5), 1683-1694. doi:10.1002/hep.22813
194. Partanen, T. A., Arola, J., Saaristo, A., Jussila, L., Ora, A., Miettinen, M., . . . Alitalo, K. (2000). VEGF-C and VEGF-D expression in neuroendocrine cells and their receptor, VEGFR-3, in fenestrated blood vessels in human tissues. *FASEB J, 14*(13), 2087-2096. doi:10.1096/fj.99-1049com
195. Pauwels, A. M., Trost, M., Beyaert, R., & Hoffmann, E. (2017). Patterns, Receptors, and Signals: Regulation of Phagosome Maturation. *Trends Immunol, 38*(6), 407-422. doi:10.1016/j.it.2017.03.006
196. Pearce, E. L., Mullen, A. C., Martins, G. A., Krawczyk, C. M., Hutchins, A. S., Zediak, V. P., . . . Reiner, S. L. (2003). Control of effector CD8(+) T cell function by the transcription factor Eomesodermin. *Science, 302*(5647), 1041-1043. doi:DOI 10.1126/science.1090148
197. Pende, D., Bottino, C., Castriconi, R., Cantoni, C., Marcenaro, S., Rivera, P., . . . Moretta, A. (2005). PVR (CD155) and Nectin-2 (CD112) as ligands of the human DNAM-1 (CD226) activating

receptor: involvement in tumor cell lysis. *Mol Immunol, 42*(4), 463-469. doi:10.1016/j.molimm.2004.07.028

198. Pende, D., Falco, M., Vitale, M., Cantoni, C., Vitale, C., Munari, E., . . . Moretta, L. (2019). Killer Ig-Like Receptors (KIRs): Their Role in NK Cell Modulation and Developments Leading to Their Clinical Exploitation. *Frontiers in Immunology, 10*. doi:ARTN 1179

199. 10.3389/fimmu.2019.01179
200. Peng, H., Jiang, X., Chen, Y., Sojka, D. K., Wei, H., Gao, X., . . . Tian, Z. (2013). Liver-resident NK cells confer adaptive immunity in skin-contact inflammation. *J Clin Invest, 123*(4), 1444-1456. doi:10.1172/JCI66381
201. Peng, H., Wisse, E., & Tian, Z. G. (2016). Liver natural killer cells: subsets and roles in liver immunity. *Cellular & Molecular Immunology, 13*(3), 328-336. doi:10.1038/cmi.2015.96
202. Potente, M., & Makinen, T. (2017). Vascular heterogeneity and specialization in development and disease. *Nat Rev Mol Cell Biol, 18*(8), 477-494. doi:10.1038/nrm.2017.36
203. Prager, I., Liesche, C., van Ooijen, H., Urlaub, D., Verron, Q., Sandstrom, N., . . . Watzl, C. (2019). NK cells switch from granzyme B to death receptor-mediated cytotoxicity during serial killing. *J Exp Med, 216*(9), 2113-2127. doi:10.1084/jem.20181454
204. Quatrini, L., Wieduwild, E., Escaliere, B., Filtjens, J., Chasson, L., Laprie, C., . . . Ugolini, S. (2018). Endogenous glucocorticoids control host resistance to viral infection through the tissue-specific regulation of PD-1 expression on NK cells. *Nat Immunol, 19*(9), 954-962. doi:10.1038/s41590-018-0185-0
205. Qureshi, O. S., Zheng, Y., Nakamura, K., Attridge, K., Manzotti, C., Schmidt, E. M., . . . Sansom, D. M. (2011). Trans-endocytosis of CD80 and CD86: a molecular basis for the cell-extrinsic function of CTLA-4. *Science, 332*(6029), 600-603. doi:10.1126/science.1202947
206. Racanelli, V., & Rehermann, B. (2006). The liver as an immunological organ. *Hepatology, 43*(2), S54-S62. doi:10.1002/hep.21060
207. Radaeva, S., Sun, R., Jaruga, B., Nguyen, V. T., Tian, Z., & Gao, B. (2006). Natural killer cells ameliorate liver fibrosis by killing activated stellate cells in NKG2D-dependent and tumor necrosis factor-related apoptosis-inducing ligand-dependent manners. *Gastroenterology, 130*(2), 435-452. doi:10.1053/j.gastro.2005.10.055
208. Raulet, D. H. (2003). Roles of the NKG2D immunoreceptor and its ligands. *Nat Rev Immunol, 3*(10), 781-790. doi:10.1038/nri1199
209. Roberts, A. D., Ely, K. H., & Woodland, D. L. (2005). Differential contributions of central and effector memory T cells to recall responses. *J Exp Med, 202*(1), 123-133. doi:10.1084/jem.20050137
210. Robinette, M. L., Bando, J. K., Song, W., Ulland, T. K., Gilfillan, S., & Colonna, M. (2017). IL-15 sustains IL-7R-independent ILC2 and ILC3 development. *Nature Communications, 8*. doi:ARTN 14601

211. 10.1038/ncomms14601
212. Robinette, M. L., Fuchs, A., Cortez, V. S., Lee, J. S., Wang, Y., Durum, S. K., . . . Immunological Genome, C. (2015). Transcriptional programs define molecular characteristics of innate lymphoid cell classes and subsets. *Nat Immunol, 16*(3), 306-317. doi:10.1038/ni.3094

213. Rocha, A. S., Vidal, V., Mertz, M., Kendall, T. J., Charlet, A., Okamoto, H., & Schedl, A. (2015). The Angiocrine Factor Rspondin3 Is a Key Determinant of Liver Zonation. *Cell Reports, 13*(9), 1757-1764. doi:10.1016/j.celrep.2015.10.049
214. Roche, P. A., & Furuta, K. (2015). The ins and outs of MHC class II-mediated antigen processing and presentation. *Nat Rev Immunol, 15*(4), 203-216. doi:10.1038/nri3818
215. Rock, K. L., Reits, E., & Neefjes, J. (2016). Present Yourself! By MHC Class I and MHC Class II Molecules. *Trends Immunol, 37*(11), 724-737. doi:10.1016/j.it.2016.08.010
216. Romero-Suarez, S., Del Rio Serrato, A., Bueno, R. J., Brunotte-Strecker, D., Stehle, C., Figueiredo, C. A., . . . Infante-Duarte, C. (2019). The Central Nervous System Contains ILC1s That Differ From NK Cells in the Response to Inflammation. *Front Immunol, 10*, 2337. doi:10.3389/fimmu.2019.02337
217. Rose, M. L., Coles, M. I., Griffin, R. J., Pomerance, A., & Yacoub, M. H. (1986). Expression of class I and class II major histocompatibility antigens in normal and transplanted human heart. *Transplantation, 41*(6), 776-780. doi:10.1097/00007890-198606000-00021
218. Sadlack, B., Kuhn, R., Schorle, H., Rajewsky, K., Muller, W., & Horak, I. (1994). Development and proliferation of lymphocytes in mice deficient for both interleukins-2 and -4. *Eur J Immunol, 24*(1), 281-284. doi:10.1002/eji.1830240144
219. Sakaguchi, S., Sakaguchi, N., Asano, M., Itoh, M., & Toda, M. (1995). Immunologic self-tolerance maintained by activated T cells expressing IL-2 receptor alpha-chains (CD25). Breakdown of a single mechanism of self-tolerance causes various autoimmune diseases. *J Immunol, 155*(3), 1151-1164.
220. Sakaguchi, S., Wing, K., Onishi, Y., Prieto-Martin, P., & Yamaguchi, T. (2009). Regulatory T cells: how do they suppress immune responses? *Int Immunol, 21*(10), 1105-1111. doi:10.1093/intimm/dxp095
221. Sallusto, F., Geginat, J., & Lanzavecchia, A. (2004). Central memory and effector memory T cell subsets: function, generation, and maintenance. *Annu Rev Immunol, 22*, 745-763. doi:10.1146/annurev.immunol.22.012703.104702
222. Sallusto, F., Lenig, D., Forster, R., Lipp, M., & Lanzavecchia, A. (1999). Two subsets of memory T lymphocytes with distinct homing potentials and effector functions. *Nature, 401*(6754), 708-712. doi:10.1038/44385
223. Sanmarco, L. M., Wheeler, M. A., Gutirrez-Vzquez, C., Polonio, C. M., Linnerbauer, M., Pinho-Ribeiro, F. A., . . . Quintana, F. J. (2021). Gut-licensed IFN gamma(+) NK cells drive LAMP1(+)TRAIL(+) anti-inflammatory astrocytes. *Nature, 590*(7846), 473-+. doi:10.1038/s41586-020-03116-4
224. Sathaliyawala, T., Kubota, M., Yudanin, N., Turner, D., Camp, P., Thome, J. J., . . . Farber, D. L. (2013). Distribution and compartmentalization of human circulating and tissue-resident memory T cell subsets. *Immunity, 38*(1), 187-197. doi:10.1016/j.immuni.2012.09.020
225. Sathe, A., & Cusick, J. K. (2021). Biochemistry, Immunoglobulin M *StatPearls*. Treasure Island (FL).
226. Satoh-Takayama, N., Dumoutier, L., Lesjean-Pottier, S., Ribeiro, V. S., Mandelboim, O., Renauld, J. C., . . . Di Santo, J. P. (2009). The natural cytotoxicity receptor NKp46 is dispensable for IL-22-mediated innate intestinal immune defense against Citrobacter rodentium. *J Immunol, 183*(10), 6579-6587. doi:10.4049/jimmunol.0901935

227. Schaer, C., Hiltbrunner, S., Ernst, B., Mueller, C., Kurrer, M., Kopf, M., & Harris, N. L. (2011). HVEM signalling promotes colitis. *PLoS One, 6*(4), e18495. doi:10.1371/journal.pone.0018495
228. Schledzewski, K., Geraud, C., Arnold, B., Wang, S., Grone, H. J., Kempf, T., . . . Goerdt, S. (2011). Deficiency of liver sinusoidal scavenger receptors stabilin-1 and -2 in mice causes glomerulofibrotic nephropathy via impaired hepatic clearance of noxious blood factors. *J Clin Invest, 121*(2), 703-714. doi:10.1172/JCI44740
229. Schmidt, A., Oberle, N., & Krammer, P. H. (2012). Molecular mechanisms of treg-mediated T cell suppression. *Front Immunol, 3*, 51. doi:10.3389/fimmu.2012.00051
230. Schneider, P., Thome, M., Burns, K., Bodmer, J. L., Hofmann, K., Kataoka, T., . . . Tschopp, J. (1997). TRAIL receptors 1 (DR4) and 2 (DR5) signal FADD-dependent apoptosis and activate NF-kappaB. *Immunity, 7*(6), 831-836. doi:10.1016/s1074-7613(00)80401-x
231. Schnoor, M., Alcaide, P., Voisin, M. B., & van Buul, J. D. (2015). Crossing the Vascular Wall: Common and Unique Mechanisms Exploited by Different Leukocyte Subsets during Extravasation. *Mediators Inflamm, 2015*, 946509. doi:10.1155/2015/946509
232. Scholzel, K., Schildberg, F. A., Welz, M., Borner, C., Geiger, S., Kurts, C., . . . Wohlleber, D. (2014). Transfer of MHC-class-I molecules among liver sinusoidal cells facilitates hepatic immune surveillance. *J Hepatol, 61*(3), 600-608. doi:10.1016/j.jhep.2014.04.028
233. Schultz, M., Tonkonogy, S. L., Sellon, R. K., Veltkamp, C., Godfrey, V. L., Kwon, J., . . . Sartor, R. B. (1999). IL-2-deficient mice raised under germfree conditions develop delayed mild focal intestinal inflammation. *Am J Physiol, 276*(6), G1461-1472. doi:10.1152/ajpgi.1999.276.6.G1461
234. Schurich, A., Berg, M., Stabenow, D., Bottcher, J., Kern, M., Schild, H. J., . . . Knolle, P. A. (2010). Dynamic regulation of CD8 T cell tolerance induction by liver sinusoidal endothelial cells. *J Immunol, 184*(8), 4107-4114. doi:10.4049/jimmunol.0902580
235. Seder, R. A., & Ahmed, R. (2003). Similarities and differences in CD4+ and CD8+ effector and memory T cell generation. *Nat Immunol, 4*(9), 835-842. doi:10.1038/ni969
236. Sedy, J. R., Gavrieli, M., Potter, K. G., Hurchla, M. A., Lindsley, R. C., Hildner, K., . . . Murphy, K. M. (2005). B and T lymphocyte attenuator regulates T cell activation through interaction with herpesvirus entry mediator. *Nat Immunol, 6*(1), 90-98. doi:10.1038/ni1144
237. Seillet, C., Huntington, N. D., Gangatirkar, P., Axelsson, E., Minnich, M., Brady, H. J., . . . Carotta, S. (2014). Differential requirement for Nfil3 during NK cell development. *J Immunol, 192*(6), 2667-2676. doi:10.4049/jimmunol.1302605
238. Seki, E., Tsutsui, H., Nakano, H., Tsuji, N., Hoshino, K., Adachi, O., . . . Nakanishi, K. (2001). Lipopolysaccharide-induced IL-18 secretion from murine Kupffer cells independently of myeloid differentiation factor 88 that is critically involved in induction of production of IL-12 and IL-1beta. *J Immunol, 166*(4), 2651-2657. doi:10.4049/jimmunol.166.4.2651
239. Seo, G. Y., Shui, J. W., Takahashi, D., Song, C., Wang, Q., Kim, K., . . . Kronenberg, M. (2018). LIGHT-HVEM Signaling in Innate Lymphoid Cell Subsets Protects Against Enteric Bacterial Infection. *Cell Host Microbe, 24*(2), 249-260 e244. doi:10.1016/j.chom.2018.07.008
240. Seong, S. Y., & Matzinger, P. (2004). Hydrophobicity: an ancient damage-associated molecular pattern that initiates innate immune responses. *Nature Reviews Immunology, 4*(6), 469-478. doi:10.1038/nri1372
241. Shamri, R., Grabovsky, V., Gauguet, J. M., Feigelson, S., Manevich, E., Kolanus, W., . . . Alon, R. (2005). Lymphocyte arrest requires instantaneous induction of an extended LFA-1 conformation

mediated by endothelium-bound chemokines. *Nature Immunology, 6*(5), 497-506. doi:10.1038/ni1194

242. Shao, Y., Saredy, J., Yang, W. Y., Sun, Y., Lu, Y., Saaoud, F., . . . Yang, X. (2020). Vascular Endothelial Cells and Innate Immunity. *Arterioscler Thromb Vasc Biol, 40*(6), e138-e152. doi:10.1161/ATVBAHA.120.314330
243. Sharpe, A. H., & Pauken, K. E. (2018). The diverse functions of the PD1 inhibitory pathway. *Nat Rev Immunol, 18*(3), 153-167. doi:10.1038/nri.2017.108
244. Shi, W., Shao, T., Li, J. Y., Fan, D. D., Lin, A. F., Xiang, L. X., & Shao, J. Z. (2019). BTLA-HVEM Checkpoint Axis Regulates Hepatic Homeostasis and Inflammation in a ConA-Induced Hepatitis Model in Zebrafish. *J Immunol, 203*(9), 2425-2442. doi:10.4049/jimmunol.1900458
245. Shibuya, A., Campbell, D., Hannum, C., Yssel, H., Franz-Bacon, K., McClanahan, T., . . . Phillips, J. H. (1996). DNAM-1, a novel adhesion molecule involved in the cytolytic function of T lymphocytes. *Immunity, 4*(6), 573-581. doi:10.1016/s1074-7613(00)70060-4
246. Shin, M. S., Kim, H. S., Lee, S. H., Park, W. S., Kim, S. Y., Park, J. Y., . . . Yoo, N. J. (2001). Mutations of tumor necrosis factor-related apoptosis-inducing ligand receptor 1 (TRAIL-R1) and receptor 2 (TRAIL-R2) genes in metastatic breast cancers. *Cancer Res, 61*(13), 4942-4946.
247. Shui, J. W., Larange, A., Kim, G., Vela, J. L., Zahner, S., Cheroutre, H., & Kronenberg, M. (2012). HVEM signalling at mucosal barriers provides host defence against pathogenic bacteria. *Nature, 488*(7410), 222-225. doi:10.1038/nature11242
248. Sivori, S., Vitale, M., Morelli, L., Sanseverino, L., Augugliaro, R., Bottino, C., . . . Moretta, A. (1997). p46, a novel natural killer cell-specific surface molecule that mediates cell activation. *J Exp Med, 186*(7), 1129-1136. doi:10.1084/jem.186.7.1129
249. Slauch, J. M. (2011). How does the oxidative burst of macrophages kill bacteria? Still an open question. *Mol Microbiol, 80*(3), 580-583. doi:10.1111/j.1365-2958.2011.07612.x
250. Smyth, M. J., Cretney, E., Takeda, K., Wiltrout, R. H., Sedger, L. M., Kayagaki, N., . . . Okumura, K. (2001). Tumor necrosis factor-related apoptosis-inducing ligand (TRAIL) contributes to interferon gamma-dependent natural killer cell protection from tumor metastasis. *J Exp Med, 193*(6), 661-670. doi:10.1084/jem.193.6.661
251. Soehnlein, O., & Lindbom, L. (2010). Phagocyte partnership during the onset and resolution of inflammation. *Nat Rev Immunol, 10*(6), 427-439. doi:10.1038/nri2779
252. Sojka, D. K., Plougastel-Douglas, B., Yang, L., Pak-Wittel, M. A., Artyomov, M. N., Ivanova, Y., . . . Yokoyama, W. M. (2014). Tissue-resident natural killer (NK) cells are cell lineages distinct from thymic and conventional splenic NK cells. *Elife, 3*, e01659. doi:10.7554/eLife.01659
253. Stan, R. V. (2007). Endothelial stomatal and fenestral diaphragms in normal vessels and angiogenesis. *J Cell Mol Med, 11*(4), 621-643. doi:10.1111/j.1582-4934.2007.00075.x
254. Stavnezer, J., & Schrader, C. E. (2014). IgH chain class switch recombination: mechanism and regulation. *J Immunol, 193*(11), 5370-5378. doi:10.4049/jimmunol.1401849
255. Steimle, V., Siegrist, C. A., Mottet, A., Lisowska-Grospierre, B., & Mach, B. (1994). Regulation of MHC class II expression by interferon-gamma mediated by the transactivator gene CIITA. *Science, 265*(5168), 106-109. doi:10.1126/science.8016643
256. Steinberg, M. W., Turovskaya, O., Shaikh, R. B., Kim, G., McCole, D. F., Pfeffer, K., . . . Kronenberg, M. (2008). A crucial role for HVEM and BTLA in preventing intestinal inflammation. *J Exp Med, 205*(6), 1463-1476. doi:10.1084/jem.20071160

257. Strauss, O., Phillips, A., Ruggiero, K., Bartlett, A., & Dunbar, P. R. (2017). Immunofluorescence identifies distinct subsets of endothelial cells in the human liver. *Sci Rep, 7*, 44356. doi:10.1038/srep44356
258. Su, G. L. (2002). Lipopolysaccharides in liver injury: molecular mechanisms of Kupffer cell activation. *Am J Physiol Gastrointest Liver Physiol, 283*(2), G256-265. doi:10.1152/ajpgi.00550.2001
259. Szafranska, K., Kruse, L. D., Holte, C. F., McCourt, P., & Zapotoczny, B. (2021). The wHole Story About Fenestrations in LSEC. *Frontiers in Physiology, 12*. doi:ARTN 735573
260. 10.3389/fphys.2021.735573
261. Takaba, H., & Takayanagi, H. (2017). The Mechanisms of T Cell Selection in the Thymus. *Trends Immunol, 38*(11), 805-816. doi:10.1016/j.it.2017.07.010
262. Takeda, K., Cretney, E., Hayakawa, Y., Ota, T., Akiba, H., Ogasawara, K., . . . Smyth, M. J. (2005). TRAIL identifies immature natural killer cells in newborn mice and adult mouse liver. *Blood, 105*(5), 2082-2089. doi:10.1182/blood-2004-08-3262
263. Takeda, K., Smyth, M. J., Cretney, E., Hayakawa, Y., Yamaguchi, N., Yagita, H., & Okumura, K. (2001). Involvement of tumor necrosis factor-related apoptosis-inducing ligand in NK cell-mediated and IFN-gamma-dependent suppression of subcutaneous tumor growth. *Cell Immunol, 214*(2), 194-200. doi:10.1006/cimm.2001.1896
264. Tamada, K., Shimozaki, K., Chapoval, A. I., Zhai, Y., Su, J., Chen, S. F., . . . Chen, L. (2000). LIGHT, a TNF-like molecule, costimulates T cell proliferation and is required for dendritic cell-mediated allogeneic T cell response. *J Immunol, 164*(8), 4105-4110. doi:10.4049/jimmunol.164.8.4105
265. Tamoutounour, S., Han, S. J., Deckers, J., Constantinides, M. G., Hurabielle, C., Harrison, O. J., . . . Belkaid, Y. (2019). Keratinocyte-intrinsic MHCII expression controls microbiota-induced Th1 cell responses. *Proc Natl Acad Sci U S A, 116*(47), 23643-23652. doi:10.1073/pnas.1912432116
266. Taylor, S., Huang, Y., Mallett, G., Stathopoulou, C., Felizardo, T. C., Sun, M. A., . . . Amarnath, S. (2017). PD-1 regulates KLRG1(+) group 2 innate lymphoid cells. *J Exp Med, 214*(6), 1663-1678. doi:10.1084/jem.20161653
267. Thery, C., Duban, L., Segura, E., Veron, P., Lantz, O., & Amigorena, S. (2002). Indirect activation of naive CD4(+) T cells by dendritic cell-derived exosomes. *Nature Immunology, 3*(12), 1156-1162. doi:10.1038/ni854
268. Thierfelder, W. E., van Deursen, J. M., Yamamoto, K., Tripp, R. A., Sarawar, S. R., Carson, R. T., . . . Ihle, J. N. (1996). Requirement for Stat4 in interleukin-12-mediated responses of natural killer and T cells. *Nature, 382*(6587), 171-174. doi:10.1038/382171a0
269. Thompson, T. W., Kim, A. B., Li, P. J., Wang, J., Jackson, B. T., Huang, K. T. H., . . . Raulet, D. H. (2017). Endothelial cells express NKG2D ligands and desensitize antitumor NK responses. *Elife, 6*. doi:10.7554/eLife.30881
270. Tian, Z., Chen, Y., & Gao, B. (2013). Natural killer cells in liver disease. *Hepatology, 57*(4), 1654-1662. doi:10.1002/hep.26115
271. Tiegs, G., Hentschel, J., & Wendel, A. (1992a). A T-Cell-Dependent Experimental Liver-Injury in Mice Inducible by Concanavalin-A. *Journal of Clinical Investigation, 90*(1), 196-203. doi:Doi 10.1172/Jci115836
272. Tiegs, G., Hentschel, J., & Wendel, A. (1992b). A T cell-dependent experimental liver injury in mice inducible by concanavalin A. *J Clin Invest, 90*(1), 196-203. doi:10.1172/JCI115836

273. Toulmin, S. A., Bhadiadra, C., Paris, A. J., Lin, J. H., Katzen, J., Basil, M. C., . . . Eisenlohr, L. C. (2021). Type II alveolar cell MHCII improves respiratory viral disease outcomes while exhibiting limited antigen presentation. *Nat Commun, 12*(1), 3993. doi:10.1038/s41467-021-23619-6
274. Toyabe, S., Seki, S., Iiai, T., Takeda, K., Shirai, K., Watanabe, H., . . . Abo, T. (1997). Requirement of IL-4 and liver NK1+ T cells for concanavalin A-induced hepatic injury in mice. *J Immunol, 159*(3), 1537-1542.
275. Trinchieri, G. (2003). Interleukin-12 and the regulation of innate resistance and adaptive immunity. *Nat Rev Immunol, 3*(2), 133-146. doi:10.1038/nri1001
276. Tsang, J. Y. S., Chai, J. G., & Lechler, R. (2003). Antigen presentation by mouse CD4(+) T cells involving acquired MHC class II : peptide complexes: another mechanism to limit clonal expansion? *Blood, 101*(7), 2704-2710. doi:10.1182/blood-2002-04-1230
277. Tu, T. C., Brown, N. K., Kim, T. J., Wroblewska, J., Yang, X. M., Guo, X. H., . . . Fu, Y. X. (2015). CD160 is essential for NK-mediated IFN-gamma production. *Journal of Experimental Medicine, 212*(3), 415-429. doi:10.1084/jem.20131601
278. Tu, Z., Bozorgzadeh, A., Pierce, R. H., Kurtis, J., Crispe, I. N., & Orloff, M. S. (2008). TLR-dependent cross talk between human Kupffer cells and NK cells. *J Exp Med, 205*(1), 233-244. doi:10.1084/jem.20072195
279. Tuganbaev, T., Mor, U., Bashiardes, S., Liwinski, T., Nobs, S. P., Leshem, A., . . . Elinav, E. (2020). Diet Diurnally Regulates Small Intestinal Microbiome-Epithelial-Immune Homeostasis and Enteritis. *Cell, 182*(6), 1441-1459 e1421. doi:10.1016/j.cell.2020.08.027
280. Ueda, H., Howson, J. M., Esposito, L., Heward, J., Snook, H., Chamberlain, G., . . . Gough, S. C. (2003). Association of the T-cell regulatory gene CTLA4 with susceptibility to autoimmune disease. *Nature, 423*(6939), 506-511. doi:10.1038/nature01621
281. van Niel, G., D'Angelo, G., & Raposo, G. (2018). Shedding light on the cell biology of extracellular vesicles. *Nat Rev Mol Cell Biol, 19*(4), 213-228. doi:10.1038/nrm.2017.125
282. Varma, T. K., Lin, C. Y., Toliver-Kinsky, T. E., & Sherwood, E. R. (2002). Endotoxin-induced gamma interferon production: contributing cell types and key regulatory factors. *Clin Diagn Lab Immunol, 9*(3), 530-543. doi:10.1128/cdli.9.3.530-543.2002
283. Vestweber, D. (2015). How leukocytes cross the vascular endothelium. *Nat Rev Immunol, 15*(11), 692-704. doi:10.1038/nri3908
284. Vignali, D. A. A., & Kuchroo, V. K. (2012). IL-12 family cytokines: immunological playmakers. *Nature Immunology, 13*(8), 722-728. doi:10.1038/ni.2366
285. Vinay, D. S., Choi, B. K., Bae, J. S., Kim, W. Y., Gebhardt, B. M., & Kwon, B. S. (2004). CD137-deficient mice have reduced NK/NKT cell numbers and function, are resistant to lipopolysaccharide-induced shock syndromes, and have lower IL-4 responses. *J Immunol, 173*(6), 4218-4229. doi:10.4049/jimmunol.173.6.4218
286. Vivier, E., Artis, D., Colonna, M., Diefenbach, A., Di Santo, J. P., Eberl, G., . . . Spits, H. (2018). Innate Lymphoid Cells: 10 Years On. *Cell, 174*(5), 1054-1066. doi:10.1016/j.cell.2018.07.017
287. von Burg, N., Chappaz, S., Baerenwaldt, A., Horvath, E., Bose Dasgupta, S., Ashok, D., . . . Finke, D. (2014). Activated group 3 innate lymphoid cells promote T-cell-mediated immune responses. *Proc Natl Acad Sci U S A, 111*(35), 12835-12840. doi:10.1073/pnas.1406908111
288. Wang, X., Peng, H., Cong, J., Wang, X., Lian, Z., Wei, H., . . . Tian, Z. (2018). Memory formation and long-term maintenance of IL-7Ralpha(+) ILC1s via a lymph node-liver axis. *Nat Commun, 9*(1), 4854. doi:10.1038/s41467-018-07405-5

289. Wang, Y., Subudhi, S. K., Anders, R. A., Lo, J., Sun, Y., Blink, S., . . . Fu, Y. X. (2005). The role of herpesvirus entry mediator as a negative regulator of T cell-mediated responses. *J Clin Invest, 115*(3), 711-717. doi:10.1172/JCI22982
290. Watanabe, N., Gavrieli, M., Sedy, J. R., Yang, J., Fallarino, F., Loftin, S. K., . . . Murphy, K. M. (2003a). BTLA is a lymphocyte inhibitory receptor with similarities to CTLA-4 and PD-1. *Nat Immunol, 4*(7), 670-679. doi:10.1038/ni944
291. Watanabe, N., Gavrieli, M., Sedy, J. R., Yang, J. F., Fallarino, F., Loftin, S. K., . . . Murphy, K. M. (2003b). BTLA is a lymphocyte inhibitory receptor with similarities to CTLA-4 and PD-1. *Nature Immunology, 4*(7), 670-679. doi:DOI 10.1038/ni944
292. Weber, L. W. D., Boll, M., & Stampfl, A. (2003). Hepatotoxicity and mechanism of action of haloalkanes: Carbon tetrachloride as a toxicological model. *Critical Reviews in Toxicology, 33*(2), 105-136. doi:Doi 10.1080/713611034
293. Weinreich, M. A., & Hogquist, K. A. (2008). Thymic emigration: when and how T cells leave home. *J Immunol, 181*(4), 2265-2270. doi:10.4049/jimmunol.181.4.2265
294. Weiss, J. M., Bilate, A. M., Gobert, M., Ding, Y., Curotto de Lafaille, M. A., Parkhurst, C. N., . . . Lafaille, J. J. (2012). Neuropilin 1 is expressed on thymus-derived natural regulatory T cells, but not mucosa-generated induced Foxp3+ T reg cells. *J Exp Med, 209*(10), 1723-1742, S1721. doi:10.1084/jem.20120914
295. Welz, M., Eickhoff, S., Abdullah, Z., Trebicka, J., Gartlan, K. H., Spicer, J. A., . . . Kastenmuller, W. (2018). Perforin inhibition protects from lethal endothelial damage during fulminant viral hepatitis. *Nat Commun, 9*(1), 4805. doi:10.1038/s41467-018-07213-x
296. Wherry, E. J., Teichgraber, V., Becker, T. C., Masopust, D., Kaech, S. M., Antia, R., . . . Ahmed, R. (2003). Lineage relationship and protective immunity of memory CD8 T cell subsets. *Nat Immunol, 4*(3), 225-234. doi:10.1038/ni889
297. Wilkinson, A. L., Qurashi, M., & Shetty, S. (2020). The Role of Sinusoidal Endothelial Cells in the Axis of Inflammation and Cancer Within the Liver. *Front Physiol, 11*, 990. doi:10.3389/fphys.2020.00990
298. Willerford, D. M., Chen, J., Ferry, J. A., Davidson, L., Ma, A., & Alt, F. W. (1995). Interleukin-2 receptor alpha chain regulates the size and content of the peripheral lymphoid compartment. *Immunity, 3*(4), 521-530. doi:10.1016/1074-7613(95)90180-9
299. Wittmann, M., Purwar, R., Hartmann, C., Gutzmer, R., & Werfel, T. (2005). Human keratinocytes respond to interleukin-18: implication for the course of chronic inflammatory skin diseases. *J Invest Dermatol, 124*(6), 1225-1233. doi:10.1111/j.0022-202X.2005.23715.x
300. Wohlfeil, S. A., Hafele, V., Dietsch, B., Schledzewski, K., Winkler, M., Zierow, J., . . . Goerdt, S. (2019). Hepatic Endothelial Notch Activation Protects against Liver Metastasis by Regulating Endothelial-Tumor Cell Adhesion Independent of Angiocrine Signaling. *Cancer Res, 79*(3), 598-610. doi:10.1158/0008-5472.CAN-18-1752
301. Wohlleber, D., & Knolle, P. A. (2016). The role of liver sinusoidal cells in local hepatic immune surveillance. *Clin Transl Immunology, 5*(12), e117. doi:10.1038/cti.2016.74
302. Wosen, J. E., Mukhopadhyay, D., Macaubas, C., & Mellins, E. D. (2018). Epithelial MHC Class II Expression and Its Role in Antigen Presentation in the Gastrointestinal and Respiratory Tracts. *Front Immunol, 9*, 2144. doi:10.3389/fimmu.2018.02144

303. Wu, C., Ferrante, J., Gately, M. K., & Magram, J. (1997). Characterization of IL-12 receptor beta1 chain (IL-12Rbeta1)-deficient mice: IL-12Rbeta1 is an essential component of the functional mouse IL-12 receptor. *J Immunol, 159*(4), 1658-1665.
304. Wu, C., Wang, X., Gadina, M., O'Shea, J. J., Presky, D. H., & Magram, J. (2000). IL-12 receptor beta 2 (IL-12R beta 2)-deficient mice are defective in IL-12-mediated signaling despite the presence of high affinity IL-12 binding sites. *J Immunol, 165*(11), 6221-6228. doi:10.4049/jimmunol.165.11.6221
305. Wu, J., Meng, Z., Jiang, M., Zhang, E., Trippler, M., Broering, R., . . . Schlaak, J. F. (2010). Toll-like receptor-induced innate immune responses in non-parenchymal liver cells are cell type-specific. *Immunology, 129*(3), 363-374. doi:10.1111/j.1365-2567.2009.03179.x
306. Xue, Y., Gao, X., Lindsell, C. E., Norton, C. R., Chang, B., Hicks, C., . . . Gridley, T. (1999). Embryonic lethality and vascular defects in mice lacking the Notch ligand Jagged1. *Hum Mol Genet, 8*(5), 723-730. doi:10.1093/hmg/8.5.723
307. Yadav, M., Louvet, C., Davini, D., Gardner, J. M., Martinez-Llordella, M., Bailey-Bucktrout, S., . . . Bluestone, J. A. (2012). Neuropilin-1 distinguishes natural and inducible regulatory T cells among regulatory T cell subsets in vivo. *J Exp Med, 209*(10), 1713-1722, S1711-1719. doi:10.1084/jem.20120822
308. Yu, Y., Tsang, J. C. H., Wang, C., Clare, S., Wang, J. X., Chen, X., . . . Liu, P. T. (2016). Single-cell RNA-seq identifies a PD-1(hi) ILC progenitor and defines its development pathway. *Nature, 539*(7627), 102-+. doi:10.1038/nature20105
309. Zamai, L., Ahmad, M., Bennett, I. M., Azzoni, L., Alnemri, E. S., & Perussia, B. (1998). Natural killer (NK) cell-mediated cytotoxicity: differential use of TRAIL and Fas ligand by immature and mature primary human NK cells. *J Exp Med, 188*(12), 2375-2380. doi:10.1084/jem.188.12.2375
310. Zammit, D. J., Cauley, L. S., Pham, Q. M., & Lefrancois, L. (2005). Dendritic cells maximize the memory CD8 T cell response to infection. *Immunity, 22*(5), 561-570. doi:10.1016/j.immuni.2005.03.005
311. Zhou, J., Peng, H., Li, K., Qu, K., Wang, B., Wu, Y., . . . Tian, Z. (2019). Liver-Resident NK Cells Control Antiviral Activity of Hepatic T Cells via the PD-1-PD-L1 Axis. *Immunity, 50*(2), 403-417 e404. doi:10.1016/j.immuni.2018.12.024
312. Zitvogel, L., Regnault, A., Lozier, A., Wolfers, J., Flament, C., Tenza, D., . . . Amigorena, S. (1998). Eradication of established murine tumors using a novel cell-free vaccine: dendritic cell-derived exosomes. *Nature Medicine, 4*(5), 594-600. doi:DOI 10.1038/nm0598-594

10 Abbreviations

4-1BBL	4-1BB ligand
7AAD	7-aminoactinomycin D
ABX	Antibiotics
ACK	Ammonium-chloride-potassium lysing buffer
ADP	Adenosine diphosphate
ALT	Alanine aminotransferase
AMO	Adenosine monophosphate
ANLN	Anilin actin binding protein
APAP	Acetaminophen
APCs	Antigen-presenting cells
ATP	Adenosine triphosphate
BCR	B cell receptor
BM	Basement membrane
BSA	Bovine serum albumin
BTLA	B and T lymphocyte attenuator
CIITA	Class II, major histocompatibility complex, transactivator
CCl_4	Carbon tetrachloride
CCR1	C-C chemokine receptor type 1
CCD2	C-C chemokine receptor type 2
CCR6	C-C chemokine receptor type 6
cDNA	Complementary DNA
CD	Cluster of differentiation
CD200R	CD200 receptor
CILP	Common ILC progenitor
CHILP	Common helper-like ILC progenitor
CLP	Common lymphoid progenitor
CLRs	C-type lectin receptors
ConA	Concanavalin A
CRD	Cystein rich domain
CTECs	Cortical thymic epithelial cells
Ctss	Cathepsin S

CTLA-4	Cytotoxic T-lymphocyte-associated protein 4
CV	Central vein
Cxcl9	Chemokine ligand 9
Cxcl10	Chemokine ligand 10
CXCR3	C-X-C chemokine receptor type 3
CXCR6	C-X-C chemokine receptor type 6
DAMPs	Damage-associated molecular patterns
DCs	Dendritic cells
D-Gal	D-galactosamine
DKO	Double knockout
DMEM	Dulbecco's modified Eagle Medium
DMSO	Dimethylsulphoxide
DN	Double negative
DNAM-1	DNAX accessory molecule-1
DR	Death receptor
EC	Endothelial cells
EMCN	Endomucin
Eomes	Eomesodermin
FACS	Fluorescence-activated cell sorting
FasL	Fas ligand
Flox	Flanked by LoxP
FoxP3	Forkhead box P3
gD	Glycoprotein
GATA3	GATA binding protein 3
GATA4	GATA binding protein 4
GF	Germ-free
GBSS	Gey's Balanced Salt Solution (GBSS)
GeoMFI	Geometric mean fluorescence intensity
GM-CSF	Granulocyte-macrophage colony-stimulating factor
GzmB	Granzyme B
Hobit	Homologue of BLIMP1 in T cells
HVEM	Herpes virus entry mediator
ICAM	Intracellular adhesion molecule
ILCP	Innate lymphoid cell progenitor

ICOSL	Inducible co-stimulator ligand
IFN-γ	Interferon gamma
Ifnγr	Interferon gamma receptor
IEC	Intestinal epithelial cells
Ig	Immunoglobulin
IL	Interleukin
IL7Rα	Interleukin-7 receptor subunit alpha (IL7R-α)
IL12R	Interleukin-12 receptor
IL15R	Interleukin-15 receptor
ILCs	Innate lymphoid cells
ILCP	Innate lymphoid cell progenitor
iTreg	Induced regulatory T cells
JAG1	Jagged Canonical Notch Ligand 1
KCs	Kupffer cells
KIRs	Killer Ig-like receptors
KLRG1	Killer Cell Lectin Like Receptor G1
KO	Knockout
LHX1	LIM homeobox 1
LMCs	Liver mononuclear cells
LPS	Lipopolysaccharide
LSECs	Liver sinusoidal endothelial cells
LT	Lymphotoxin
LTi	Lymphoid tissue-inducing cells
Lyve1	Lymphatic vessel endothelial hyaluronan receptor 1
MCP-1	Monocyte-chemotatic protein-1
MIC	MHC I chain-related molecules
MHC	Major histocompatibility complex
MTECs	Medullary thymic epithelial cells
MULT1	Murine UL16 binding protein-like transcript
NaCl	Sodium chloride
NCR	Natural cytotoxicity receptor
NFAT	Nuclear factor of activated T-cells
NFκB	Nuclear factor kappa-light-chain-enhancer of activated B cells
NK cells	Natural killer cells

NKP	NK progenitor
NKT cells	Natural killer T cells
NLR	NOD-like receptors
NOD	Nucleotide oligomerization domain
NPCs	Non-parenchymal cells
ns	Not significant
nTreg	Natural regulatory T cells
OX40L	OX40 ligand
PAMPs	Pathogen-associated molecular patterns
PBS	Phosphate-buffered saline
PCCM	Primary cell culture media
PD-1	Programmed cell death protein 1
PD-L1	Programmed death-ligand 1
PMA	Phorbol myristate acetate
POR	Cytochrome P450 oxidoreductase
PRRs	Pattern recognition receptors
PT	Portal triad
RAE-1	Retinoic acid early transcript 1
RAG	Recombination-activated genes
RIG-I	Retinoic acid-inducible gene I
RIN	RNA integrity number
RLR	RIG-I-like receptors
RNA	Ribonucleic acid
Rorγt	RAR-related orphan receptor gamma
Rpm	Revolutions per minute
RPMI	Roswell Park Memorial Institute
Rspo3	R-spondin3
RT-PCR	Real time polymerase chain reaction
Rxrα	Retinoic X receptor alpha
scRNA seq	Single-cell RNA sequencing
SEM	Standard error of the mean
SLOs	Secondary lymphoid organs
SMCs	Smooth muscle cells
SOX2	SRY (sex determining region Y)-box 2,

SPF	Specific-pathogen-free
Stab	Stabilin
SP	Single positive
STAT	Signal transducer and activator of transcription
Tbet	T-box expressed in T cells
TCR	T cell receptor
T_{CM}	Central memory T cells
T_{EM}	Effector memory T cells
T_N	Naïve T cells
Th1 cells	Type 1 helper T cell
Th2 cells	Type 2 helper T cell
Th17 cells	Type 17 helper T cell
TLR	Toll-like receptors
TLSP	Thymic stromal lymphopoeitin
TGF-β	Transforming growth factor-β
TNF	Tumor necrosis factor
TNFSF	Tumor necrosis factor super family
TRAIL	TNF-related apoptosis-inducing ligand
TRIF	TIR-domain-containing adapter-inducing interferon-β
Treg	Regulatory T cells
TSA	Deacetylase inhibitor trichostatin
TW	Transwell
VCAM	Vascular cell adhesion protein
VEGFR2	Vascular endothelial growth factor receptor 2
WT	Wild type
YFP	Yellow fluorescent protein

11 Acknowledgements

I would like to thank my supervisor Prof. Dr. Adelheid Cerwenka for offering me the opportunity to perform my PhD's study in her lab. She has supported me by allowing me to pursue my experimental plans, giving me advice, and initiating collaborations with other groups. Perhaps one of the most important people that has assisted me to finish my thesis is Dr. Ana Stojanovic. She has guided my projects, provided me with numerous great ideas, and has always been positive about my data.

I am thankful to Prof. Dr. Ana Martin-Villalba for being the first referee of my thesis, the chair of my PhD defense, and TAC member. Moreover, I want to acknowledge Prof. Dr. Viktor Umansky and Prof. Dr. Peter Angel, who agreed to be in my thesis examination committee. In addition, I would like to thank Prof. Dr. Hellmut Augustin for being a member of my TAC committee.

I am very grateful to be in the best PhD's office of Immunobiochemie. In a chronological order of friendship duration, I first thank Mingeum for always listening to my data and all sorts of daily topics, discussing them with me, helping with my experiments, and stealing my hand cream, Vitamin C, and foods without any mercy. Next would be the boat party team, including Irene (are we friends?) and Tomas, in which we endured together the past 4 years of PhD hardships like a boat sailing against the direction of the stream. And special thanks to Sophia, who came later and joined my LSEC team, working together with me for all crazy experiments, organizing my messy bench, and playing Kpop songs for me. Then it would be Francesco, the best advocate of western democracy, who has made me thought that he is more like an American than an European. Also Silvina, who is the most chilled person that I have ever met in my life. And finally Andy and Bianca, two young bright PhD's students who will inherit our legacy. Thank you everyone for making my life in Germany here so meaningful.

I am also very thankful for having Petra, the master of mouse, to help breed, pack, genotype, and order the mice. A big thank to Sina, who has always helped me to solve my Visa problems, which often I think they are harder than my PhD's project, to ensure that I would not be an illegal resident here. I would also like to thank other lab members for their supports, and previous lab members including Margareta, Jana, and Marian.

最后，我想感谢我生命中最重要的人，也就是我的父亲 – 施新胜，和我的母亲 – 蔡芳婷。感谢他们从来不会限制我想做的事，而是支持我所做的任何决定。因为他们的支持，我才能出国留学完

成我的梦想。我也要感谢我的弟弟 – 施嘉豪，在我不在马来西亚的这许多年，都是他在陪伴着我的父母。我还要感谢我两个最重要的朋友 – 林道显和洪晓双。在我在德国的这几年，依然把我当成朋友，与我分享生活的一切。

时光飞逝，五年读博时间就此结束。我感谢在这段期间帮助我的每一个人，希望有缘大家再相见。